PARAMETRIC OPTIMIZATION OF A DI-CI ENGINE FUELLED WITH BUTANOL/DIESEL BLENDS FOR IMPROVED PERFORMANCE AND EMISSION CHARACTERISTICS

A Thesis submitted in partial fulfillment of the requirements for the award of the degree of

DOCTOR OF PHILOSOPHY

by

KATTELA SIVA PRASAD

Roll No: 716126

DEPARTMENT OF MECHANICAL ENGINEERING
NATIONAL INSTITUTE OF TECHNOLOGY
WARANGAL – 506004
TELANGANA STATE, INDIA.
JULY– 2021

PARAMETRIC OPTIMIZATION OF A DI-CI ENGINE FUELLED WITH BUTANOL/DIESEL BLENDS FOR IMPROVED PERFORMANCE AND EMISSION CHARACTERISTICS

A Thesis submitted in partial fulfillment of the requirements for the award of the degree of

DOCTOR OF PHILOSOPHY

by

KATTELA SIVA PRASAD

Roll No: 716126

under the supervision of

Prof. S. SRINIVASA RAO

&

Dr. V. R. K. RAJU

Associate Professor

Department of Mechanical Engineering

DEPARTMENT OF MECHANICAL ENGINEERING

NATIONAL INSTITUTE OF TECHNOLOGY

WARANGAL – 506004

TELANGANA STATE, INDIA.

JULY– 2021

THESIS APPROVAL FOR Ph. D.

This thesis entitled **"Parametric optimization of a DI-CI engine fuelled with butanol/diesel blends for improved performance and emission characteristics"** by **Mr. Kattela Siva Prasad** is approved for the degree of Doctor of Philosophy.

Examiners

_____

_____

_____

Supervisors

Dr. S. Srinivasa Rao
Professor
Department of Mechanical Engineering
NIT Warangal

Dr. V. R. K. Raju
Associate Professor
Department of Mechanical Engineering
NIT Warangal

Chairman
Prof. A. Kumar
Head, Mechanical Engineering Department,
NIT Warangal.

NATIONAL INSTITUTE OF TECHNOLOGY

WARANGAL – 506 004, Telangana State, INDIA

CERTIFICATE

This is to certify that the thesis entitled **"Parametric optimization of a DI-CI engine fuelled with butanol/diesel blends for improved performance and emission characteristics"** submitted by **Mr. Kattela Siva Prasad**, **Roll No. 716126**, to **National Institute of Technology, Warangal** in partial fulfillment of the requirements for the award of the degree of **Doctor of Philosophy in Mechanical Engineering** is a record of bonafide research work carried out by him under our supervision and guidance. This work has not been submitted elsewhere for the award of any degree.

Dr. S. Srinivasa Rao
(Supervisor)
Professor
Department of Mechanical Engineering,
National Institute of Technology,
Warangal - 506004, Telangana State.

Dr. V. R. K. Raju
(Co-Supervisor)
Associate Professor
Department of Mechanical Engineering,
National Institute of Technology,
Warangal - 506004, Telangana State.

Prof. A. Kumar
Chairman-DSC
Head of the Department
Department of Mechanical Engineering
National Institute of Technology
Warangal -506 004, Telangana, India.

NATIONAL INSTITUTE OF TECHNOLOGY

WARANGAL – 506 004, Telangana State, INDIA

DECLARATION

This is to certify that the work presented in the thesis entitled "**Parametric optimization of a DI-CI engine fuelled with butanol/diesel blends for improved performance and emission characteristics**", is a bonafide work done by me under the supervision of **Prof. S. Srinivasa Rao** and **Dr. V. R. K. Raju,** and was not submitted for the award of any degree to any other University or Institute.

I declare that this written submission represents my ideas in my own words and where ever others ideas or words are included have been adequately cited and referenced with the original sources. I also declare that I have adhered to all principles of academic honesty and integrity and have not misrepresented or fabricated or falsified any idea/data/fact/source in my submission. I understand that any violation of the above will cause for disciplinary action by the institute and can also evoke penal action from the sources which have thus not been properly cited or from whom proper permission has not been taken when needed.

Place: Warangal.

Date:

Kattela Siva Prasad
Research scholar
Roll No: 716126

Dedicated

to

ALMIGHTY GOD,

My Family

My Teachers and friends who encouraged me

ACKNOWLEDGEMENTS

I would like to express my sincere gratitude and profound indebtedness to **Prof. S. Srinivasa Rao** and **Dr. V. R. K. Raju**, Associate professor, Mechanical Engineering Department, NIT Warangal for giving me an opportunity to carry out doctoral work under their esteemed supervision. This work is a reflection of their thoughts, ideas and concepts. Prof. S. Srinivasa Rao and Dr. V. R. K. Raju look at things in the right perspective, and it has truly been a learning experience working with them. I owe a lot to them for making me a part of the continuity of the profession.

I extend my sincere gratitude to **Prof. N. V. Ramana Rao,** Director, National Institute of Technology Warangal, India for providing the necessary facilities and encouragement throughout my work.

I am thankful to **Prof. A. Kumar**, Head, Department of Mechanical Engineering, NIT Warangal and other faculty members of the department for their encouragement and support extended during this period.

Its my great opportunity to express my deepest gratitude to the Departmental Scrutiny Committee members, **Dr. A. Veeresh Babu**, Associate Professor and **Dr. G. Naga Srinivasulu**, Associate Professor, Department of Mechanical Engineering, and **Dr. S. Vidyasagar**, Associate Professor, Department of Chemical Engineering for their adeptness and many discussions during the research period.

My sincere thanks also go to **Prof. C. S. P. Rao, Prof. P. Bangaru Babu, Prof. N. Selvaraj and Prof. R. Narasimha Rao** former HoDs, Department of Mechanical Engineering, National Institute of Technology, Warangal, for their encouragement, for providing access to the laboratory and research facilities. Without their precious support it would not have been possible to conduct this research.

I wish to convey my heartfelt thanks to **Prof. G. Amba Prasad Rao**, National Institute of Technology, who taught me Advanced IC engine course and motivated me in understanding the concepts in completing my research work.

I wish to convey my heartfelt thanks to **Sri. G. R. K. Gupta**, Associate Professor National Institute of Technology Warangal, for continuous motivation and support.

I am grateful to **Dr. M. Raja Vishwanathan,** Assistant Professor, Department of Humanities & Social Science, NIT Warangal, for his constant support.

I would like to extend my heartfelt thanks to **Mr. Rama Chander**, **Mr. Ravi** and **Mr. Sathish** Technical Staff of Thermal Engineering Lab and **Mr. M. V. Vijay Kumar,** Office staff of Mechanical Engineering Department, NIT Warangal for their constant help and encouragement.

I also like to express my sincere thanks to all my friends and colleagues specially, to Dr. Ganji Prabhakar Rao, Dr. Manoj Kumar, Mr. Chandrasekhar, Mr. Sasidhar and Mr.Ganesh Gawale.

A special debt of deep gratitude to my parents and family members for their unceasing sacrifices, endeavors and encouragement.

Finally, I would also like to acknowledge the help given by all the persons who have directly or indirectly supported the work.

(Kattela Siva Prasad)

CONTENTS

Chapter 5

Numerical studies - Results and Discussion

Parametric study to identify the ranges of the operating parameters of a DI-CI engine through numerical analysis

Chapter 6

Parametric optimization of a DI-CI engine fuelled with butanol/diesel blends using response surface methodology

LIST OF FIGURES

LIST OF TABLES

NOMENCLATURE

aTDC - After top dead center

bTDC - Before top dead center

Bu00 - Pure diesel (100% of diesel fuel)

Bu20 - 20% butanol + 80% diesel

Bu30 - 30% butanol + 70% diesel

Bu40 - 40% butanol + 60% diesel

BTE - Brake thermal efficiency (%)

BSEC - Brake specific energy consumption (kJ/kWh)

BSFC - Brake specific fuel consumption (kg/kWh)

CI - Compression ignition

CR - Compression ratio

CD - Combustion duration (deg CA)

CO - Carbon monoxide

CN - Cetane number

CA - Crank angle

CRDI - Common rail direct injection

EGT - Exhaust gas temperature (^{0}C)

EGR - Exhaust gas recirculation

FIP - Fuel injection pressure (bar)

HD - Heavy duty

HS - High speed

HCCI - Homogeneous charge compression ignition

ISFC - Indicated specific fuel consumption (kg/kWh)

ISEC - Indicated specific energy consumption (kJ/kWh)

ID - Ignition delay (ID) (deg CA)

IHRR - Instantaneous heat release rate (J/deg)

IHR - Integrated heat release (J0

LD - Light duty

LFDI - Lean Fuel Distribution Index

NHR - Net heat release (J/deg)

RoPR - Rate of pressure rise (bar/deg)

RFDI - Rich Fuel Distribution Index

RSM - Response surface methodology

TFDI - Target Fuel Distribution Index

UBHC - Unburned hydrocarbons

VCR - Variable Compression Ratio

WC - Water cooled

ABSTRACT

The rapid depletion of fossil fuels, surging oil prices, stringent emission regulations and the environmental considerations are motivating researchers to develop a well performed engine with less emissions. Therefore, there is a compulsion to develop a new combustion technology along with clean renewable fuels. Among the different technologies, HCCI technology has been observed to be an effective way to decrease the NOx and soot emissions simultaneously in the CI engine. The present work deals with the HCCI combustion characteristics of a CI engine fuelled with butanol/diesel blends.

The present study deals numerical and experimental analysis for evaluating the combustion, performance and emission characteristics of a CI engine fuelled with butanol/diesel blends. Numerical analysis was carried out by varying four operating parameters, i.e., Compression ratio (CR), Fuel injection pressure (FIP), Exhaust gas recirculation (EGR) and Start of injection (SOI), and with different butanol/diesel blends (0, 20%, 30% and 40% of butanol-by volume, designated as Bu00, Bu20, Bu30 and Bu40) by using CONVERGE CFD simulation software. Response surface methodology (RSM) was used to obtain the relation between the input parameters and output responses. Three output responses, viz., indicated specific fuel consumption (ISFC), NOx and soot emissions were considered in the present study. The optimum combinations of the input parameters for the four test fuels were found with the objective of minimizing the three output responses. The homogeneity of the air-fuel mixture was estimated using Target Fuel Distribution Index (TFDI). Experimental studies were also carried out on a VCR DI-CI engine by varying different operating parameters (CR, EGR and FIP) with different butanol/diesel blends. These experimental results were used for validation of the numerical results.

It was observed from the analysis of the results that the optimum combination of the input parameters resulted in better performance and lower emissions as compared to the respective baseline configuration performance for all the four butanol/diesel blends. It was observed from the comparison of the optimum values of the operating parameters for the four blends that with increase in the butanol content in the blends from Bu00 to Bu40, the optimum FIP, optimum SOI and the optimum EGR are decreasing, while the optimum CR is more or less constant. It was also observed that for the optimized case the TFDI increased by 19.3%, 21.3%, 24.1% and 27.2% for Bu00, Bu20, Bu30 and Bu40 respectively as compared to their respective baseline configurations. Improved TFDI with simultaneous reduction of NOx and soot emissions with the optimized configuration is an indication of near HCCI mode of combustion in all the cases. Thus, the use of Bu40 as an alternate fuel in a CI engine with the optimum values of the operating parameters is justified, and recommended as a replacement for convectional diesel fuel.

Chapter 1

Introduction

1.1. Introduction

IC engines are widely used in different industrial sectors and transportation sector. IC engines are classified based on the type of ignition as Spark Ignition (SI) and Compression Ignition (CI) engines. The operation of the SI engine is limited by lower part load efficiencies owing to its lower compression ratio. In IC engines, CI engines constitute a major portion in the transportation sector, heavy-duty machinery sector, agriculture machinery, industrial and power development owing to higher energy conversion efficiency and power development compared to SI engines. However, there are certain problems with the present use of fossil fuels in CI engines such as the harmful engine emissions and the rapid depletion of fossil fuels.

Among the different CI engine emissions, NOx and soot are considered to be more objectionable as they are hazardous to both environment and human life. To reduce these emissions and meet the strict emission regulation conditions, researchers are studying many advanced combustion strategies such as HCCI with EGR, different injection strategies, fuel reformulation and after-treatment system, etc. HCCI system is different from the conventional combustion system of CI engines. HCCI technology has been found to be an effective way to reduce NO_x and soot emission simultaneously in CI engines, by applying exhaust gases to cylinder, which decreases the overall combustion temperature and oxygen concentration [1,2]. These effects reduce the formation of NO_x emissions although the reduction in oxygen concentration usually causes an increase in the soot, UBHC and CO emissions [3,4]. Retarding

the start of fuel injection timing (SOI) can also reduce NO_x emission with a small penalty on soot and fuel economy. Another method is reformulation of diesel fuel with biofuel. Diesel fuelled HCCI suffers from limited premixing time resulting from ignition delay and difficulties in achieving spray vaporization at low temperature and pressure, due to the higher value of cetane number (CN), high viscosity, high boiling point of diesel fuel [5,6]. These problems can be successfully handled by using alcohol-based fuels, which have higher self-ignition temperature (SIT), higher volatility and lower CN. Addition of biofuel to conventional diesel fuel increases the renewable energy utilization and therefore ensures energy security.

Another problem with the use of fossil fuels is that they are getting depleted at an alarming rate. This is also another reason for the large-scale research in finding alternate fuels for the IC engines. The use of biofuels such as biodiesel, biogas and bio-alcohol is attractive not only because they are renewable in nature but also they help in decreasing the greenhouse gas emissions as well as soot and NOx emissions from CI the engine [7,8].

Biofuels mostly include biodiesel, biogas and bio-alcohols. Among the biofuels, bio-alcohols are an attractive proposition. Once again, among the alcohols the lower chain alcohols (ethanol and methanol) are prominently used as a substitute of gasoline in SI engines. However, the lower chain alcohols have lower energy density, higher LHV and inferior cetane number (CN) compared to the diesel fuel. These shortcomings of lower chain alcohols make them less attractive for wide spread use as in the conventional CI engine [9].

On the other hand, higher-chain alcohols such as butanol, propanol and n-octanol have properties closer to that of diesel. Even among the higher-chain alcohols, butanol is a more attractive fuel as a substitute for diesel in CI engines. Among the higher chain alcohols, butanol has the lowest viscosity while the other higher chain alcohols have higher viscosity than the diesel fuel. The molecular structure of butanol (C_4H_9OH) has more oxygen atoms when compared to biodiesel, thereby potentially leading to decrease of emissions, primarily soot[10]. Butanol has higher LHV than conventional diesel fuel, which is helpful for the reduction of the in-cylinder temperature, and consequently reduction in NOx emission formation [11]. Therefore, butanol shows some additional advantages as an alternative to fossil fuels in the CI engines, compared to ethanol and methanol. Though butanol is a promising alternative fuel, the production rate of butanol from fermentation process is lower compared to ethanol fermentation

process [12]. However, in the present research study, butanol/diesel blends are used as fuel in the CI engine.

1.2. Objective of the present work

The objective of the present work is to substitute the fossil fuel (diesel) with renewable fuel (butanol) in a DI-CI engine to the maximum extent possible with minimum modifications to the existing engine. In the first stage, experiments were carried out with butanol/diesel blends for validation purposes. In the next step, a complete engine model was designed and developed using CONVERGE CFD software. The work focuses on the validation of VCR engine models for diesel and butanol/diesel blends (Bu00, Bu20, Bu30 and Bu40). Once each of these models were validated, the models were further analysed for the effect of different parameters such as Compression Ratio, Fuel Injection Pressure, Exhaust Gas Recirculation and Start of Injection. In the next step, DOE analysis was used to analyse the effects of these parameters and their interaction effects on the engine characteristics to obtain the relation between the input and output response factors, and obtain optimum conditions. The optimum parameters were simulated using the CONVERGE CFD software and compared to the performance and emission characteristics for both baseline and optimum cases. The mixture homogeneity of the optimum and baseline cases was also compared for all the four test fuels, viz., Bu00, Bu20, Bu30 and Bu40.

1.3. Structure of the thesis

The thesis comprises of seven chapters. Chapter 1 provides a brief introduction to IC engines, pollutants and their effects on humans and the environment. It also details advantages and disadvantages of different types of biofuels/ blends. Chapter 2 presents a critical literature review on butanol/diesel blends, and individual parameters effects (CR, FIP, EGR and SOI) on the combustion, performance and emission characteristics of CI engines. Further, this chapter also focuses on the literature related to optimization of parameters using RSM method. This is accompanied by the research gaps identified from the literature survey, and conclusions drawn from the literature review. All the objectives of the present research work are also included. In the next chapter, i.e., Chapter 3, the methods adopted for carrying out experimental and numerical studies of DI-CI engine using CONVERGE CFD software are presented. The

procedure for preparation of blends, their properties and methods of experimentation are explained. The preparation of the DI-CI engine Model, mathematical modelling, different physical, chemical and combustion models, reaction mechanism and grid independency test have also been discussed in this chapter. In Chapter 4, firstly, the influence of butanol/diesel blends on the engine performance and emission characteristics of a VCR engine are presented. In the second phase, the influence of different operating parameters along with butanol/diesel blends on the engine performance and emission characteristics are presented. In Chapter 5, numerical simulation studies to analyse the parametric effects on the characteristics of CI engine and the parametric range for each of the individual parameters are discussed. In Chapter 6, the results and findings are discussed for different test fuels. The validation of numerical models for different test fuels are first discussed in the chapter. In the next step, optimization technique (RSM) was used to minimise ISFC, soot and NOx emissions. The comparison of the optimized and baseline cases performance also figure in the discussion. Finally, the homogeneity of air-fuel mixture is discussed for both optimized and baseline configuration. Chapter 7 presents the conclusions of the work and scope for future research.

Chapter 2

Literature Review

This chapter presents a summary of the experimental and numerical studies on the performance and emission characteristics of CI engines operating with different blends (butanol/diesel). The effect of different operating parameters on the performance and emission characteristics of CI engine fuelled with butanol are also discussed in this section. Further, some important findings from the literatures have been summarized.

2.1. State of the art CI engine

Many researchers have investigated the development of IC engines from the time engines came into existence. CI engines have always enjoyed an upper hand over SI engine owing to higher energy conversion, higher power development and wider range of applications. CI engine has many advantages over the SI engine. The CI engine shows higher thermal efficiency, and also produces lower CO and HC emissions than the SI engine. But, the main disadvantage of CI engines is producing higher NOx and soot emissions than the SI engine. These emissions are harmful to both the environment and human life. Nowadays, engine manufacturers are using various controlling techniques like fuel injection pressure, fuel injection timing and EGR for controlling the CI engine combustion. In order to reduce the emissions and meet the emission regulations, recent studies have suggested many advanced combustion strategies such as HCCI, different injection strategies, fuel reformulation and after-treatment system etc. From the literature, it is clean that among the various technologies, HCCI technology is one of the best method to reduce the NOx and soot emission simultaneously in the CI engine.

HCCI combustion concept involves a combined characteristic of SI and CI engine. In HCCI mode, a well-mixed air-fuel (homogeneous charge) and oxidizer are compressed to the point of auto ignition conditions inside the combustion chamber. The HCCI combustion concept mainly involves low temperature combustion of a homogeneous air-fuel mixture, which leads to simultaneous reduction of NOx and soot emission. However, the main challenge of HCCI concept is that it requires preparation of homogeneous air-fuel charge in a short interval of time, lacks control of combustion timing and has limited power output. Diesel fuelled HCCI suffers from limited premixing time resulting in shorter ignition delay and difficulties in achieving spray vaporation at low temperature and pressure, due to higher cetane number (CN) and higher boiling point of diesel. These problems can be successfully handled by using alcohol fuels due to their higher self-ignition temperature, higher volatility and lower cetane number. Engine models based on HCCI concept using renewable fuels are also available in literature. Very few studies have provided complete and well validated models that include accurate physical property data as well as detailed description of the fuel chemistry. It is important to expand simulation studies by incorporating validated numerical techniques by adopting different fuel options like renewable fuel blends.

In the present study an alcohol based fuel i.e., butanol was used in the experiments and for numerical analysis. Butanol, a higher chain alcohol, is a promising alternative fuel to diesel in the CI engine. Butanol consists of a straight chain 4-carbon alcohol. Butanol has other forms of isomers such as normal butanol (n-butanol), secondary butanol, iso-butanol and tert-butanol.

These butanol isomers exist with the location of hydroxyl group (-OH) being different in the molecular structure, with different carbon chains. Among these n-butanol and iso-butanol show better performance and give lower emissions. In the present study, n-butanol was considered. Butanol can be used in the CI engines in any one of the following three modes:

1. As a blend (blend of butanol and diesel with different volume fractions of butanol in the blend).
2. In Dual fuel mode, with butanol being premixed with air and diesel as the main fuel.
3. As an additive in a ternary blend of diesel and biodiesel

In the present study, butanol/diesel blends were used as the fuel in CI engine. Literature on the performance and emission characteristics of CI Engines operating with butanol/diesel blends is presented in the section that follows.

2.2. Performance, combustion and emissions characteristics of butanol in CI engines

Butanol has lower polarity that shows better miscibility with gasoline and diesel fuel. Butanol has lower density and viscosity than diesel fuel. Butanol has properties such as lower CN, higher auto-ignition temperature (AIT) and greater volatility compared to diesel. Butanol/diesel blends are hydrophilic in nature and do not require any special blending agents. Butanol/diesel blends are stable for many days due to the stable mixture formation ability of butanol. Another noteworthy advantage is that higher content of butanol can blend in diesel fuel without using any solvent. It indicates that higher content of renewable fuel can be utilized. Several kinds of research suggest that butanol can substitute up to 40% in convention diesel fuel without any alterations in the existing diesel engine [13,14]. These benefits make butanol/diesel blends attractive as an alternative to pure diesel and motivated researchers to engage in research in the area.

2.2.1. Effect of butanol/diesel blends on the performance, combustion and emission characteristics of CI engine

Literature on the performance and emission characteristics of CI engines operating with butanol/diesel blends under various ranges of operating conditions are presented in this section.

Literature survey reveals that studies were conducted on the use of butanol/diesel blends in CI engines without any modifications to the engine operating parameters or with minor modifications to the engine operating parameters. The influence of butanol/diesel blends on the performance, combustion and exhaust gas emission characteristics in various CI engines without modification to the engine operating parameters is presented in this section.

Rakopoulos et al.[15] experimentally studied the influence of two different butanol/diesel blends (8% and 16% - by volume) on the performance of a six-cylinder, turbocharged, water-

cooled, Heavy-duty (HD), Direct injection (DI), Mercedes-Benz diesel engine at various engine speeds (1200 and 1500 rpm) and loads (3.56, 7.04. 10.52-BMEP). Their results revealed that butanol/diesel blends slightly elevated the in-cylinder pressure and heat release rate (premixed combustion). It was interpreted that the butanol/diesel blends have longer ignition delay due to the lower cetane number of butanol, which increases the ignition delay and also increases the premixed fuel for combustion after the start of ignition. UBHC emissions increased, and NOx, CO and soot emissions reduced with the addition of butanol content in the blends compared to pure diesel fuel.

Karabektas and Hosoz [16] investigated the impact of butanol/diesel blends (5% to 20% of butanol-by volume) on the performance and emissions of a CI engine at different engine speeds. They found that with an increase of butanol content in the blend, the brake power (BP), CO, soot and NOx emissions reduced, whereas the UBHC emissions increased. It was explained that the addition of butanol to diesel fuel causes the leaning effect on the blends due to lower stoichiometric ratio and thus lowered the CO emissions. Similarly, NOx emission decreased with increase of butanol percentage, due to lower combustion temperatures and prolonged ignition delay of the blend. With increase of butanol amount in the blend, UBHC emissions increased due to lower cetane number of butanol. The lower cetane number of the blends reduces the self-ignition characteristics of the blends and promotes quenching effect on the lean mixture zone. It was also observed that with increase in the butanol content in the blends, the exhaust gas temperature decreased compared to pure diesel operation. It was explained that this was due to the lower energy content of the blends, and the consequent lower combustion temperature. CO emissions reduced with increase of butanol amount in the blends, due to the oxygen content in butanol that enhances the air-fuel mixture in the rich zone.

An experimental study was carried out by Dogan [17] to evaluate the performance of a CI engine using butanol/diesel blends (5% to 20% by volume) at a speed of 1500 rpm and at different loads. It was observed that BTE increased for butanol blend operation as compared to diesel fuel operation. It was due to the higher burning velocity (higher flame speed) of butanol blends and the oxygenated nature of butanol blends leading to improved diffusion combustion process compared to the diesel fuel.

Ozsezen et al. [18] experimentally evaluated the effect of iso-butanol/diesel blends (by volume - 5% to 20% of butanol) on the exhaust emission and performance characteristics of a

six-cylinder, turbocharged, HD CI engine at a speed of 1400 rpm and varied loads (150, 300 and 450Nm). It was found that with the increase of butanol percentage in the blend, the BSFC increased and BTE decreased. It was attributed to the lower calorific value of the blend and as a result, more amount of fuel was consumed to attain the same engine power. The peak in-cylinder pressure and HRR slightly increased compared to the diesel fuel operation, whereas CO, NO_x and soot emissions significantly reduced and the UBHC emissions slightly raised with the use of iso-butanol/diesel blends.

Satsangi and Tiwari [19] investigated the influence of butanol/diesel blends (by volume, 0-20%) on the combustion noise, vibrations, performance and emissions characteristics of a CI engine. The experimental outcomes showed that butanol/diesel blends produced higher combustion noise, vibration, rate of pressure rise and heat release rate compared to diesel fuel, mostly at higher load. It was also observed that butanol/diesel blends showed better decrease in emissions with little penalty on performance. They suggested that butanol blends are more suitable for diesel engine applications.

Al-hasan et al. [20] performed experiments on a single cylinder CI engine fuelled with iso-butanol/diesel blend (10%, 20%, 30% and 40% of butanol by volume) at different speeds and loads. Their results showed that iso-butanol content up to 30% showed better performance than diesel fuel. With further increase of iso-butanol percentage to 40%, the BSFC drastically increased while the BTE drastically decreased than other blends and diesel fuel. It was also observed that as the engine speed increases, the air-fuel ratio (AFR) and exhaust gas temperature decreased for blends compared to diesel fuel. It was explained that the air-fuel ratio decreased due to the increase of fuel mass flow rate with increase in the engine speed for blends.

2.2.2. Parametric study with butanol/diesel blends on the combustion, performance and emission characteristics of CI engine

Design of efficient engine depends on several operating and design parameters, which can influence the performance and emission characteristics of the engine. This section shows the literature on major parameters that impact the performance and emission characteristics of a CI engine. The parametric study of the CI engine (CR, SOI, EGR, FIP and different injection strategies) in terms of performance and emission characteristics of the CI engine fuelled with butanol/diesel blends are presented in this section.

Experimental and numerical analysis (CFD-AVL) was carried out by Lamani et al. [21] to study the effect of oxygenated fuel i.e., butanol/diesel blends (0 to 30% volume of butanol) by varying the SOI (9^0, 12^0, 15^0, and 18^0 CA bTDC) on a twin cylinder CI engine. Their results showed that BTE increased by 4.5, 6, and 8% for the butanol-diesel blends of 10%, 20% and 30% respectively. The maximum BTE for the butanol-diesel blends of 10%, 20% and 30% were 38.4%, 40.19, 40.9 and 41.7% respectively, which were obtained at an SOI of 12^0 bTDC for diesel fuel and 15^0 bTDC for the blends. From the numerical analysis, it was observed that most of the fuel burns in the premixed phase due to higher flame speed of the blend. NOx and soot emissions decreased with increase in the butanol fraction in diesel fuel. This is because advanced SOI leads to early start of combustion, causing higher cylinder temperature. It results in fast chemical reaction between carbon and oxygen in the combustion chamber which increases the oxidation process. As a result, it produces lower soot and CO, and higher NOx emissions.

Merola et al. [22] examined the influence of butanol/diesel blend (20% of butanol-Bu20) on the emission characteristics of a four cylinder turbocharged CI engine by varying the start of injection (SOI) (-3, -5 and -8^o CA bTDC) and fuel injection pressure (FIP) (100, 120, 140 and 160 MPa). The studies were carried out using optical methods (UV-visible digital imaging and natural emission spectroscopy) and conventional methods. They concluded that Bu20 butanol/diesel blend promotes higher concentration and faster formation of OH radicals inside the cylinder. This effect led to advance in soot oxidation phase that promotes smokeless emission in advanced injection condition.

Liu et al. [23] investigated the effect of n-butanol/diesel blends under early-injection partially premixed combustion (PPC) (0 to -25^o CA bTDC) and pre-injection strategy (-25^o CA bTDC to -75^o CA bTDC) in a four-cylinder turbocharged intercooled CI engine. The test outcomes showed that as the proportion of butanol in the blend increased, peak HRR increased, heat release duration reduced and the peak value of the accumulation mode particles reduced. As the injection timing was advanced, the in-cylinder temperature became lower when the fuel was injected, and the fuel-injection penetration distance was longer and the fuel distribution range was expanded, which reduced the probability of the collision and condensation of nucleation mode particle. As the pre-injection ratio was increased, the pre-injection combustion phase showed bimodality (two peak pressures and heat releases rate) compared to the single injection strategy. It may be the reason that when using n-butanol/diesel blends, the peak values of the

cool-flame reaction increase with an increase of pre-injection fuel quantity. With the advancing of injection timing (single injection mode), the GMD (Gross Mean Diameter) of PM got reduced for diesel fuel, whereas for the butanol/diesel blend, it was almost unchanged. This was because the blending of butanol makes the oxygen concentration of the fuel increase, which is conducive for the oxidation of soot particles in high temperature.

Chen et al.[24] studied the effect of higher fraction of butanol content (40% of butanol by volume -Bu40) along with different EGR rates on the characteristics of a HD-CI engine by experimental and numerical analysis (CONVERGE CFD Code). They found that the Bu40 blend has longer ignition delay, faster burning rate and higher in-cylinder pressure compared to the diesel fuel operation. The butanol blend developed higher NOx emission owing to high-temperature region and lower soot due to better air-fuel distribution, and higher CO owing to lower exhaust gas temperature during the late expansion process. For the blend, it was showed that the effect of EGR was to decrease NO_x emissions significantly, with no obvious effect on the soot emission. A combination of higher butanol fraction along with medium EGR rate (30%) was shown to have the potential to accomplish ultra-low soot and NO_x emissions.

Huang et al.[25] examined the impact of pilot injection timing and pilot injection fuel proportion with butanol-diesel blends (20 and 30% v/v) and medium EGR rate (25%) on the performance of a HD-CI engine. They found that advancing the pilot injection timing reduced the HRR peak value of the pre-injected fuel, increased the peak value of HRR of the main-injected fuel slightly, reduced the combustion peak pressure value in the main injection period, and increased the maximum pressure rise rate. The advancement of the pilot-injection timing led to a decrease in soot and NO_x emissions; but BTE decreased while BSFC increased. Increase in the pilot injection fuel proportion elevated the HRR peak value of the pre-injected fuel, reduced the HRR peak value of main-injected fuel, increased the combustion peak pressure value, along with BSFC and NO_x emission, while soot emission reduced at first and then increased**.**

Nayyar et al. [26] determined the optimum blending ratio and operating parameters for improving the performance and emission characteristics of CI Engines. Experiments were performed on a single cylinder VCR diesel engine fuelled with butanol blend (10% to 25% by volume). Their results showed that 20% of butanol/diesel blend would give lower emissions and

better performance at higher CR (18.5) compared to diesel fuel. The addition of butanol in the diesel fuel decreased CO, soot and NOx emissions whereas UBHC emissions raised.

Maurya et al. [27] analyzed the nano size particle emission characteristics of diesel/butanol fuelled stationary (non-road) CI engine. Experiments were conducted at a constant speed of 1500 rpm for three compression ratios (16, 17 and 18) and FIP (170, 200 and 220 bar) at various engine loads. Their experimental results showed that the total particle concentration reduced with increase in engine operating loads. Moreover, the addition of butanol in the diesel fuel led to a decrease in the soot particle concentration. The peak particle concentration was higher for lower compression ratio.

He et al. [28] studied the effect of ethanol/diesel (15%-by volume) and butanol/diesel blends (15% and 40% by volume) with different EGR rates on the combustion characteristics, emissions, total particle number concentration and particle matter size distribution of DI CI engine at higher loads. The test outcomes showed that with rise in the butanol amount in the blend and the EGR rate, the premixed combustion phase and the peak heat release rate in the premixed combustion phase increased. The ITE increased with the addition of butanol content but it decreased with increased EGR rate. With the addition of butanol, the total particle number concentration (TPNC) decreased. Eventually, it was apparent that at higher loads, the combination of higher alcohol content of blend and medium EGR rate could achieve better performance and lower emissions.

Fayad [29] experimentally studied the effect of fuel injection strategy (injection pressure and injection timing) operated with 20% of butanol/diesel blend on the characteristics of CI engine. The test outcomes showed that higher fuel injection pressure improves the performance than lower pressure for both fuels. At advanced injection timing, the performance of 20% butanol/diesel blend is higher than that of diesel fuel. Finally they concluded that a combination of 20% butanol/diesel blend with advanced injection can improve the performance and reduce harmful (total hydrocarbons (THC) and carbon monoxide (CO)) emission in the exhaust.

Emiroglu [30] examined the effect of fuel injection pressure with 10% of butanol/diesel blends on the performance and emission characteristics of single cylinder diesel engine. The test results showed that butanol/diesel blend have higher BTE and BSFC, longer ignition delay and shorter combustion duration. With an increase in FIP, the maximum cylinder pressure, HRR

elevated. It was also found that with an increase in FIP, NOx emission increased while smoke emission decreased.

2.2.3. Response surface methodology (RSM)

RSM is one of the optimization techniques used in engineering applications. RSM, as a statistical and mathematical method, is useful to obtain a relation between the responses and the input parameters with an objective of maximization or minimization of the response values. RSM has been widely used in many applications in the manufacturing sector for design and development of new products, as well as in enhancing the existing design of the products.

It is observed from the literature survey that a few studies were conducted to study the effect of butanol blends on the performance and emission characteristics of CI Engines by varying multiple operating parameters of the CI Engine, and optimum values of the operating parameters were determined using different optimization techniques such as Response surface methodology. This section presents a review of this literature.

Saravanan et al. [31] studied the effect of varying three operating parameters, viz., FIP (200-240 bar), SOI (19-25° bTDC) and EGR rate (10-30%) on the performance of diesel engine fuelled with iso-butanol /diesel (40% of butanol by volume) blend using experimental and statistical analysis (RSM method). Response surface methodology (RSM) was used to model the measured responses such as smoke opacity, NOx, BSFC and BTE. They found that FIP of 240bar, SOI of 23°CA bTDC, less than 30% of EGR rate were optimum parameters for the given engine configuration.

In another study, Nayyar et al. [32] investigated experimentally the effect of butanol/diesel blends (10-25% by volume) on the characteristics of CI engine, by varying compression ratio (CR) (16.5, 17.5, 18.5 and 19.5), SOI (19-25° bTDC), and FIP (180-220 bar) at different loads (12, 16, 20 and 24 Nm). RSM was used for optimization. Their outcomes exhibited that at higher CR, 20% of blend showed improved performance, improved the BTE (5.54%) and reduced the NO_x (15.96%) and soot (59.56%) emissions. A CR of 18.5, SOI of 23 °CA bTDC and FIP of 210 led to optimum conditions for diesel fuel, while optimum conditions for Bu20 fuel was CR of 19.5, SOI of 23 °CA bTDC and FIP of 210.

2.2.4. Special emissions with butanol/diesel blends

Carbonyl compounds are non-regulated and poisonous gas emissions. They are highly reactive with atmosphere and cause cancer in human beings. Ballesteros et al. [33] experimentally studied the carbonyl compound emission characteristics of a Nissan Euro 5 M1D-Bk diesel engine with ethanol/diesel (10%- by volume) and butanol/diesel (16% of butanol by volume). The experiment was carried out in four different modes of European driving cycle. The experimental results showed that the butanol/diesel blends produce lower carbonyl emissions compared to the ethanol/diesel blend.

Zhang et al. [34] studied the influence of butanol/diesel blend and pentanol/diesel blend (10% and 20%-by volume) on the performance, emissions of particulate matter and carbonaceous particulate of a single cylinder CI engine. Their results showed that the particulate matter and organic carbon (OC) and elemental carbon (EC) emissions were reduced with blended fuels. Both the blends have higher oxygen content that could be effectively delivered to pyrolysis zone of the burning diesel spray to suppress soot formation and EC emissions. It was also shown that butanol blends produced lower soot and EC compared to pentanol blends. It was because butanol has higher oxygen and lower cetane number than pentanol that led to increase in ignition delay and more amount of fuel burned in the premixed combustion mode.

Zhang et al. [35] studied the effect of butanol/diesel blends (5%, 10%, 15% and 20% by volume) on the particulate emissions on a non-road CI engine. Their results showed that polycyclic aromatic hydrocarbon (PAHs) emissions and their carcinogenic potency increased with blends containing greater than 10% of butanol. It was observed that increase in the butanol percentage in the blend consequently reduced the elemental carbon (EC) and increased the organic carbon (OC) emissions compared to the pure diesel fuel.

Another study, by Choi and Jiang [36], was on the effect of diesel fuel blend with n-butanol (5, 10 and 20% - v/v) on the individual hydrocarbons (IHC) and PM of a CI engine. The outcomes revealed that with the addition of butanol, more ethylene and benzene are emitted under low load conditions. This is attributed to the fact that butanol blends have higher oxygen content, which reduces aromatic compounds from the diesel fuel. It was also found that more than 10% of butanol in the butanol/diesel blend produced higher non-regulated formaldehyde (HCHO) emission compared to diesel fuel, under low engine load conditions. This was on account of the fact that there was lower combustion temperature under lower load conditions.

Eventually, it was suggested that using less than 10% of n-butanol in the blended fuel is a better option to decrease PM. It was also observed that the 5% and 10% of butanol blends emitted PM with particles sizes lower than 50 nm.

2.3. Homogeneous Charge Compression Ignition (HCCI) or Low Temperature Combustion (LTC) of butanol blends in CI engine

Homogeneous Charge Compression Ignition (HCCI) or Low temperature combustion (LTC) can be accomplished by proper air-fuel mixing which can be oxidized at a low temperature, preceded by a prolonged ignition delay period [37]. HCCI is one of the promising solutions which offers simultaneous reduction of soot and NOx emissions [38]. The most commonly used strategies to succeed in LTC operations are retarded injection timing and EGR rate [39]. Introducing higher EGR rate reduces engine performance by worsening the combustion process and as a result, there is increased UBHC and CO emission. Late SOI leads to reduction in ITE and increase in soot emission [40]. Biofuels such as butanol were observed to be more suitable for LTC combustion using DI strategy under higher pressure, EGR and port fuel injection (PFI). Butanol has lower CN, higher SIT and higher volatility. Lower CN increases the ignition delay which leads to better fuel-air mixing, and higher volatility increases the vaporization rate and is thus favourable to achieve LTC. Butanol is a favourable fuel for achieving HCCI owing to its low reactive and high volatile nature compared to diesel fuel.

2.3.1. Combustion, performance and emission characteristics with butanol/diesel blend

This section presents a comprehensive review of the ability of butanol in aiding HCCI operation in CI engine.

Valentino et al. [41] investigated the influence of butanol/diesel blends (by volume of 20% and 40%) on the characteristics of a turbocharged engine, equipped with a common-rail injection system DI CI engine by changing the SOI, intake oxygen concentration and FIP. The experimental results showed that both the blends reduced NO_x and soot emissions with a small penalty on specific fuel consumption. It was also found that the early start of injection and low injection pressure (100-120MPa) can achieve partial premixed low temperature combustion. In addition, higher butanol blends produced high combustion noise compared to diesel fuel.

Zhang et al. [38] investigated the impact of n-butanol blends (20% and 40% by volume), along with EGR on the performance of a heavy duty CI engine, and compared the engine performance with ethanol or methanol and n-butanol fuelled CI engine performance results. The fuel injection timing was adjusted such that CA50, which represents the crank angle of 50% mass fraction burned, was fixed at 8 ^{0}CA ATDC. The fuel injection pressure was fixed at 1600 bar. Their results indicated that with increase in n-butanol content in blend, the ignition delay period got extended, the pressure rise rate increased and the ITE slightly improved. It was also found that with increase in butanol percentage in the blend, soot emissions and NO proportion decreased but NO_2 proportion increased. It was observed that with the addition of n-butanol, the emissions of CO and THC decreased at higher EGR levels. The soot emission decreased greatly, with the increase of butanol fraction. In addition, with increase in EGR rate, the methane (CH_4) emissions increased, but the addition of n-butanol reduced CH_4. It may be observed these results are quite different since this is a heavy-duty engine.

Han et al. [42] assessed the effect of different fuels (gasoline, ethanol and butanol) to enable the LTC at high load operation. Their results showed that when butanol content was injected in the intake port, it deteriorates the combustion efficiency due to its premature auto-ignition. They also found that butanol fuel is more suitable for achieving LTC mode in CI engine under high FIP, supercharging and EGR than with diesel operation. The gasoline/diesel blend can also achieve LTC by port injection but it required sophisticated control over supercharging and EGR. It was suggested that low reactive fuel such as methanol is more suitable for aiding LTC at a higher load.

In another study, Gu et al. [43] evaluated the effect of iso-butanol/diesel and normal-butanol/diesel blends (15% and 30% by volume) in aiding the LTC in CI engines. Experiments were carried out on a CRDI CI engine at light/medium load along with various EGR rates and SOI. The results showed that iso-butanol/diesel blends presented longer ignition delay, higher combustion pressure and higher premixed HRR than normal-butanol/diesel blends. But, smoke emission was lower for n-butanol/diesel blends compared to iso-butanol/diesel blends and NOx emissions reduced slightly for both blends compared to diesel fuel. They suggested that a combination of lower EGR, late SOI and butanol blends can attain LTC mode and simultaneously decrease soot and NOx emissions.

Most of the above studies have focused on butanol/diesel blends during the LTC operation. Yang et al. [44] studied the effect of butanol (0%, 10%, 20% and 30% v/v) blended with gasoline to achieve LTC conditions in CI engine. Experiments were carried out for different butanol/gasoline blends and EGR rates on a single cylinder CI engine. Their results showed that the addition of butanol reduced soot emission. They also found that higher percentage of butanol causes release of higher content of primary individual hydrocarbons (IH) such as Ethylene (C2H4), Propylene (C3H6), n-Pentane (NC5) and iso-Pentane (IC5). With the addition of butanol, formaldehyde and acetaldehyde emission also increased.

Zhou et al. [45] examined the soot precursor emission characteristics of butanol/diesel blend during LTC operation of a six-cylinder turbocharged CI Engine. Experiments were carried out by varying the blending ratio, SOI, supercharging and EGR rate. The test consequences showed that with increasing butanol percentage in the blend, the formation of soot precursors such as naphthalene, benzene, pyrene and phenanthrene were delayed and the final amount of precursor produced also gets reduced.

Zheng et al. [46] examined the effect of supercharging and EGR rate on the combustion phasing and controllability of n-butanol HCCI in a single-cylinder CI Engine with high CR (18.2:1). In the case of diesel fuel for HCCI operation, direct multiple injections technique was adopted to form a homogeneous mixture, whereas in the case of n-butanol fuel HCCI operation, port fuel injection technique was adopted to prepare the premixed air-fuel mixture. From the experimental results, it was shown that n-butanol fuel in HCCI operation developed lower pressure rise rate and bulk temperature compared to diesel fuel in HCCI operation. The ignition delay for butanol was longer than for diesel in HCCI mode of operation. Their results showed that HCCI mode of operation with butanol achieved ultra-low soot and NO_x emissions without much dependence on EGR rate compared to diesel. At low-to-medium engine loads, the super charging and EGR rate had smaller impact on the emissions and the performance. However, at higher loads, both boost pressure and EGR rate were required to control the combustion phasing and higher-pressure rise rate for higher thermal efficiency. It was observed that in HCCI mode of operation, butanol as fuel would give 25% more efficiency compared to diesel in HCCI combustion mode.

In another study, Rajesh and Saravanan [47] studied the combined effect of iso-butanol/diesel (10%, 20%, 30% and 40% v/v) blends, SOI (23° and 21° bTDC) and EGR rate (10%, 20%, and 30%) on diesel engine. Experimental results showed that a combination of 40% iso-butanol/diesel blend, medium EGR (30%) and late SOI can reduce NO_x emissions and soot emission with little drop in performance. Finally, it was reported that a higher percentage of iso-butanol blend required higher EGR rate to accomplish simultaneous reductions of NO_x and soot emissions.

Rajesh and Saravanan [48] compared the effect of two higher alcohol blends (butanol/diesel and pentanol/diesel) on the characteristics of a CI Engine. The results showed that butanol blends are superior in EGR tolerance and have better influence in trade-off of NO_x-soot emissions compared to pentanol blend. Finally, it was concluded that a combination of higher alcohol blends, lower EGR rate, and late injection can achieve partially premixed LTC mode and simultaneous reduction in NO_x and soot emissions.

Zhu et al. [49] studied the influence of n-butanol/diesel blend(butanol-by volume of 30%) and neat diesel (D100) with different intake oxygen concentrations (IOC) (15%, 17%, 19%, and 21%) for enabling premixed low temperature combustion (PLTC). A new reduced reaction mechanism was developed for neat diesel (D100), n-butanol/diesel blend (30% of butanol-by volume) for combustion and emission analysis. The results exhibited that with the reduction of IOC at intake, the HRR of diesel increased, while HRR of B30 first increased and then reduced. The NO_x emissions for both the fuels reduced, but slightly differed between them. The soot emission was very low for B30 compared to D100 under the same IOC. It was also observed from the study of chemical kinematics that the addition of butanol content causes a slowdown in the oxidation of n-heptane and toluene, because OH radicals were consumed.

Table 2.1. shows the detail summary of the literature on the use of butanol/diesel blends in CI engines.

1 Table 2.1. Summary of the literature on the use of butanol/diesel blends in CI engines.

Investigator	Type of Engine used	Type of used Fuel	Test conditions and variables	Performance and combustion	Emissions
Sahin and Asku [50]	RENAULT K9K 700 Four-cylinder, four stroke, turbocharged, WC, CRDI CI engine.	Addition of n-butanol (2%, 4%, and 6% -(v/v)- Bu2, Bu4 and Bu6) to diesel fuel.	Different loads and speeds	• Little increase in HRR, peak pressure rise and BSFC for all blends at all speeds compared to diesel fuel.	• Lower soot emissions for all the blends compared to diesel fuel. • NO_x emissions reduced for Bu2 and Bu4 whereas increased for Bu6 compared to diesel fuel.
Rakopoulos et al.[15]	Six-cylinder, four-stroke, turbocharged, HD DI diesel engine, Rated power: 177KW, CR: 18:1.	n-butanol (8%, and 16% (v/v)) (Bu8 and Bu16) in diesel fuel.	Different loads and speeds (1200 and 1500 rpm).	• Higher BSFC and BTE with the addition of butanol percentage.	• Lower NOx, lower soot, lower CO and higher UBHC with the addition of butanol to diesel fuel.
Karabektasans and Hosoz[16]	Single-cylinder, four stroke, DI-CI engine,	Addition of iso-butanol (5%, 10%, 15% and 20% (v/v))(IBu5, IBu10, IBu15, and IBu20) in diesel fuel	At different speeds (1200 and 2800 rpm).	• Increased BSFC from IBu5 to IBu20 blend. • BTE increased for IBu5 and IBu10 whereas decreased for IBu15 and IBu20 blends.	• Lower NOx and CO and higher UBHC for all butanol/diesel blends.
Dogan [17]	modified Single-cylinder, four-stroke naturally aspirated, HS, water-cooled DI CI engine	Addition of n-butanol (5%, 10%, 15% and 20% -(v/v)) (Bu5, Bu10, Bu15 and Bu20) to diesel fuel	Different loads at 2600 rpm	• Higher BTE and BSFC for all blends • Decreased exhaust gas temperature for all blends	• Less NOx, soot, CO and higher UBHC emission with the addition of butanol to diesel.
Siwale et al.[51]	Four-Cylinder, four-stroke, CI engine	Addition of n-butanol (5%, 10% and 20% -(v/v)- Bu5, Bu10 and Bu20) to diesel	Different loads and speeds	n/a	• Lower NOx, lower soot, lower CO and higher UBHC with the addition of butanol to diesel.

		fuel			
Ozsezen et al. [18]	Six-cylinder, four -stroke, turbocharged, HD, DI diesel engine.	Addition of iso-butanol (5%, 10%, 15% and 20% (v/v)) (IBu5, IBu10, IBu15, and IBu20) to diesel fuel	Different loads at 1400 rpm	• Lower BTE and higher BSFC for all blends. • Increased HRR and pressure rate with the addition of iso-butanol.	• Inferior NOx, soot, CO and higher UBHC emission with the addition of butanol to diesel fuel.
Rakopoulos et al. [52]	Single- cylinder, four stroke, HS, WC, DI-CI engine	n-butanol (8%, 16% and 24% (v/v) - Bu8, Bu16, Bu24) in diesel fuel	Three different loads, 2000 rpm, Standard injection timing.	• Higher BSFC and BTE with the addition of butanol percentage at all loads.	• Lower NOx, lower soot, lower CO and higher UBHC with the addition of butanol to diesel fuel.
Campos et al. [53]	Three-cylinder, four stroke, Water cooled DI CI engine. CR:18.5:1	n-butanol (10%, 15%, 20% 25% and 30% (v/v)-Bu10,Bu15, Bu20, Bu25 and Bu30) and Pentanol (10% 15%, 20% and 25% (v/v)-P10, P15, P20 and P25).	Different loads and speeds.	• Increased BTE for alcohol/diesel blends compared to diesel fuel. • Up to 30% of butanol and 25% of pentanol can be suitable for diesel engine without any modification.	n/a
Al-hasan et al. [20]	Single- cylinder, four stroke, HS, WC, DI-CI engine	Addition of iso-butanol (10%, 20% , 30% and 40% (v/v)) (IBu10, IBu20, IBu30, and IBu40) to diesel fuel	Different loads and speeds	• Iso-butanol content up to 30% showed better performance. • Air/fuel ratio and exhaust gas decreased for blends	n/a
Miers et al. [54]	Four-cylinder, four- stroke, CRDI, CI engine	n-butanol (20% and 40%-volume based (v/v)) (Bu20, Bu40) used in diesel fuel	Hot and cold start urban and highway drive cycle tests for 35mph and 55mph under	• Increased BSFC for blends under all conditions.	• NOx emission decreased for Bu20 and Bu40 under urban drive cycle whereas increased for highway drive cycle. • Lower soot, CO and higher UBHC for B20 and Bu40.

			steady-state test condition		
Lamani et al. [21]	Two-cylinder, four stroke, ware cooled, CRDI CI Engine	Addition of butanol (10%, 20%, and 30%(v/v)) (Bu10, Bu20, and Bu30) to diesel fuel	Different SOI (9°, 12°, 15°, and 18°)	• BTE was increased for all the blends. • Higher BTE for Bu00 is 38.4% at 12° BTDC, for Bu10, Bu20 and Bu30 are 40.1%9, 40.9%, and 41.7% at 15° BTDC, respectively.	• Less smoke, NO_x and CO emissions with increasing of butanol content.
Merola et al. [22]	Four-cylinder, four stroke, turbocharged, WC,CRDI CI engine	Addition of 20% (v/v) butanol (Bu20) in diesel fuel	Injection pressure (100 - 160 MPa) at 2500 rpm,	• Minor penalty of BSFC for blend.	• Butanol blend (Bu20) allowed to accomplish smoke less emission at lower IP (100 MPa) than diesel fuel (120 MPa).
Yao et al. [55]	Six-cylinder, inter cooled, heavy-duty (HD), turbocharged, CRDI, WC, CI engine.	n-butanol (5%, 10% and 15% (v/v) (Bu5, Bu10 and Bu15) in diesel fuel.	To maintain NO_x emission constant (2.0g/kWh) at BMEP 1.16MPa and 1840 rpm, used EGR rate and Multiple injection strategies.	• Less impact on BSFC with the addition of butanol content.	• Lower soot and CO emissions with increase of butanol percentage. • Larger soot reduction and higher CO emission with early pilot injection • Lower soot and CO emission with post-injection strategy. • Soot emission decreased for all injection strategy with increase in butanol content.
Liu et al. [23]	Four-cylinder turbocharged intercooler diesel engine	Addition of butanol content in diesel fuel.	Variation of injection timing: Single injection: (0 to -20 bTDC) and Pre-injection: (-25 to -75 bTDC).	• Under a single injection strategy, the addition of butanol increased the peak value of HRR, shortened the heat release rate and delayed the start of combustion. • Under the pre-injection strategy, the injection timing is earlier than -−25° CA ATDC, the pre-injection combustion phase exhibits bimodality and with increasing of butanol ratio,	• Under a single injection strategy, the GMD was reduced for Bu00 with early injection. But GMD was unchanged for Bu30 and Bu50. • Under the pre-injection condition, total number and mass of concentration of the particulates reduced with the addition of butanol and the GMD of the particles was reduced when the pre-injection timing was changed from 25 to 35° CA ATDC.

				the cold -flame reaction stage decreased and the whole stage of premixed combustion was delayed.	
Chen et al. [24]	1-Cylinder, Water cooled, CRDI DI CI engine with EGR system.	Addition of 40% butanol (Bu40) in diesel fuel.	Different EGR rates at 1400 rpm.	• Bu40 blend develops longer ignition delay and higher cylinder pressure.	• Lower soot and CO, but higher NO_x emission with the addition of butanol to diesel • For Bu40, with EGR rate, NO_x emission decreased and no impact on soot.
Huang et al. [25]	Four-cylinder, HS DI diesel engine.	Addition of 20% and 30% of butanol (Bu20 and Bu30) in diesel fuel.	Different Pilot injection timing and pilot injection mass under medium EGR (25%).	• Advancing the pilot injection timing, the cylinder peak pressure value decreases, but the MPRR rises. • Increasing the pilot injection fuel mass, peak in-cylinder pressure increased.	• Advancing the pilot injection timing, NO_x and soot emissions reduced. • Increasing the pilot injection fuel mass, NO_x emissions increases and soot emission decline at first and then increased.
Zheng et al. [56]	Four-cylinder, Four - stroke turbocharged DI diesel engine	Addition of gasoline (G30), n-butanol (Bu30), gasoline/n-butanol (DGB) in diesel fuel.	Two-stage injection strategies (pilot-main and main-post) with four different fuels under high EGR rate (46%).	• Adopting pilot injection near to main injection can effectively decrease the peak of premixed heat release rate and MPRR.	• Soot emissions reduce with the addition of gasoline or/ and butanol. • The soot emission increases first and then declines with the retard of post-injection timing. • With increasing of the pilot-main interval, NO_x emissions reduce first and then increase, whereas CO and THC emissions increase • With increasing of the main-post interval, NO_x emissions decrease whereas CO and THC emissions increase.
Huang et al. [57]	Four-cylinder, Four - stroke turbocharged, diesel engine	Addition of gasoline (D70G30), n-butanol (D70Bu30), gasoline/n-butanol (D70G15Bu15) in diesel fuel.	Four different fuels under varies EGR rates	• As the EGR ratio increased, the combustion pressure and HRR of D100 and D70Bu30 decreased, whereas the BSFC increased.	• As the EGR ratio increased up to 25%, the soot and CO emissions not significantly varied for the fuel blends.

Rajesh kumar et al. [58]	Kirloskar Single-Cylinder, DI-CI engine.	Addition of 30% of iso- butanol (ISB30) in diesel fuel.	At different loads	• ISB30 has higher pressure rise and longer ignition delay than diesel fuel	• For ISB30, NOx, CO and soot emissions reduced whereas the UBHC emissions increased.
Zheng et al. [59]	Four-cylinder, CRDI Turbocharged diesel engine.	Addition of 10% and 20% of butanol (nBu10 and nBu20) and iso- butanol (isoBu10 and isoBu20) in diesel fuel.	Conducted the experiments on LD and HD engines.	• Both alcohol blends show the same start of combustion and identical HRR. • Butanol exhibited good cold start performance in LD engine.	• Less soot formation for the both blends in both types of engines. • Alcohol blends showed much less soot than diesel fuel in both types of engines due to the higher oxygen content in the blends, but cause slightly increased NO_x formation.
Kumar and Pali [60]	Single-cylinder, Four stroke, water cooled diesel engine.	Addition of (5%, 10% and 20%) butanol in biodiesel.	At different loads.	• BTE was higher for all blends.	• For blends, soot, NOx and CO emissions reduced, whereas UBHC emissions raised slightly.
Zheng et al. [61]	Single-cylinder, Four stroke, water cooled diesel engine.	Addition of 20% of butanol (Bu20), ethanol (E20) and dimethylfuran (DMF20) in diesel fuel.	At different loads and 50% of EGR rate.	• Higher ITE for pure biodiesel and three fuel blends than diesel fuel, especially at high load and high EGR rates.	• Less smoke and higher NO_x emissions for Bu20 and DMF20. • Less HC and CO emissions for all the three blends at higher loads.
Wei et al. [62]	Four-cylinder, Four - stroke turbocharged DI diesel engine	Addition of gasoline (D70G30), n-butanol (D70Bu30), gasoline/n-butanol (D70G15Bu15) in diesel fuel.	Different engine load conditions with a constant speed of 1800 rpm	• Blends produced higher-pressure rise, longer ignition delay and shorter combustion duration than diesel fuel.	• CO emissions reduced, and NO_x and UBHC emissions slightly increased under medium and high engine load conditions for all the blends.
Nayyar et al. [26]	Single cylinder, Four - Stroke diesel engine equipped with a water cooled.	Addition of (10%, 15%, 20% and 25%) butanol (Bu10, Bu15, Bu20 and Bu25) in diesel fuel.	Different loads and parameters (CR, SOI and FIP)	• BSFC increases with the addition of butanol. • Bu20 blend exhibited better performance and lower emission at higher CR than the diesel fuel.	• With increasing of butanol content, soot and NO_x emissions were lower whereas UBHC emissions increased.

Lapuerta et al. [63]	Four-cylinder, four-stroke, turbocharged intercooler, CRDI diesel engine equipped EGR system.	Addition of 10%, 13%, 16% and 20% butanol (Bu10, Bu13, Bu16 and Bu20) in diesel fuel.	Varies loads	• No change in engine efficiency with the addition of butanol.	• The particulate emission reduced with the addition of butanol content up to 16% and then increased. • No variation in NO_x emission with the addition of butanol. • Higher CO and UBHC emissions for all blends.
Satsangi and Tiwari [19]	Single-cylinder, four stroke, naturally aspirated, DI-CI Genset engine	Addition of n-butanol (4.9%, 9.8%, 14.6% and 19.5% -(v/v)-Bu1, Bu2, Bu3 and Bu4) to diesel fuel	Different loads	• Butanol/diesel blend produced more pressure, HRR, and RoPR, more noise and vibrations as compared to diesel, especially at high engine load.	• Lower NO_x, lower soot, lower CO and higher UBHC with the addition of butanol to diesel.
Emiroglu and sen[64]	Single-cylinder, four stroke, air cooled, DI-CI Genset engine	n-butanol (10%(v/v)-Bu10), ethanol (10%-E10) and methanol (10%-M10) in diesel fuel	Different loads	• Cylinder pressures and HRR of the alcohol blends are higher than that of diesel. • Lower BTE, higher BSFC for alcohol than diesel fuel.	• Higher NO_x, lower values soot, UBHC and CO emissions for all the alcohols than diesel fuel.
Ahmed et al. [65]	Six- cylinder, four stroke, turbocharged DI- CI Diesel engine.	Addition of 5%, 15%, and 25% butanol (Bu5, Bu15, and Bu25) in diesel fuel.	Different engine speeds (1000 and 2000 rpm) at four different loads.	• BTE improved for the higher blend (Bu25).	• Less CO and NO_x emissions for all the blends. • The CO_2 and UBHC emissions for all the blends increased.
Maurya et al. [27]	Kirloskar TV1 single-cylinder, DI-CI engine.	Addition of 10%, 20%, and 30% butanol (Bu10, Bu20, and Bu30) in diesel fuel.	Compression ratios (16-18) and nozzle opening pressures (170-220 bar) at different engine loads. RSM analysis was used	n/a	• The total particle concentration decreased with increase in load and reduced with the addition of butanol content.

			for optimization.		
He et al. [28]	Modified single- cylinder, DI diesel engine.	Addition of 15% ethanol (E15) and 15%, and 40% butanol (Bu15, and Bu40) in diesel fuel.	Combination alcohol additive and EGR rate.	• With the addition of alcohol and EGR rate, the peak heat release rate in the premixed increased. • ITE increased with the addition of alcohol but it reduced with EGR.	• Total particle number concentration (TPNC) decreased with the addition of alcohol, but it increased with EGR rate. • Higher alcohol and medium EGR showed lower TPNC.
Fayad [29]	Single-cylinder, DI-CI engine.	Addition of 20% of butanol content (Bu20) in diesel fuel.	Different fuel injection strategy (SOI and FIP)	• Higher FIP and advanced SOI improved the performance for butanol/diesel blends.	• The Combination of 20% of butanol/diesel and advanced SOI can be improved the performance and reduced the harmful gases.
Emiroglu [30]	Single-cylinder, DI-CI engine.	Addition of 10% of butanol content (Bu10) in diesel fuel.	Different FIP	• Higher BTE and BSFC for butanol/diesel blend at all FIP. • With increases in FIP, the Maximum cylinder pressure and HRR increased.	• With increases in FIP, NOx emission increased while soot emission decreased for butanol/diesel blends.
Saravanan et al. [31]	Single cylinder, Four - Stroke, DI diesel engine.	40% of iso-butanol (IBu40) in diesel fuel.	Optimization of parameters (FIP, SOI and EGR) using the RSM approach.	• At 240bar, 23°CA bTDC and 30% EGR rate was predicted to be optimum for this particular engine.	
Nayyar et al. [32]	Single cylinder, Four - Stroke, DI diesel engine.	Addition of 10%, 15%, 20% and 25% butanol (B10, B15, B20 and B25) in diesel fuel.	Different blending ratio and operating parameters (CR, SOI and FIP)	• At higher CR of 19.5, B20 blend showed better performance and lower soot emissions. • The optimum condition for diesel case is a CR of 18.5, SOI of 23 °CA bTDC and FIP of 210 bar. • The optimum condition for Bu20 case is CR of 19.5, SOI of 23 °CA bTDC and FIP of	• For B20, soot (59.56%) and NO_x (15.96%) reduced at full load compared to diesel.

				210 bar.	
Zhang et al. [34]	Single-Cylinder, DI CI engine,	Addition of 10% and 20% of butanol (Bu10 and Bu20) and pentanol (P10 and P20) in diesel fuel.	Three different engine loads at constant engine speed.	• Marginally varied the BSFC and BTE for both blends	• Reduces the particulate mass, EC and total counts of volatile particles for both blends • Butanol blends reduce the EC formation and a higher emission reduction in solid and volatile particles than pentanol blends. • Both blended fuels reduce the organic carbons (OC).
Zhang et al. [35]	Single-cylinder, naturally aspirated, CRDI, WC CI engine with, EGR system.	Addition of 5, 10, 15 and 20% of butanol in diesel fuel.	Different loads	n/a	• Increases in butanol content in blends polycyclic aromatic hydrocarbon (PAHs) increased. • Addition of butanol content in diesel fuel reduced the EC and increased the OC.
Choi et al.[66]	Four Cylinder, four-stroke, turbocharged, CRDI CI engine with cooled EGR system	Addition of n-butanol (5%, 10%, and 15% -(v/v)- Bu5, Bu10 and Bu15) to diesel fuel	Different European Stationary Cycle (ESC) test	n/a	• NO_x emissions reduced at low load and increased at higher load with addition of butanol content. • The total mass of PM reduced for all blends. • Higher formaldehyde and THC emission for all blends at lower load • Lower formaldehyde emission and higher PAH for all blend at higher load •
Lopez et al. [67]	Four-cylinder, Four - stroke turbocharged DI diesel engine	Addition of 10% of hydrous ethanol (HE10) and n-butanol fumigation (nBu10) in diesel fuel	At different loads	• Both blends produce higher premixed combustion peaks, faster combustion rate, and lower in-cylinder temperature. • BTE and BSFC are better for butanol blends than hydrous ethanol.	• Both alcohols reduce the soot and NO_x emissions and increase the THC and CO emissions. • Butanol fumigation showed the best trade-off (PM vs NO_x + THC) among all the fuels tested.
Valentino et al. [68]	Four-Cylinder, turbocharged, Water-cooled,	Addition of 40% butanol (Bu40) and 40% of	Different SOI and FIP	• Higher ignition delay for blends.	• Lower NO_x emission at moderate intake oxygen content and injection pressure (100-

	CRDI CI engine.	gasoline (G40) in diesel fuel.		• Higher BTE for Bu40 than G40. • Lower combustion noise for B40 and G40 with late injection timing	120MPa) for Bu40 and G40. • Better controlling of FIP, SOI and O2 at intake can achieve the LTC operation.
Valentino et al. [41]	Four-cylinder, turbocharged CRDI DI diesel engine.	Addition of 20% and 40% butanol in diesel (Bu20 and Bu40).	Direct injection of both the blends. EGR rate in terms of oxygen reduction (19% to 19.5%)	BSFC increased for all the blends with EGR rate.	• Early start of injection and low injection pressure can achieve the LTC operation.
Gu et al. [43]	Six- Cylinder, four stroke, CRDI CI engine equipped with cooled EGR system,	Addition of n-butanol (15% and 30% -(v/v) Bu15 and Bu30) and iso-butanol (15% and 30% (v/v)-IBu15 and IBu30) in diesel fuel	Different loads, injection timing and EGR rates at a constant speed (1000 rpm).	• Longer ignition delay for butanol/diesel blend than iso-butanol/diesel blend • BSFC was constant at a low EGR rate and decreased at the late injection timing	• Lower soot emission for butanol/diesel blend than iso-butanol/diesel blend • NOx emissions were constant at low EGR rate and decreased at high EGR rate and late injection timing. • Soot emissions were constant at low EGR rate and increased at high EGR rate and late injection timing. • CO emissions were increased at low EGR rate and constant at high EGR rate • Combination of lower EGR rate and late SOI and butanol can enable the LTC mode and lower NOx and soot emission.
Lannuzzi et al. [69]	Four-cylinder, 4 valve, DI diesel engine	Addition of 20% of butanol in diesel fuel.	Different injection strategies under two oxygen concentrations	• Higher BSFC for all the blends under all injection strategies.	• Butanol/diesel blends produced lower UBHC emission than the gasoline/diesel blends at any injection strategy.
Yang et al. [44]	Single-cylinder, four stroke, CRDI DI diesel engine.	Addition of 10%, 20% and 30% of butanol in gasoline fuel.	EGR rate (0-45%)	BSFC increased for all the blends with EGR rate.	• Addition content in blends reduced the soot emission. • Higher percentage of butanol causes release of higher content of primary individual hydrocarbons.
Rajesh and Saravanan [47]	Single-cylinder, four strokes, VCR DI diesel	Addition of iso-butanol content (0-40%) in diesel	Direct injection. EGR rate (30%) and Injection		• Higher percentage of iso-butanol/diesel required higher EGR rate to accomplish simultaneously reduction of NOx and soot

	engine.	fuel.	timing (21 and 23° bTDC)		emission.
Zhu et al. [49]	Four-cylinder, CRDI DI diesel engine.	30% butanol+70% diesel (B30)	Direct injection, Different intake oxygen concentrations (IOC).	With decrease in the IOC, the maximum HRR of D100 increased, while the maximum HRR of B30 first increased and then decreased.	• At the same IOC, NO_x and soot emissions reduced with the addition of butanol.

2.4. Observations from the literature review

- Experimental studies were carried out on the use butanol fuel up to 40% (v/v) (by blending with diesel fuel) in the conventional CI engines. But, the effects on the performance and emissions were not clearly established.
- The effect of varying the individual operating parameters such as CR, FIP, SOI and EGR were studied with the specific objective of decreasing NOx emissions or soot emissions. But simultaneous reduction of emissions without compromising the performance was not thoroughly studied.
- There are inconsistent conclusions on the effect of butanol on brake thermal efficiency. However, most of the researchers concluded that with an increase in butanol fraction in the butanol/diesel blend, BTE slightly increased due to higher burning velocity and a wider fraction of fuel burning.

2.5. Gaps observed from the literature review

It is noticed from the literature review that the following areas were not much focused on:

- Less work is available on the utilization of higher content of butanol in butanol/diesel blends in the DI-CI engine and its effect on the performance and emission characteristics.
- Little work has been carried out on DI-CI engine fuelled with butanol-diesel blends as a fuel to achieve HCCI mode.
- Limited work has been carried out for achieving mixture homogeneity of DI-CI engine fuelled with butanol/diesel blends by simultaneously varying different operating parameters (CR, FIP, SOI and EGR).
- Limited work has been carried out for achieving better performance of DI- CI engine using parametric optimization of the engine operating variables.
- Interaction effects of the engine operating parameters on the performance and emission characteristics of CI engine has not been thoroughly studied.

2.6. Objectives

Based on the literature review and gaps observed, the following objectives were chosen:

- To analyze numerically the effect of different operating parameters such as CR, EGR, FIP and SOI on the performance and emission characteristics of a CI engine operated with butanol/diesel blends (Bu00, Bu20, Bu30 and Bu40).
- To identify the optimum values of the operating parameters for HCCI mode of operation using RSM technology.
- To study experimentally the performance and emissions characteristics of a DI-CI engine with different butanol/diesel blends (Bu00, Bu20, Bu30 and Bu40).
- To study experimentally the performance and emissions characteristics of a DI-CI engine with different butanol/diesel blends (Bu00, Bu20 and Bu40) by varying the CR, FIP and EGR.

Chapter 3

Research Methodology

This chapter describes the methodology adopted for the experimental as well as the numerical studies of a DI-CI engine. The procedure to prepare the butanol/diesel blends and properties of the blends are explained. This chapter also discusses the experimental set-up and the experimental procedure. The mathematical modelling of the DI-CI engine, different physical, chemical, combustion models, reaction mechanisms and grid independency test have been discussed in this chapter. This chapter also includes a detailed procedure to execute CONVERGE CFD software based simulation and presents a detailed flow chart of the research work.

3.1. Experimental methodology

Experiments were conducted to evaluate the performance of a DI- CI engine with diesel and butanol/diesel blends. The influence of the engine operating parameters for such as EGR, FIP and CR on the performance characteristics of the engine fuelled with butanol/diesel blends were experimentally studied. The present chapter discusses the methodology adopted in determining the properties of butanol/diesel blends. Experiments were carried out on a variable compression ratio (VCR) engine. The results of these experimental studies mentioned above are presented in chapter 4. The experimental results were then used for validating the numerical studies carried out as part of the present thesis work.

3.1.1 Materials and methods

As mentioned in chapter 2 dealing with the literature survey, n-butanol was chosen as a potential fuel substitute for diesel in the CI engine. Experiments were performed with

butanol/diesel blends. The preparation of butanol/diesel blends and the determination of some of the properties of these fuels are described in this section.

3.1.1.1. Test fuel preparation

n-butanol is a 4-carbon structure straight chain alcohol (C_4H_9OH). It was purchased from a local retailer at Warangal. Similarly, diesel fuel was also bought from a local supplier. Butanol and diesel blends were prepared using a homogenizer. Three blends, 20%, 30% and 40% by volume of butanol in the blends, designated as Bu20, Bu30 and Bu40 respectively, were prepared. The details of the homogenizer and method of preparation of the blends are presented in Appendix A.

3.1.1.2. Measurement of the properties of test fuels

Experiments were carried out to measure some of the properties of the test fuels. The density, viscosity and calorific value of the test fuels were measured with the facilities available in the department. The density of the test fuels was measured using hydrometer. The viscosity was measured using Redwood viscometer. Bomb calorimeter was used to determine the calorific values of test fuels. The details of the equipment used and the test procedures are presented in Appendix A for the test fuels. From the properties of the test fuels, the stoichiometric ratio and percentage of oxygen available in the test fuels were estimated. The detailed calculations are presented in Appendix A. The properties of the test fuels are presented in Table 3.1.

Table 3.1. Properties of diesel, butanol and butanol/diesel blends.

Properties	**Diesel**	**Butanol**	**Bu20**	**Bu40**
Density (kg/m^3) (40 ^0C)	820	800	813	807
Viscosity (mm^2/s) (40 ^0C)	2.82	2.22	2.7	2.57
Calorific Values (MJ/kg)	43.50	33.10	41.58	40.21

It is observed from the table that with increase in the percentage volume amount of butanol in the butanol/diesel blend, the viscosity of the blend decreases. It is desirable that the viscosity of the CI engine fuel should be as small as possible. Smaller viscosity facilitates better atomization of the fuel in the combustion chamber during fuel injection. This also aids in complete combustion resulting in higher performance of the engine. However, lower

viscosity of the fuels may result in more wear and tear of the fuel injection system components. It can also be observed from the table that with an increase of butanol fraction in the blend, the density of the blend decreases. The calorific value of the blend also decreases with increase in the butanol fraction in the blends as shown in the table. This decrease in the calorific value, combined with decrease in the density of the blends may affect the amount of heat supplied to the engine. For a given engine and fuel injection system, less mass of the fuel will be supplied, and this in turn releases less heat. This may result in a small derating of the engine, i.e., decrease in the power output of the engine, unless it is compensated by better combustion and performance**.**

3.1.2. Experimental set-up of the VCR engine test rig

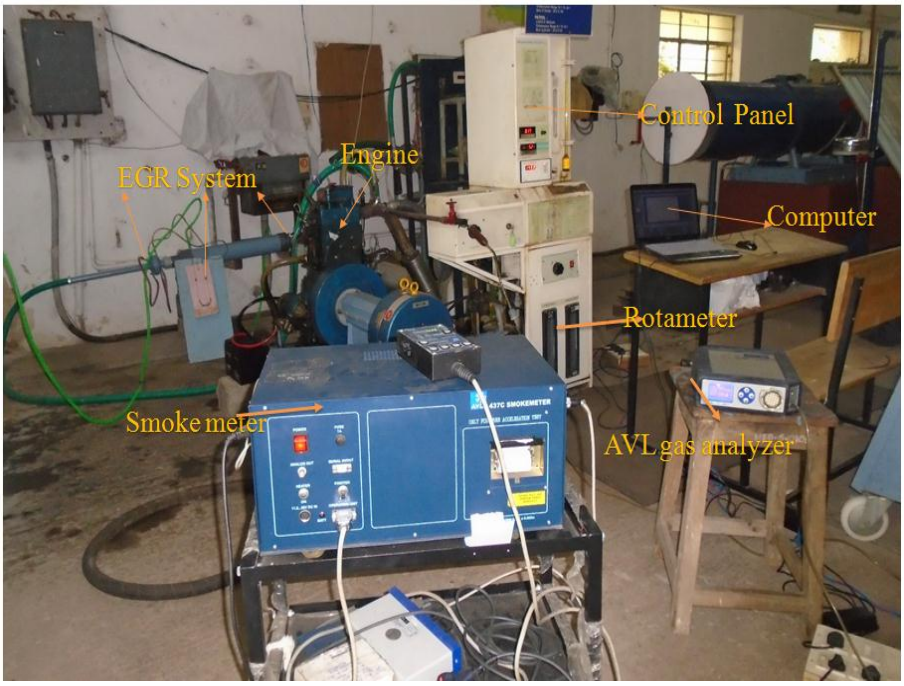

Fig. 3.1. Engine experimental set-up of the VCR engine test rig.

Experiments were conducted on a standard VCR engine to evaluate the influence of butanol/diesel blends as fuel on the performance, combustion and emission characteristics. Figure 3.1 shows the layout of the experimental set-up. The detailed specifications of the VCR engine set-up are shown in Table 3.2. Provision exists in the engine set-up to vary the compression ratio (CR) and fuel injection pressure (FIP). An additional set-up has been fabricated and attached to the engine set-up for enabling exhaust gas recirculation. The details

of the experimental set-up are presented in Appendix A. The detailed procedure and equations used to determine the EGR rate are presented in Appendix A.

Table 3.2. Detailed engine specifications.

Name of the description	Details/value
Engine type	4-Stroke, vertical, water-cooled, Direct Injection
Make and Model	Kirloskar-TV1
No. of cylinders	Single cylinder
Stroke (m)	0.110
Bore (m)	0.0875
Connecting rod length (m)	0.234
Rated speed (rpm)	1500
Rated power (kW)	3.5
Compression ratio range	12:1 to 18:1
Number of injection holes and diameter (m)	3 and 0.000255
Fuel injection timing variation	17 to 29° bTDC
Nozzle injection pressure (bar)	220
Fuel used	Diesel and butanol/diesel blends
Type of Combustion Chamber	Hemispherical combustion chamber
Loading type	Eddy current dynamometer
Dynamometer arm length (mm)	185

Experiments were conducted in two phases. In the first phase, experiments were conducted on the VCR engine with baseline configuration: CR of 17.5, FIP of 220 bar, SOI of 23^{o} CA bTDC and EGR of 0%, using different test fuels (Bu00, Bu20, Bu30 and Bu40). In the second phase, experiments were conducted to evaluate the influence of three different engine parameters, viz., EGR, CR and FIP on the characteristics of the CI engine fuelled with diesel and different butanol/diesel blends. Experiments were conducted by varying the exhaust gas recirculation (EGR of 0%, 10%, 20% and 30%), compression ratio (CR of 14:1, 15:1, 16:1, 17.5:1 and 18:1) and fuel injection pressure (FIP of 200 bar, 220 bar, 240 bar, 260 bar and 280 bar). Thus, a total of 36 tests were conducted. Each of these tests was repeated at least 3 times for ensuring consistency in the results. In each of these tests, constant speed

(1500 rpm) was maintained. In each of these tests, the load was varied from "No load" to "rated load" in five steps. The combustion characteristics were evaluated in terms of the in-cylinder pressure, neat heat release (NHR), ignitron delay (ID), combustion duration (CD) and rate of pressure rise (RoPR). The performance characteristics were evaluated in terms of specific energy consumption and brake thermal efficiency. Similarly, the emission characteristics were determined by measuring the NOx, soot, UBHC and CO emissions in the engine exhaust gas. The model calculations and the uncertainty analysis are presented in Appendix A.

3.2. Simulation Studies

Simulation analysis were carried out using CONVERGE CFD software to study the influence of different engine parameters such as FIP, CR, EGR and SOI on the performance and emission characteristics of a DI-CI engine operated with different butanol-diesel blends (Bu00, Bu20, Bu30 and Bu40). A design matrix was developed by using Design expert software. A total set of 29 simulation experiments were run in the present study for each one of these four fuels. In the next step, optimum set values of these four input parameters were found with an objective of minimization of the output response factors, viz., ISFC, soot and NOx. Finally, confirmation test was carried with the optimum set values. Similarly, the mixture homogeneity was also estimated.

3.2.1. Description of CONVERGE software

CONVERGE is an innovative CFD code which can eliminate grid generation issues in the simulation. It can solve both the classic steady state assumption problem and even transient state problems in fluid flow, which is difficult to solve using the standard methods. It can solve both compressible and incompressible flow problems without encountering any issues. The unique thing about CONVERGE is that it can easily solve fluid flow problems with various chemical species. The requirement for solving problems which involve different chemical species is to import the chemical reaction mechanism and the thermodynamic property data of the specific chemical species. Thus, it is a very attractive solution to the problems involving different chemical species such as air-fuel mixture and the blends of different fuels along with petrol or diesel in an engine simulated environment. The nature of complexity of CONVERGE software is further alleviated as it can deal with not only stationary surfaces but also model the moving surfaces. Engine simulations are dynamic in nature due to the movement of the piston inside the engine cylinder. Since CONVERGE can

model the moving piston inside the cylinder, the computational results are far more accurate than any other CFD software product. Secondly, CONVERGE is not restricted to simple geometry problems. Very complex and intricate geometries can be modelled in CAD (Computer Aided Design) software packages such as SOLIDWORKS or CREO and imported into the CONVERGE software for performing simulations.

The simulation model used in the present analysis included different combustion, physical and chemical models as shown in Table 3.3. Spray modelling includes the following sub-models: spray wall interaction, spray atomization, vaporisation, collision, breakup and turbulent dispersion. A KH–RT model [70] represented spray atomization and breakup. Discrete multi-component vaporisation model [71] was used to model the vaporisation process. Turbulence was modelled using RNG k-ε model. The SAGE combustion model was also incorporated in the CONVERGE CFD code. In addition, Zeldovich mechanism and Hiroyasu-NSC model were employed in the simulation analysis to compute NOx and soot formation, respectively [72]. In addition, conservation equations, transport of passive scalars, species and turbulence are also incorporated to simulate the IC engine combustion phenomena. The details are presented in Appendix B.

Table 3.3. Details of numerical models used for simulation.

Spray model	KH-RT model
Combustion model	SAGE
Vaporisation model	Multi-component vaporisation model
Turbulence model	RNG k-ε model
NOx model	Zeldovich mechanism
Soot model	Hiroyasu-NSC model

3.2.2. Preparation of the engine geometry surface

Before running the engine simulations, it is required to generate the surface of the engine model. The ‘make_surface’ utility inbuilt in the CONVERGE software was used for developing the engine surface for running the simulations in this project. In the present analysis, HCC geometry (Hemispherical Combustion Chamber) was considered. HCC curve profile points were obtained from CREO CAD software using 2D sketching. The combustion chamber of an internal combustion engine consists of a piston bowl, cylinder head and cylinder wall. To make the surface using ‘make_surface’ utility, two files are required: Bowl profile and Head profile. Bowl profile consists of the coordinate points of the piston bowl

curve. Head profile contains the data points of the straight line starting from the origin up to the last point. Using these two files with 'make_surface' command, the run was developed for the engine geometry.

3.2.3. Engine geometry, boundary and initial conditions

Figure 3.2 shows the engine computational model. The model consists of a piston bowl, a piston head and one injector (three nozzle holes). The Computational domain has around 300,000 cells.

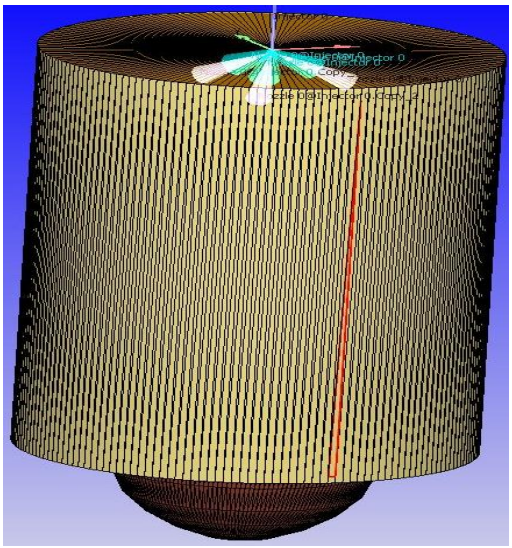

Fig. 3.2. Computational domain of the VCR engine.

Table 3.4. Boundary and initial conditions.

Initial Conditions	
Inlet air pressure (kPa)	101
Inlet air temperature (K)	300
Temperature boundary conditions (Law of Wall)	
Material	Aluminium
Head temperature (K)	475
Piston wall temperature (K)	500
Cylinder wall temperature (K)	450
Velocity boundary conditions	
Head	Stationary
Piston wall	Translating
Cylinder wall	Stationary

Turbulence kinetic energy (tke) boundary conditions	
Cylinder wall, Piston wall and Head	Zero normal gradient
Turbulent dissipation (td) boundary conditions	
Cylinder wall, Piston wall and Head	Wall model

The initial conditions and boundary conditions are tabulated in Table 3.4. Total Kinetic Energy is given by $\kappa = 3/2*(UI)^2$, where U is the velocity and I is the initial turbulence intensity. Turbulent dissipation is given by $\varepsilon=C_{\mu}^{3/4}\kappa^{3/2}le^{-1}$ where, ε is the turbulent dissipation, C_{μ} is a model constant, κ is the turbulent kinetic energy and le is the length scale.

3.2.4. Grid independence test

Grid independence test was carried out to find the optimum grid size. In the present work, three different grid sizes were considered, viz., 1 mm, 1.4 mm and 2 mm. Figure 3.3 depicts the influence of grid size on the pressure-crank angle variation. From the figure it is observed that for decreasing the grid size from 2 mm to 1.4 mm, there is some improvement, but decreasing the grid size further to 1mm, there is very little improvement. The computational time increased for 1mm grid size by 30% and 58.4% respectively as compared to 1.4 mm and 2 mm grids. Therefore, a grid size of 1.4 mm was considered in all the simulation studies.

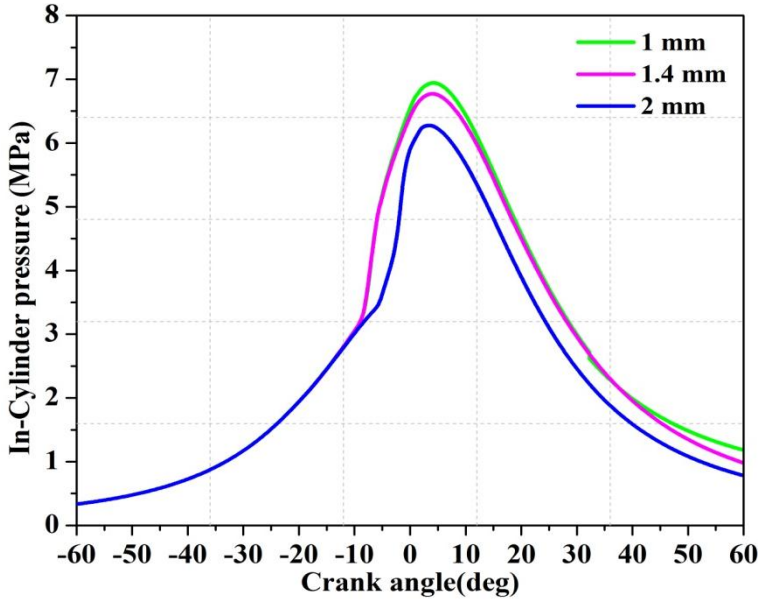

Fig. 3.3. Grid independent test for different grid sizes.

3.2.5. Response surface methodology (RSM)

RSM is a mathematical and statistical method, useful to obtain the relation between input parameters and output responses, with an objective of minimization or maximization of the output response values. In the present study, four input parameters viz., CR, FIP, SOI and EGR, and three output responses, viz., ISFC, soot and NOx were considered. Design matrix was developed by using Box-Behnken method, for numerical analysis. In this method, each variable was maintained at 3 equal intervals. Since there are 4 variables and 5 centre points, there were a total of 29 experiments. A total set of 29 experiments were run using CONVERGE CFD software. Different steps in the method are depicted in figure 3.4.

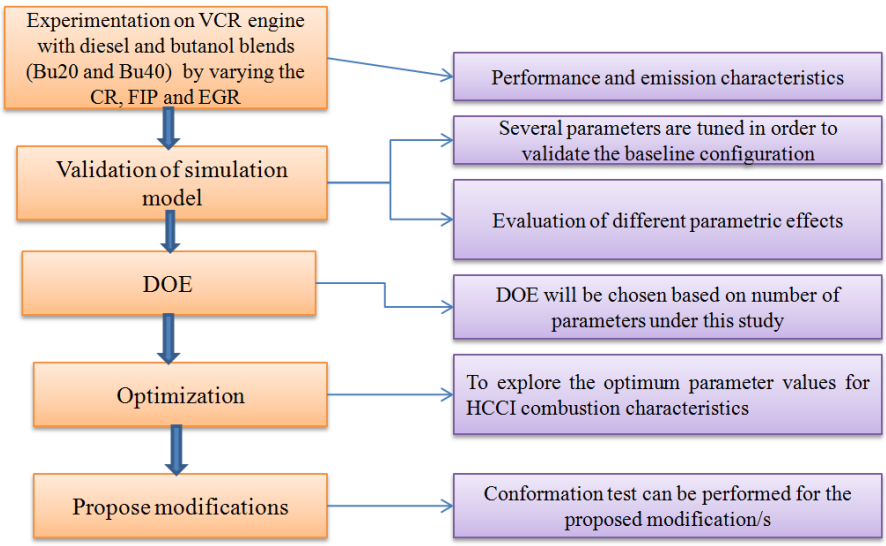

Fig. 3.4. Flow chart of methodology for research work.

3.2.6. Estimation of mixture homogeneity of air-fuel

Homogeneity of the air-fuel mixture inside the engine cylinder was estimated based on the Fuel Distribution Index (FDI). The fuel distribution index is defined as the ratio of mass of evaporated fuel in the combustion chamber to the total mass of fuel injected in the combustion chamber. The fuel distribution index was expressed in terms of target, rich and lean conditions [73]. The practical target equivalence ratio (Φ) range was considered from 0.3 to 1.2 [74]. The homogeneity of the mixture was expressed in the range of 0 to 1. The Fuel Distribution Index formulae are shown in equations (3.1) to (3.3)

$$M_F = \sum (M_{FL} + MF_{FT} + M_{FR}) \tag{3.1}$$

$$LFDI = \frac{M_{FL}}{M_F}$$

$$TFDI = \frac{M_{FT}}{M_F} \quad (3.2)$$

$$RFDI = \frac{M_{RT}}{M_F}$$

$$LFDI+TFDI+RFDI=1 \quad (3.3)$$

Where, LFDI refers to Lean fuel distribution index, TFDI refers to Target fuel distribution index, RFDI refers to Rich fuel distribution index, M_F is the total amount of fuel injected inside the combustion chamber, M_{FL} is the amount of fuel available in the lean mixture zone (Φ <0.3), M_{FR} is the amount of fuel available in the rich mixture zone (Φ >1.2), M_{FT} is the amount of fuel available in the target mixture zone (Φ - 0.3 to 1.2).

Summary

This chapter described the methodology adopted for both experimental studies and numerical analysis. CONVERGE was used for engine simulations. RSM was employed for design of experiments in all the four cases. The methodology for estimating the mixture homogeneity of air-fuel was also discussed.

Chapter 4

Experimental Studies - Results and Discussion

Experimental studies on the performance and emission characteristics of a DI-CI engine operated with butanol/diesel blends

The objective of the present work is to substitute a fossil fuel (diesel) with renewable fuel (butanol) to the maximum extent possible with minimum modifications to the existing engine. In pursuit of this objective, experiments were conducted on a conventional CI engine (VCR engine) using different test fuels (Bu00, Bu20, Bu30 and Bu40) of baseline configuration (CR: 17.5; FIP: 220 bar; EGR: 0%; and SOI: 23^{o} CA bTDC). Experiments were also performed by varying different operating parameters such as EGR, FIP and CR using these butanol/diesel blends as the fuel. The performance, combustion and emission characteristics of the engine are evaluated. The details are discussed here.

4.1. Experimental studies on the combustion, performance and emission characteristics of a CI engine operated with different butanol/diesel blends

Experiments were conducted on a conventional CI engine (VCR engine) using different test fuels (Bu00, Bu20, Bu30 and Bu40) with the baseline configuration of the engine (CR: 17.5; FIP: 220 bar; EGR: 0%; and SOI: 23^{o} CA bTDC). In each one of these tests, constant speed (1500 rpm) performance test was carried out. The performance and emission characteristics were analysed. The peak in-cylinder pressure, net heat release (NHR), exhaust gas temperature (EGT), rate of pressure rise (RoPR), ignition delay (ID), combustion duration (CD), brake specific energy consumption (BSEC), brake thermal efficiency (BTE) , NOx, soot, unburned hydrocarbons (UBHC) and carbon monoxide (CO) were compared for diesel and butanol/diesel blends at different loads.

4.1.1. Combustion and performance characteristics for butanol/diesel blends

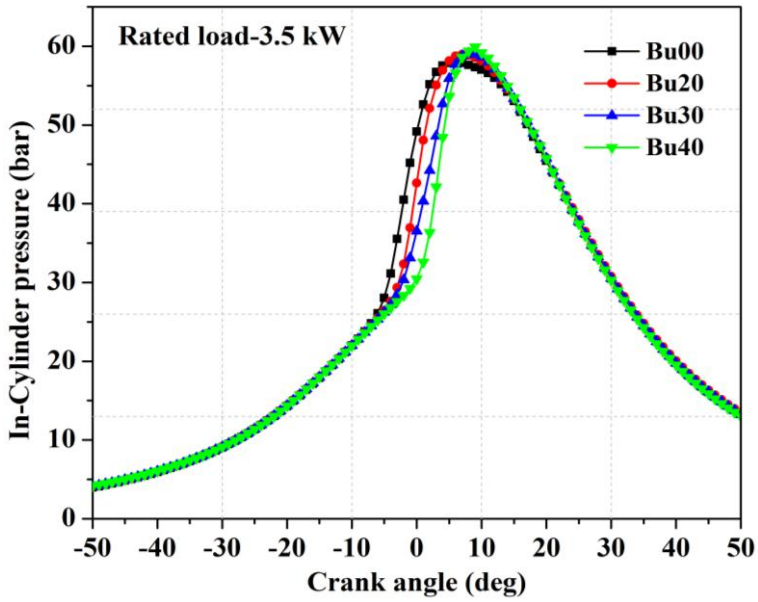

Fig. 4.1. Variation of in-cylinder pressure with crank angle for different butanol/diesel blends at rated load.

Figure 4.1 shows the variation of in-cylinder pressure with crank angle for different butanol/diesel blends. It is observed from the figure that increase of butanol fraction in the blend from 0% to 40% increased the peak in-cylinder pressure marginally compared to diesel fuel (Bu00) operation. The in-cylinder pressure increased by 1.72%, 1.96%, and 3.28% for Bu20, Bu30 and Bu40 respectively compared to diesel fuel operation. Similarly, it can be seen from figure 4.2 that butanol/diesel blends developed higher NHR compared to diesel fuel. The peak NHR increased by 9.24%, 13.43% and 15% for Bu20, Bu30 and Bu40 respectively compared to diesel fuel operation. It can also be observed from figure 4.2 that the NHR in the premixed combustion zone raised significantly with increase in butanol content in the blends. These trends can be explained taking into consideration the properties of butanol, diesel and butanol/diesel blends. Butanol has a lower cetane number of 25, compared to 52 for diesel. Thus, with increase of butanol content in the blend, the cetane number (CN) of the blend reduces proportionately. The reduction in the CN manifested in the form of increase in the ignition delay (ID) period from 18.76 to 20.5 deg CA, as seen in figure 4.2. In a way, the longer ID period results in better mixing of air and fuel, which leads to better combustion. As a result, the peak in-cylinder pressure and NHR increases. Similar results were obtained by Chen et al. [14].

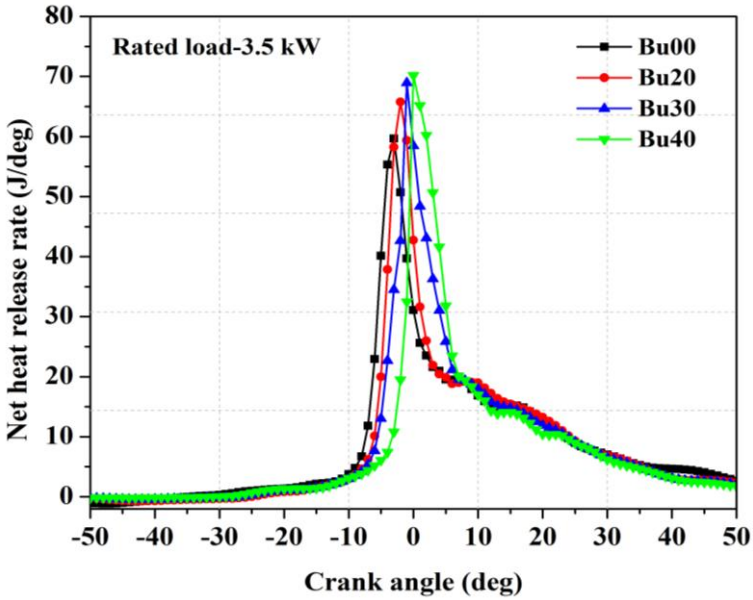

Fig. 4.2. Variation of NHR with crank angle for different butanol/diesel blends at rated load.

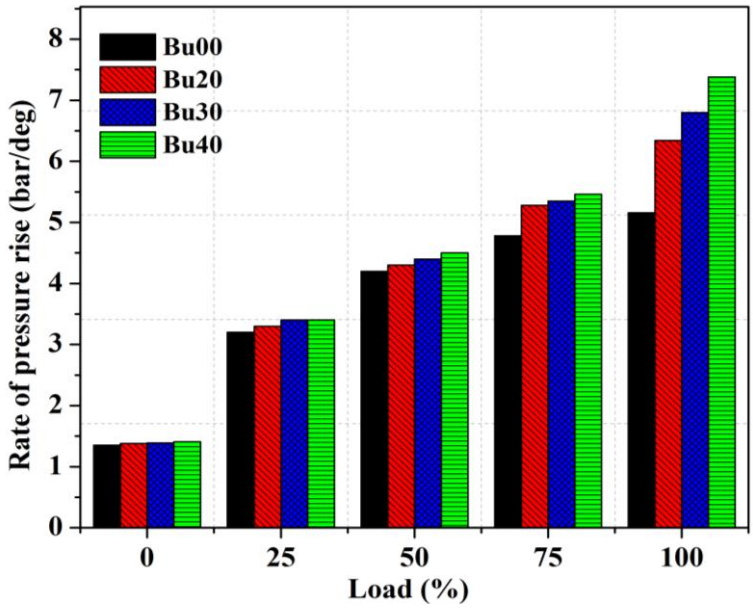

Fig. 4.3. Comparison of rate of pressure rise for different butanol/diesel blends at different loads.

Figure 4.3 depicts the rate of pressure rise (RoPR) for different butanol/diesel blends under different loads. RoPR represents the combustion noise of the engine. A value beyond 8 bar/deg CA (crank angle) is generally not desirable for CI engine [75]. It is observed from the figures that with the increase of butanol content in the blends, the RoPR increased. The RoPR values are 5.16 bar/deg, 6.34 bar/deg, 6.8 bar/deg and 7.38 bar/deg for Bu00, Bu20, Bu30 and Bu40 respectively, at the rated load conditions. The reason may be that butanol blends have lower cetane number, which leads to longer ignition delay; as a result of which,

more fuel gets accumulated in the premixed zone. The large amount of accumulated fuel causes intense heat release and hence higher RoPR. From the literature also [38] it is observed that butanol/diesel blends result in higher RoPR. These results also help in determining the maximum amount of butanol fraction in the butanol/diesel blends, which can be used in the existing CI engines without major modifications to the engine. Based on these results of RoPR, Bu40 is considered as the upper limit in the present work.

Figure 4.4 shows a comparison of ignition delay for different butanol/diesel blends under different loads. Ignition delay (ID) is generally defined as the time duration expressed in terms of the crank angle (CA) between the start of injection (SOI) to the start of combustion (SOC) of fuel. In this study, ID is considered as the crank angle between the start of fuel injection to 10% of mass fraction burned, MFB10. The ID increased with increase in the butanol content in the blend. Butanol has higher LHE and lower CN compared to diesel fuel. As a result, it absorbs more heat energy from the cylinder wall, prolongs the ignition delay and delays the SOC. The ID values are 18.76, 19.46, 19.98 and 20.5 deg CA for Bu00, Bu20, Bu30 and Bu40 respectively, at the rated load.

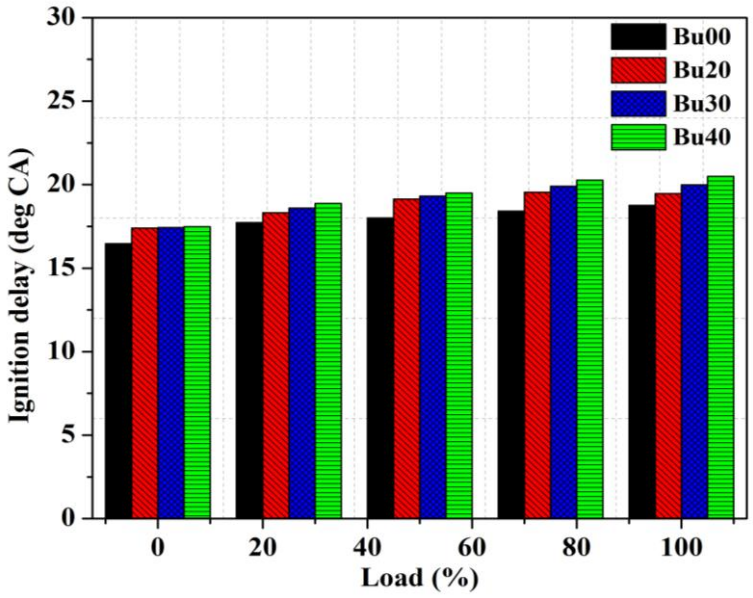

Fig. 4.4. Comparison of ignition delay for different butanol/diesel blends under at different loads.

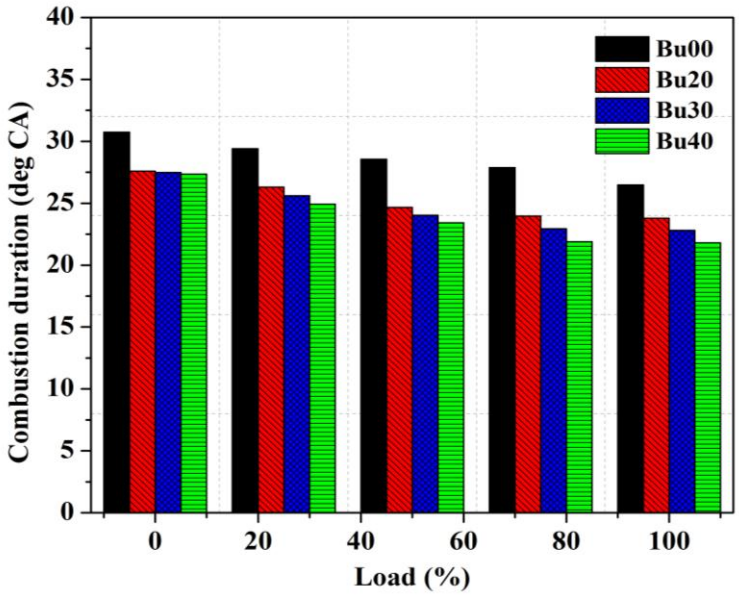

Fig. 4.5. Comparison of combustion duration for different butanol/diesel blends under different loads.

The comparison of combustion duration (CD) for butanol/diesel blends under different loads is shown in figure 4.5. The CD is the time duration expressed in terms of the crank angle between the start of combustion (SOC) and the end of combustion (EOC). In the present study, the CD is considered as the crank angle interval of MFB10 (10% of mass fraction burned) to MFB90 (90% of mass fraction burned). In general, EOC is tough to identify because of incomplete combustion and loss of heat in the combustion chamber due to crevices [76]. It is observed from the figure that the CD reduced with increase of butanol fraction in the blends. This is because butanol has lower cetane number and higher latent heat of evaporation compared to diesel, which leads to longer ignition delay and as a consequence, more fuel accumulating in the premixed zone. This fuel burns rapidly in the premixed zone and less fuel burns in the diffusion zone. Hence, the CD reduced with increase of butanol content in the blends. The CD values are 26.47, 23.8, 22.8 and 21.8 deg CA for Bu00, Bu20, Bu30 and Bu40 respectively, at the rated load. Similar results were observed for alcohol-based fuels in the literature also [77].

Figure 4.6 depicts the variation of EGT for different butanol/diesel blends. It can be observed from the figure that at any load on the engine, the EGT reduces with increase of butanol content in the blends. The EGT values are 327 ^{0}C, 320 ^{0}C, 314 ^{0}C and 310 ^{0}C for Bu00, Bu20, Bu30 and Bu40, respectively at the rated load condition. The main factors causing an impact on the EGT are the energy content of the fuel, latent heat of evaporation (LHE) and oxygen content in molecular structure. Although butanol/diesel blends have

higher molecular oxygen content, which gives rise to higher combustion temperature, the higher value of LHE of butanol blends has more dominant effect than the molecular oxygen content. This results in a decrease in-cylinder temperature and as a result, lowers the exhaust temperature. Similar trends are observed in the literature also [52]**.**

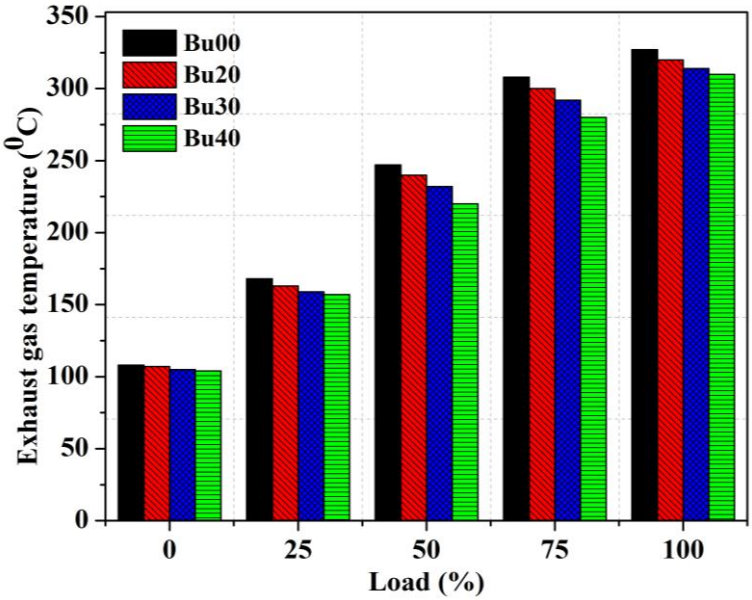

Fig. 4.6. Variation of EGT for different butanol/diesel blends at different loads.

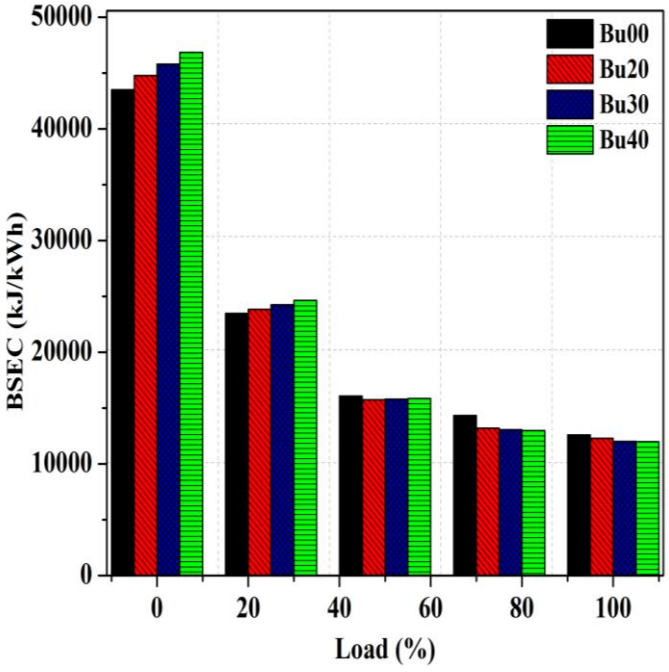

Fig. 4.7 (a) Variation of BSEC for different butanol/diesel blends at different loads.

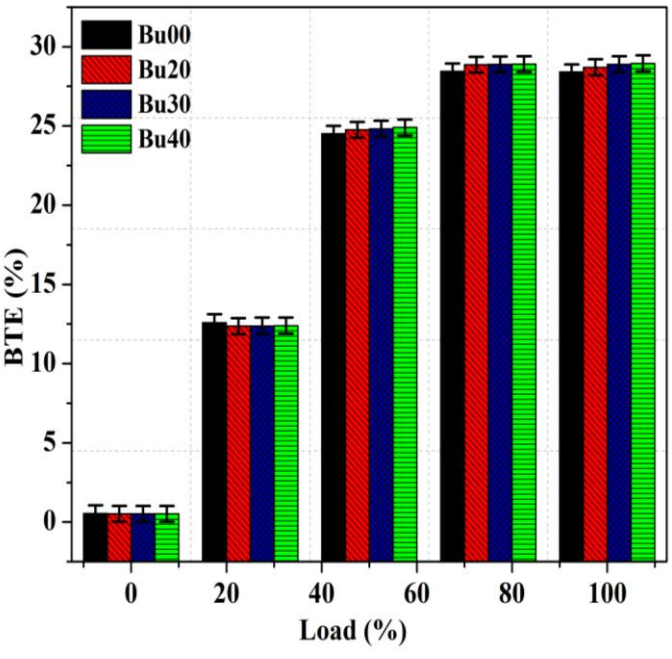

Fig. 4.7 (b) Variation of BTE (with error analysis) for different butanol/diesel blends at different loads.

The variation of BSEC and BTE for different butanol/diesel blends under different loads is shown in figure 4.7 (a). The experimental results reveal that the BTE increases with increase of butanol content in the blend. The BTE increased by 1.04%, 1.69% and 1.89 % for Bu20, Bu30 and Bu40 blends compared to the diesel fuel operation at the rated load condition. It can be observed from the figure that BSEC decreases with increase in the load, and the minimum value of BSEC is obtained at the rated load condition. Brake specific energy consumption (BSEC) measures the energy input required to develop a unit power. The least value of BSEC shows better efficiency of fuel consumption. BSEC is the product of calorific value and SFC. BSEC is used for comparing different fuels. BSEC decreased by 2.54%, 4.74% and 4.93% for Bu20, Bu30 and Bu40 blends compared to the diesel fuel operation at the rated load conditions. This can be credited to the molecular oxygen present in butanol, which leads to improved combustion of the fuel, particularly in the diffusion combustion mode.. In addition, the flame-burning speed also has an important effect on BTE [78]. Higher flame speed improves thermal efficiency. The burning speed of diesel is 33 cm/s while that of butanol is 45 cm/s. In addition, butanol blends have lower viscosity than diesel fuel, which improves the fuel atomization process, thereby enhancing combustion. All these factors contribute to increased BTE for butanol/diesel blends compared to the diesel fuel [79]. Similar results were also observed in the literature [15,17,80]. The maximum possible error in the calculation of BTE was found to be 5.3%, as shown in figure 4.7(b). Uncertainty analysis was carried out to estimate the uncertainty in the calculated results. The details are presented in the Appendix A.

4.1.2. Emission characteristics of butanol/diesel blends

Figure 4.8 illustrates the comparison of NOx emissions for different butanol/diesel blends under different loads. The NOx emissions increase with increase in the load for all the blends, as shown in figure 4.8. However, at any load, the NOx emissions are higher for diesel fuel compared to the butanol blends. NOx emissions decreased with increase of butanol content in the blends. NOx emissions reduced by 7.96%, 10.33% and 12.9% for Bu20, Bu30 and Bu40 blends respectively compared to the diesel fuel at the rated load. It may be attributed to the reason that butanol blends have higher LHE compared to the diesel fuel. Therefore, the introduction of butanol content into the cylinder reduces the in-cylinder charge temperature and also the combustion temperature. This results in lower NOx formation. Similar trends were also observed in the literature [15,17,81].

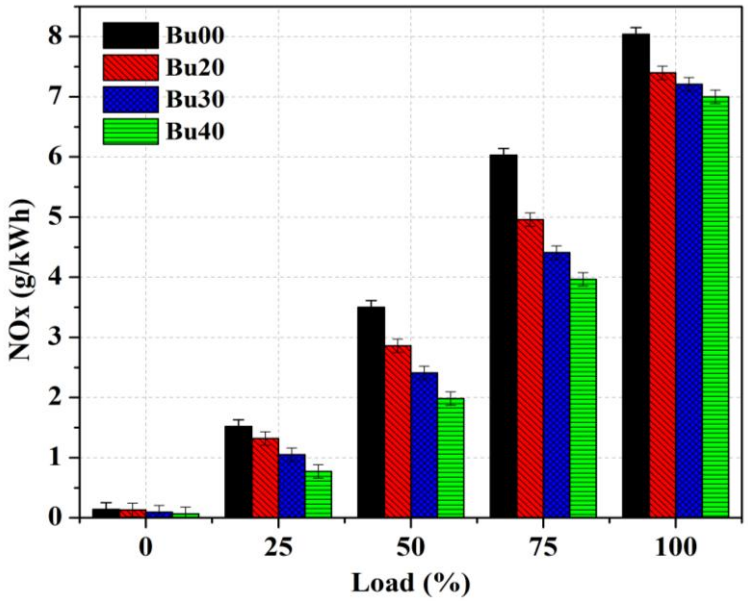

Fig. 4.8. NOx emissions for different butanol/diesel blends at different loads.

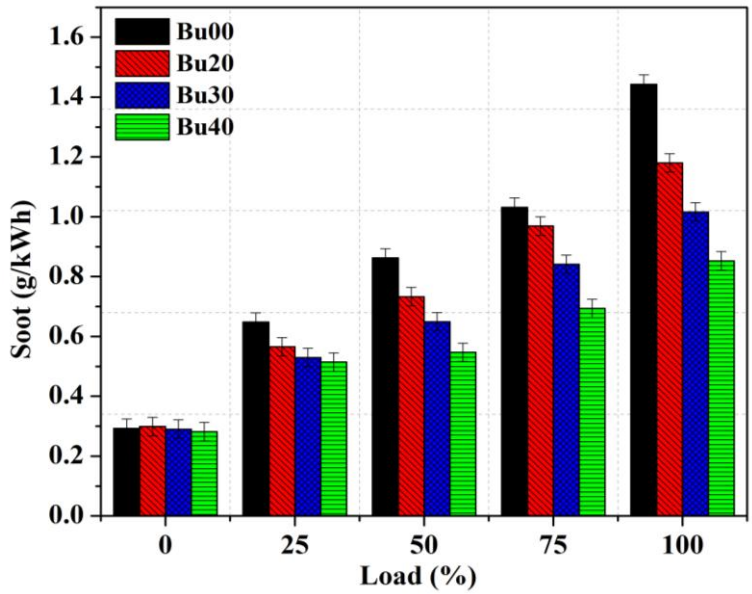

Fig. 4.9. Soot emission for different butanol/diesel blends under different loads.

The soot emission for different butanol/diesel blends at different loads is shown in figure 4.9. It is observed from the figure that for all the butanol/diesel blends, the soot emission increased with increase in the load. The experimental results demonstrate that the soot emissions drastically reduced with increase of butanol fraction in the blends compared to the diesel fuel operation. The soot emission reduced by 18.22%, 29.59% and 40.92% for Bu20, Bu30 and Bu40 compared to the diesel fuel at the rated load condition. Even though the CI engine operates on overall lean air-fuel ratio, there exists rich fuel zones inside the combustion chamber, where incomplete combustion results in the formation of soot. Since,

butanol has molecular oxygen present in its structure it facilitates better combustion in the rich fuel zones also. Thus, it helps in decreasing the soot growth rate in the rich fuel zone [16,17,81].

Figure 4.10 depicts the comparison of UBHC emissions for different butanol blends under different loads. It is observed from the figure that the UBHC emissions increase with increase of butanol content in the blends compared to diesel fuel operation. The UBHC emissions increased by 25.33%, 38.4% and 45.5% for Bu20, Bu30 and Bu40 respectively, compared to the diesel fuel operation at the rated load condition. Butanol/diesel blends have higher LHE, which leads to a quenching effect in the lean mixture zone. Therefore, UBHC emissions are higher for butanol/diesel blends [15–17,81].

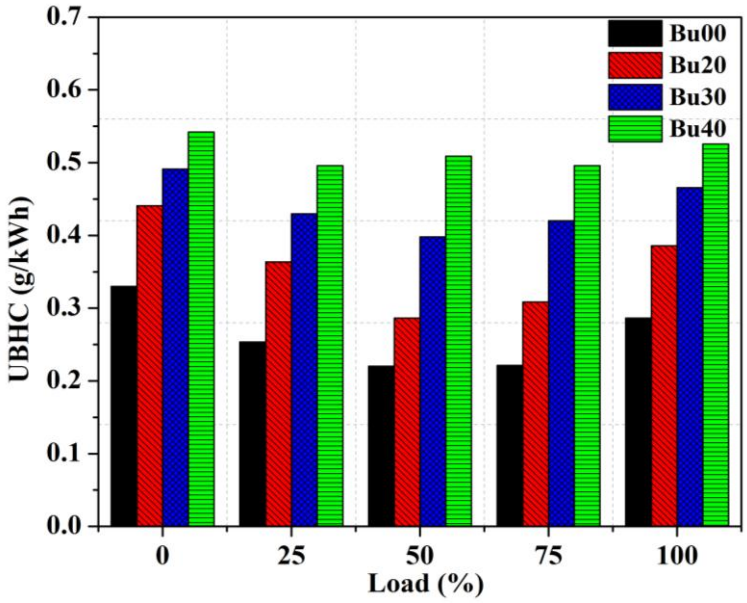

Fig. 4.10. UBHC emission for different butanol/diesel blends under different loads.

Figure 4.11 depicts the variation of CO emissions for diesel and butanol/diesel blends. It is observed from the figure that CO emissions decrease with the increase of butanol content in the blends. The CO emissions decreased by 20.68%, 26.72% and 32.5 % for Bu20, Bu30 and Bu40 respectively, compared to diesel fuel operation at the rated load condition. This is because butanol/diesel blends have higher oxygen content in molecular structure, which facilitates complete combustion in the rich fuel zones, thereby decreasing the CO emissions [16,17].

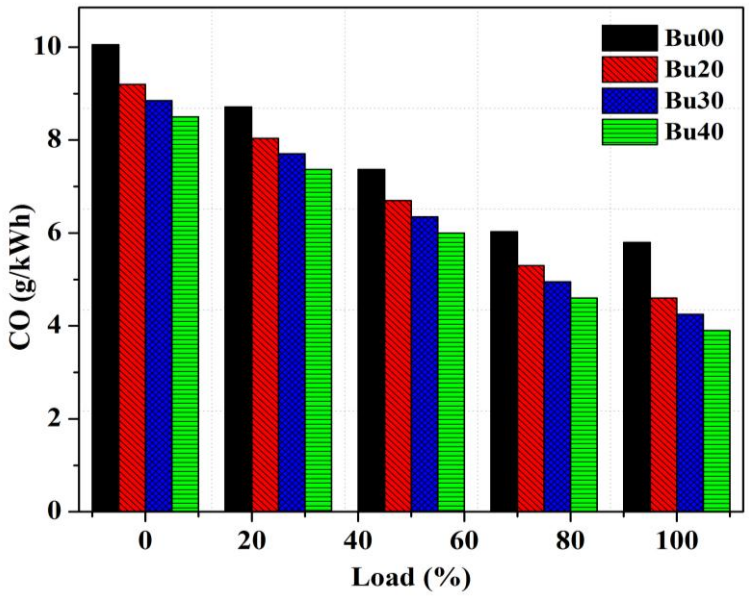

Fig. 4.11. CO emission for different butanol/diesel blends under different loads.

4.2. Effect of exhaust gas recirculation (EGR) on the characteristics of a CI engine

It is observed from previous results that increase in the butanol content in butanol/diesel blends increases the UBHC while it reduces the soot, NOx and CO emissions. However, the reduction in NOx emissions is relatively smaller compared to the reduction in soot emissions. The reduction in NOx emission is smaller at higher loads compared to the lower and medium loads. In order to overcome these problems (NOx emission and RoPR) associated with butanol/diesel blends, Exhaust Gas Recirculation (EGR) was considered as an option. In the present experimental study, the EGR was varied form 0 to 30%, keeping the other parameters constant.

4.2.1. Effect of EGR on the combustion and performance characteristics of the CI engine fuelled with butanol/diesel blends

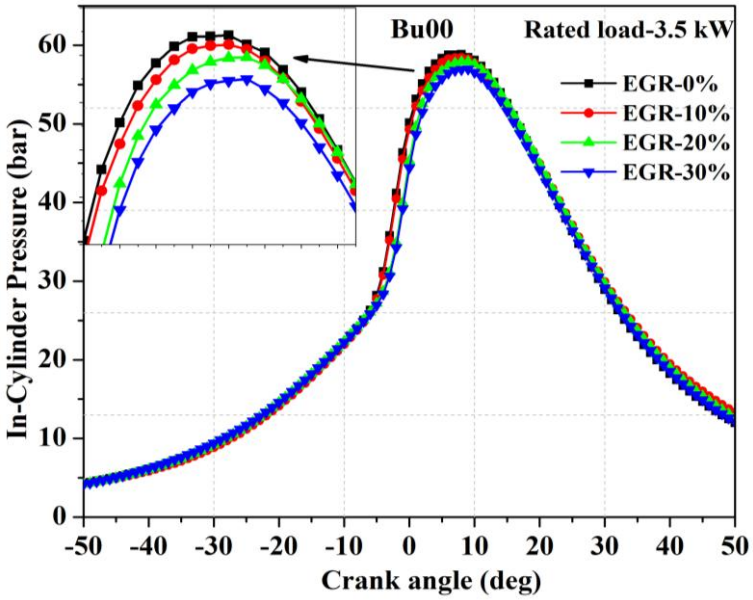

Fig. 4.12. Variation of the in-cylinder pressure with crank angle for diesel fuel for various EGR rates at rated load.

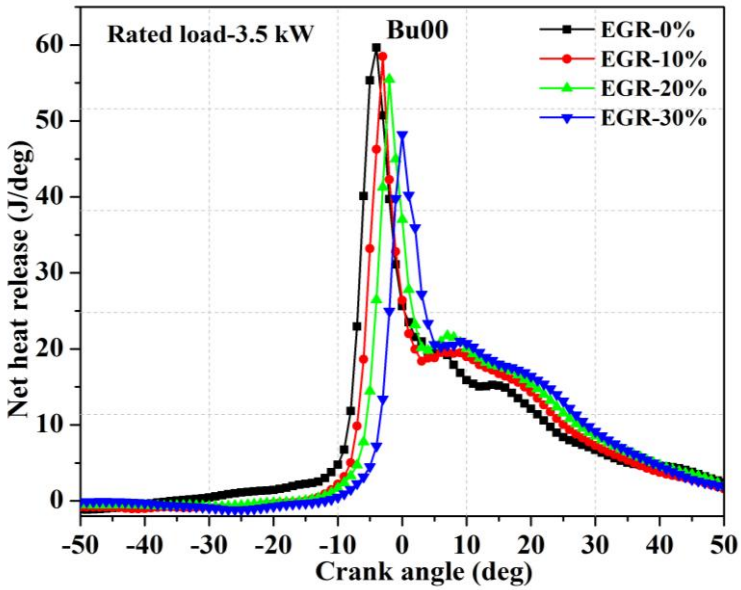

Fig. 4.13. Variation of NHR with crank angle for diesel fuel for various EGR rates at rated load.

Figure 4.12 and 4.13 shows the variation of in-cylinder pressure and NHR for diesel fuel (Bu00) operation for different EGR rates. It is observed from figure 4.12 that with the increase in the EGR rate from 0 to 30%, the peak in-cylinder pressure decreased and the ignition delay increased (18.76 to 24.76 deg CA) (as shown in figure 4.18) compared to the

baseline configuration (without EGR). The peak in-cylinder pressure decreased by 1.4%, 2.5%, 3.48% for 10%, 20% and 30% EGR fraction respectively, compared to the baseline configuration (i.e., without EGR) at the rated load conditions. It is observed from figure 4.13 that with the introduction of EGR, the NHR in the premixed combustion zone decreased significantly whereas in the diffusion combustion zone it increased. This is due to decrease in oxygen availability in the charge, following the replacement of air by the EGR. It led to longer ignition delay that provides ample time to mix the fuel with air that increased the amount of premixed charge fuel. But, reduction in oxygen concentration in the charge reduces the premixed combustion, thereby generating a negative effect on the premixed charge. As a result, there was lowering of peak in-cylinder pressure and increase in ignition delay [82,83]. Similar trends were observed for the other blends also (Bu20 and Bu40) as shown in figures 4.14, 4.15, 4.16 and 4.17.

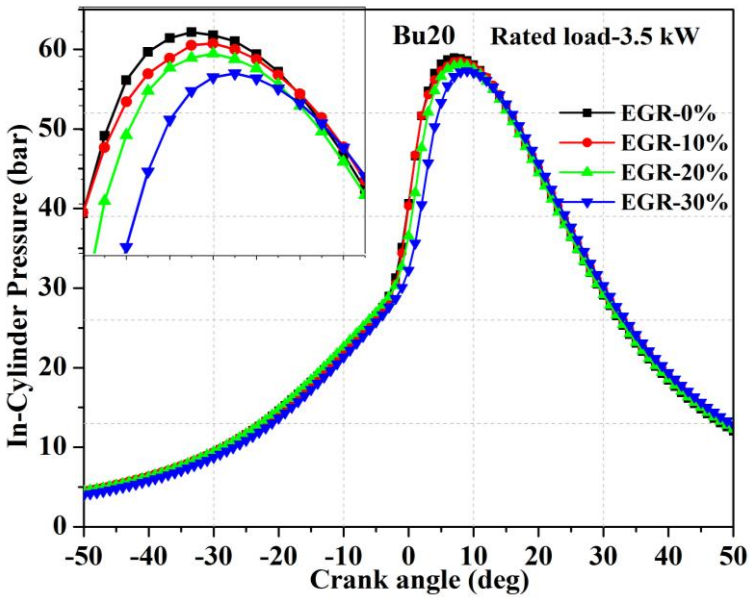

Fig. 4.14. Variation of in-cylinder pressure with crank angle for Bu20 blend for various EGR rates at rated load.

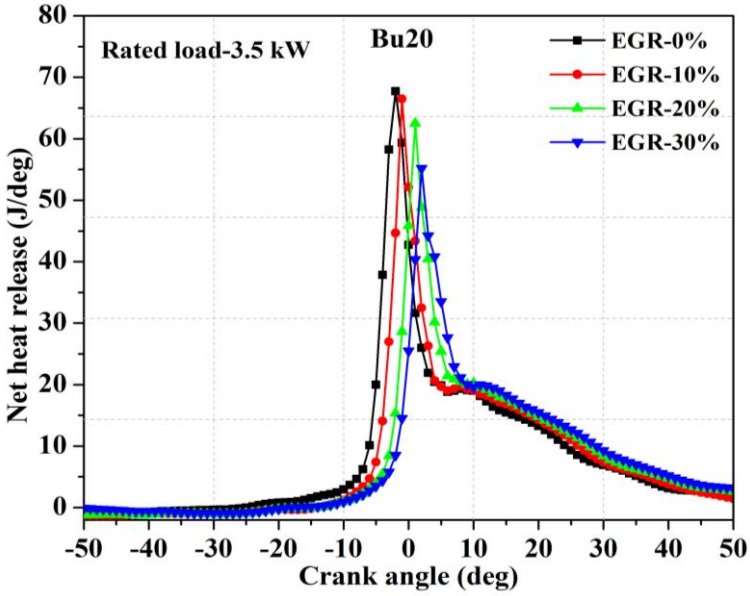

Fig. 4.15. Variation of NHR with crank angle for Bu20 blend for various EGR rates at rated load.

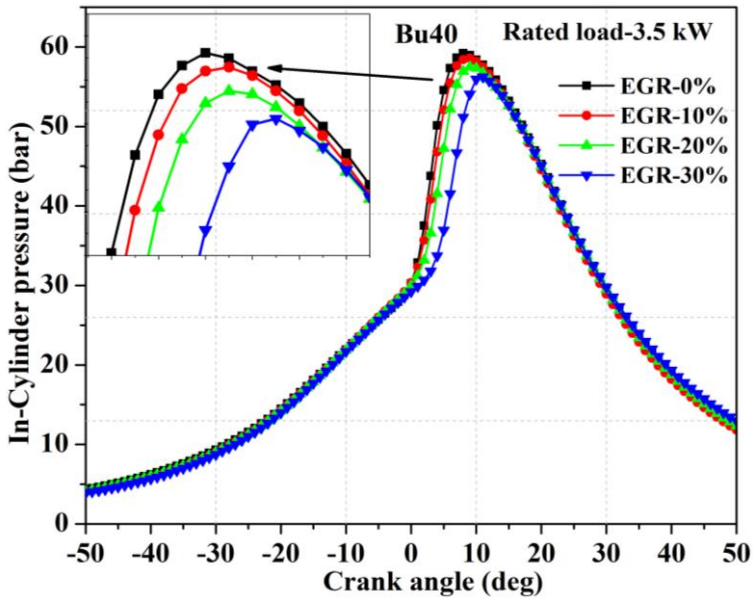

Fig. 4.16. Variation of in-cylinder pressure with crank angle for Bu40 blend for various EGR rates at rated load.

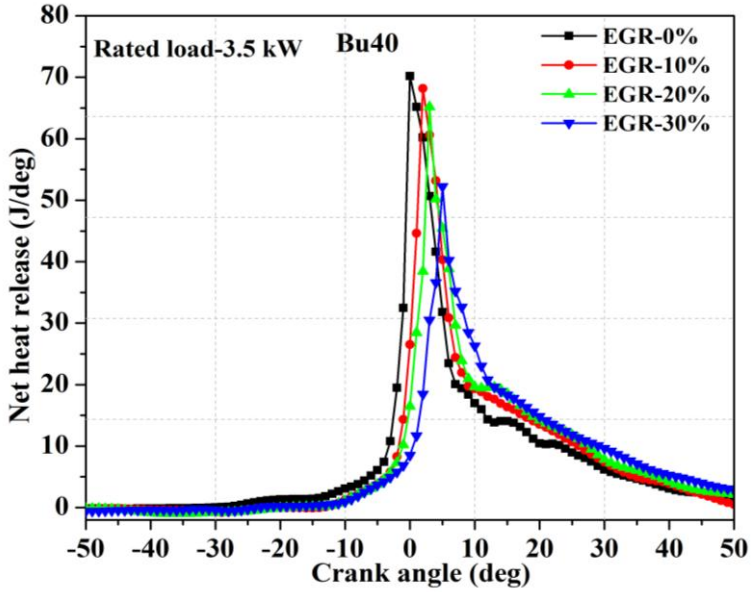

Fig. 4.17. Variation of NHR with a crank angle for Bu40 blend for various EGR rates at rated load.

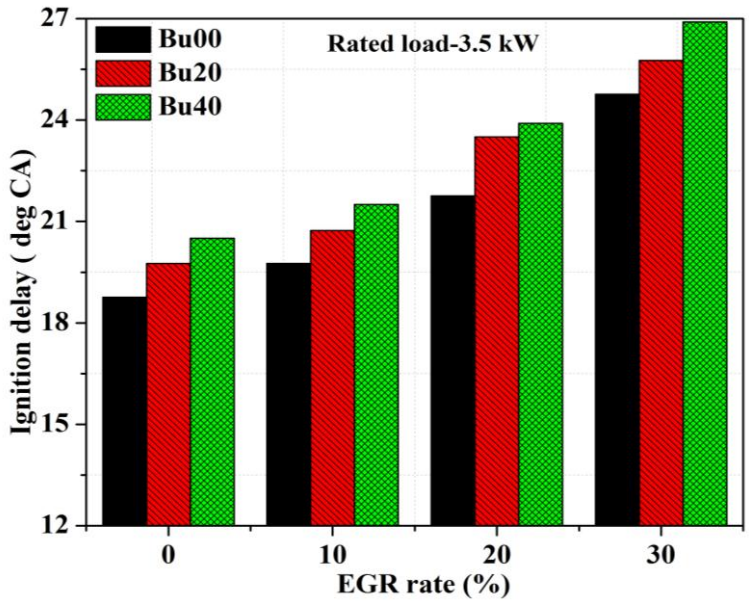

Fig. 4.18. Comparison of ignition delay for different blends at different EGR rates at the rated load.

Figure 4.19 shows the rate of pressure rises (RoPR) for different test fuels at different EGR rates. RoPR represents the combustion noise of the engine. It can be observed from the figure that for all the three test fuels (Bu00, Bu20 and Bu40), the RoPR decreases with increase of EGR from 0 to 30%. This is similar to the effect of EGR on the NHR. Similar results were obtained in the literature also [84].

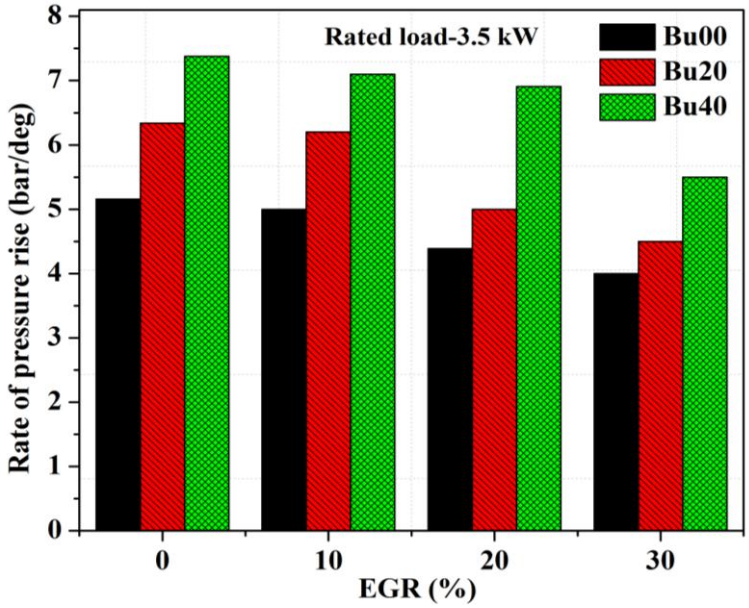

Fig. 4.19. Rate of pressure rise for diesel and butanol/diesel blends at different EGR rates at rated load.

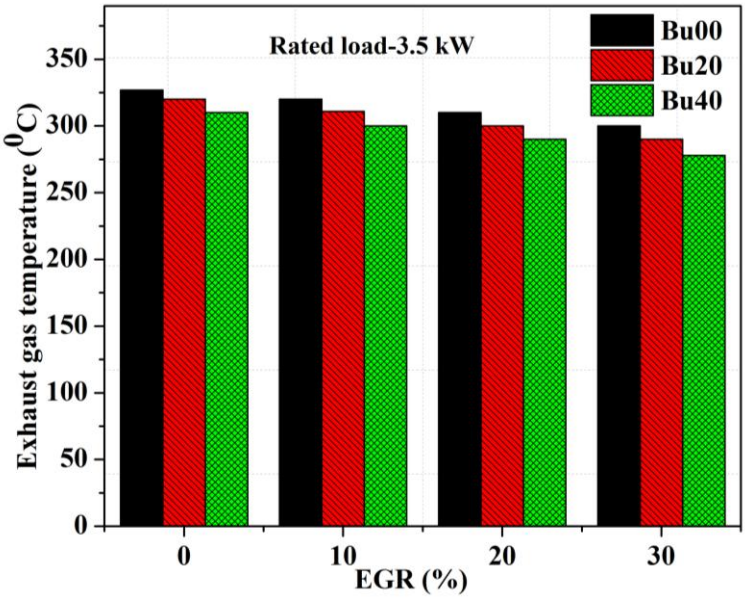

Fig. 4.20. Variation of EGT for diesel and butanol/diesel blends for various EGR rates at rated load.

Figure 4.20 illustrates the effect of EGR on the exhaust gas temperature (EGT) for diesel fuel and different butanol/diesel blends operation. It is observed from the figure that with an increase in the EGR rate from 0 to 30%, the EGT reduced for all the test fuels compared to the respective baseline configuration (without EGR). It may be reasoned that as the EGR rate increases, there will be a proportionate reduction in the oxygen quantity in the

charge. Hence, incomplete combustion occurs, resulting in lower combustion temperature and thus a reduction in the EGT [47].

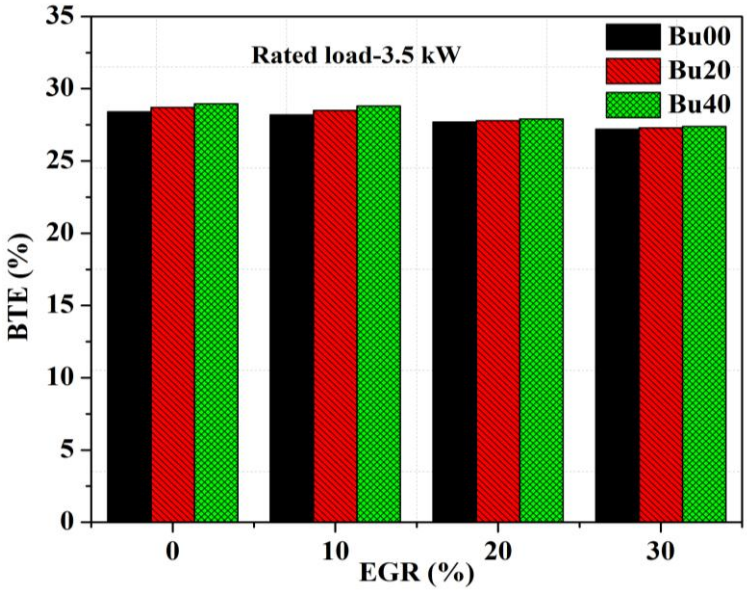

Fig. 4.21. Variation of BTE for diesel and butanol/diesel blends for various EGR rates at the rated load.

Figure 4.21 shows the variation of BTE for diesel and butanol/diesel blends at different EGR rates. It is observed from the figure that the BTE is slightly reduced for all the three test fuels with increase in the EGR rate from 0% to 30%. The reason may be deficiency of oxygen concentration in the combustion chamber because of the replacement of air by the exhaust gas, which slow down the combustion process and burning rate resulting in lowering of BTE.

4.2.2. Effect of EGR on the emission characteristics of the CI engine

Figure 4.22 shows the variation of NOx emissions for the three test fuels at different EGR rates at the rated load. It can be observed that with increase in the EGR rate from 0% to 30%, the NOx emission decreased significantly. The NOx emission formation is mainly dependent on oxygen concentration inside the cylinder, in-cylinder temperature, and the residence time of exhaust gas inside the cylinder. Increasing the EGR in the fresh charge reduces the flame temperature and in-cylinder temperature caused by the replacement of fresh air with inert gases (CO_2 and H_2O). This is called the dilution effect. Since the specific heat of the inert gases is more than that of fresh air, the inert gases absorb more heat compared to the fresh air. This is called thermal effect. Because of the dilution effect and thermal effect, the combustion gases absorb more heat released by combustion, leading to the lowering of

combustion temperature and flame temperature, because of which the NOx formation is reduced. NOx emissions decreased for Bu00 by 7.9%, 22.8% and 53.9% and for Bu20 by 11.6%, 30.1% and 60.2%, and for Bu40 by 13.3%, 35% and 67% at 0%, 10%, 20% and 30% EGR rates, respectively.

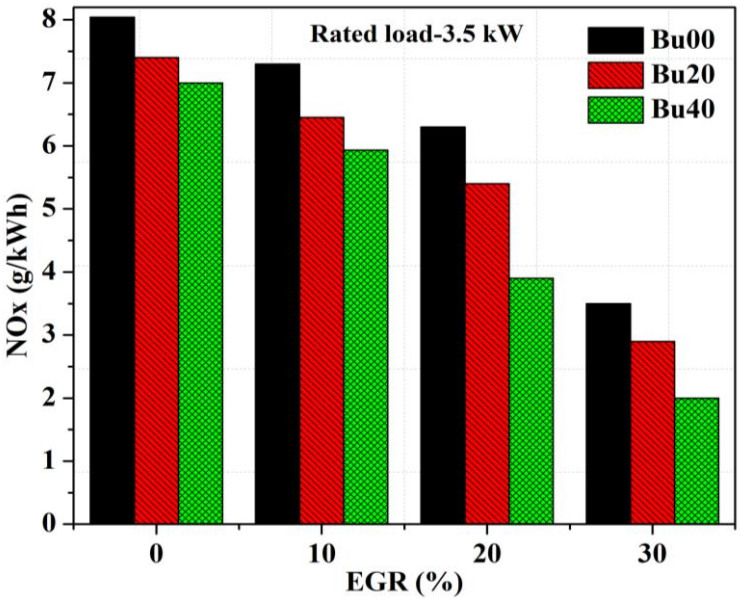

Fig. 4.22. Variation of NOx emission for diesel and butanol/diesel blends for various EGR rates at the rated load.

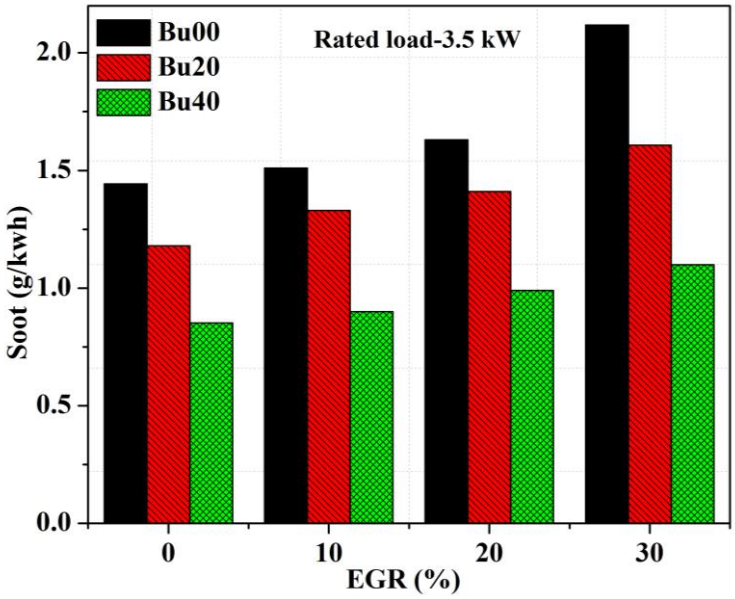

Fig. 4.23. Variation of soot emission for diesel and butanol/diesel blends for various EGR rates at the rated load.

It can be seen from figure 4.23 that with increase in the EGR rate, the soot emissions increase for all test fuels compared to the respective baseline configuration (without EGR). Increasing the EGR rate in the charge increases the local equivalence ratio, decreases the oxygen concentration causing incomplete combustion, and promotes soot growth rate. Soot emissions increased for Bu00 by 4.4%, 11.8% and 31.7% and for Bu20 by 7.6%, 12.7% and 23.1%, and for Bu40 by 5.5%, 14.1% and 21.7% at 0%, 10%, 20% and 30% EGR rates, respectively.

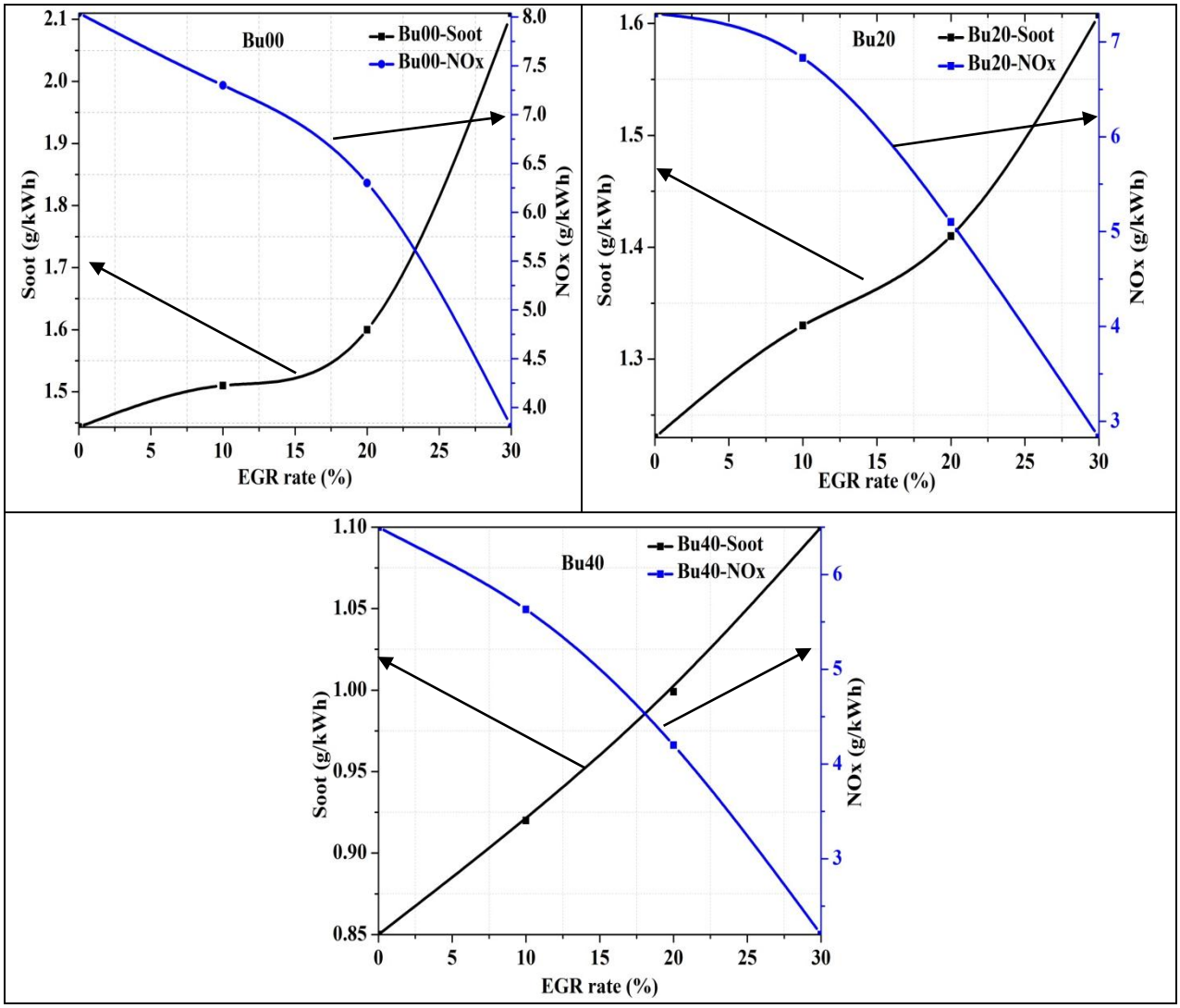

Fig. 4.24. Trade-off between soot and NOx emission for diesel and butanol/diesel blends at various EGR rates.

Figure 4.24 shows the trade-off curves between the soot and NOx emissions for diesel and different butanol/diesel blends at the rated load conditions for different EGR rates. It is observed from the figure that the trade-off relation between the soot and NOx occurs between 20% to 30% of EGR rate for diesel. However, as the butanol content in the fuel is increased

(for Bu20 and Bu40) it occurs between 10% to 20%. From the figure, it is clearly observed that the addition of butanol content in the blends, reduces the EGR rate requirement for reduction of NOx emission compared to baseline configuration.

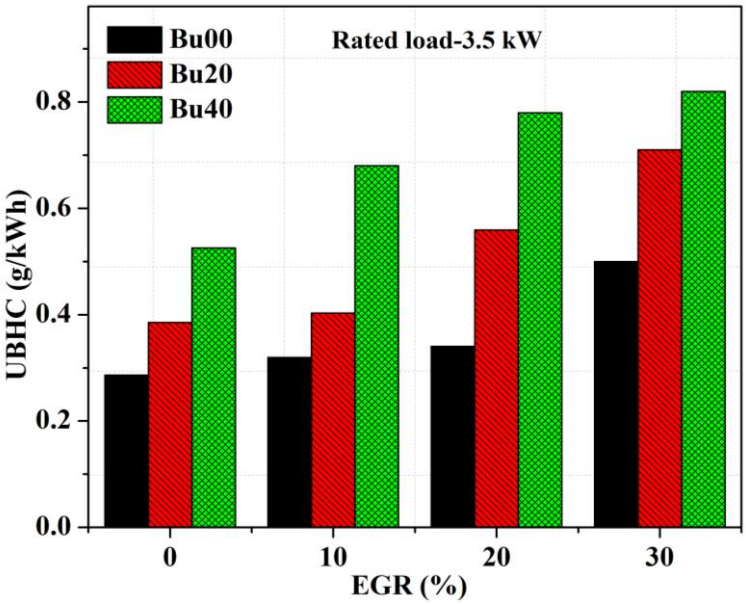

Fig. 4.25. Variation of UBHC emission for diesel and butanol/diesel blends for various EGR rates at the rated load.

The variation of UBHC emission for diesel and butanol/diesel blends for various EGR rates is shown in figure 4.25. UBHC emissions increased with increase in EGR rates in the charge. Increasing EGR rate reduces oxygen content in the charge that causes lowering of flame temperature, which results in the formation of large flame quenching zones where combustion cannot happen easily. UBHC emissions increased for Bu00 by 10.9%, 15.92% and 42.7% and for Bu20 by 14.86%, 31.06% and 45.6%, and for Bu40 by 22.5%, 32.2% and 48.5% at 0%, 10%, 20% and 30% EGR rates, respectively.

Figure 4.26 indicates the variation of CO emission for diesel and butanol/diesel blends at various EGR rates. CO emissions increased with increase in the EGR rates for all the test fuels. CO emission increased for diesel by 3.8%, 13.4% and 32% at 10%, 20% and 30% EGR rates, respectively compared to baseline configuration. Similarly, CO emission increased for Bu20 by 7%, 18%, and 31%, and for Bu40 by 10%, 29%, and 40% at 10%, 20% and 30% EGR rates, respectively compared to their respective baseline configurations. This is owing to oxygen deficiency in the charge associated with EGR, which results in incomplete combustion and therefore higher CO emission. However, butanol/diesel blends have lower CO emissions compared to diesel fuel. The reason is that, the molecular oxygen

of the butanol partially compensates oxygen-deficiency under EGR operation, thereby reducing CO emissions for butanol/diesel blends compared to diesel fuel.

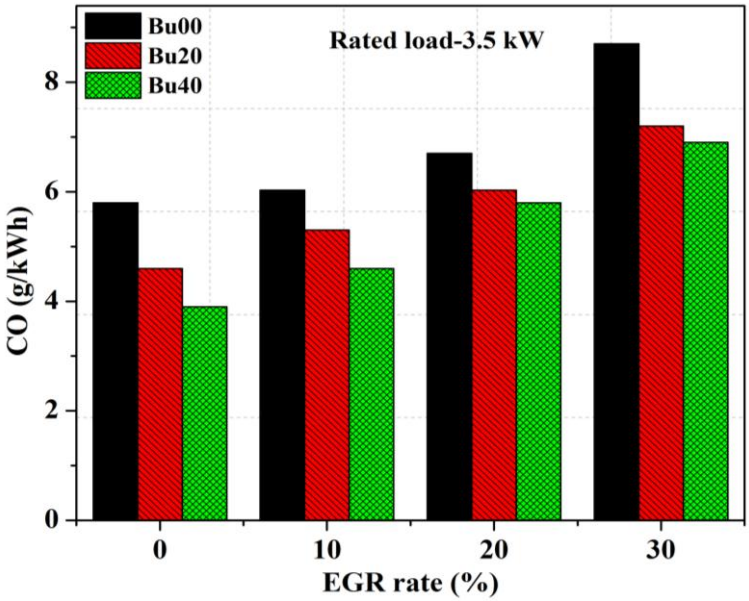

Fig. 4.26. Comparison of CO emission for diesel and butanol/diesel blends for various EGR rates at the rated load.

4.3. Effect of FIP on the combustion, performance and emission characteristics of CI engine fuelled with diesel and different butanol/diesel blends

The combustion, performance and emissions characteristic of CI engine operated with diesel and butanol/diesel blends at different fuel injection pressure (200 to 280 bar in steps of 20 bar) were studied. The peak in-cylinder pressure, NHR, ID, BTE, EGT, NOx, soot, UBHC and CO were compared for diesel and butanol/diesel blends at different fuel injection pressures.

4.3.1. Combustion and performance analysis for butanol/diesel blends under different FIPs

Figures 4.27 and 4.28 illustrate the variation of in-cylinder pressure and net heat release (NHR) with crank angle with diesel fuel at different FIPs. It can be observed from the figure that as the FIP is increased from 200 bar to 260 bar, the peak in-cylinder pressure and NHR increased, however beyond 260 bar FIP, both of them decreased. Similarly, the ignition delay (as shown in figure 4.28 and 4.34) decreases with increase in FIP from 200 bar to 260

bar: with further increase in FIP to 280 bar, the ignition delay increases. Higher FIP provides better-atomized fuel droplets and increased ease of fuel spray inside the combustion chamber. This results in the fuel having a larger surface area of contact in the combustion chamber. Therefore, combustion occurs at different locations, resulting in higher values of NHR and peak in-cylinder pressure. However, there exists an optimum FIP, beyond which adverse consequences creep in. As the FIP is increased, no doubt the droplet size decreases, but simultaneously the air entrainment with the surrounding fuel droplet decreases. Similarly, if the FIP is too high, there is a possibility of the fuel impinging on the piston surface and the cylinder walls. In both the cases, it results in incomplete combustion and loss of performance. Probably this may be the reason for the reduction of peak in-cylinder pressure and NHR at 280 bar for Bu00 [85][86].

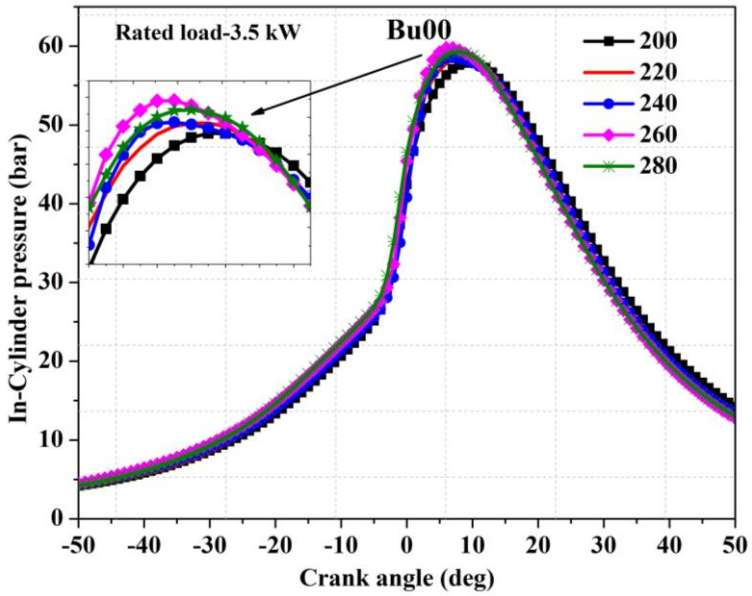

Fig. 4.27. Variation of in-cylinder pressure with a crank angle for diesel fuel at different FIPs at rated load.

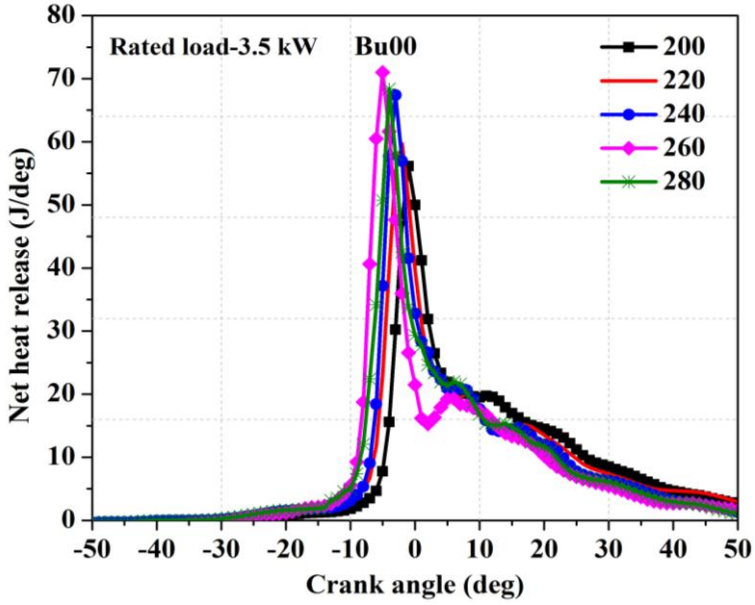

Fig. 4.28. Variation of neat heat release with crank angle for diesel fuel at different FIPs at rated load.

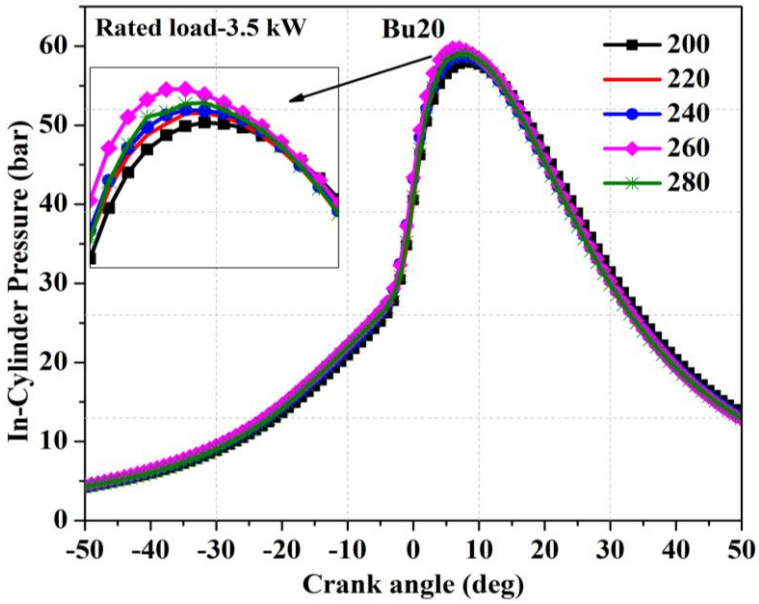

Fig. 4.29. Variation of in-cylinder pressure with crank angle for Bu20 blend at different FIPs at rated load.

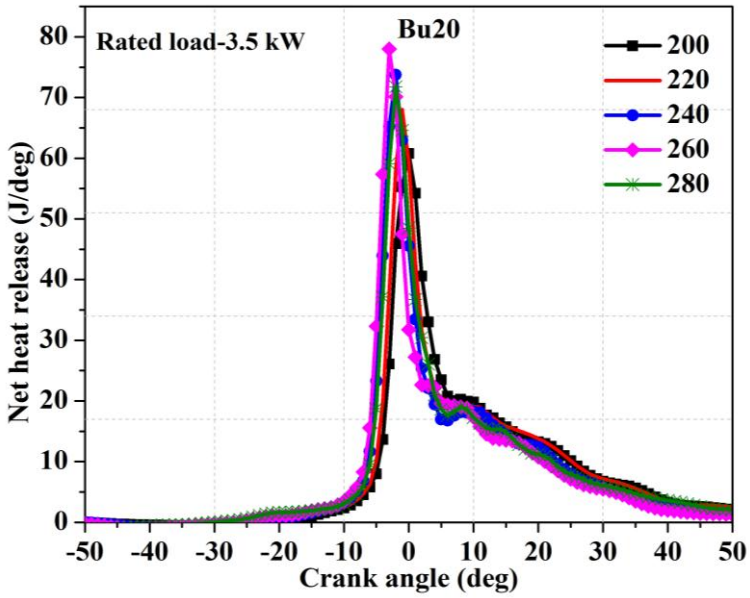

Fig. 4.30. Variation of neat heat release with a crank angle for the Bu20 blend at different FIPs at rated load.

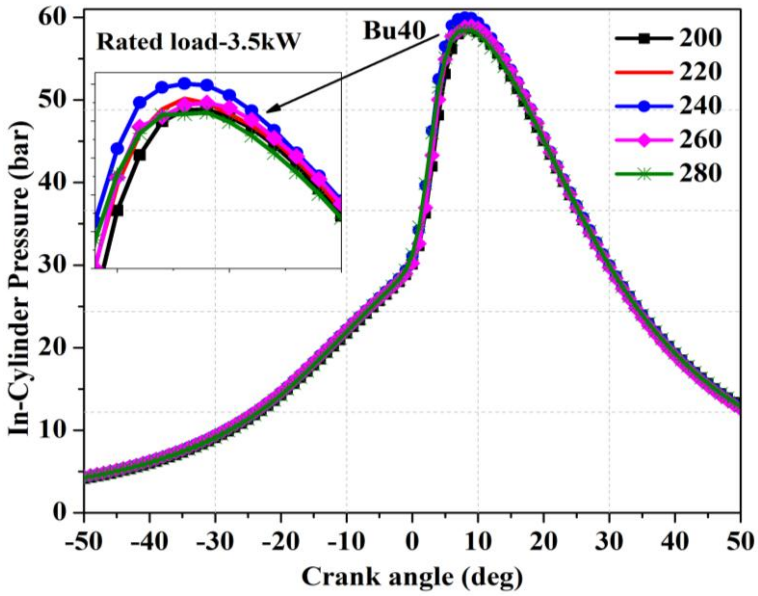

Fig. 4.31. Variation of in-cylinder pressure with crank angle for Bu40 blend at different FIPs at rated load.

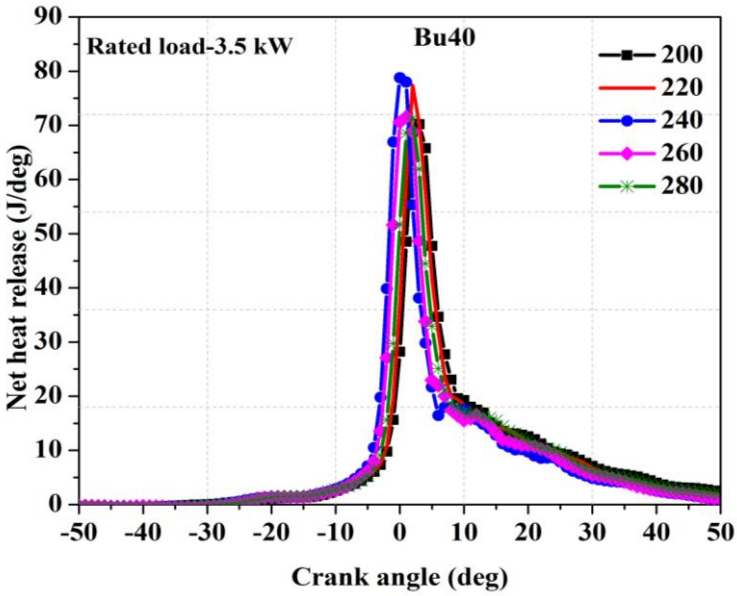

Fig. 4.32. Variation of neat heat release with the crank angle for Bu40 blend at different FIPs at rated load.

Similar trends were observed for Bu20 and Bu40 test fuels also as shown in figures in 4.29, 4.30, 4.31 and 4.32. Figure 4.33 shows a comparison of the peak in-cylinder pressures at different FIPs for the three test fuels. It is observed that the optimum value of FIP for Bu20 is the same as that of Bu00, i.e., 260 bar. However, for Bu40 test fuel, the optimum FIP is 240 bar. Butanol has lower viscosity than diesel. The increase in butanol content in the blends leads to a reduction in the viscosity of the blend. The lower viscosity of blend (Bu40) causes longer penetration inside the combustion chamber. The longer penetration of fuel results in better mixing of air-fuel mixture and leads to complete combustion. Therefore, Bu40 blend requires lower values of FIP to achieve complete combustion compared to Bu00 and Bu20.

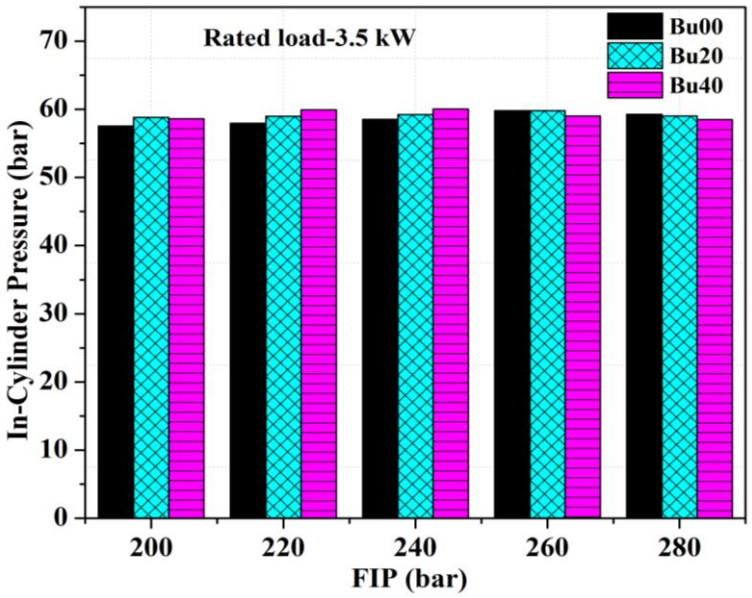

Fig. 4.33. Comparison of peak in-cylinder pressure at the rated load for different test fuels at different FIPs.

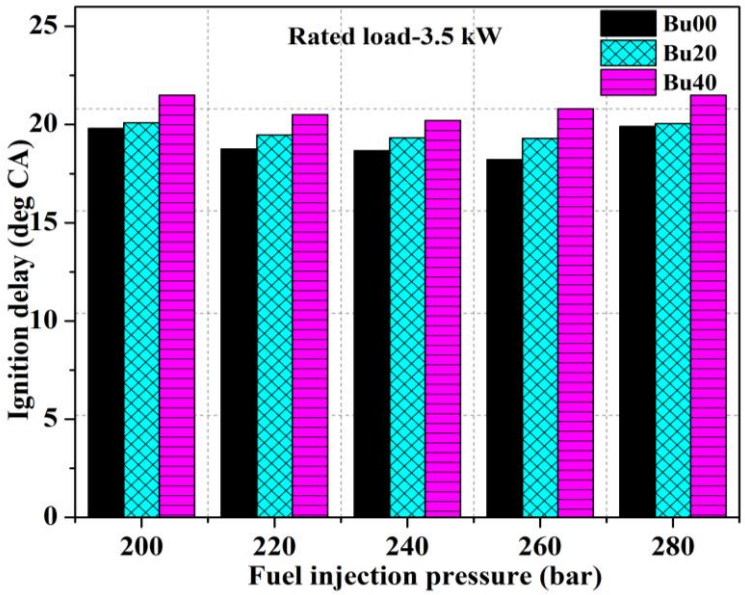

Fig. 4.34. Variation of ID for diesel and butanol/diesel blends at different FIPs at rated load.

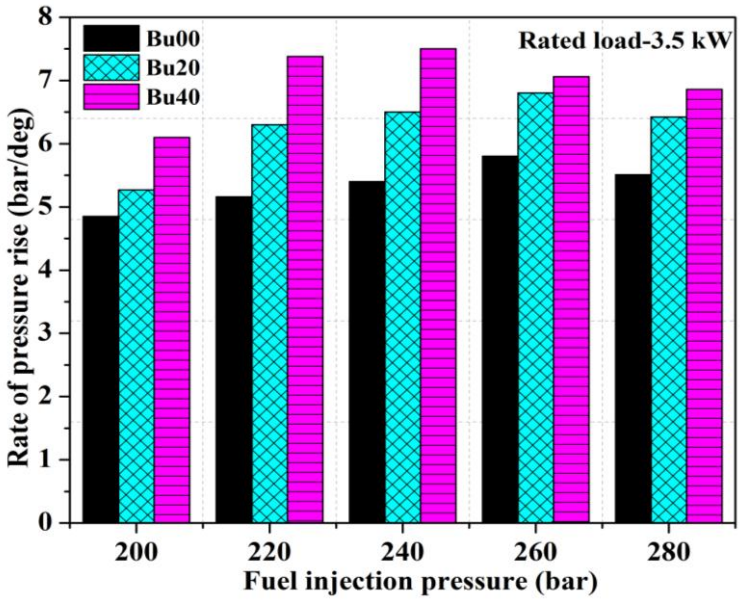

Fig. 4.35. Comparison of RoPR for different test fuels at different FIPs at rated load.

RoPR increases with increase in the FIP from 200 to 260 bar for Bu00 and Bu20 blend, and from 200 to 240 bar for Bu40 blend. But, upon further increase in the FIP beyond these respective FIPs, the RoPR decreases as shown in figure 4.35. The higher RoPR for Bu00 is at 260 bar (5.8 bar/deg), for Bu20 blend at 260 bar (6.8 bar/deg) and for Bu40 blend at 240 bar (7.48 bar/deg). These trends are similar to that of peak in-cylinder pressures and NHR.

The variation of EGT for diesel and butanol/diesel blends at different FIPs is shown in figure 4.36. It is observed from the figure that the EGT of the blends is lower than that for pure diesel. This can be attributed to better atomization, easy evaporation of fuel droplets and better mixing of air-fuel. Further increase in the FIP beyond the optimum FIP decreases the EGT due to fuel impingement on the wall, as a result of which there is incomplete combustion.

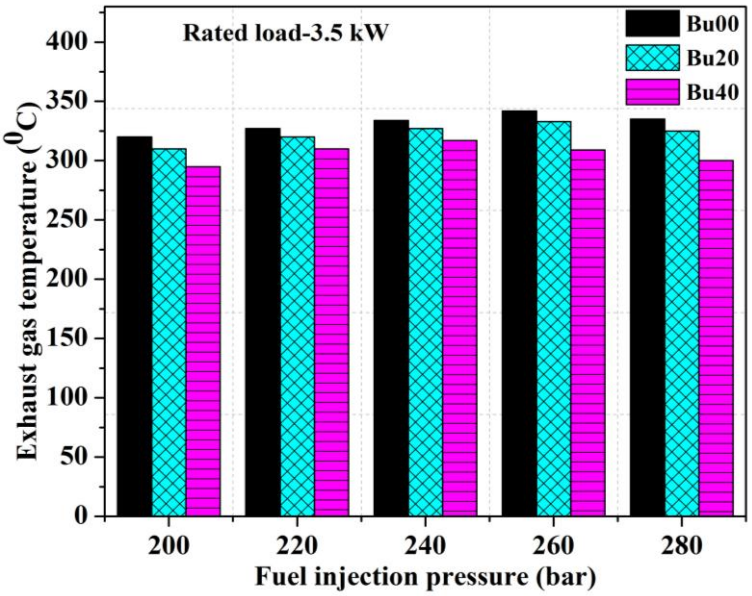

Fig. 4.36. Variation of EGT at the rated load for diesel and butanol/diesel blends at different FIPs.

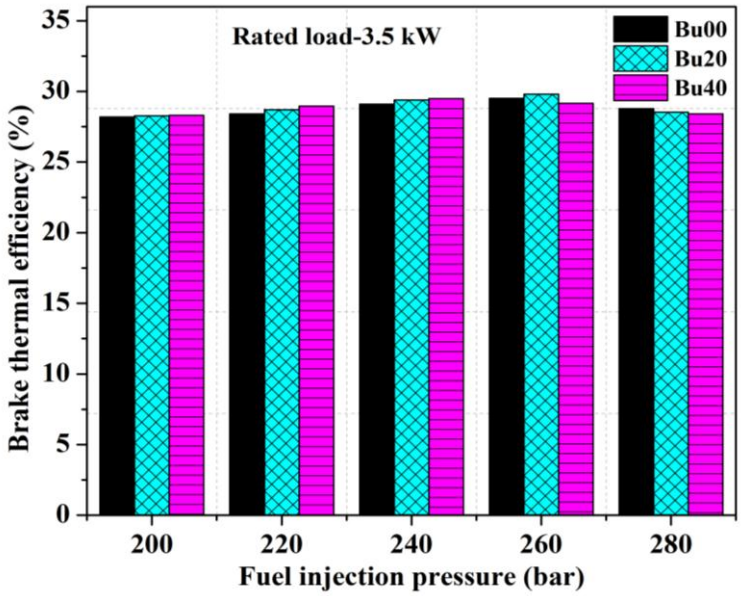

Fig. 4.37. Variation of BTE at the rated load for diesel and butanol/diesel blends at different FIPs.

Figure 4.37 shows the effect of FIP on the BTE for three test fuels. The highest BTE for Bu00 and Bu20 fuels was occurring at 260 bar, while for the Bu40 blend it was at 240 bar. As mentioned earlier, increase in the FIP results in decrease in the fuel droplet size during fuel injection. This enables faster evaporation of the fuel and better mixing with the surrounding air. This enhances the combustion efficiency and increases the BTE. On the other hand, very higher FIPs result in extremely small fuel particles. Hence, the air entrainment with the surrounding fuel droplet decreases and also there is a possibility of the

fuel impinging on the piston surface and the cylinder walls. This decreases the combustion efficiency and hence the BTE.

4.3.2. Emission analysis for butanol/diesel blends under different FIPs

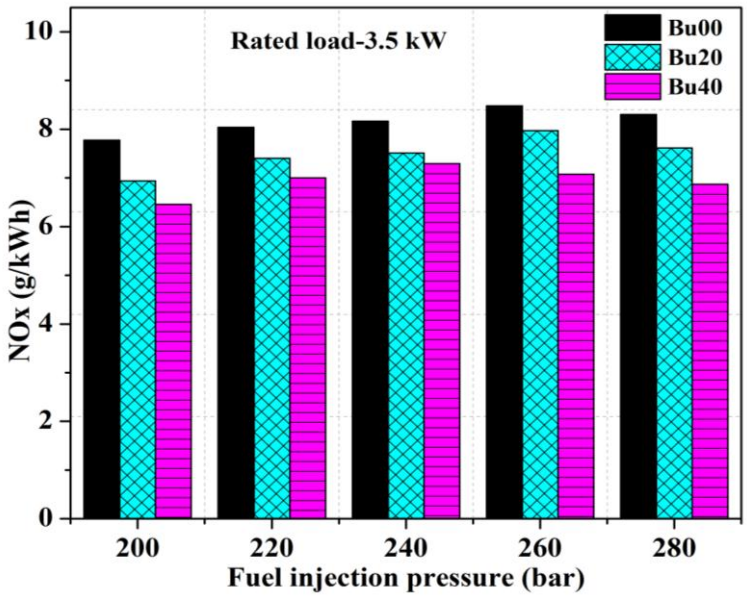

Fig. 4.38. Variation of NOx at the rated load for different FIP for diesel and butanol/diesel blends.

Figure 4.38 shows the variation of NOx for diesel and butanol/diesel blends at different FIPs. It is observed from the figure that NOx emissions are smaller for butanol/diesel blends compared to diesel fuel at all the FIPs. The highest NOx emissions appear for diesel at 260 bar (8.48 g/kWh), for Bu20 blend at 260 bar (7.9 g/kWh) and for Bu40 blend at 240 bar (7.07 g/kWh). It is observed that with increasing the butanol content in blends, the NOx emissions decrease. This is because butanol/diesel blends have higher latent heat of vaporization compared to diesel fuel. Therefore, the induction of butanol into the cylinder results in reduced charge temperature as well as the combustion temperature. As a result, it lowers the NOx emissions. It was also found that NOx emissions increased with increase in FIP up to 260 bar for Bu00, Bu20 blends and upto 240 bar for Bu40 blend. Any further increase in the FIP, decreased the NOx emissions. This may be due to the lower combustion temperature and lower NHR in the premixed combustion phase as explained earlier.

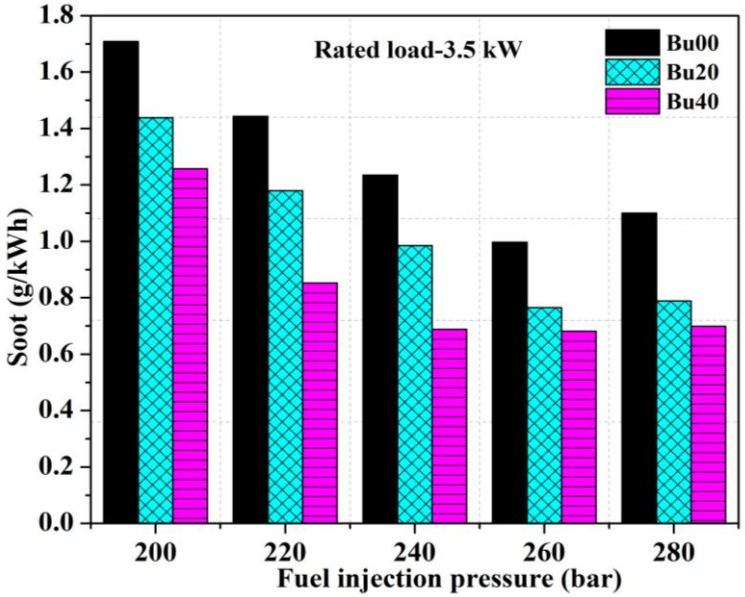

Fig. 4.39. Variation of soot for different FIP for diesel and butanol/diesel blends at the rated load.

The variation of soot emission for diesel and butanol/diesel blends at different FIPs is shown in figure 4.39. It is observed from the figure that the soot emissions are considerably lower for butanol/diesel blends compared to diesel fuel at all the FIPs. This is because butanol/diesel blends have higher molecular oxygen content that will participate in the rich fuel zones reducing soot growth rate in the process. It is also observed from the figure that the soot emissions decrease with increase in the FIP up to 260 bar for diesel and Bu20 blend, and up to 240 bar for Bu40 blend. The lowest soot emission appears for diesel at 260 bar (0.99 g/kWh), for Bu20 blend at 260 bar (0.76 g/kWh) and for Bu40 blend at 240 bar (0.69 g/kWh). However, with further increase in the FIP, the soot emissions significantly increased. Thus, it appears that there is an optimum value of FIP for every test fuel.

Figure 4.40 shows variation of UBHC for diesel and butanol/diesel blends at different FIPs. It was observed from the figure that the UBHC emissions are significantly higher for the butanol/diesel blends compared to diesel fuel at all the FIPs. The UBHC emissions decreased with increase in the FIP up to 260 bar for diesel and Bu20 blend, and up to 240 bar for Bu40 blend. However, with further increase in the FIP, the UBHC emissions significantly increased. The lowest UBHC emission appears for diesel at 260 (0.2228 g/kWh), for Bu20 blend at 260 bar (0.365 g/kWh) and for Bu40 blend at 240 bar (0.51 g/kWh).

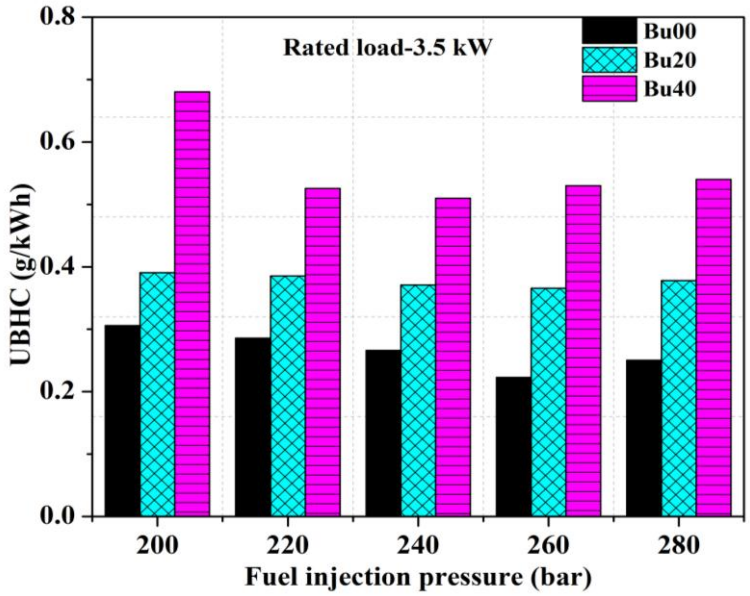

Fig. 4.40. Variation of UBHC for different FIP for diesel and butanol/diesel blends at the rated load.

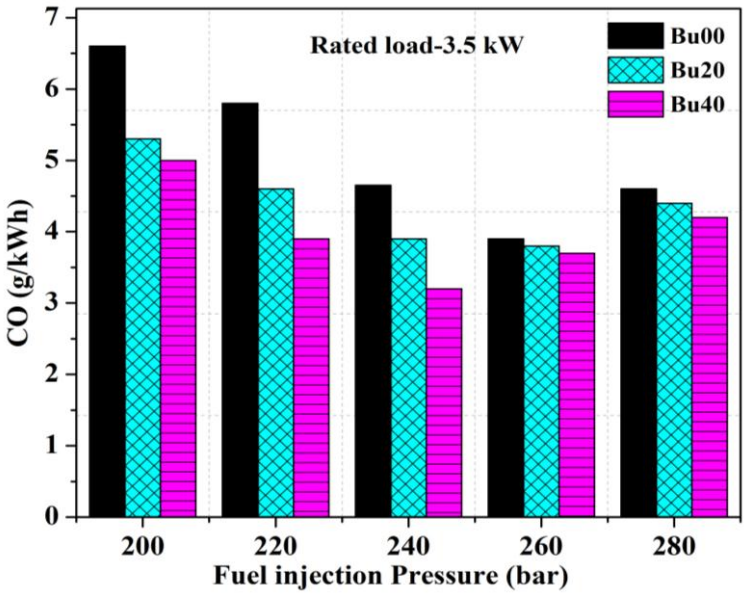

Fig. 4.41. Variation of CO emission for diesel and butanol/diesel blends for different FIPs at the rated load.

CO emission is a manifestation of incomplete combustion of the fuel. It is observed from figure 4.41 that the CO emission decreases with increasing of FIP from 200 to 260 bar for diesel fuel and Bu20 blend, and from 200 to 240 bar for Bu40 blend. However, with further increase in the FIP, the CO emissions significantly increased. These trends are similar to soot emission.

4.4. Effect of compression ratio on the combustion, performance and emission characteristics of CI engine fuelled with butanol/diesel blends

The performance, combustion and emissions characteristic of a CI engine fuelled with the three test fuels, i.e., Bu00, Bu20 and Bu40 at different compression ratios (CR) were studied. The peak in-cylinder pressure, NHR, ID, BTE, EGT, NOx, soot, UBHC and CO were compared for diesel and butanol/diesel blends at various compression ratios (CR) (14, 15 16, 17.5 and 18).

4.4.1. Combustion and performance analysis of butanol/diesel blends at different CRs

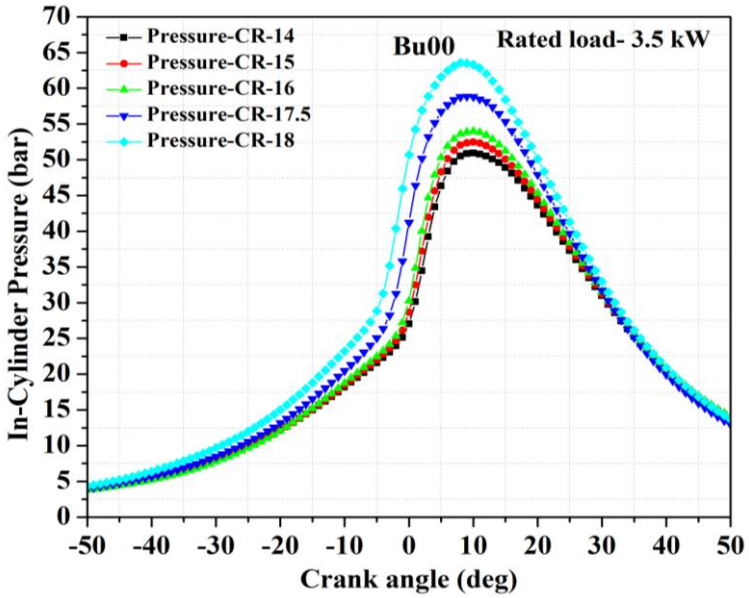

Fig. 4.42. Variation of in-cylinder pressure for diesel fuel at different CRs at rated load.

The variation of peak in-cylinder pressure and NHR with the crank angle for diesel fuel operation of the engine for different CRs at the rated load is shown in figures 4.42 and 4.43. It is noticed from the figure that as the CR is increased from 14 to 18, the peak in-cylinder pressure increased. As the CR is increased, the pressure and temperature of air inside the combustion chamber increase, thereby enhancing the mixing of air and fuel contributing to better combustion. As a result, the peak in-cylinder pressure increases with increase in the CR from 14 to 18. Similarly, as seen in figure 4.43, the NHR also increases and the ignition delay decreases (figure 4.49) with increase in the CR from 14 to 18. Also, it is observed that at higher CR, the NHR is higher in the premixed combustion zone whereas it

is lower in the diffusion combustion zone. This is because the fuel is injected into the charge which is at higher pressure and temperature, which causes early combustion.

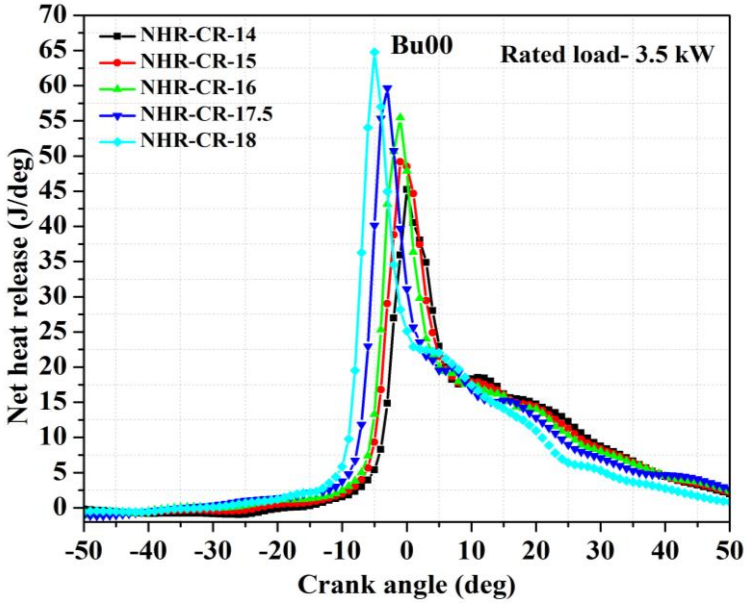

Fig. 4.43. Variation of NHR for diesel fuel at different CRs at rated load.

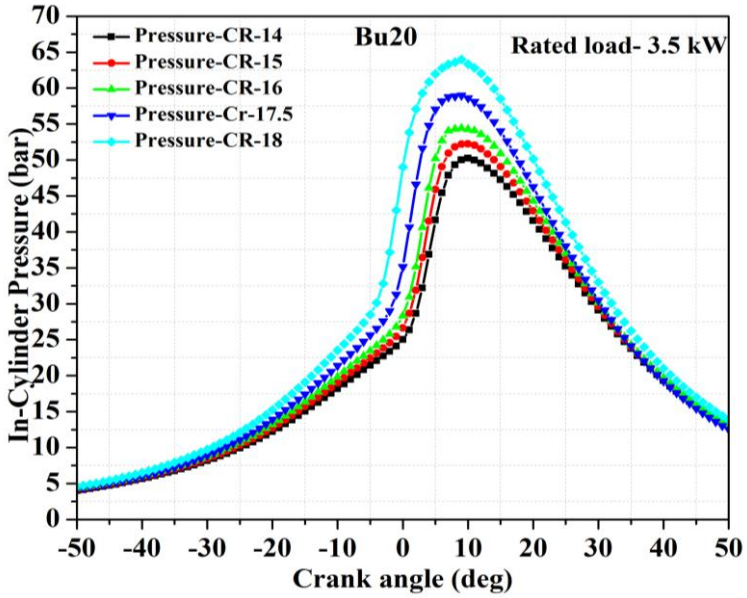

Fig. 4.44. Variation of in-cylinder pressure for Bu20 at different CRs at rated load.

Figures 4.44, 4.45, 4.46 and 4.47 depict the comparison of in-cylinder pressure and NHR for different butanol/diesel blends (Bu20 and Bu40) under different CR at the rated load. From the figures it is observed that, as the CR is increased from 14 to 18, the peak in-cylinder pressure increases for all butanol/ diesel blends. As mentioned earlier, the initial pressure and temperature of air inside the combustion chamber increase with increase in the CR. As seen from the figures, butanol/diesel blends have longer ignition delay and higher

NHR in the premixed combustion. This is because butanol/diesel blends have higher latent heat of vaporization and lower cetane number, which causes accumulation of a large quantity of fuel in the premixed zone. As a result, longer ignition delay and higher NHR occur in the premixed zone.

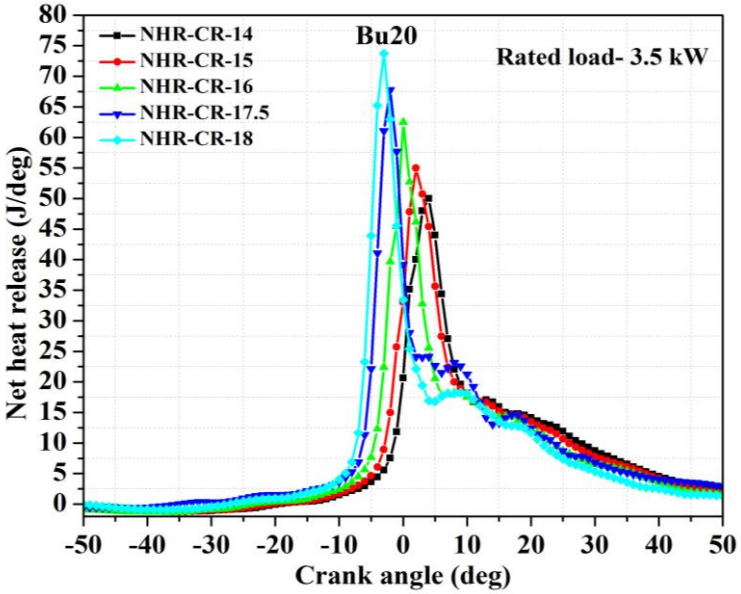

Fig. 4.45. Variation of NHR for Bu20 at different CRs at rated load.

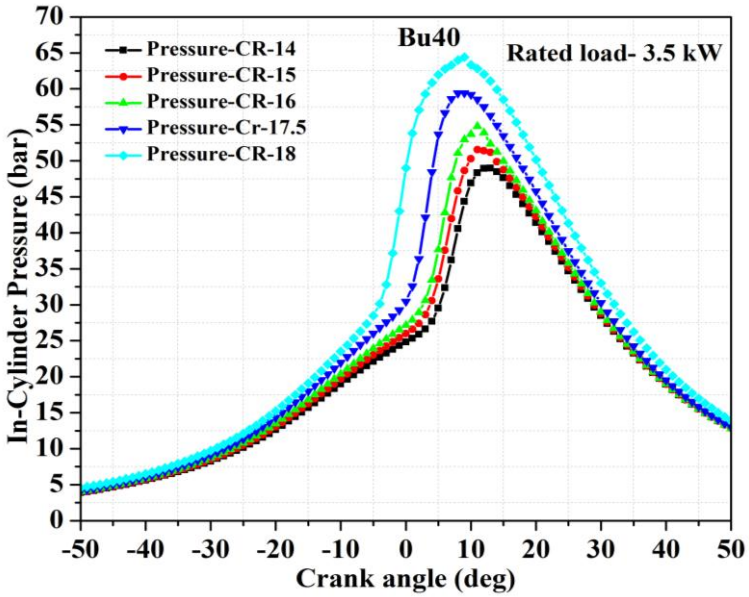

Fig. 4.46. Variation of in-cylinder pressure for Bu40 at different CRs at rated load.

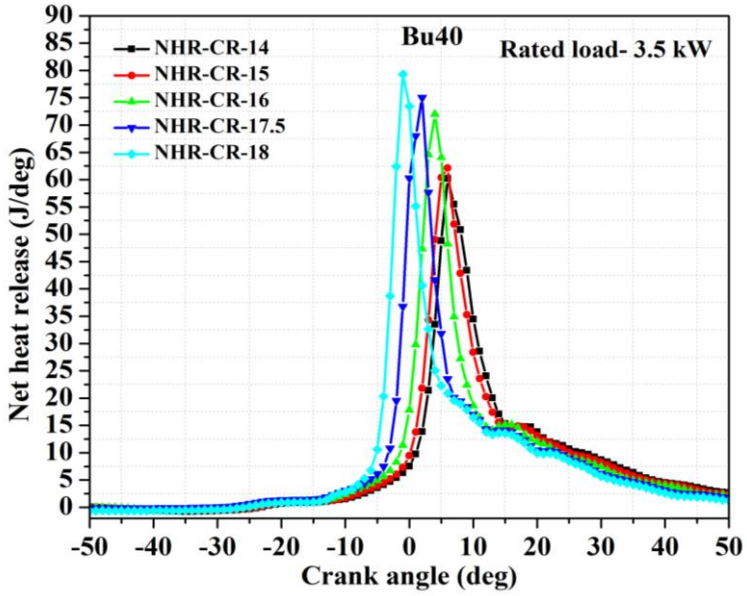

Fig. 4.47. Variation of NHR for Bu40 at different CRs at rated load.

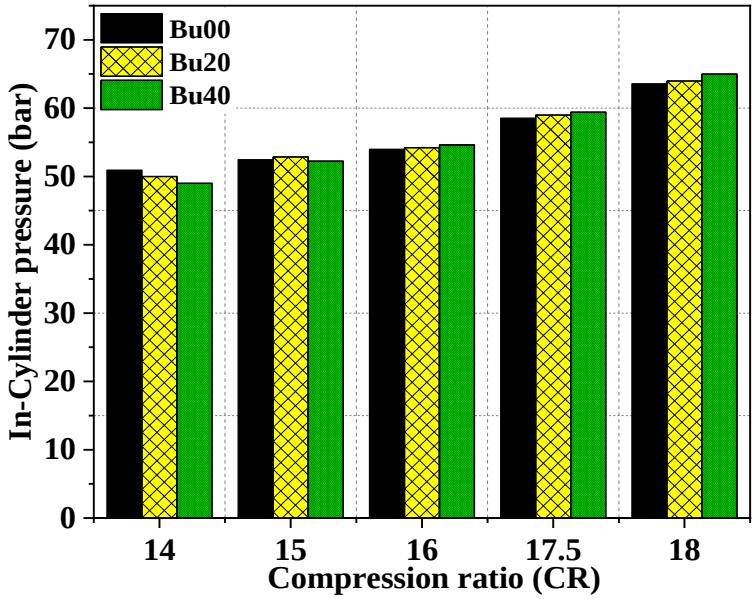

Fig. 4.48. Comparison of in-cylinder pressure at the rated load for different test fuels at different CRs.

Figure 4.48 depicts the comparison of in-cylinder pressure for different test fuels at different CR. It is observed from the figure that at lower CR, the butanol/diesel blends develop lower peak in-cylinder pressure compared to diesel. However, at higher CRs, it is the other way, i.e., the peak in-cylinder pressure is more for the butanol/diesel blends compared to diesel. At lower CR, the initial pressure and temperature are less. These lower temperature and pressure are not sufficient for early start of combustion. This causes longer ignition delay, leading to the combustion process extending into the expansion stroke. As a result, it reduced the peak in-cylinder pressure.

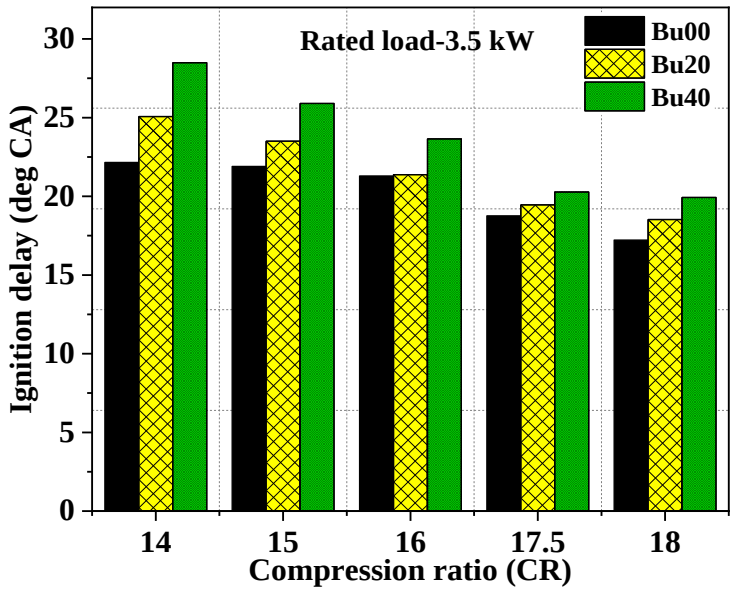

Fig. 4.49. Comparison of ignition delay at the rated load for different test fuels at different CRs.

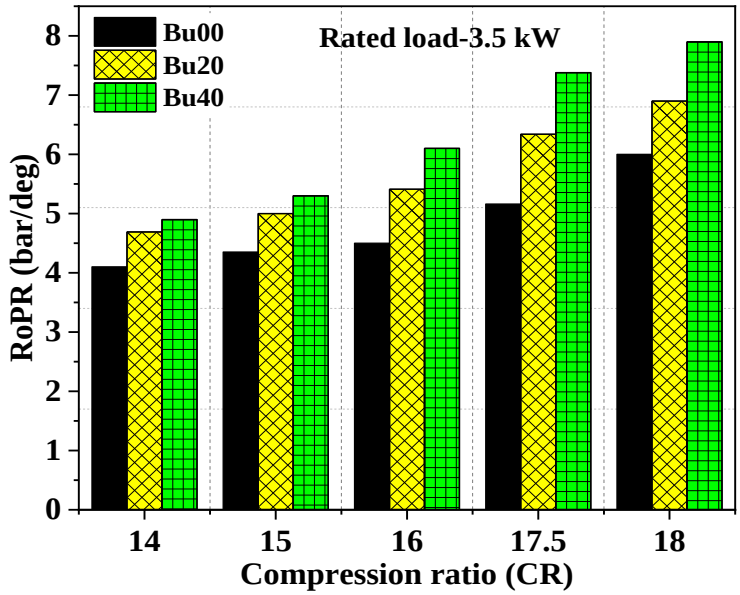

Fig. 4.50. Comparison of RoPR at the rated load for different test fuels at different CRs.

Figure 4.50 shows the variation of RoPR for different test fuels. It is noticed from the figure that increase in the CR from 14 to 18 results in the RoPR to increase for all the test fuels. With increase in the CR, the pressure and temperature increase during the engine compression process. This may facilitate rapid burning of fuel and release of heat energy in the premixed combustion zone. Similar trends for butanol/diesel were noticed from the figure. Butnol/diesel blends have higher RoPR than diesel fuel. This may be attributed to lower CN of butanol blends which causes prolonged ignition delay, as a result of which more

fuel accumulates in the premixed zone. This large amount of fuel releases higher heat release causing higher RoPR.

Figure 4.51 shows the comparison of EGT for different test fuels at different CRs. It is seen from the figure that as the compression ratio is increased from 14 to 18, the EGT increased for all the test fuels. These trends are similar to the peak in-cylinder pressure and NHR. It is also observed that the EGT was lower for the blends compared to diesel fuel at all the CRs.

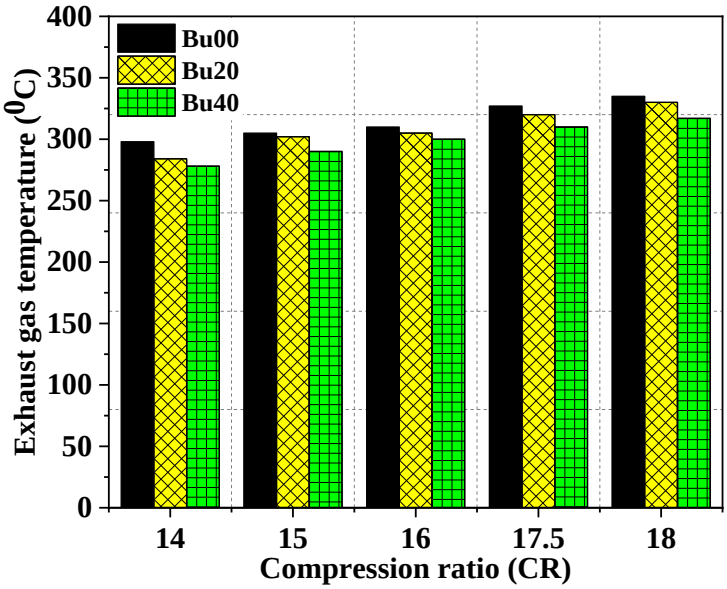

Fig. 4.51. Comparison of EGT at the rated load for different test fuels at different CRs.

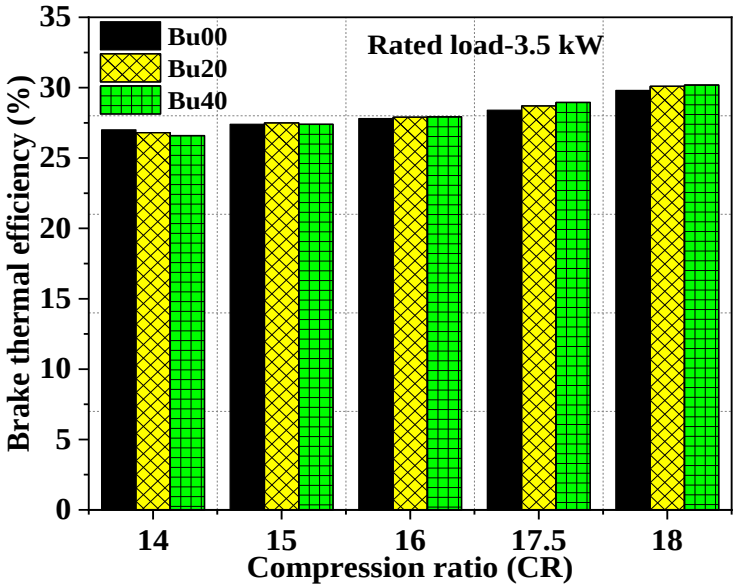

Fig. 4.52. Comparison of BTE at the rated load for different test fuels at different CRs.

From figure 4.52 it is observed that with increase in the CR from 14 to 18, the BTE increases for all test fuels. This is due to the fact that an increase in the CR causes complete combustion because the fuel is injected into a higher temperature and pressure chage which leads to better mixing of fuel with air and faster evaporation of fuel and better combustion.

4.4.2. Emission analysis for butanol/diesel blends at different CRs

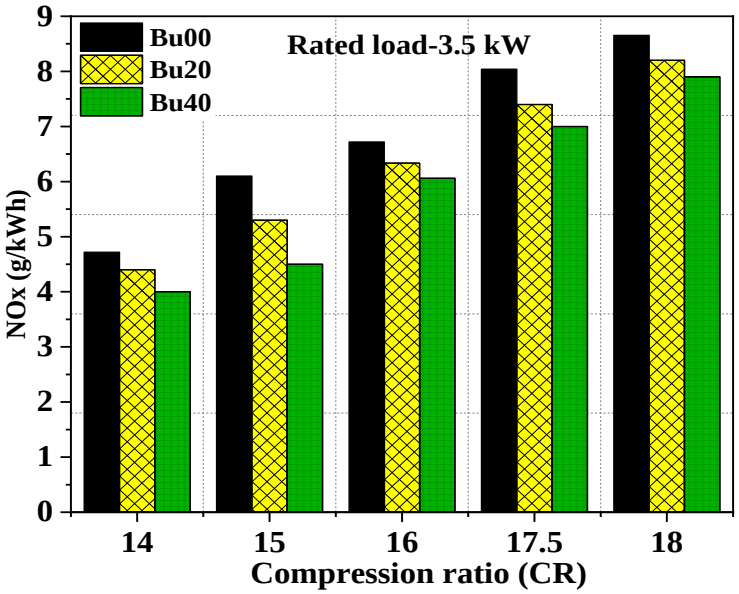

Fig. 4.53. Comparison of NOx for different test fuels at different CRs at rated load.

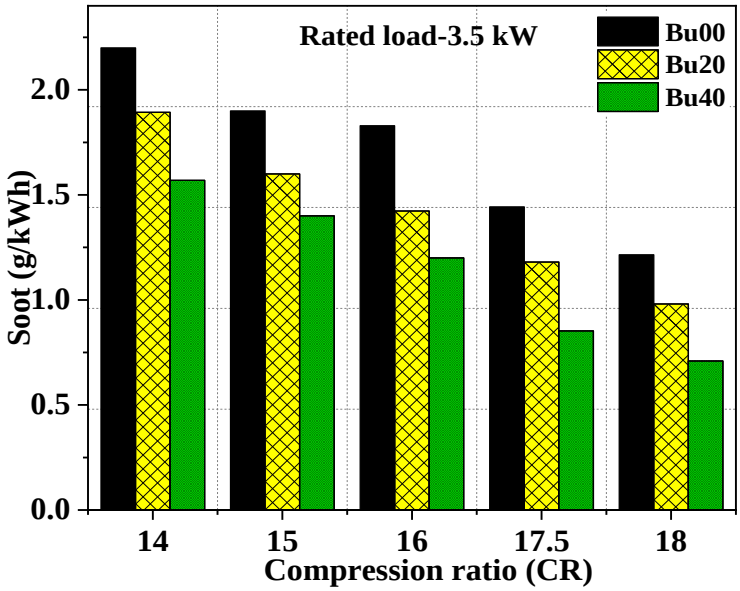

Fig. 4.54. Comparison of soot for different test fuels at different CRs at rated load.

As seen from figure 4.53 that increase in the CR from 14 to 18, increases the NOx emissions for all the test fuels. This may be on account of better combustion of fuel, which leads to higher temperature and as a result higher NOx emission formation. The NOx emission increased by 45.6%, 43% and 41.2% for Bu00, Bu20 and Bu40 when the CR was increased from 14 to 18.

The soot emissions for different butanol/diesel blends and diesel for different CR at the rated load are shown in figure 4.54. It is observed from the figure that the soot emission significantly decreases for all the test fuels with increase in the CR from 14 to 18. Higher CR develops higher swirl and turbulence inside the combustion chamber leading to better mixing of air and fuel and, as a result lower soot emission formation. Butanol/diesel blends develop lower soot emissions compared to diesel fuel at all the CRs. This is owing to the fact that butanol fuel has higher oxygen content in molecular structure, which helps complete combustion in the fuel-rich zone. Therefore, the soot growth rate decreases with increase of the volume fraction of butanol in the blends. The second reason may be that butanol has lower viscosity, density and higher volatility which leads to better mixing of fuel with air resulting in lower soot formation. The soot emission decreased by 41%, 48% and 55.25% for Bu00, Bu20 and Bu40, when CR increased from 14 to 18.

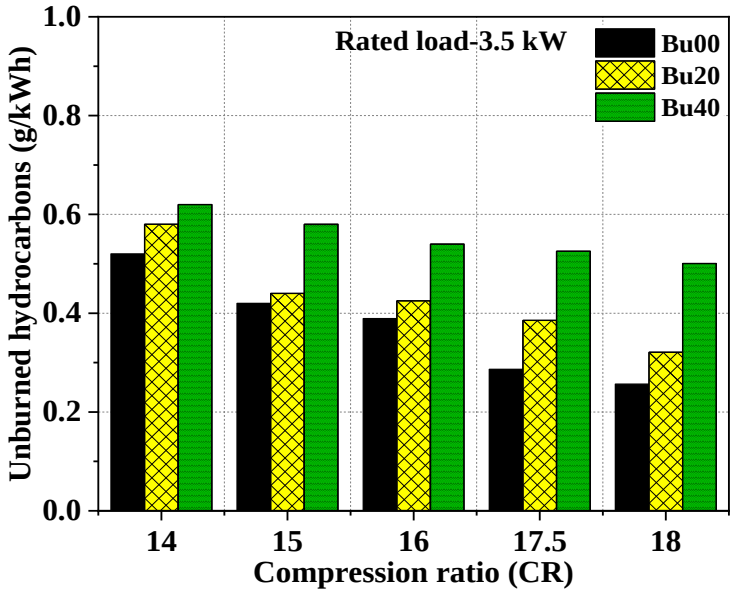

Fig. 4.55. Comparison of UBHC at the rated load for different test fuels at different CRs.

Figure 4.55 portrays the comparison of UBHC emissions for butanol/diesel blends and diesel fuel at different CRs. It can be seen from the figure that with increase in the CR from 14 to 18, the UBHC emissions significantly decreased. This is due to the rise in air

temperature at higher CR, improvement in combustion temperature that leads to better combustion, resulting in lower UBHC emission formation. The UBHC emission reduced by 50.25%, 44.62% and 22.5 % for Bu00, Bu20 and Bu40 blend with increase in CR from 14 to 18 at the rated load.

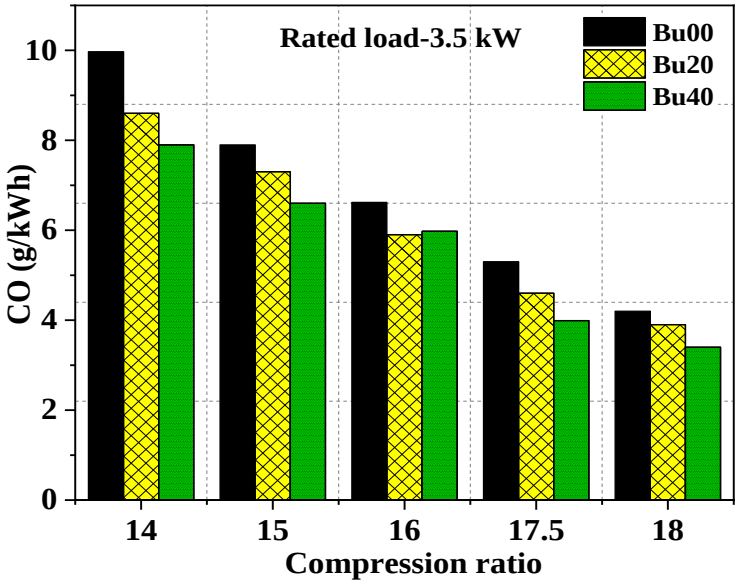

Fig. 4.56. Variation of CO emission at the rated load for different test fuels at different CRs.

Figure 4.56 depicts the comparison of CO emissions for different butanol/diesel blends for different CRs at the rated load. As shown in the figure, the CO emissions decrease with increase in the CR from 14 to 18 for all the test fuels. At higher CR, the CO emissions decrease due to better mixing of air and fuel. The CO emission decreased by 48.2%, 53.3% and 59.5% for Bu00, Bu20 and Bu40 blend with increase in the CR from 14 to 18 at the rated load.

4.5. Major Observations

Experimental studies were carried out to evaluate the influence of butanol/diesel blends (by volume of 20%, 30% and 40% butanol) on the combustion, performance and emission characteristics of a DI-CI engine at constant speed and varying loads. Experiments were also carried out to study the influence of EGR, FIP and CR on the characteristics of different test fuels. The effect of increasing the EGR rate up to 30%, CR from 14 to 18, and FIP from 200 to 280 bar was investigated for diesel and different butanol/diesel blends. The following conclusions were drawn from the experimental study:

- **At the baseline configuration of the engine**
  - The peak in-cylinder pressure was higher by 1.72%, 1.96% and 3.28% for Bu20, Bu30 and Bu40 blends, respectively compared to diesel fuel operation with the baseline configuration of the engine. The peak NHR was higher by 9.24%, 13.43% and 15% for Bu20, Bu30 and Bu40 respectively compared to diesel fuel operation.
  - The BSEC decreased by 2.54%, 4.74% and 4.93% for Bu20, Bu30 and Bu40 blends compared to diesel fuel operation at the rated load conditions. The BTE increased by 1.04%, 1.69% and 1.89% for Bu20, Bu30 and Bu40 blends compared to diesel fuel operation.
  - The RoPR increased with the increase of butanol content in the blends. The RoPR values were 5.16 bar/deg, 6.34 bar/deg, 6.8 bar/deg and 7.38 bar/deg for Bu00, Bu20, Bu30 and Bu40. This also indicates that the maximum permissible volume fraction of butanol in the blends is around 40%, without making any major modification to the engine configuration.
  - With increase in the butanol content, the ignition delay period increased, while the combustion duration decreased for butanol/diesel blends compared to diesel fuel.
  - With increase of butanol content in the blends, the soot, NOx and CO emissions decreased while the UBHC emissions increased compared to diesel fuel operation.
  - From the experiments it is observed that it is possible that up to 40% of butanol fraction (Bu40) can be used in the butanol/diesel blends, and the blends can replace diesel as fuel in the CI engine without major modifications to the engine.

- **Effect of EGR**

  - With increases in the EGR rate from 0 to 30%, the peak in-cylinder pressure, NHR and BTE decreased for all the test fuels, viz., Bu00, Bu20 and Bu40.
  - With increase in the EGR rate from 0 to 30%, the NOx emissions decreased drastically for all the butanol/diesel blends compared to diesel fuel operation. The NOx emissions decreased by 53.9%, 60.2% and 67% for Bu00, Bu20 and Bu40 blend at 30% EGR rate at the rated load compared to the baseline configuration.
  - The soot emissions decreased for all the butanol/diesel blends compared to diesel fuel without EGR. However, with EGR, the soot emissions increased slightly up to 20% EGR and drastically beyond 20% EGR, for all the blends.

- UBHC and CO emissions increased with increase of EGR for all the butanol/diesel blends compared to diesel fuel.

- **Effect of FIP**
  - It appeared that there exists an optimum FIP to every test fuel at which the performance was better and the emissions were minimum. However, this optimum FIP was found to be different for different test fuels. This optimum FIP was found to decrease with increase in the butanol content in the bend. For Bu00 and Bu 20 it was 260 bar while for Bu40 it was 240 bar.

- **Effect of CR**
  - Increasing the CR from 14 to 18 increased the peak in-cylinder pressure, NHR, EGT and BTE for all butanol/diesel blends and diesel fuel also.
  - With increase in the CR, the NOx emissions increased whereas the soot emissions decreased for all the test fuels.
  - The UBHC and CO emissions decreased with increase in the CR for all the test fuels.

Chapter 5

Numerical Studies - Results and Discussion

Parametric study to identify the ranges of the operating parameters of a DI-CI engine through numerical analysis

The objective of the present work is to study the effect of the engine operating parameters on the performance and emission characteristics of a DI-CI engine fuelled with different butanol/diesel blends. It was observed from the literature that the combustion and emission characteristics of a CI engine fuelled with biofuels is significantly influenced by the engine operating parameters. In the present study four operating parameters, viz., CR, FIP, EGR and SOI are considered to evaluate their effect on the engine performance and combustion characteristics, viz., ISFC, soot and NOx. But, the specific range of each one of these input parameters is not explicitly available in the literature. As a first step in the numerical analysis, the ranges of each one these four input parameters were identified by carrying out simulation experiments taking into consideration their effect on the three output parameters. The details of validation of the simulation model with the experimental results is discussed first. The effect of variation of the operating parameters on the engine combustion and emission characteristics is presented next. Finally, the ranges of the operating parameters considered for further studies is discussed.

5.1. Validation of the numerical model

Numerical studies were carried out on the same model of the VCR engine which was used for experimentation as discussed in Chapter 4. Initially, the numerical model was validated by comparing the simulation results with experimental results for diesel fuel (Bu00). Validation of the numerical results was done using experimental data by comparing

the performance (in-cylinder pressure) and emission (NOx and soot) characteristics. Experiments were carried out as discussed in Chapter 4, on a VCR DI-CI engine with diesel (Bu00) as the fuel. The engine validation was carried out for diesel fuel (Bu00), i.e., when the engine was running on pure diesel (Bu00). In this study, three different conditions (**case 1:** CR: 17.5, FIP: 220 bar, SOI: -23^{o} CA bTDC, EGR: 0%; **case 2:** CR: 17.5, FIP: 240 bar, SOI: -23^{o} CA bTDC, EGR: 0%, and **case 3:** CR: 17.5, FIP: 220 bar, SOI: -23^{o} CA bTDC, EGR: 20%,) were taken for validation and attempts were made to check the errors and trends between experimental and simulation results. Figure 5.1 shows the comparison of the simulation results with the experimental results in terms of pressure vs. crank angle variation. The trends of the simulation results are similar to that of the experimental results. It is observed that the maximum deviation in the peak in-cylinder pressure between the simulation and the experimental results was approximately 4.01 bar, which accounts for a difference of around 5.8%. Table 5.1 shows the comparison between the simulation and experimental results of emission and performance characteristics. The simulation results are nearly in good agreement with experimental results as the maximum difference between them is around 10%. However, the simulation values of the peak in-cylinder pressure were greater than the experimental values. This may be due to the fact that in a physical engine, blow by losses takes place, i.e., during compression stroke the gases may escape from the crevice region and end up with lower in-cylinder pressure, while in the simulation studies, this effect was not considered. Probably this may be the reason for the discrepancy between the experimental and simulation values of peak in-cylinder pressure. Based on the comparison of these characteristics, it was concluded that the simulation results are nearly in good agreement with the experimental results and further studies were carried out using the simulation model.

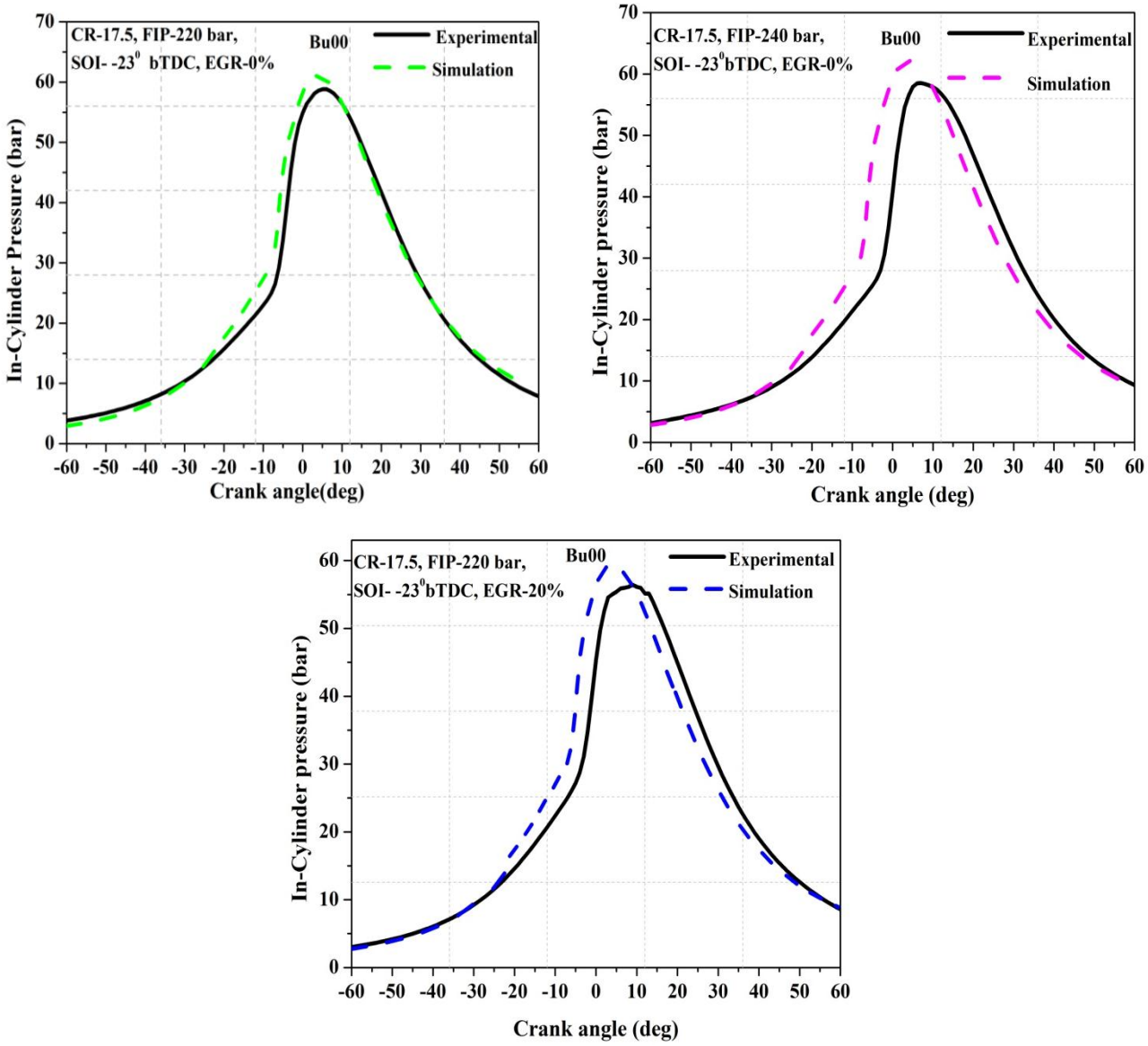

Fig. 5.1. Comparison of the simulation results with experimental data of the variation of in-cylinder pressure with crank angle for Bu00.

Table 5.1. Comparison of simulation and experimental results of performance and emissions for diesel fuel (Bu00).

	In-Cylinder pressure (bar)			**NOx (g/kWh)**			**Soot (g/kWh)**		
	Case 1	**Case 2**	**Case 3**	**Case 1**	**Case 2**	**Case 3**	**Case 1**	**Case 2**	**Case 3**
Experimental	57.95	58.12	53.99	8.04	8.16	6.3	1.44	1.23	1.63
Simulation	60.5	62.13	56.34	8.3	9.1	6.41	1.51	1.29	1.85
Error (%)	4.21	5.8	4.17	1.51	10.3	1.71	4.6	4.65	9.4

5.2. Effect of the engine operating parameters on the performance and emission characteristics

Having validated the numerical model with the experimental results, simulation studies were carried out by varying each one of the four operating parameters, viz., CR, FIP, EGR and SOI. The effect of varying the individual parameters was studied by keeping the other three parameters constant at the engine base configuration values of CR: 17.5, FIP: 220 bar, EGR: 0% and SOI: -23º CA bTDC. The effect of varying the operating parameters on the ISFC, soot and NOx emissions was analysed. Simulation studies were carried out by varying these input parameters in the following ranges: compression ratio (CR) from 14 to 19, fuel injection pressure (FIP) from 200 to 300 bar, exhaust gas recirculation (EGR) from 0 to 40% and, start of injection (SOI) from -17º CA bTDC to -32º CA bTDC. All the simulation runs were carried out at rated the load and the rated speed of the engine (1500 rpm). The analysis of these simulation studies is presented in the following sections.

5.2.1. Effect of compression ratio (CR) on the performance and emission characteristics

CR is defined as the ratio of total volume to clearance volume. So, the CR mainly depends on the clearance volume and total volume of the cylinder. In an actual engine, it is quite easy to achieve lower CR whereas higher CR is limited by the lowest possible clearance volume when the position of piston is at TDC. The minimum clearance volume for any particular piston bowl is fixed and thereby restricts the CR on the higher side. The CI engine can operate with a compression ratio of 12 to 24. In the present analysis, the CR is fixed from 14 to 19, due to the design constraints of the VCR engine.

The numerical analyses were carried out by varying the compression from 14 to 19. The effect of CR on the in-cylinder combustion characteristics is discussed in the following sections.

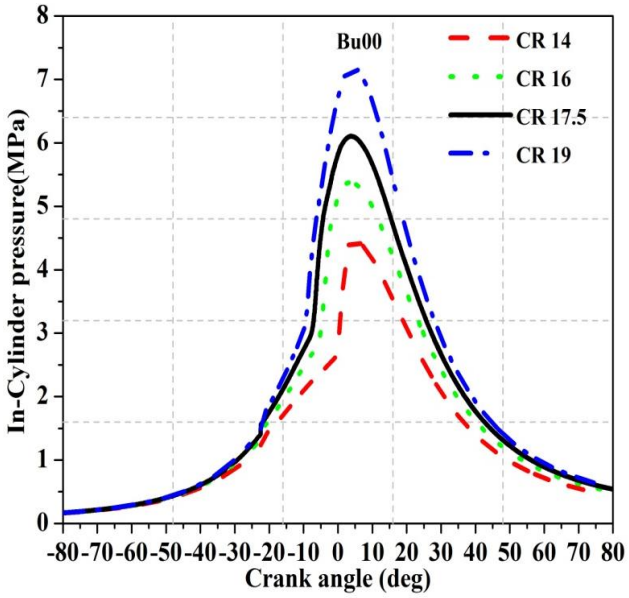

Fig. 5.2. Variation of in-cylinder pressure with crank angle for different CRs.

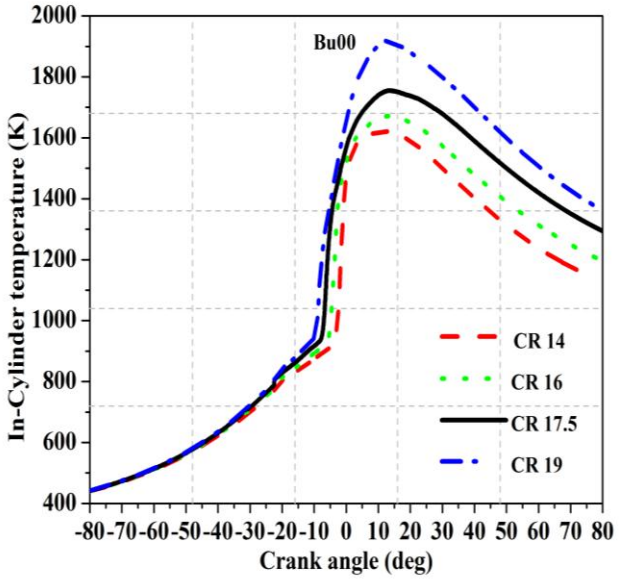

Fig. 5.3. Variation of in-cylinder temperature with crank angle for different CRs.

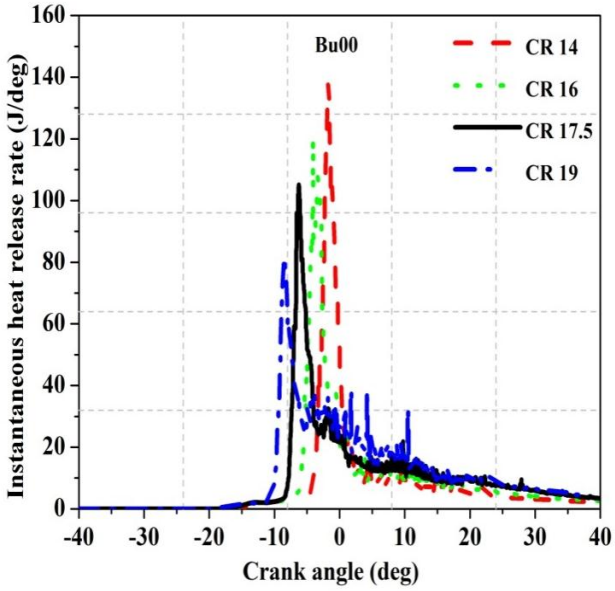

Fig. 5.4. Variation of instantaneous heat release rate with crank angle for different CRs.

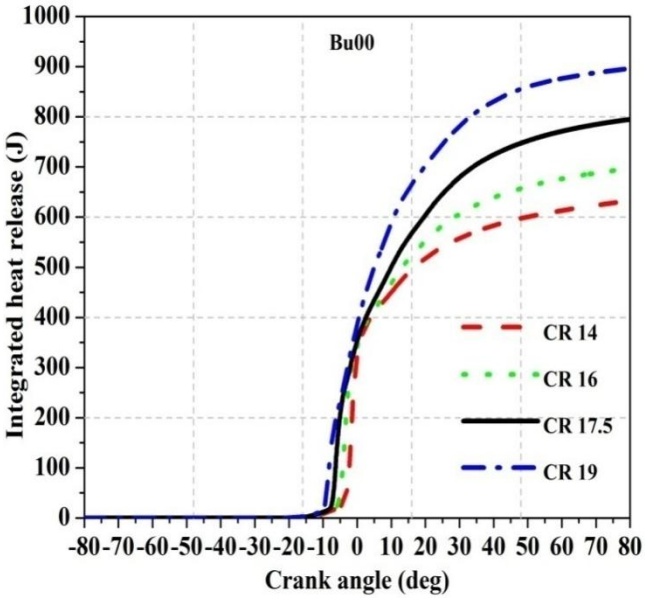

Fig. 5.5. Variation of integrated heat release with crank angle for different CRs.

From the figures 5.2 and 5.3, it is observed that as the CR is increased from 14 to 19, the peak in-cylinder pressure increases from 47 bar to 76 bar and the in-cylinder temperature increases from 1653 K to 1930 K. This is due to the reason that as the CR increases, the pressure and temperature of the charge increase, and as a result the ignition delay reduces. The ignition delay is reduced from 19.52 to 11.52 CA, as the CR is increased from 14 to 19. At higher CR, the instantaneous heat release rate (IHRR) is lower in the premixed combustion zone, whereas IHRR is higher in the diffusion combustion zone (figure 5.4). Since the ignition delay is short, only a small quantity of accumulated fuel is available during

the ignition delay period and this results in lower peak IHRR during the premixed combustion zone. However, the integrated heat release (IHR) (accumulated heat release) (figure 5.5) increases from 628 J to 923 J, as the compression ratio is increased from 14 to 19. Because of higher pressure and temperature of the charge, the combustion process also progresses rapidly.

Figure 5.6 shows that as the CR is increased the swirl ratio increases (from 1 to 1.7), which contributes to better mixing of air-fuel, and hence better combustion. Figure 5.7 shows the fuel distribution index at different crank angles (from crank angle 0 to 35° CA aTDC). At 0° CA aTDC, the TFDI (Target Fuel Distribution Index) for CR of 14 and CR of 19 were observed to be 15.2% and 28.2% respectively. Similarly, at 35° CA aTDC, the TFDI for CR of 14 and CR of 19 were observed to be 41.72% and 77.72% respectively. Thus, it can be observed that at any instant, as the CR is increased, the TFDI increases. For the increase of CR from 14 to 19, at 35° CA aTDC, the TFDI increased by 46.56%. The increase in the TFDI is associated with a proportionate reduction in the RFDI and LFDI. The RFDI and LFDI reduced with 35.2% and 79.19% respectively at 35° CA aTDC, as the CR is increased from 14 to 19. This shows that better fuel distribution occurred at higher CR, as a result of which there was better air-fuel mixing. The cumulative effect of these factors resulted in increased IHR. Increased IHR results in higher values of peak in-cylinder pressure and temperature.

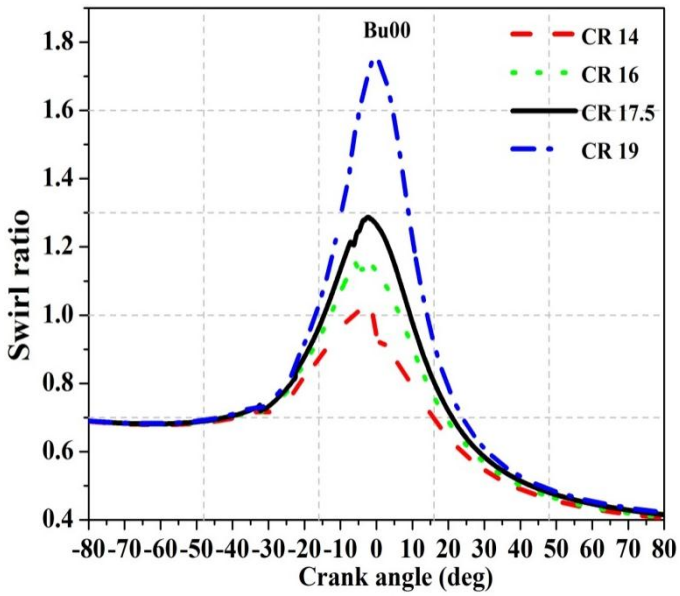

Fig. 5.6. Variation of swirl ratio with crank angle for different CRs.

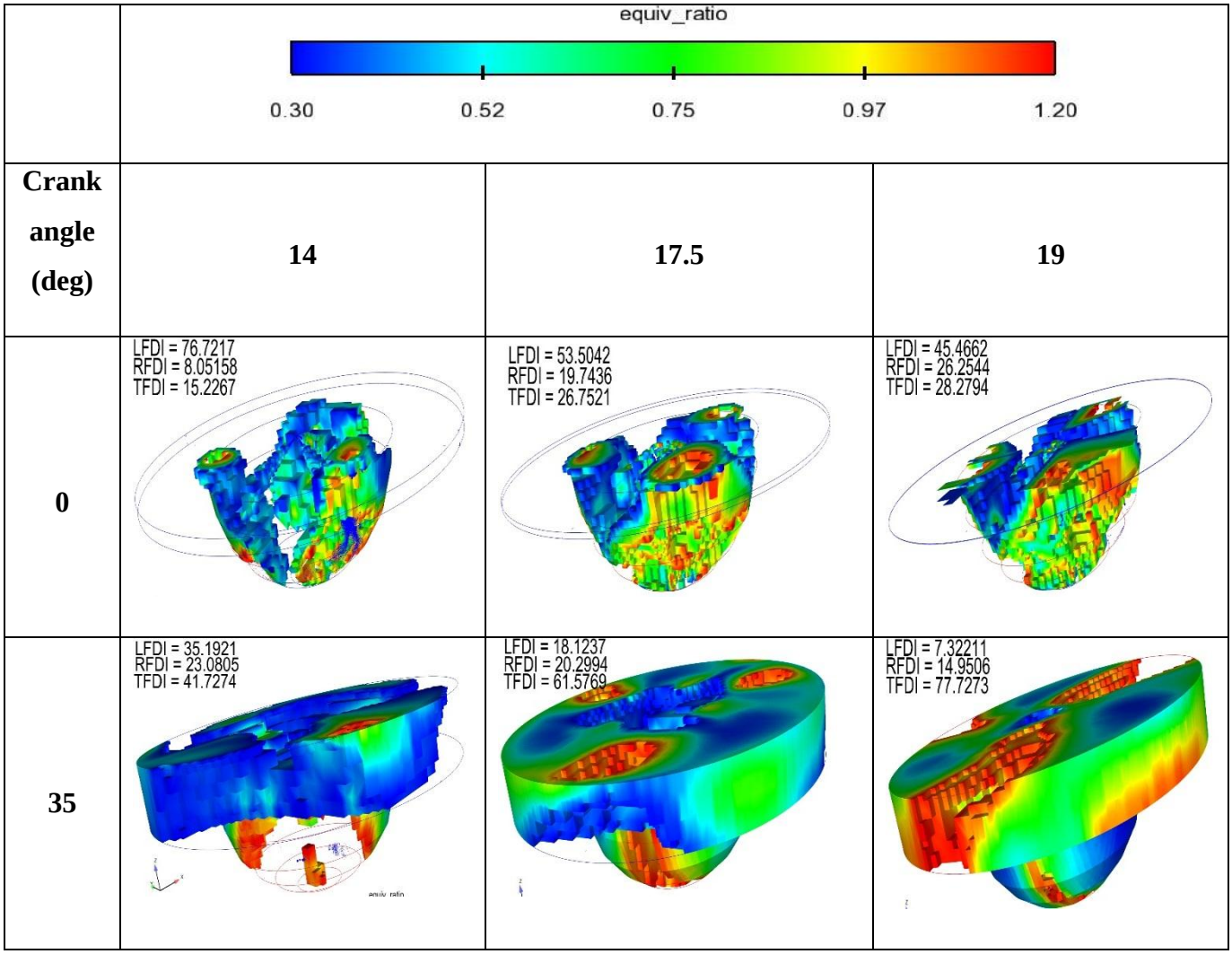

Fig. 5.7. Variation of fuel distribution index with crank angle for different CRs.

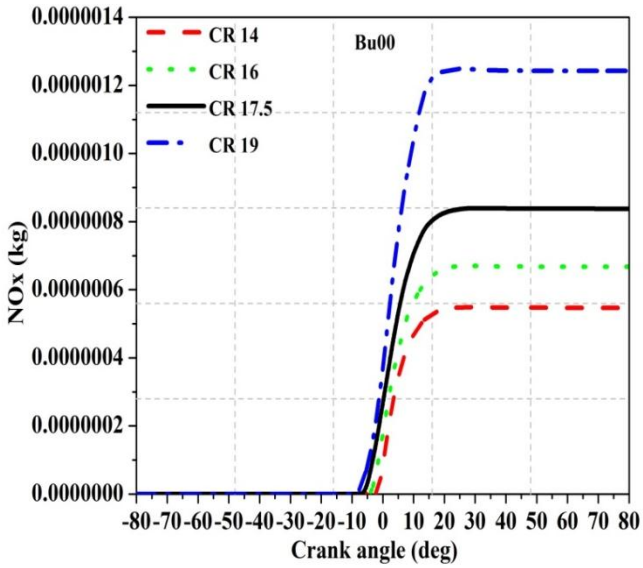

Fig. 5.8. Variation of NOx emission with crank angle for different CRs.

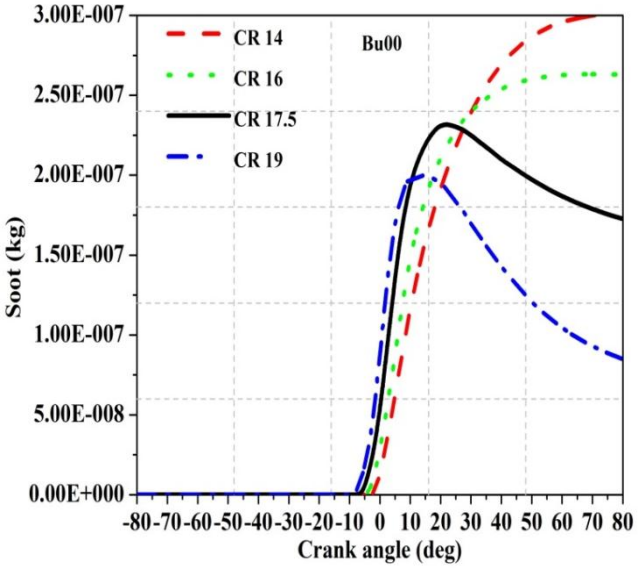

Fig. 5. 9. Variation of soot emission with crank angle for different CRs.

It can be seen from figure 5.8 that with an increase in the CR, the NOx emission increased. This is because the in-cylinder temperature increases (as shown in figure 5.3), which is favourable to increase the NOx emissions. From figure 5.9, it can be observed that the soot emission decreases with increase in the CR. This may be because of increased soot oxidation process caused by higher swirl ratio (figure 5.6), which is attained at higher CR.

It is observed from figure 5.10 that with increase in the CR, the UBHC emissions decrease. This is because at higher CR, the in-cylinder temperature increases, which leads to better combustion. It is also observed that as the CR is increased, the CO emission (figure 5.11) decreases, whereas the CO_2 emission (figure 5.12) increases. At higher CR, sufficient amount of heat is delivered; as well as the higher swirl ratio leads to better oxidation of CO emission. Hence, CO_2 emission increases with increase in the CR.

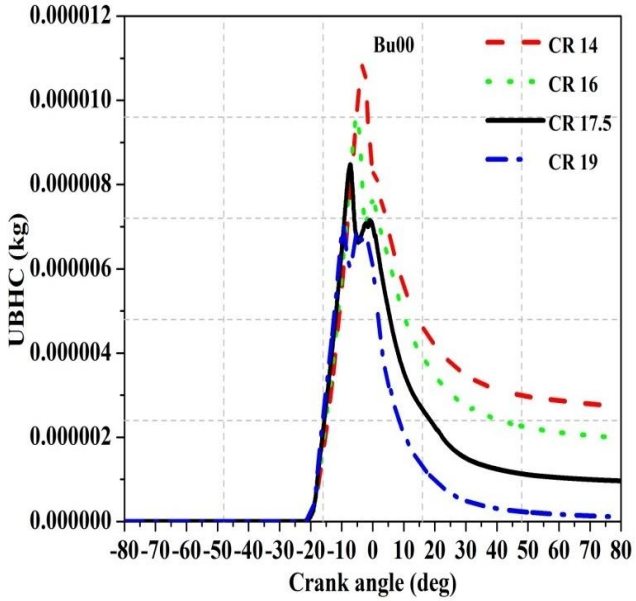

Fig. 5.10. Variation of UBHC with crank angle for different CRs.

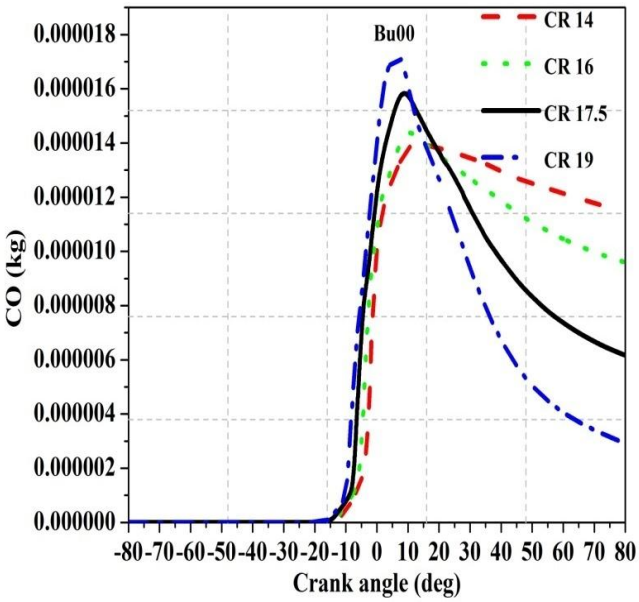

Fig. 5.11. Variation of CO with crank angle for different CRs.

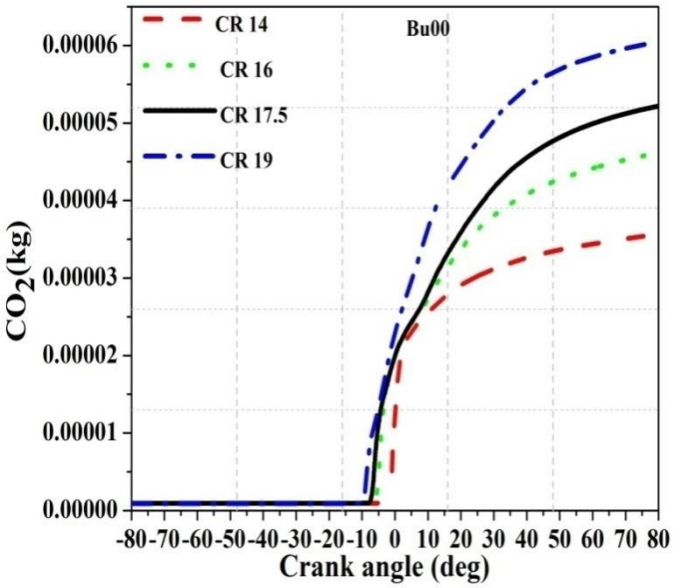

Fig. 5.12. Variation of CO_2 with crank angle for different CRs.

Figure 5.13 shows the effect of CR on the ISFC. As the CR is increased from 14 to 19, the ISFC decreased from 281 g/kWh to 191 g/kWh, around 32% decrement. Figure 5.14 shows the effect of CR on the NOx emission. As the CR is increased from 14 to 19, the NOx emission increases from 6.3 g/kWh to 12.3 g/kWh, around 48% increase. It can be seen from figure 5.14 that soot emission decreased from 3.5 g/kWh to 0.5 g/kWh (around 85% decreased) as CR increased from 14 to 19.

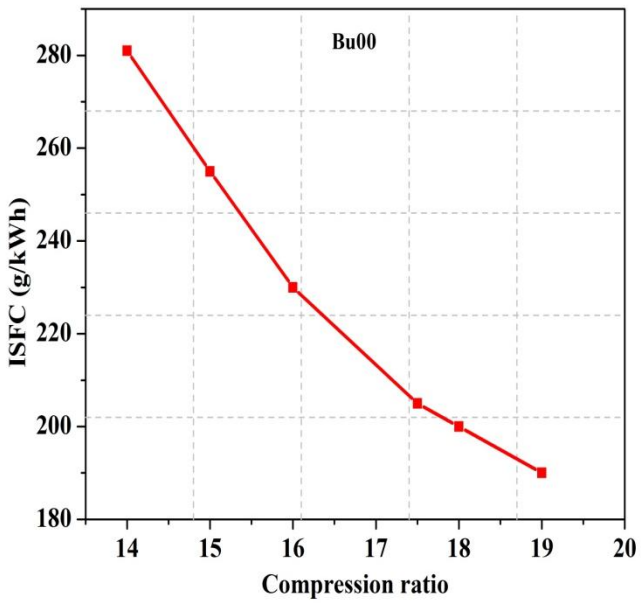

Fig. 5.13. Variation of IFSC with different CRs.

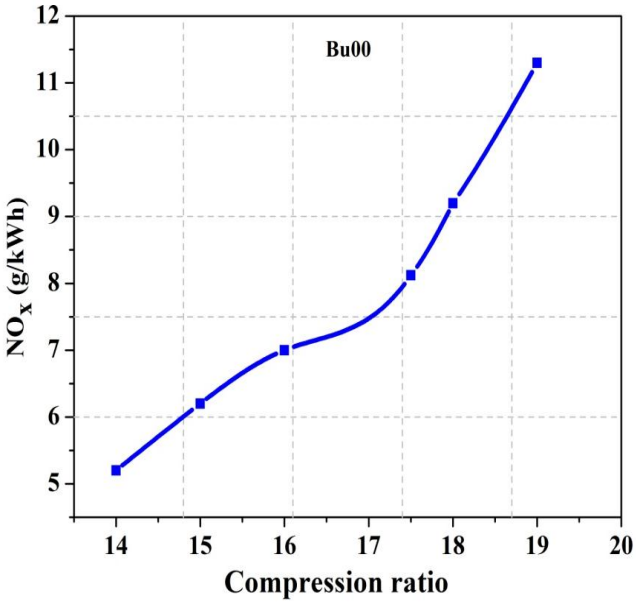

Fig. 5.14. Variation of NOx with different CRs.

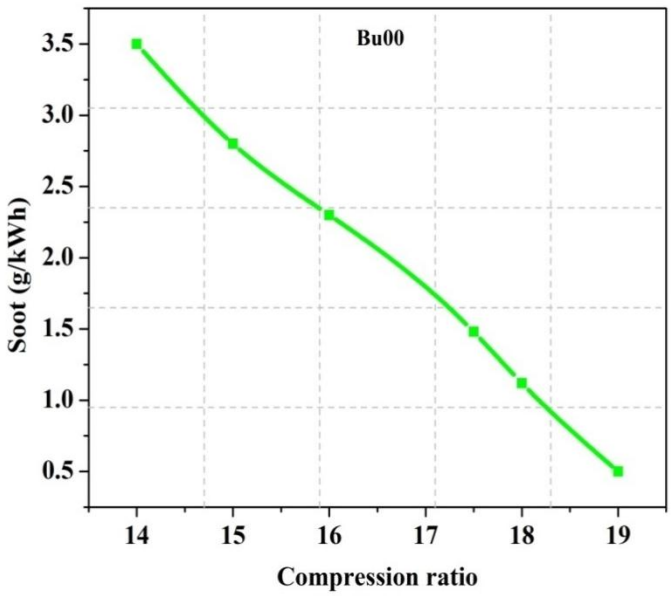

Fig. 5.15. Variation of soot with different CRs.

5.2.2. Effect of fuel injection pressure (FIP) on the performance and emission characteristics

FIP is the pressure at which the fuel is injected into the cylinder through the fuel injection system. FIP has a major role on the performance and emission characteristics of the engine. The FIP system is used in the engine to achieve better atomization and longer penetration into combustion chamber. Higher FIP provides better atomization of fuel particles in shorter duration, and hence results in higher combustion efficiency. The common rail direct injection (CRDI) engines can operate up to 3000 bar. Gasoline direct injection (GDI) can operate up to 200 bar. Therefore, the fuel injection pressure depends on the type of engine. The Kirloskar - TV1 VCR engine can operate at 200 bar to 280 bar. In the present numerical analysis, the FIP is varied from 200 bar to 300 bar.

Simulation runs were carried out by varying the FIP from 200 bar to 300 bar with all the other parameters being kept constant (CR of 17.5, EGR- 0% and SOI of -23º CA bTDC, at baseline configuration). It is observed from figures 5.16 and 5.17 that as the FIP is increased, the peak in-cylinder pressure increases from 59 to 64 bar, and the mean in-cylinder temperature increases from 1716 K to 1850 K. It may be explained that as the FIP is increased, it results in better atomization and easy vaporization of the fuel inside the combustion chamber. This causes the fuel to have larger contact surface area and better air-fuel mixing in the combustion chamber. Better atomization also results in decrease in the physical ignition delay, and this proportionately decreases the overall ignition delay period

(decreased from 10.5 to 9.8 CA from the figure 5.18). Therefore, combustion occurs simultaneously at different locations, resulting in higher value of IHR (figure 5.19). The IHR (accumulated heat release) increased from 812 J to 890 J, as the FIP increased.

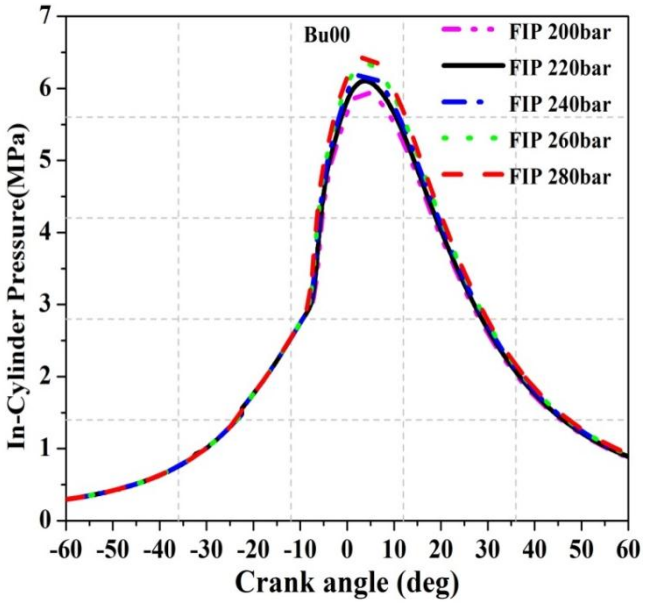

Fig. 5.16. Variation of in-cylinder pressure with crank angle for different FIPs.

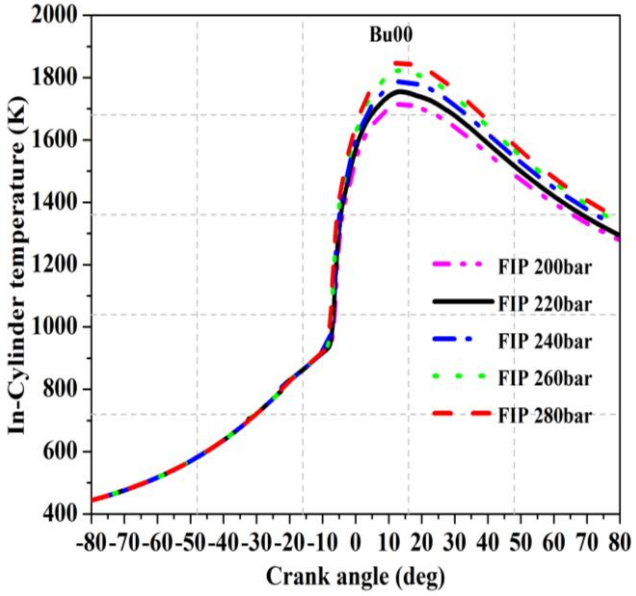

Fig. 5.17. Variation of in-cylinder temperature with crank angle for different FIPs.

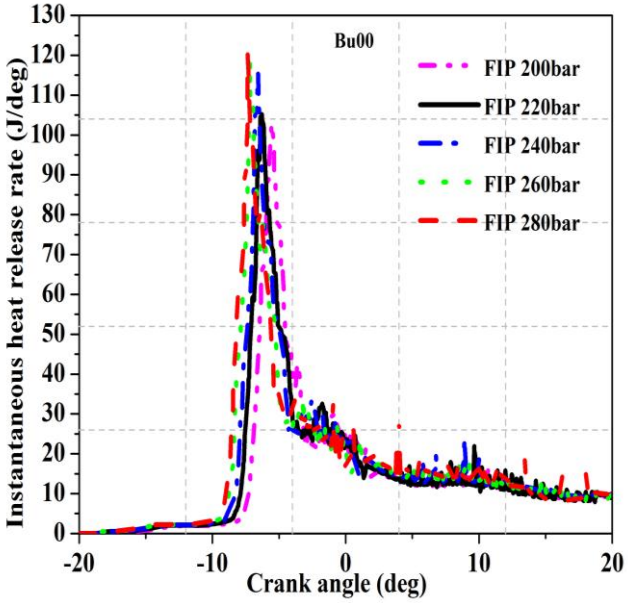

Fig. 5.18. Variation of IHRR with crank angle for different FIPs.

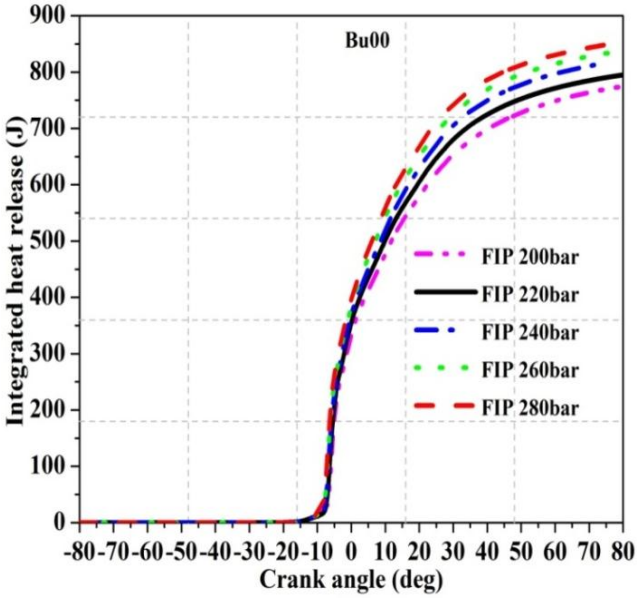

Fig. 5.19. Variation of IHR with crank angle for different FIPs.

The fuel distribution index at different crank angles is shown in figure 5.20. From the figure it is evident that as the FIP is increased from 200 to 280 bar, the TFDI increased by 15.4%, at 35° CA aTDC. Similarly, at 35° CA aTDC, the LFDI and RFDI decreased by 37.79% and 9.48% respectively. This indicates that higher FIP provides better air-fuel

mixture inside cylinder. The cumulative effect of all these factors results in increased IHR. The increased IHR results in higher values of peak in-cylinder pressure and temperature.

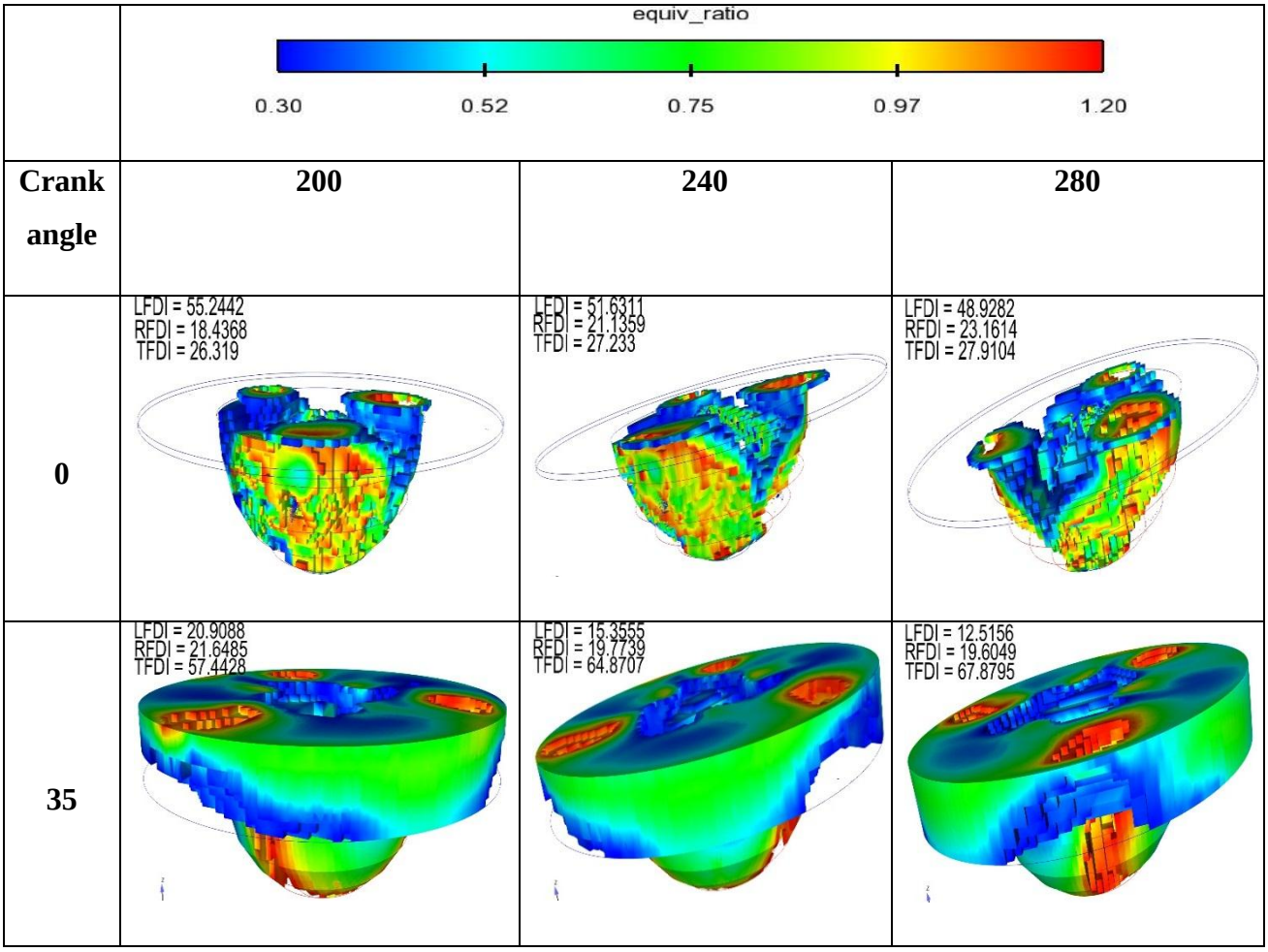

Fig. 5.20. Variation of fuel distribution index with crank angle for different FIPs.

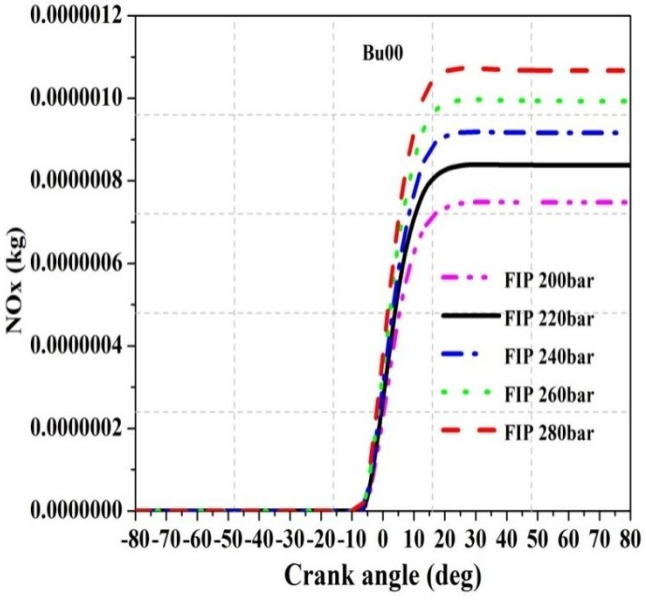

Fig. 5.21. Variation of NOx emission with crank angle for different FIPs.

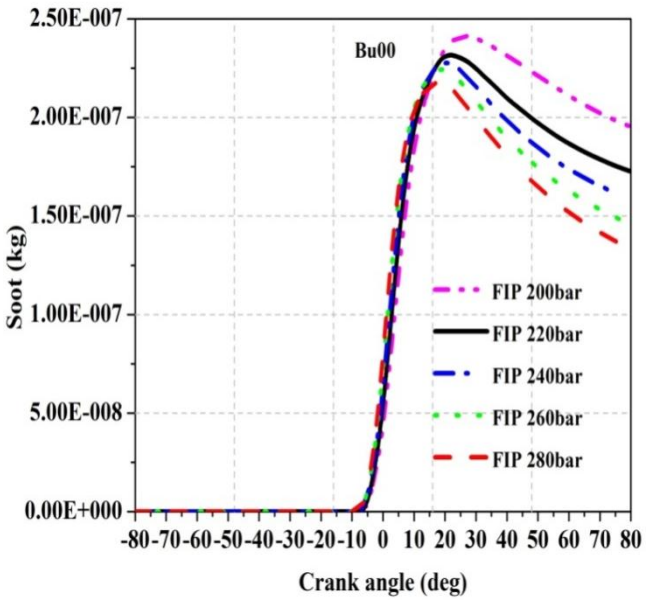

Fig. 5.22. Variation of soot emission with crank angle for different FIPs.

From the figures 5.21 and 5.22, it is observed that with increase in the FIP, the NOx emission increases whereas the soot emission reduces. This is due to better mixing of air-fuel and fuel penetration inside the combustion chamber. Therefore, it reduces the soot emissions whereas the NOx emissions increase due to higher combustion temperature (figure 5.17).

The UBHC emissions decrease with increase in the FIP (figure 5.23). This is because at higher FIP, the in-cylinder temperature increases, which leads to lowering UBHC emission. Also, it was observed that as the FIP is increased, the CO emission (figure 5.24) decreased whereas the CO_2 emission (figure 5.25) increased. At higher FIP, the fuel droplets size is very small and more contact surface area is available for combustion and as a result better homogeneous air –fuel mixture is formed. This causes better oxidation of the CO emission. Hence, the CO_2 emission increases with increase in the FIP.

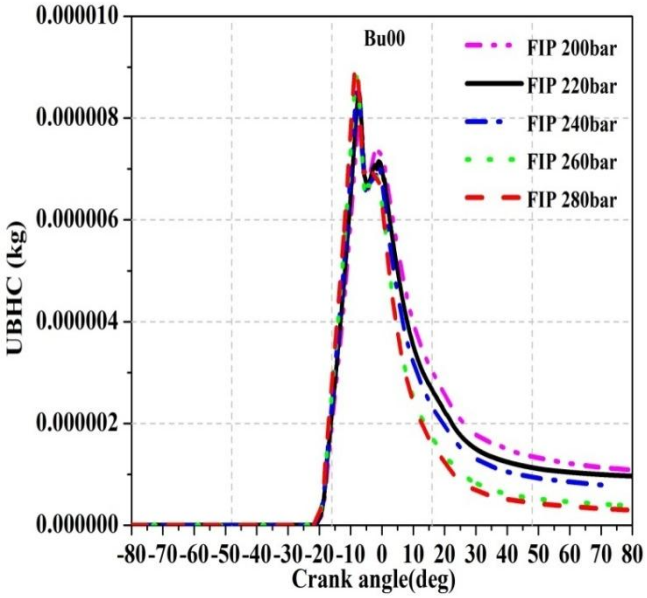

Fig. 5.23. Variation of UBHC emission with crank angle for different FIPs.

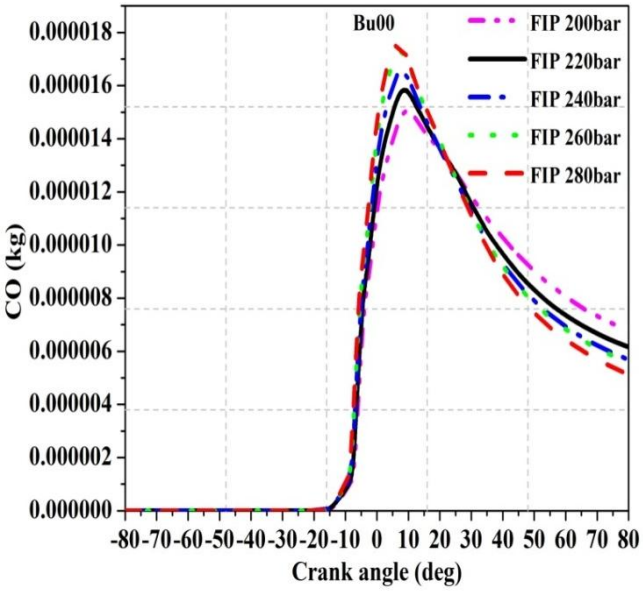

Fig. 5.24. Variation of CO emission with crank angle for different FIPs.

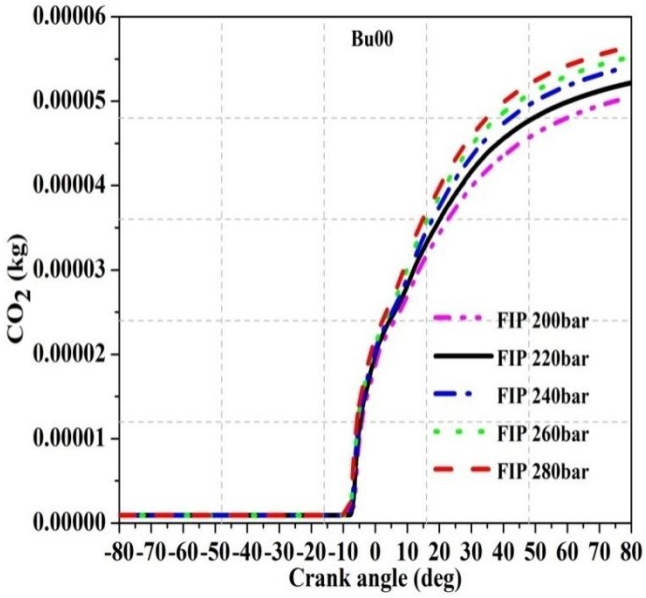

Fig. 5.25. Variation of CO_2 emission with crank angle for different FIPs.

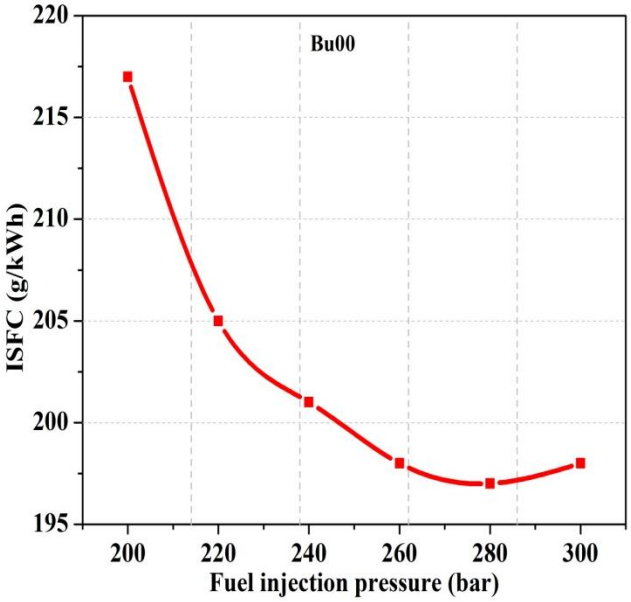

Fig. 5.26. Effect of FIP on the ISFC.

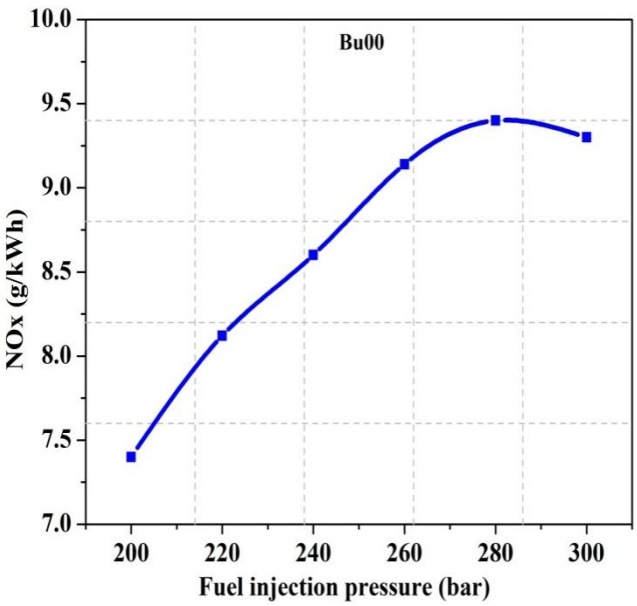

Fig. 5.27. Effect of FIP on the NOx.

It can be seen from the figure 5.26 that as the FIP is increased from 200 bar to 280 bar, the ISFC decreased from 217 g/kWh to 197 g/kWh (around 9% decreased). It is noticed from figures 5.27 and 5.28 that as the FIP is increased from 200 bar to 280 bar, the NOx emissions increased from 7.4 g/kWh to 9.6 g/kWh (around 23% increase) and the soot emissions decreased from 1.73 g/kWh to 0.95 g/kWh (around 45% decrease).

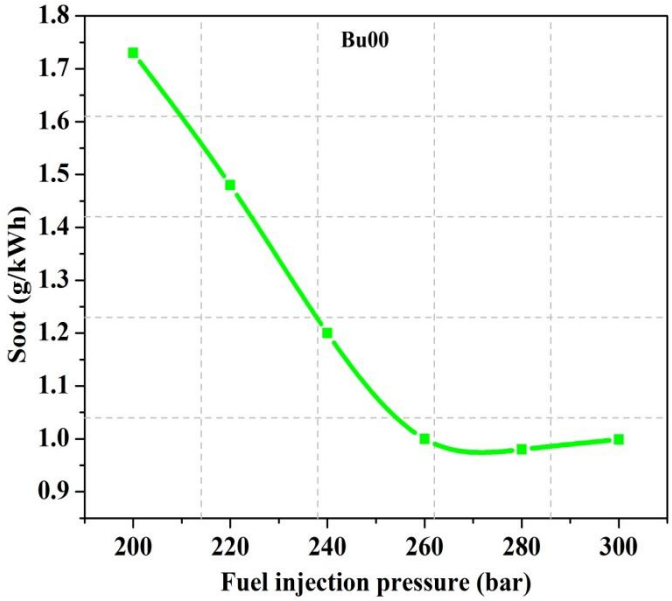

Fig. 5.28. Effect of FIP on the soot.

Crank angle	280	300
35	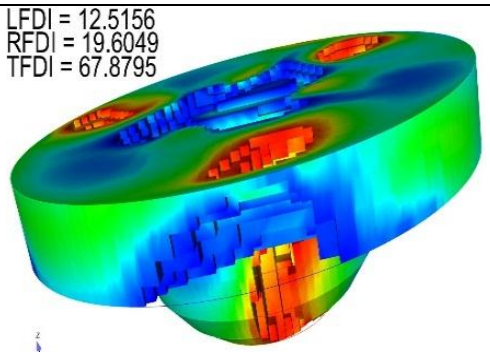	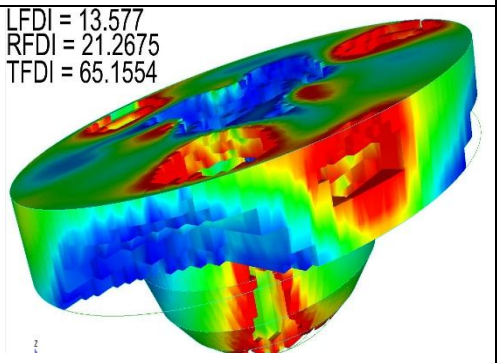

Fig. 5.29. Variation of fuel distribution index for different FIPs (280 bar and 300 bar).

On further increasing FIP from 280 to 300 bar, the ISFC, NOx and soot emission trends are reverse. This is because, if the FIP is too high, there is a possibility of the fuel impinging on the piston surface and the cylinder walls. From the Table 5.2, it is clearly observed that as FIP increased from 200 bar to 280 bar, the TFDI increased whereas the LFDI and RFDI decreased. Further increase in FIP from 280 bar to 300 bar, TFDI is decreased whereas the LFDI and RFDI increased. Figure 5.29 shows the fuel distribution index for different FIPs. At 35° CA aTDC, the RFDI (Rich Fuel Distribution Index) for FIP of 280 bar and FIP of 300 bar were observed to be 19.6 % and 21.62% respectively. Thus, it can be observed that at 35° CA aTDC, as the FIP is increased the 280 bar to 300 bar RFDI increased by 7.2% (It means the rich fuel (red colour) is increased at cylinder wall-more

fuel). It results in incomplete combustion and loss of performance. Probably this may be the reason for the increase in ISFC and soot emission at 300 bar for diesel fuel.

Table 5.2. Variation of fuel distribution index for different FIPs at 35º CA aTDC.

FIP (bar)	LFDI	RFDI	TFDI
200	20.09	21.64	57.44
220	18.12	20.29	61.57
240	15.35	19.77	64.87
260	13.25	19.70	65.85
280	12.51	19.60	67.87
300	13.57	21.2	65.15

5.2.3. Effect of exhaust gas recirculation (EGR) on the performance and emission characteristics

EGR has limited range for conventional DI-CI engine due to its trade-off between the soot and NOx emission. To find the best trade-of-relation between the NOx and soot, the simulation runs were carried out by varying the EGR rate from 0 to 40% with all the other parameters being kept constant (CR of 17.5, SOI of -23º CA bTDC and FIP of 220 bar-at baseline configuration).

External EGR is a well-known technique to reduce the NOx emissions in the diesel engine. The recirculated exhaust gas contains more CO_2 and H_2O, compared to the fresh charge which contains O_2 and N_2. The specific heats of CO_2 and H_2O are higher compared to the specific heats of O_2 and N_2. Therefore, the introduction of EGR into the cylinder results in lowering the gas temperature and cylinder temperature during the combustion process. This is called the thermal effect of EGR. As the EGR rate is increased, it results in reducing the oxygen content in the fresh charge. This is called the dilution effect of EGR. Simultaneously, with the introduction of EGR, the recirculated water vapour and CO_2 of EGR dissociate during combustion, modifying the combustion process. In particular, the endothermic

dissociation of H_2O results in a decrease of the flame temperature. This is called the chemical effect of EGR.

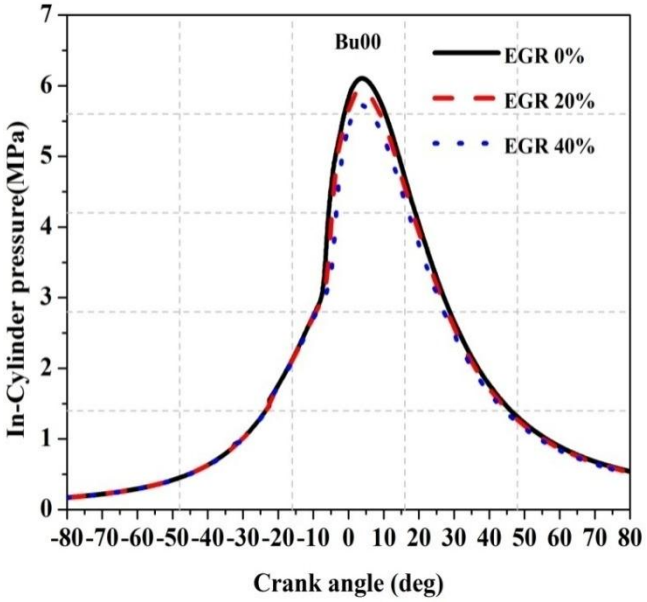

Fig. 5.30. Variation of in-cylinder pressure with crank angle for different EGR rates.

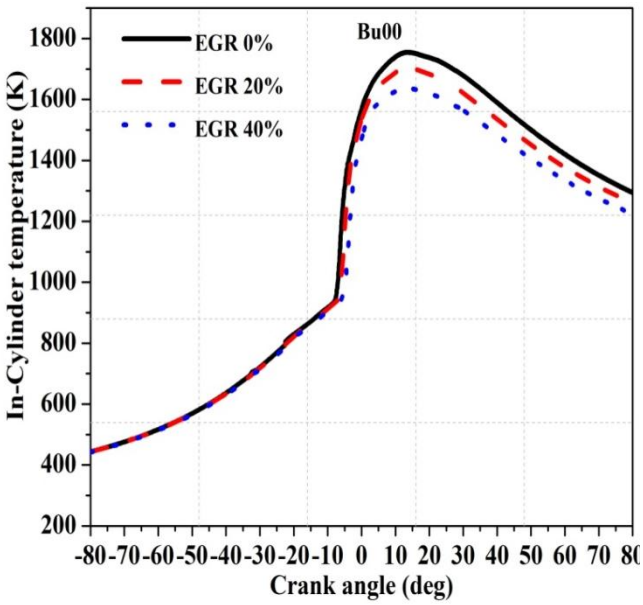

Fig. 5.31. Variation of in-cylinder temperature with crank angle for different EGR rates.

From figures 5.30 and 5.31, it was observed that the in-cylinder pressure decreases from 61 bar to 56 bar, and also, the mean in-cylinder temperature decreases from 1754 K to 1630 K with increase of the EGR rate from 0 to 40%. As mentioned earlier, this is due to the thermal effect, the charge temperature decreases with increase of the EGR and hence the ignition delay period increases proportionately. Because of the thermal effect, the mean in-cylinder temperature decreases (figure 5.31). This results in sluggish combustion in the premixed combustion region and proportionately the in-cylinder pressure and temperature decrease. The dilution effect results in incomplete combustion, and thereby reduces the IHRR and IHR (figures 5.32 and 5.33). As the EGR rate is increased, the oxygen content in the air-fuel mixture is reduced, which creates larger a region of the rich air-fuel mixture.

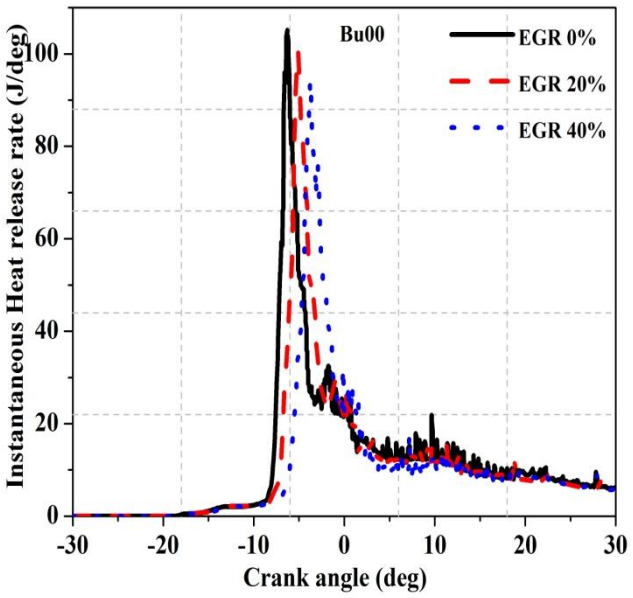

Fig. 5.32. Variation of IHRR with crank angle for different EGR rates.

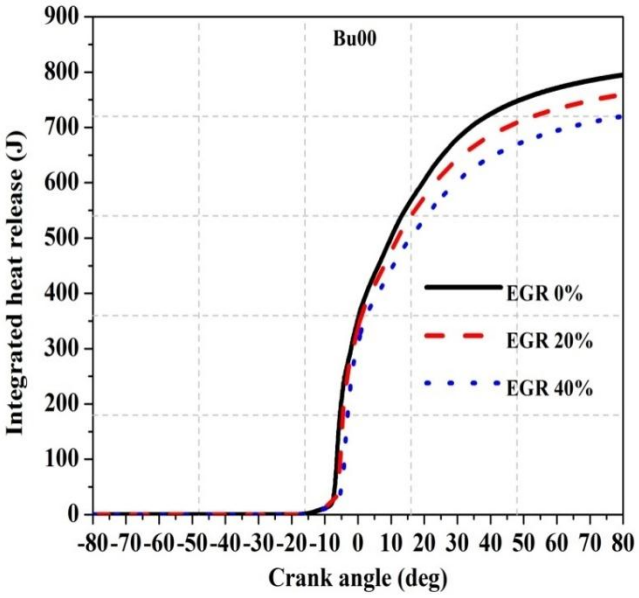

Fig. 5.33. Variation of IHR with crank angle for different EGR rates.

Crank angle	EGR-0	EGR-20	EGR-40
0	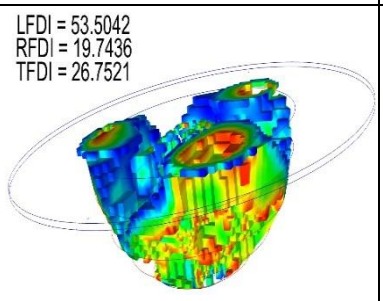	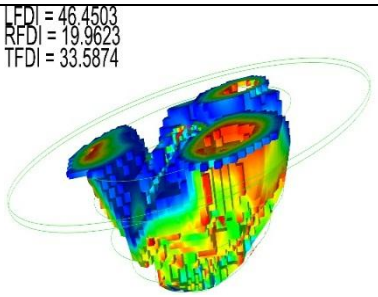	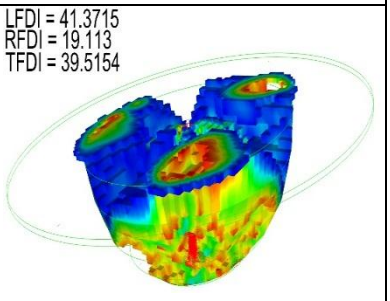
35	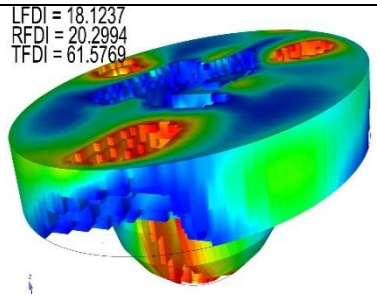	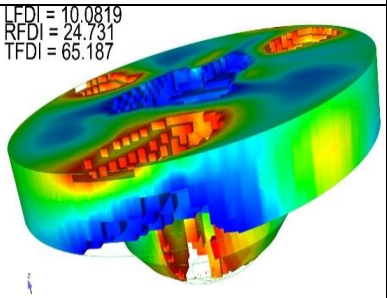	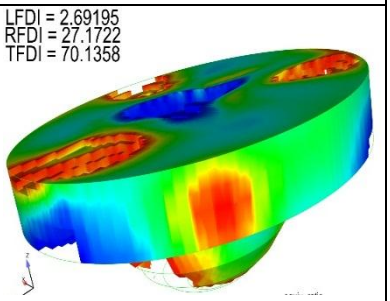

Fig. 5.34. Variation of fuel distribution index with crank angle for different EGR rates.

Figure 5.34 shows the variation of fuel distribution index for different EGR rates. From the figure it is observed that as the EGR rate is increased from 0 to 40%, at the instant of 35^{o} CA aTDC, the TFDI and RFDI increased by 12.3% and 25.65% respectively whereas the LFDI decreased by 85.15%. From fuel distribution index it was observed that TFDI increased only moderately whereas the RFDI increased considerably. The increase in the RFDI results lack of oxygen content in the premixed combustion zone, which leads to formation of rich air-fuel mixture zone (RFDI is increased by 25.65%), which causes incomplete combustion. Therefore, the introduction of EGR into the cylinder reduces the in-cylinder pressure, temperature and IHR. The performance of the engine also deteriorates.

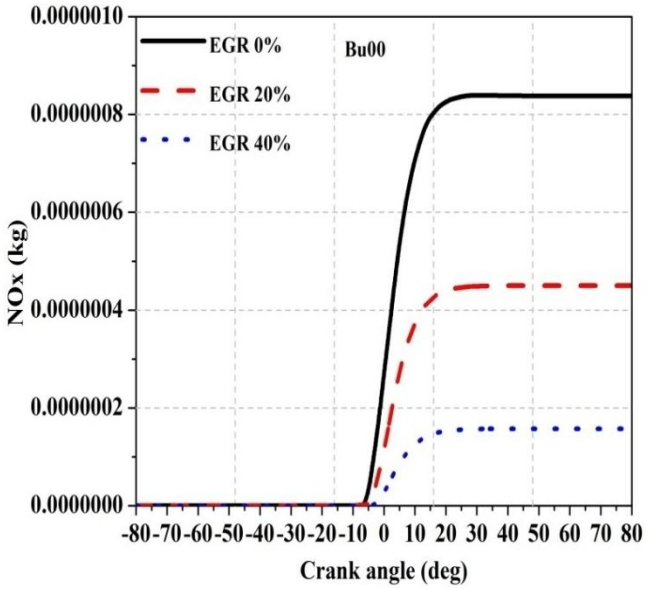

Fig. 5.35. Variation of NOx emissions with crank angle for different EGR rates.

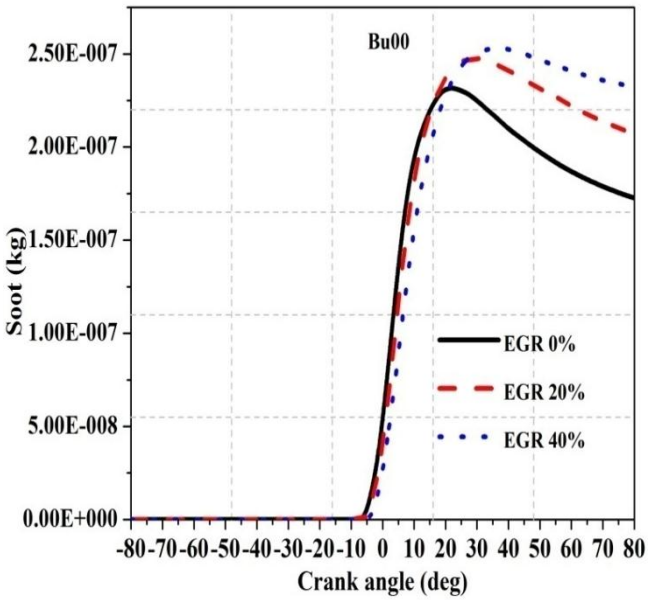

Fig. 5.36. Variation of soot emissions with crank angle for different EGR rates.

The effect of introducing EGR on the NOx and soot emissions is shown in figure 5.35 and 5.36 respectively. The NOx emissions reduced as the EGR rate is increased from due to the cumulative effect of thermal effect, dilution effect and chemical effect. Soot emissions increased with increase of the EGR rate due to incomplete combustion caused by the dilution effect.

With increase of the EGR rate, the UBHC and CO emissions (figures 5.37 and 5.38) increase, whereas the CO_2 emission (figure 5.39) decreases. This is due to incomplete combustion caused by the dilution effect. This also results in lower mean temperature during

the combustion process. Hence, the UBHC and CO emissions increase and the CO_2 emission decreases.

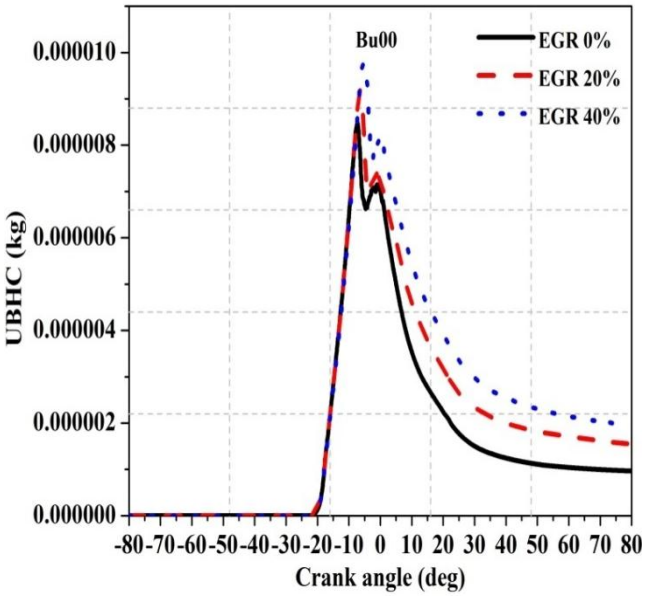

Fig. 5.37. Variation of UBHC emissions with crank angle for different EGR rates.

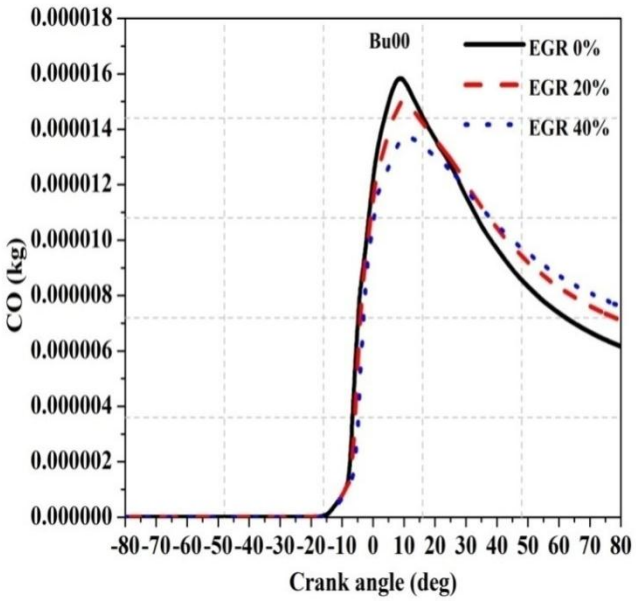

Fig. 5.38. Variation of CO emissions with crank angle for different EGR rates.

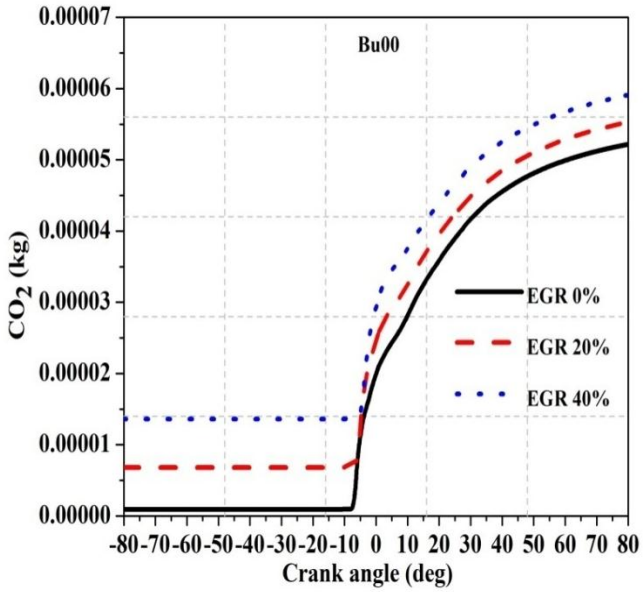

Fig. 5.39. Variation of CO_2 emissions with crank angle for different EGR rates.

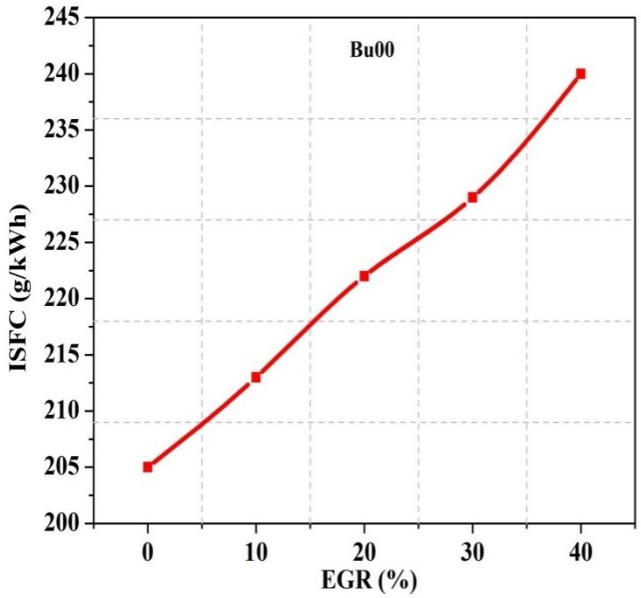

Fig. 5.40. Effect of EGR rate on the ISFC.

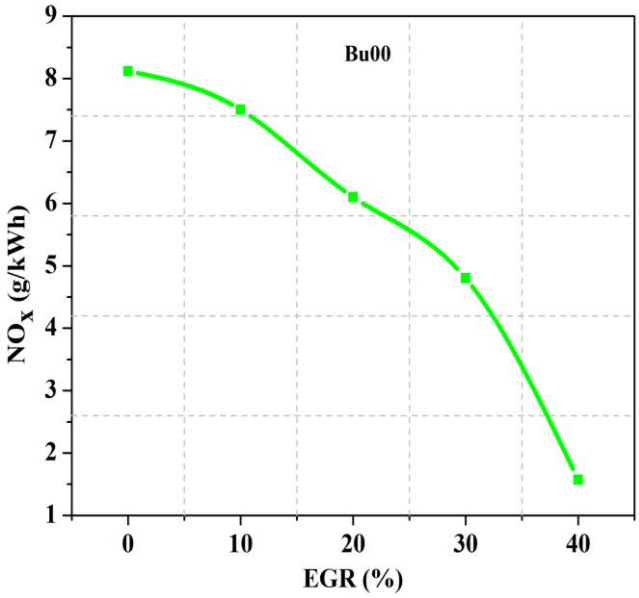

Fig. 5.41. Effect of EGR rate on the NOx.

Figure 5.40 shows the effect of EGR on the ISFC. As the EGR rate is increased from 0 to 40%, the ISFC increases from 205 g/kWh to 237 g/kWh (around 13.5 % increase). Figures 5.41 and 5.42 show the effect of EGR on the NOx and soot emission. As the EGR rate is increased from 0 to 40%, the NOx emissions get reduced from 8.12 g/kWh to 1.57 g/kWh (around 80% decrease) and the soot emissions increased from 1.48 g/kWh to 3 g/kWh (around 51% increase).

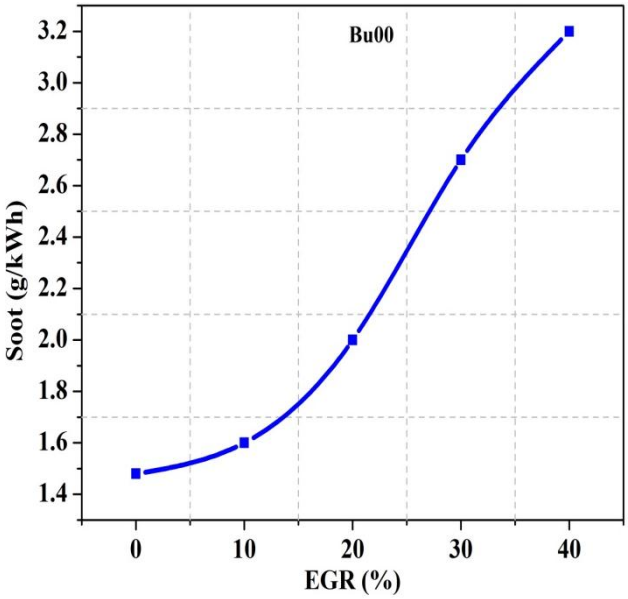

Fig. 5.42. Effect of EGR rate on the soot.

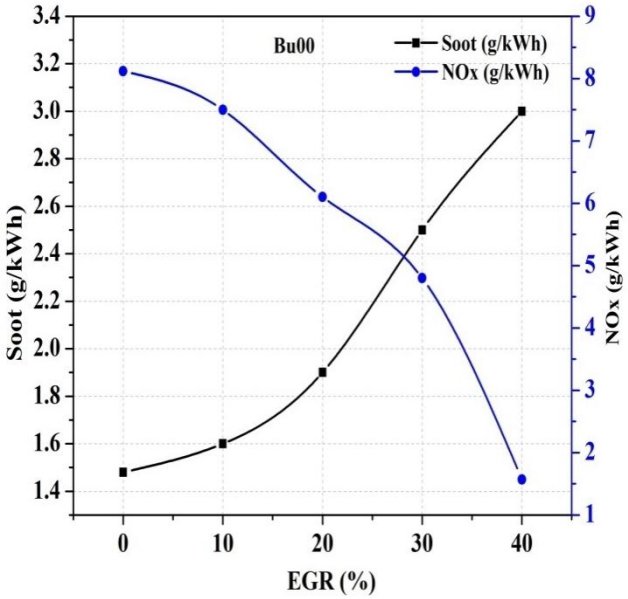

Fig. 5.43. Trade-off between soot and NOx emission for diesel at different EGR rates.

Figure 5.43 depicts the trade-off curves between the soot and NOx emissions for diesel fuel for different EGR rates at the rated load. It is observed that the trade-off relation between NOx and soot emission appears between 20% to 30% of EGR rate for Bu00.

5.2.4. Effect of start of injection (SOI) on the performance and emission characteristics

The objective of the present section is to find the operating range of SOI with safe operation. Simulation runs were carried out to study the influence of the start of injection (SOI) by varying it from -17º CA to -32º CA bTDC, on the performance and emission characteristics of the engine with the other parameters being kept constant (CR of 17.5, EGR rate of 0% and FIP of 220 bar- at baseline configuration).

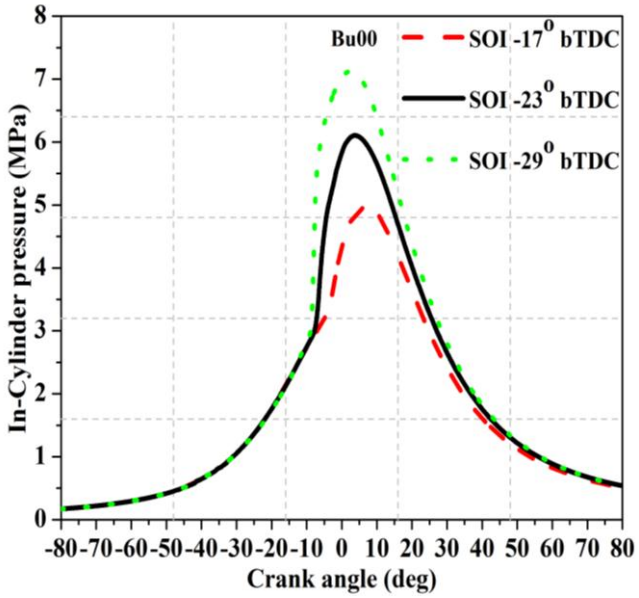

Fig. 5.44. Variation of in-cylinder pressure with crank angle for different SOIs.

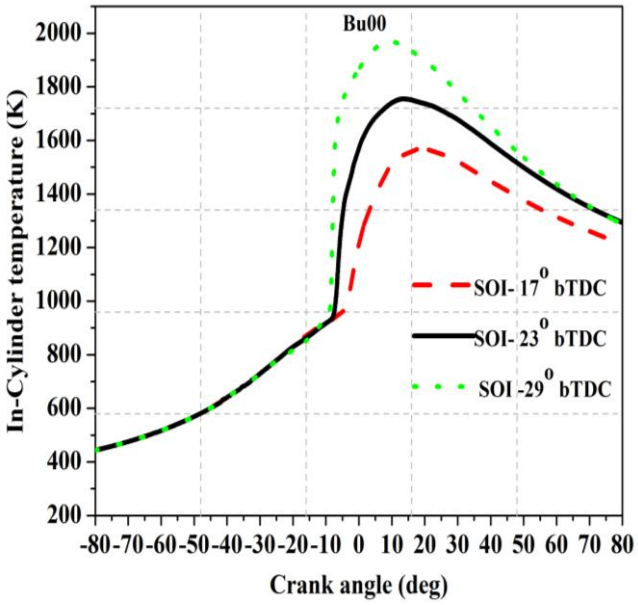

Fig. 5.45. Variation of in-cylinder temperature with crank angle for different SOIs.

Figures 5.44 and 5.45 show the variation of in-cylinder pressure and in-cylinder temperature. It can be seen from the figures that as the SOI is advanced from -17º CA to -29º CA bTDC, the peak in-cylinder pressure increased from 49 bar to 74 bar and the peak in-cylinder temperature increased from 1550 K to 1950 K. Similarly, the instantaneous heat release rate significantly increased in the premixed combustion phase, from 40 J/deg to 330 J/deg, as the SOI is advanced, but with a corresponding reduction in the diffusion combustion mode (figure 5.46). Also, there is a significant increase in the integrated heat release (IHR) from 700 J to 830 J as the SOI is advanced (figure 5.47). As the fuel injection timing is advanced, the in-cylinder temperature and pressure at the instant of fuel injection are lower inside the cylinder, which is not sufficient to ignite the fuel; it leads to the accumulation of

the fuel during the ignition delay. On the other hand, advancing the SOI makes more time available for the fuel to mix and diffuse into the air. This helps in more homogeneous charge preparation (figure 5.48). This also results in the diffusion of fuel to lean air-fuel ratio regions. Because of the homogeneous charge preparation, ignition occurs simultaneously at a number of locations, resulting in greater IHR. The longer ignition delay leads to rapid burning rate and the pressure and temperature inside the cylinder rise suddenly. Hence, most of the fuel burns in the premixed mode, causing maximum peak heat release rate, maximum cumulative heat release and shorter combustion duration.

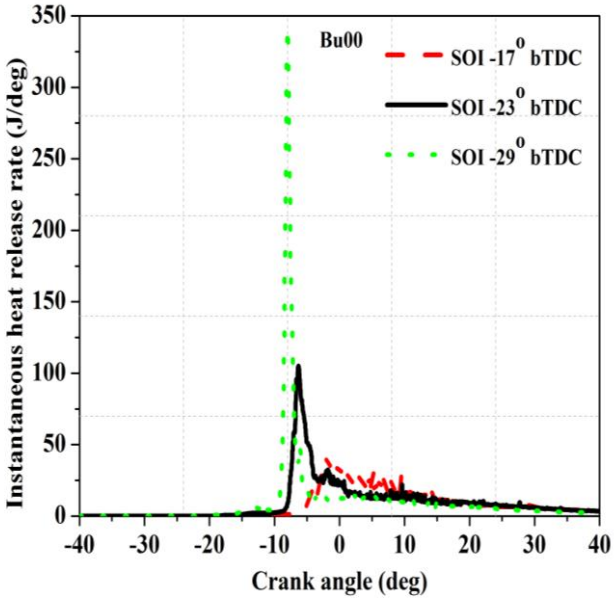

Fig. 5.46. Variation of IHRR with crank angle for different SOIs.

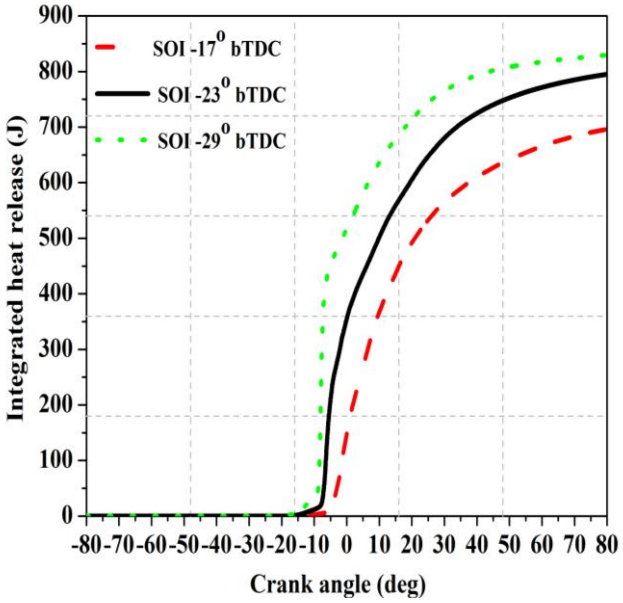

Fig. 5.47. Variation of IHR with crank angle for different SOIs.

The variation of fuel distribution index at different crank angles for different SOIs is shown in figure 5.48. From the figure it is observed that as the SOI is advanced the TFDI increases and the RFDI and LFDI decrease. It can be observed that at 35^o CA aTDC, the TFDI increased by 45.18%, whereas the RFDI and LFDI reduced by 37.6% and 68.04% respectively. This shows that advanced SOI provides better air-fuel mixture (homogeneous charge), which leads to better performance. This is the reason for the increase in the peak in-cylinder pressure and temperature as the SOI is advanced.

Crank angle	-17	-23	-29
0	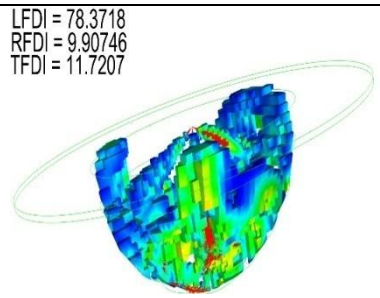	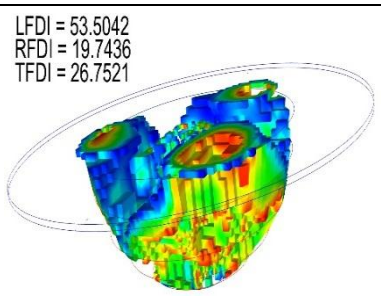	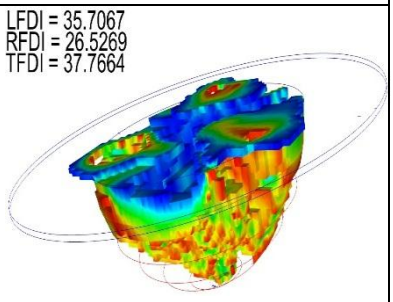
35	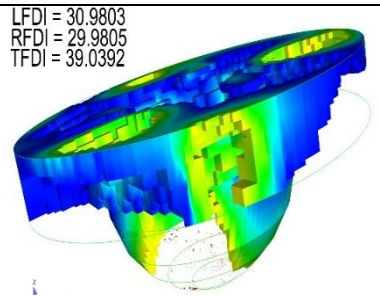	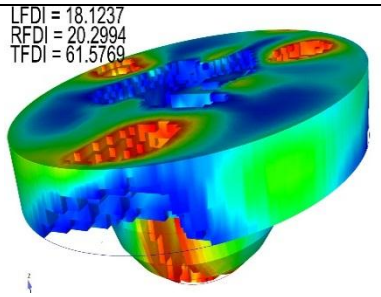	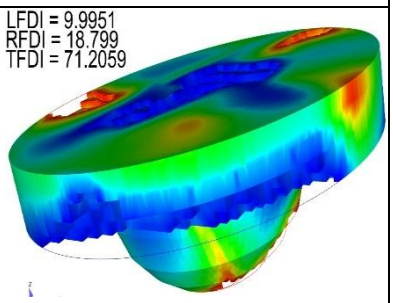

Fig. 5.48. Variation of fuel distribution index with crank angle for different SOIs.

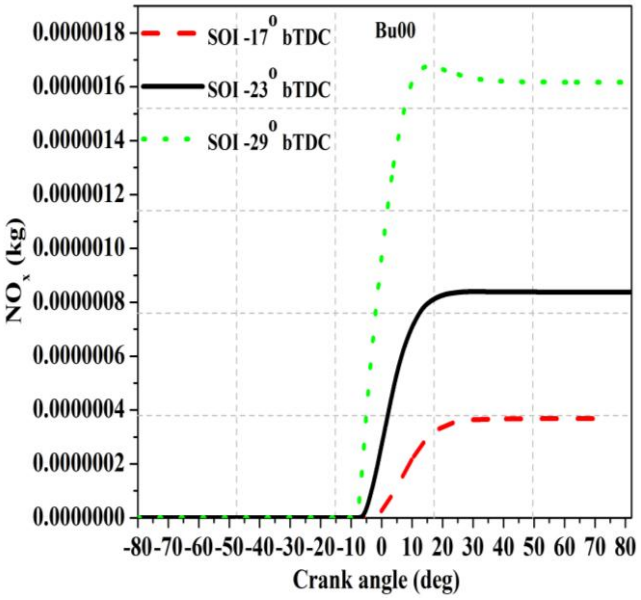

Fig. 5. 49. Variation of NOx with crank angle for different SOIs.

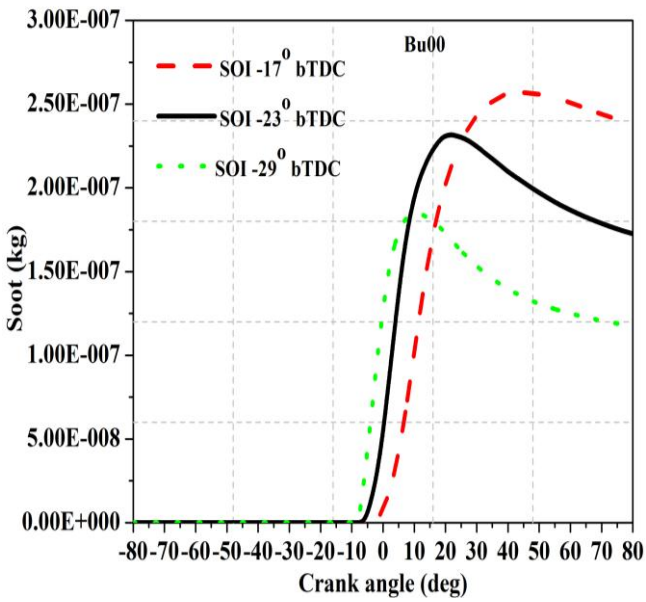

Fig. 5. 50. Variation of soot with crank angle for different SOIs.

Figures 5.49 and 5.50 show the variation of NOx and soot emissions at different SOIs. It is observed from the figures that as the SOI is advanced from -17º CA to -29º CA bTDC, the NOx emissions increase and the soot emissions decrease. The increment in the NOx is

because of higher in-cylinder temperature caused by the premixed burning. The decrease in the soot emission is because of better mixing of air and fuel by early injection leading to higher rate of oxidation of soot at higher in-cylinder temperatures.

Figures 5.51 and 5.52 show the variation of UBHC and CO emissions at different SOIs. It can be seen from the figure that as the SOI is advanced from -17º CA to -29º CA bTDC, the UBHC and CO emissions decrease. This is due to the reason that as the SOI is advanced, it enhances the mixture homogeneity, increases the in-cylinder temperature, and as a result lower UBHC and CO missions and higher CO_2 emission (figure 5.53) are formed.

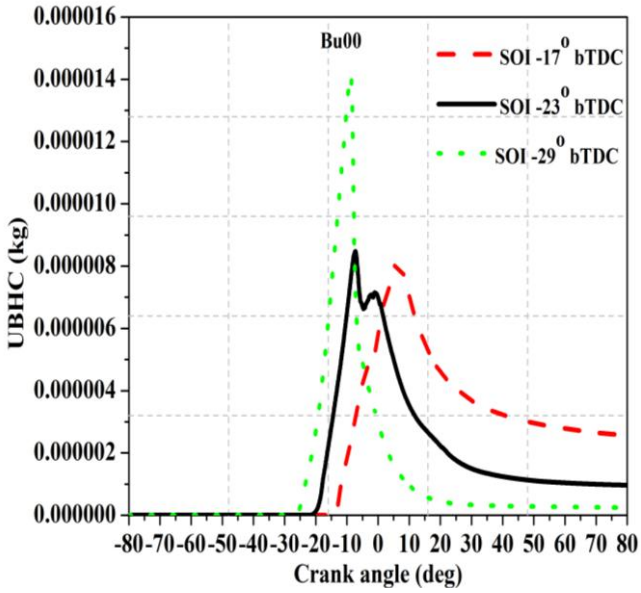

Fig. 5.51. Variation of UBHC with crank angle for different SOIs.

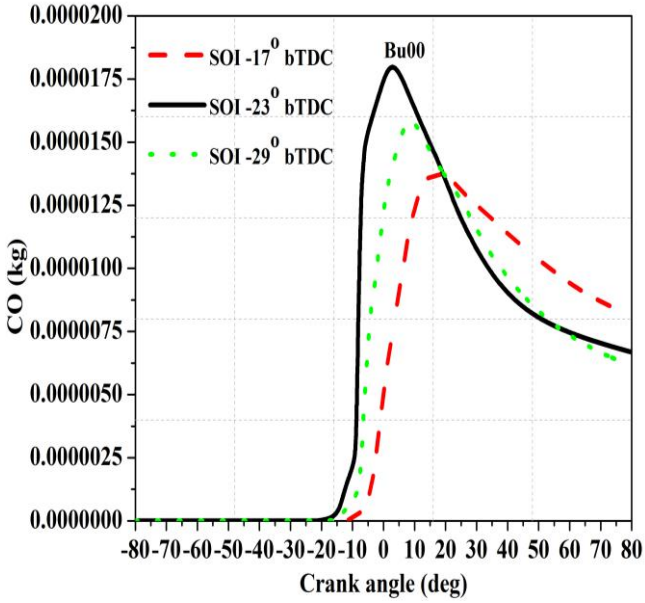

Fig. 5.52. Variation of CO with crank angle for different SOIs.

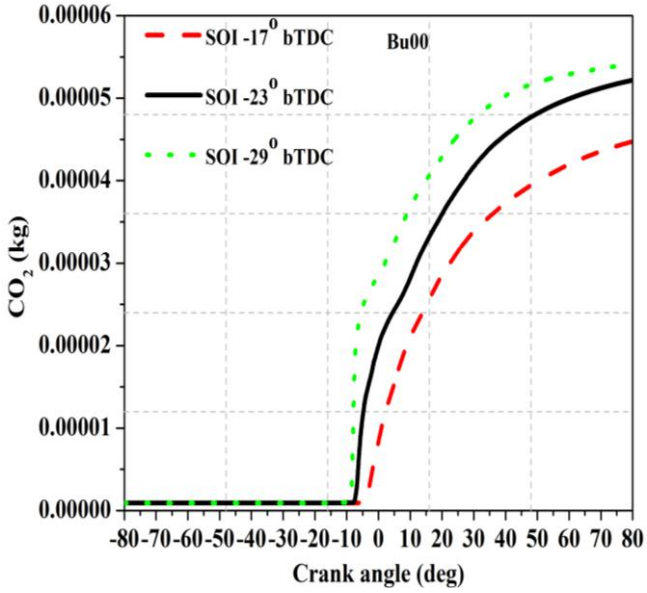

Fig. 5.53. Variation of CO_2 with crank angle for different SOIs.

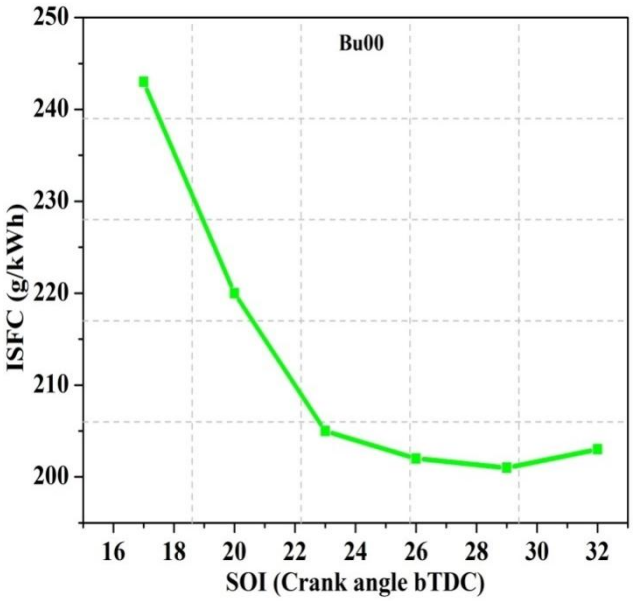

Fig. 5.54. Effect of SOI on the ISFC.

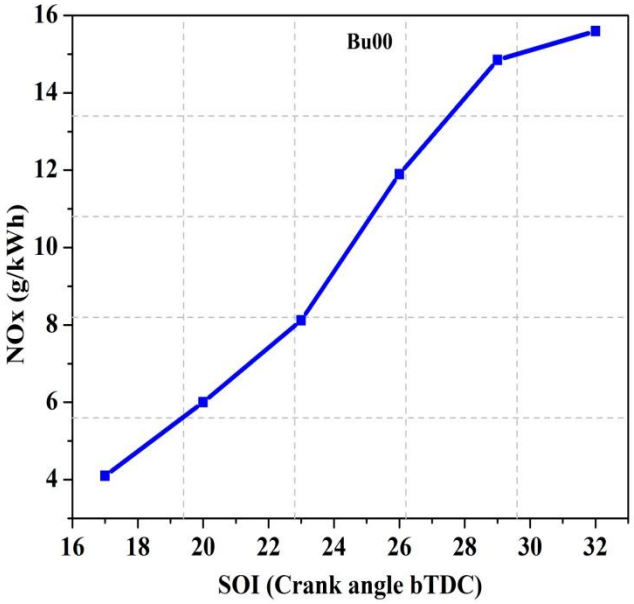

Fig. 5.55. Effect of SOI on the NOx.

Figure 5.54 shows the effect of SOI on the ISFC. It is observed from the figure that as the SOI is advanced from -17 to -29^{o} CA bTDC, the ISFC decreased from 243 to 202 g/kWh. This is because advanced SOI provides ample time for air-fuel mixing, which causes better homogeneity of air-fuel mixing and as a result better combustion efficiency. Further, advancing the SOI from -29 to -32^{o} CA bTDC, the performance decreases due to more compression effect (negative work done) caused by the early start of combustion. Thus, ISFC increased, as the SOI is advanced from -29 to 32^{o} CA bTDC.

It is observed from figure 5.55 that that as SOI is advanced from -17 to -29^{o} CA bTDC, the NOx emission increased from 4.1 to14.26 g/kWh (around 71% increase). It is observed from figure 5.56 that as SOI is advanced from -17 to -29^{o} CA bTDC, the soot emission decreased from 2.43 to 0.95 g/kWh (around 62% reduction). For any further advancement of SOI, the rate of decrease in soot is very less. From the above it is observed that range of SOI from -17 to -29^{o} CA bTDC is preferable for any given CI engine.

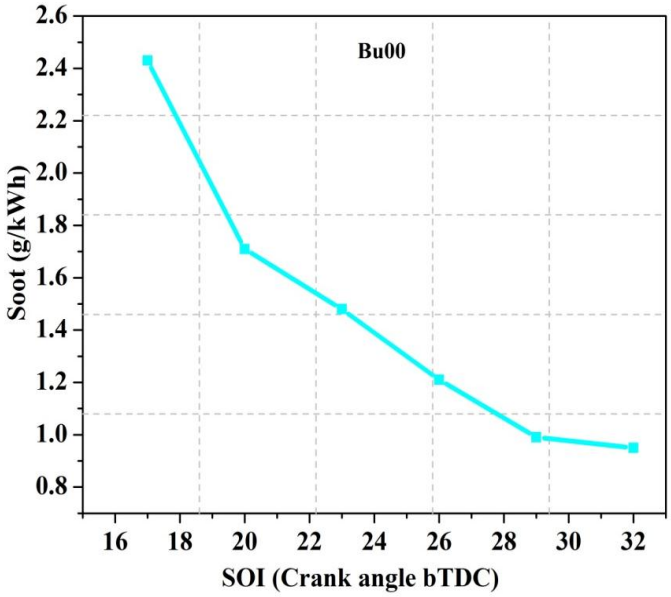

Fig. 5.56. Effect of SOI on the soot.

5.3. Selection of the ranges for the operating parameters

It was observed from the parametric study that increase in the CR drastically reduces the soot and ISFC, whereas it significantly increases the NOx emissions. Higher FIP is favourable in decreasing the soot and helps a little in improving the ISFC, but it increases the NOx emissions. However, this not monotonous. With increase in the FIP from 280 to 300 bar, the ISFC and soot increase, while the NOx emission decreased. As the SOI is advanced, it greatly reduces the soot emission, whereas it increases the NOx emission. It is also observed that advancing of SOI results in lower power output due to higher compression work. With increase in the EGR, the NOx emission drastically reduces whereas the soot emission and ISFC increase. From the trade-off between the soot and NOx it was observed that the optimum value of EGR was found to be between 20 to 30% of EGR. Therefore, operating ranges of the four input parameters for further numerical studies were selected as follows: CR is varied from 14 to 19, FIP is varied from 200 to 280 bar, SOI is varied from -17 to -29^{o} CA bTDC, and EGR is varied from 0 to 30%.

5.4. Major observations

In chapter 5, numerical studies were carried out for analysing the effect of engine operating parameters on the performance and emission characteristics of the DI-CI engine. Based on the analysis, suitable ranges were identified for further numerical analysis.

The following major conclusions have been drawn from the numerical analysis:

Effect of individual Parameters

- As the CR was increased from 14 to 19, the ISFC and soot emission decreased by 32% and 85% respectively, whereas the NOx emission increased by 48%.
- With increase in the FIP from 200 to 280 bar, the ISFC and soot emission decreased by 9% and 45% respectively, whereas the NOx emission increased by 23% for diesel fuel. On further increase in the FIP, the performance decreased.
- As the EGR rate was increased from 0 to 40%, the ISFC and soot emission increased by 13.5% and 51% respectively, whereas the NOx emission drastically reduced by 80%. From the trade-off between soot and NOx, it is evident that the optimum value of EGR appeared to be around 30%.
- An advancement of fuel injection timing i.e., SOI from -17 to -29° CA bTDC, the ISFC and soot emission decreased by 17.28% and 60% respectively, whereas the NOx emission increased by 71.2%. For a further advancement of SOI from -29 to -32^{o} CA bTDC, the performance decreased due to more compression effect caused by early start of combustion.
- Based on the simulation studies and taking into consideration the effect on the combustion and emission characteristics expressed in terms of the ISFC, soot and NOx emissions, the ranges of the operating parameters are identified as: CR: 14 to 19, FIP: 200 to 280 bar, SOI: -17 to -29^{o} CA bTDC, and EGR: 0 to 30%.
- Further the numerical studies were carried out over these ranges as discussed in the next chapter.

Chapter 6

Parametric optimization of a DI-CI engine fuelled with butanol/diesel blends using response surface methodology

The aim of present work is to determine the set of optimum values of the operating parameters of a DI-CI engine fuelled with butanol/diesel blends for achieving better performance with lower emissions. To achieve this objective, initially, the engine model was validated with experimental data for all the test fuels. In the present study four different operating parameters (CR, FIP, EGR and SOI - input parameter) were considered. The engine parametric ranges were identified as discussed in the previous Chapter-5 and the same ranges were considered in the present analysis. In the next step, optimization technique was used to minimise the ISFC, NOx and soot emission. Simulation results were obtained corresponding to this optimized sets of values and the results were compared with the baseline configuration. The homogeneity of the air-fuel mixture was also compared for the optimized and baseline configurations. Simulation studies were carried out for four different butanol/diesel blends, viz., Bu00, Bu20, Bu30 and Bu40. The optimum set of the operating parameters for each one of these fuel blends was identified. A comparison of the variation of the values of these operating parameters from Bu00 to Bu40 was also studied. For the sake of brevity, detailed analysis pertaining to Bu00 and Bu40 test fuels only is presented in this Chapter. The details pertaining to Bu20 and Bu30 test fuels are presented in the Appendix C.

6. 1. Determination of optimal engine parameters using RSM for the DI-CI engine fuelled with diesel fuel (Bu00)

6.1.1. Enabling HCCI mode of the CI engine with diesel fuel (Bu00) using RSM technique

The validation of the numerical model for diesel duel (Bu00) operation was shown in chapter 5. Simulation studies were carried out on the engine model considered, by varying different operating parameters. The effect of varying the operating parameters (called as input parameters) on the output parameters (called as output responses) was evaluated and, optimal values of the input parameters, which give the best performance, were evaluated using RSM. In the present work, four operating parameters (factors) were considered and their levels are shown in Table 6.1. A design matrix (for four factors and three levels) was developed using Box–Behnken method for numerical analysis. All the experiments (29 rums) were simulated in CONVERGE CFD and the outcomes are summarized in Table 6.2. In this study, a chemical reaction mechanism comprising about 349 reactions and 76 species, developed by Wang et al.[87], was chosen to simulate the diesel and butanol/diesel blend models.

Table 6.1. Factors and levels for numerical analysis.

Factors	**Levels**		
	1	2	3
Compression ratio (CR)	14	16.5	19
Fuel injection pressure (FIP) (bar)	200	240	280
Start of injection (SOI) (bTDC)	17	23	29
Exhaust gas recirculation (EGR) (%)	0	15	30

Table 6.2. Experimental design matrix and their responses**.**

Run order	**CR**	**FIP (bar)**	**SOI (bTDC)**	**EGR (%)**	**ISFC (g/kWh)**	**Soot (g/kWh)**	**NOx (g/kWh)**
1	14	240	23	0	285	3.31	5.99
2	16.5	240	17	0	228.4	3	6.43
3	16.5	240	23	15	225.11	2.61	5.54
4	16.5	240	23	15	225.11	2.61	5.54
5	19	240	23	30	190	1.1	4.5

6	16.5	200	23	30	231.5	3.3	2.37
7	19	280	23	15	184.5	0.42	8.78
8	16.5	280	23	30	221.2	2.57	3.73
9	19	240	23	0	183.1	0.53	13
10	16.5	240	23	15	225.11	2.61	5.54
11	19	240	17	15	185	0.7	4.33
12	19	240	29	15	194	0.48	13.52
13	16.5	240	23	15	225.11	2.61	5.54
14	16.5	280	23	0	199	1.69	10.8
15	16.5	280	29	15	208	1.15	11.2
16	19	200	23	15	188	0.91	6.96
17	16.5	280	17	15	229	2.27	3.6
18	16.5	240	29	30	218	2.78	5.2
19	16.5	240	29	0	195	1.12	14.8
20	16.5	200	29	15	211.3	2.15	8.5
21	16.5	200	23	0	224.3	2.313	7.9
22	14	200	23	15	312.2	3.5	2.9
23	14	240	17	15	354.3	3.7	2.5
24	16.5	240	23	15	225.11	2.61	5.54
25	14	240	29	15	245	2.5	6.5
26	14	240	23	30	302.7	3.9	1.8
27	16.5	240	17	30	251.65	2.373	2
28	14	280	23	15	268.54	3.3	4.34
29	16.5	200	17	15	260	2.44	2.62

6.1.2. ANOVA analysis for the DI-CI engine fuelled with diesel fuel (Bu00)

Analysis of variance (ANOVA) was used to verify the significance of the input parameters and their interaction effects. ANOVA gave the P value for all the response parameters (i.e., ISFC, NOx and soot), as shown in Table 6.3, 6.4 and 6.5. P-values of less than 0.05, indicate that the factor is significant at 95% confidence level. Similarly, P-value less than 0.0001 implies that the factor is significant at 99% confidence level.

From the ANOVA, it is observed that ISFC was most influenced by CR (71.8%), followed by SOI (9.75%), FIP (2.37%) and EGR (1.74%), as shown in Table 6.3. This implies that even a small increase in the CR has a significant effect on the ISFC. SOI has a moderate effect on the ISFC and in the decreasing order of influence, EGR has the least influence on the ISFC. The interaction of CR x SOI (7.28%) has a moderate influence on the ISFC followed, by CR x FIP (0.83%) and FIP x SOI (0.39%). The square term of the CR (4.06%) also has some impact on ISFC.

For Soot emission, CR (73.24%) is the most influential parameter, followed by SOI (5.24%), EGR (4.66%) and FIP (2.92%). The interactions of SOI x EGR (4.46%) has some influence followed by CR x SOI (0.81%) and FIP x SOI (0.58%). The square terms of CR (4.08%), SOI (3.36%) and FIP (1.08%) also have some impact on the soot emission.

EGR (36.85%) has the highest impact on the NOx emission, followed by SOI (34.85%), CR (17.45%) and FIP (2.98%). The interaction of CR x SOI (1.92%) has a moderate influence on the NOx emission, followed by SOI x EGR (1.9%), CR x EGR (1.32%), FIP x SOI (0.21%) and FIP x EGR (0.16%). The square effects of SOI (1.47) and EGR (0.57%) also have some influence on the NOx emissions.

Table 6.3. ANOVA analysis for ISFC for diesel fuel operation.

Source	**Sum of Squares**	**df**	**Mean Square**	**F-value**	**p-value**		Percentage contribution
Model	47669.42	14	3404.96	142.17	< 0.0001	significant	99.85
A-CR	34469.09	1	34469.09	1439.26	< 0.0001		71.8
B-FIP	1141.92	1	1141.92	47.68	< 0.0001		2.37
C-SOI	4682.73	1	4682.73	195.53	< 0.0001		9.75
D-EGR	837.51	1	837.51	34.97	< 0.0001		1.74
AB	403.21	1	403.21	16.84	0.0011		0.83
AC	3498.72	1	3498.72	146.09	< 0.0001		7.28
AD	29.16	1	29.16	1.22	0.2884		0.06
BC	191.82	1	191.82	8.01	0.0134		0.39
BD	56.25	1	56.25	2.35	0.1477		0.117
CD	0.0156	1	0.0156	0.0007	0.98		0.0003
A^2	1952.6	1	1952.6	81.53	< 0.0001		4.06

B^2	25.94	1	25.94	1.08	0.3156		0.05
C^2	69.1	1	69.1	2.89	0.1115		0.14
D^2	56.88	1	56.88	2.37	0.1456		0.11
Residual	335.29	14	23.95				
Lack of Fit	312.12	10	31.21	5.39	0.0594	not significant	
Pure Error	23.17	4	5.79				
Total	48004.71	28					

Table 6.4. ANOVA analysis for soot for diesel fuel operation.

Source	**Sum of Squares**	**df**	**Mean Square**	**F-value**	**p-value**		Percentage contribution
Model	29.14	14	2.08	119.83	< 0.0001	significant	99.59
A-CR	21.52	1	21.52	1239.15	< 0.0001		73.24
B-FIP	0.8603	1	0.8603	49.54	< 0.0001		2.92
C-SOI	1.54	1	1.54	88.85	< 0.0001		5.24
D-EGR	1.37	1	1.37	79.09	< 0.0001		4.66
AB	0.021	1	0.021	1.21	0.2898		0.071
AC	0.2401	1	0.2401	13.83	0.0023		0.81
AD	0.0001	1	0.0001	0.0058	0.9406		0.00034
BC	0.1722	1	0.1722	9.92	0.0071		0.58
BD	0.0029	1	0.0029	0.1648	0.6909		0.0098
CD	1.31	1	1.31	75.29	< 0.0001		4.46
A^2	1.2	1	1.2	68.84	< 0.0001		4.084
B^2	0.3181	1	0.3181	18.32	0.0008		1.082
C^2	0.9876	1	0.9876	56.87	< 0.0001		3.36
D^2	0.0041	1	0.0041	0.2366	0.6342		0.013
Residual	0.2431	14	0.0174				0.82
Lack of Fit	0.2246	10	0.0225	4.85	0.0708	not significant	
Pure Error	0.0185	4	0.0046				

Total	29.38	28					

Table 6.5. ANOVA analysis for NOx for diesel fuel operation.

Source	**Sum of Squares**	**df**	**Mean Square**	**F-value**	**p-value**		**Percentage contribution**
Model	348.34	14	24.88	275.38	< 0.0001	significant	99.12
A-CR	61.02	1	61.02	675.34	< 0.0001		17.45
B-FIP	10.45	1	10.45	115.69	< 0.0001		2.98
C-SOI	121.86	1	121.86	1348.6	< 0.0001		34.85
D-EGR	128.84	1	128.84	1425.9	< 0.0001		36.85
AB	0.0361	1	0.0361	0.3995	0.5375		0.01
AC	6.73	1	6.73	74.53	< 0.0001		1.92
AD	4.64	1	4.64	51.4	< 0.0001		1.32
BC	0.7396	1	0.7396	8.19	0.0126		0.21
BD	0.5929	1	0.5929	6.56	0.0226		0.16
CD	6.68	1	6.68	73.96	< 0.0001		1.9
A^2	0.1149	1	0.1149	1.27	0.2784		0.03
B^2	0.0128	1	0.0128	0.1416	0.7123		0.003
C^2	5.17	1	5.17	57.26	< 0.0001		1.478
D^2	2.02	1	2.02	22.36	0.0003		0.57
Residual	1.26	14	0.0904				0.36
Lack of Fit	1.18	10	0.1182	5.73	0.0535	not significant	
Pure Error	0.0825	4	0.0206				
Total	349.6	28					

6.1.3. Error analysis of the regression model for DI-CI engine fuelled with diesel fuel (Bu00)

Having obtained the values of the three output responses corresponding to different combinations of input parameters, regression equations were obtained for each one of these three output parameters as a function of input parameters. The regression statistics of fit (R^2), adjusted R^2 and predicated R^2 for the three output responses are shown in Table 6.6. It can be

observed from the table that the difference between the values of adjusted R^2 and predicated R^2 is less than 0.2 for all the responses, which indicates that the models were able to fit the data with reasonably good accuracy. Figure 6.1 shows the normal probability vs. residuals for the three output responses, i.e., ISFC, soot and NOx emissions. The plot of normal probability vs. residual is one of the diagonal plots, which is used to check whether the residuals follow a normal distribution or not. It can be observed from the figures that most of the residuals accumulated on the straight line. This implies that the errors between the simulations results and the regression-based equations for the three output responses were normally distributed. Hence, the fitted models adequately represent the simulation results. This indicates that the regression equations are accurate enough to correlate the results.

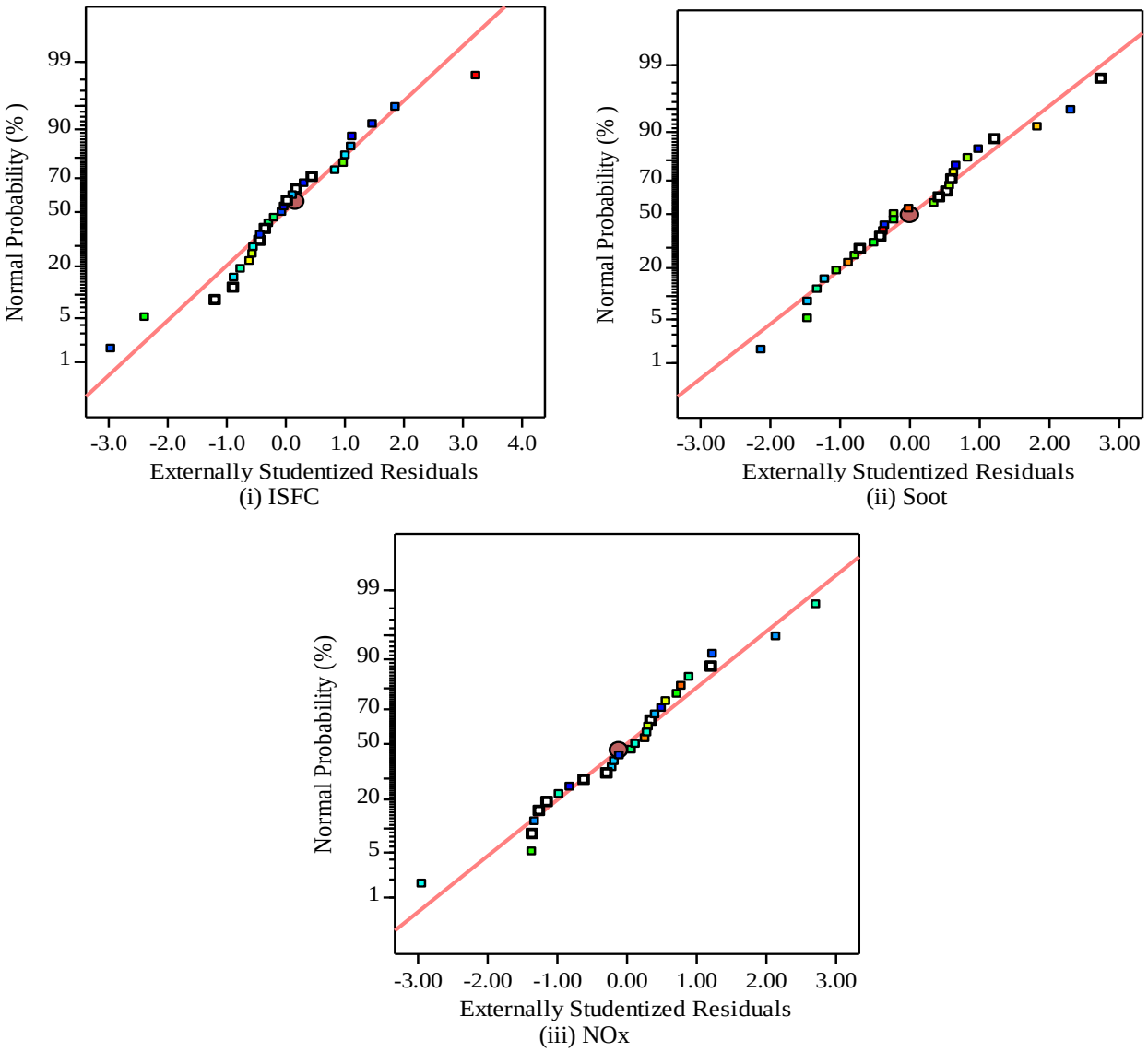

Fig. 6.1. Normal probability versus residuals plots for ISFC, soot and NOx for diesel fuel.

Table 6.6. Model evaluation for ISFC, soot and NOx for diesel fuel

Parameters	**ISFC**	**Soot**	**NOx**
R^2	0.9981	0.9936	0.9972
Adjusted R^2	0.9961	0.9873	0.9945
Predicted R^2	0.9898	0.9660	0.9864
(Adjusted R2) - (Predicted R2)	0.0063	0.0213	0.0081
Adeq. Precision	50.3	44.43	59.71

6.1.4. Interaction effects of the operating parameters on the performance of DI-CI engine fuelled with diesel fuel (Bu00)

Interaction arises when considering the relation between two or more variables, and it expresses a situation in which the effect of one variable on an outcome depends on the state of a second variable. From the ANOVA table it is observed that six interaction effects are available in the table. Among them, the most influential interaction parameters has been considered in the present analysis. From ANOVA analysis it was observed that, the interaction effect of CR and SOI had a strong influence on the ISFC. The interaction effect of SOI and EGR exercised a strong impact on the soot. Similarly, the NOx emissions were affected by the interaction effect of CR and SOI. Figures 6.2 (i to iii) depict the combined influence of CR and SOI at different FIPs on the ISFC for Bu00 test fuel. The reddish and bluish colour regions in the contour plot represent the higher and lower values of ISFC respectively, while the greenish colour region represents in-between values. As seen from the figure that ISFC is lower at higher CR and at advanced SOI for all FIPs, which is represented by bluish colour. Advancing the SOI (higher value of SOI) makes more time available for the fuel to mix and diffuse into the air. This helps in more homogeneous charge preparation. This also results in the diffusion of the fuel to the lean air-fuel ratio regions. Because of the homogeneous charge preparation, ignition occurs simultaneously at a number of locations, resulting in greater combustion. Similarly, increase in the CR increases the initial pressure and temperature of the charge, which helps in better mixing of the air and fuel, and hence better combustion. From the figure it is observed that as the FIP is increased from 200 bar to 280 bar, (from figures (i) to (iii)), ISFC decreases, i.e., the ISFC is smaller at higher FIP. This is because increase in the FIP reduces the fuel droplet size, which helps in easy evaporation of the fuel droplets in the combustion chamber in a short interval of time.

Because of this, the combustion process enhances, which leads to reduced ISFC. Thus, the cumulative effect of three input parameters is that at higher CR, higher SOI (advanced SOI) and higher FIP, the ISFC is the lowest.

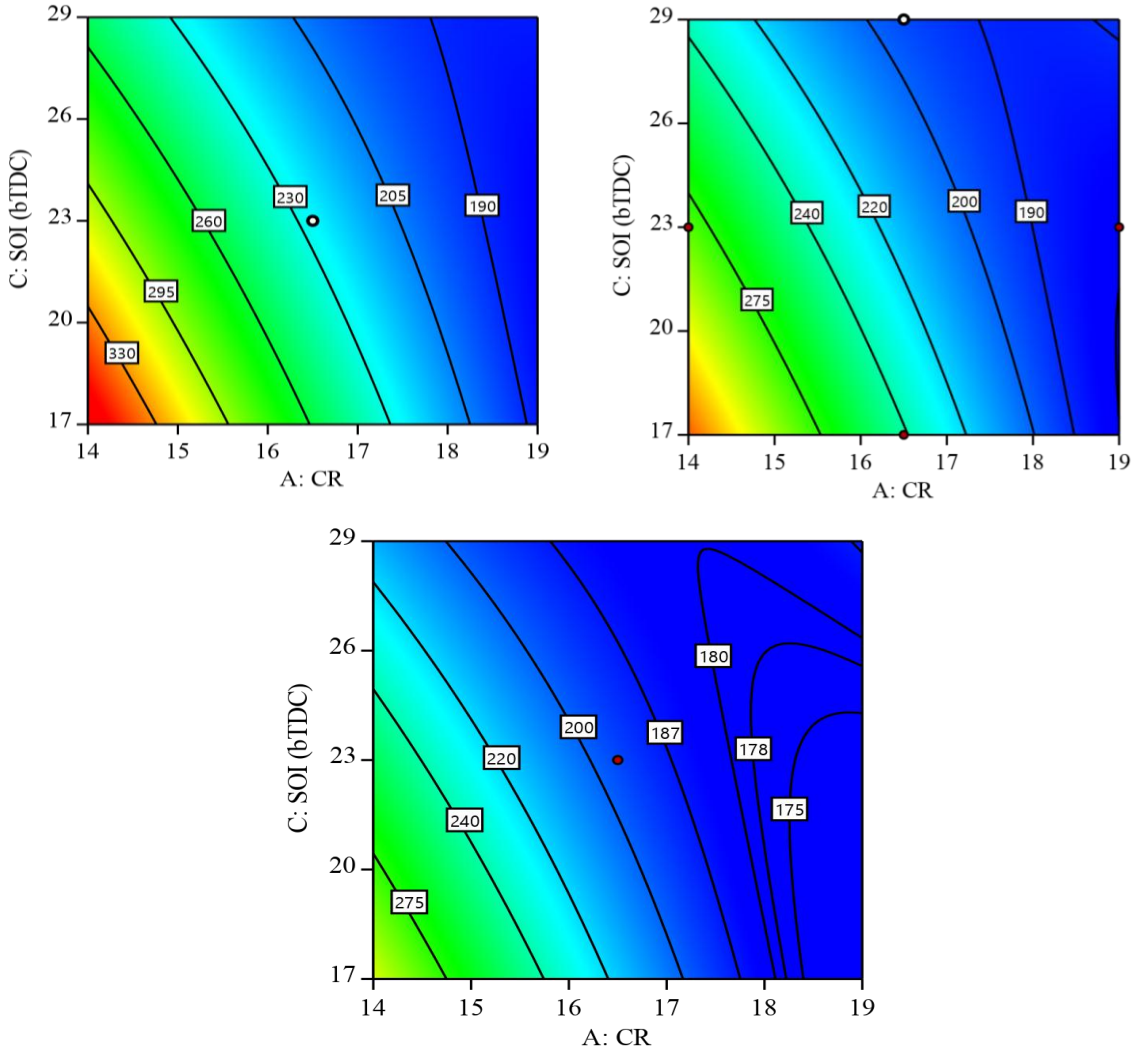

Fig. 6.2. Interaction effect of CR and SOI on the ISFC at different FIPs (i) 200 bar (ii) 240 bar and (iii) 280 bar for Bu00.

It can be observed that at FIP of 200 bar and at SOI of 23° CA bTDC, ISFC decreases from 300 to 185 g/kWh, i.e., a decrease in 115 g/kWh as the CR is increased from 14 to 19. On the other hand, at 280 bar FIP and at SOI of 23° CA bTDC, the reduction in ISFC is only 78 g/kWh (250-172 g/kWh) for the same change in the CR from 14 to 19. This shows that at higher FIP, the effect of CR on the ISFC is less. Similarly, at 200 bar FIP and CR of 16.5, the reduction in ISFC is 55 g/kWh (260-205 g/kWh) for an increase of SOI from 17 to 29° CA bTDC. On the other hand, at 280 bar FIP and CR of 16.5, the reduction in ISFC is only

36 g/kWh (218-182), for the same increase of SOI from -17 to -29° CA bTDC. This shows that at higher FIP, the effect of SOI on the ISFC is low.

It can also be observed from the figures that as the CR is increased from 14 to 19, the effect of SOI on the ISFC diminishes, which is seen in the form of almost vertical lines of constant ISFC at higher CR. It can be observed from figure 6.2 (iii) that at the FIP of 280 bar, the effect of CR on the ISFC is not monotonous. Initially, at smaller CRs, the ISFC decreases with increase in the CR. But beyond some optimum value, the ISFC increases with increase in the CR. Form the nature of the curves (the curves are no more smooth curves but look like inverted V-shaped curves) it appears that there exists an optimum CR corresponding to which the ISFC is minimum, and with further increase in the CR there is an increase in the ISFC. Similarly, at lower CRs the ISFC decreases with increase in the SOI, but at a higher CR of 19, the ISFC increases with increase in the SOI.

Figure 6.3 depicts the interactive effect between SOI and EGR on the soot emission at different CRs. From the figure it is observed that the soot emission is the minimum at advanced SOI and lower EGR for all the CRs, which is showed by a bluish colour. CR has a strong effect on the soot emission. At a lower CR of 14, increasing the EGR results in increased soot emission. On the other hand, increase in the SOI results in reduced soot emission. It can also be observed from figure 6.3 (iii) that at higher CR of 19, the effect of EGR and SOI on the soot is almost negligible, and the soot emissions are lowest throughout the present ranges of EGR and SOI. It can be explained that as the CR is increased, the pressure and temperature of the charge during compression stroke increase. This increases the combustion temperature and the combustion efficiency. It results in complete combustion of the fuel, thereby reducing the soot emissions. Similarly, higher CR induces higher turbulence and swirl. It enhances the mixing of the fuel with air, thereby reducing the formation fuel-rich zones. This also reduces the soot emissions.

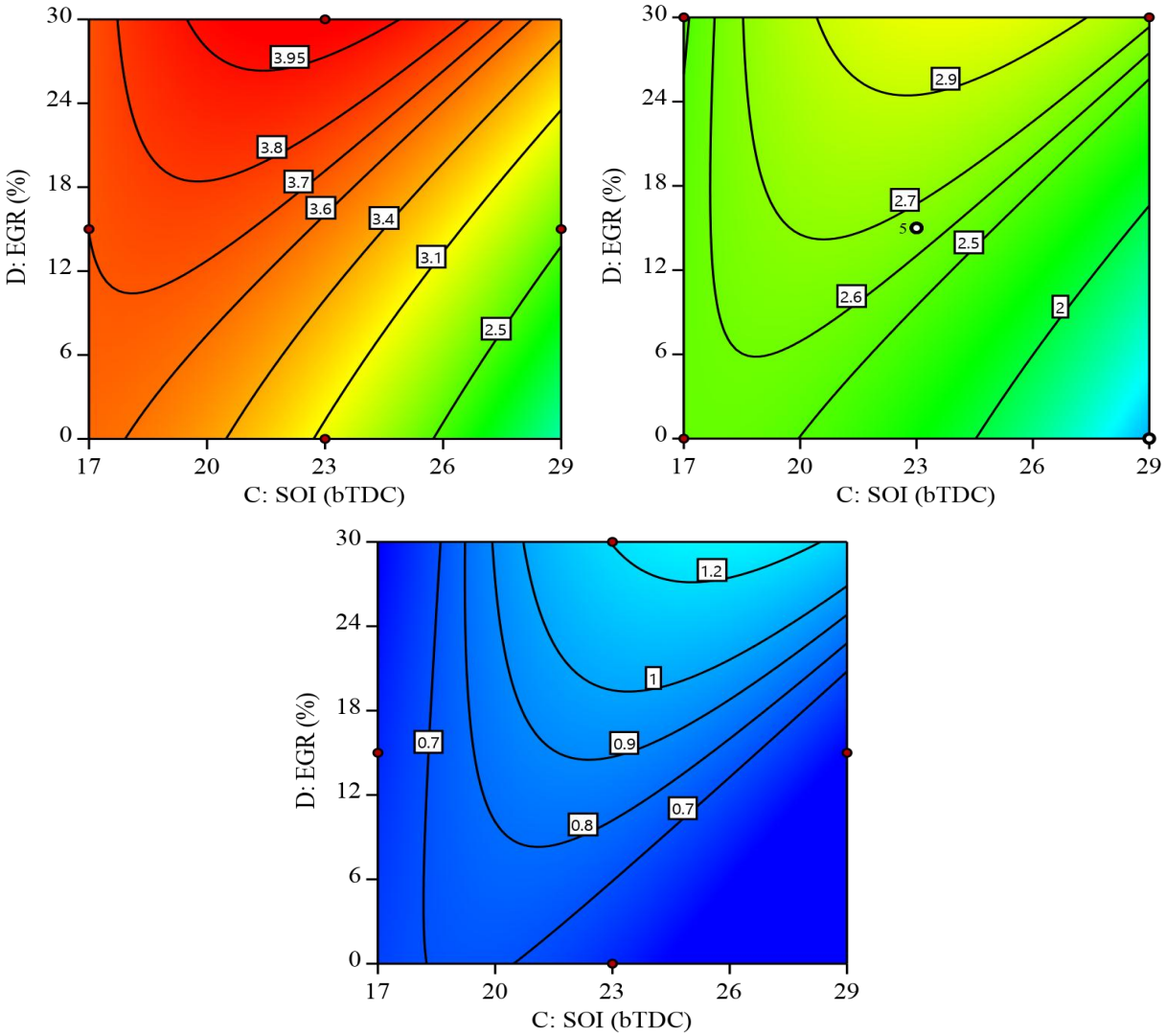

Fig. 6.3. Interaction effect of SOI and EGR on the soot at different CRs (i) 14 (ii) 16.5 and (iii) 19 for Bu00.

The combined influence of CR and SOI at different EGRs on the NOx for Bu00 operation is shown in figures 6.4 (i to iii). It can be seen from the figures that all the input parameters have strong influence on the NOx emissions, i.e., the NOx emissions are higher at higher CR, or advanced SOI, or reduced EGR. It can be seen that the interaction effects between CR and SOI are similar at all values of EGR, as reflected in the similar nature of curves for all the three EGRs. The CR and SOI interaction line is a straight line having negative slope, i.e. smaller SOI and higher CR combination shows the same NOx emission as higher SOI and lower CR combination. It is observed that at smaller values of SOI, (late injection or retarded injection) and smaller values of CR, NOx emissions are lower at all EGRs. On the other extreme, at higher SOI and higher CR, NOx emissions were higher. This can be explained as follows. As the SOI is delayed, the combustion continues to the

expansion stroke, along with associated heat losses during the expansion and this results in lower temperatures. Similarly, the residence time of the high temperature gases in the combustion chamber also gets reduced. Both the factors decrease the NOx formation. Similarly, at lower CRs, the temperature and pressure of the charge will be less, resulting in lower combustion temperature and hence lower NOx. It can be seen from figures 6.4 (i) to (iii) that as the EGR is increased from 0 to 30%, the NOx emission decreases. This can be explained by the fact that since the EGR introduces a volume of combustion products back into the cylinder, it affects the normal combustion process and combustion efficiency. This is because with EGR (owing to the associated dilution effect and thermal effect) the specific heat of the charge (which contains CO_2 and H_2O) increases. It causes reduction in the flame temperature. And also, with EGR, there is a reduction in the intake of oxygen content. Both these factors prevent the NOx formation.

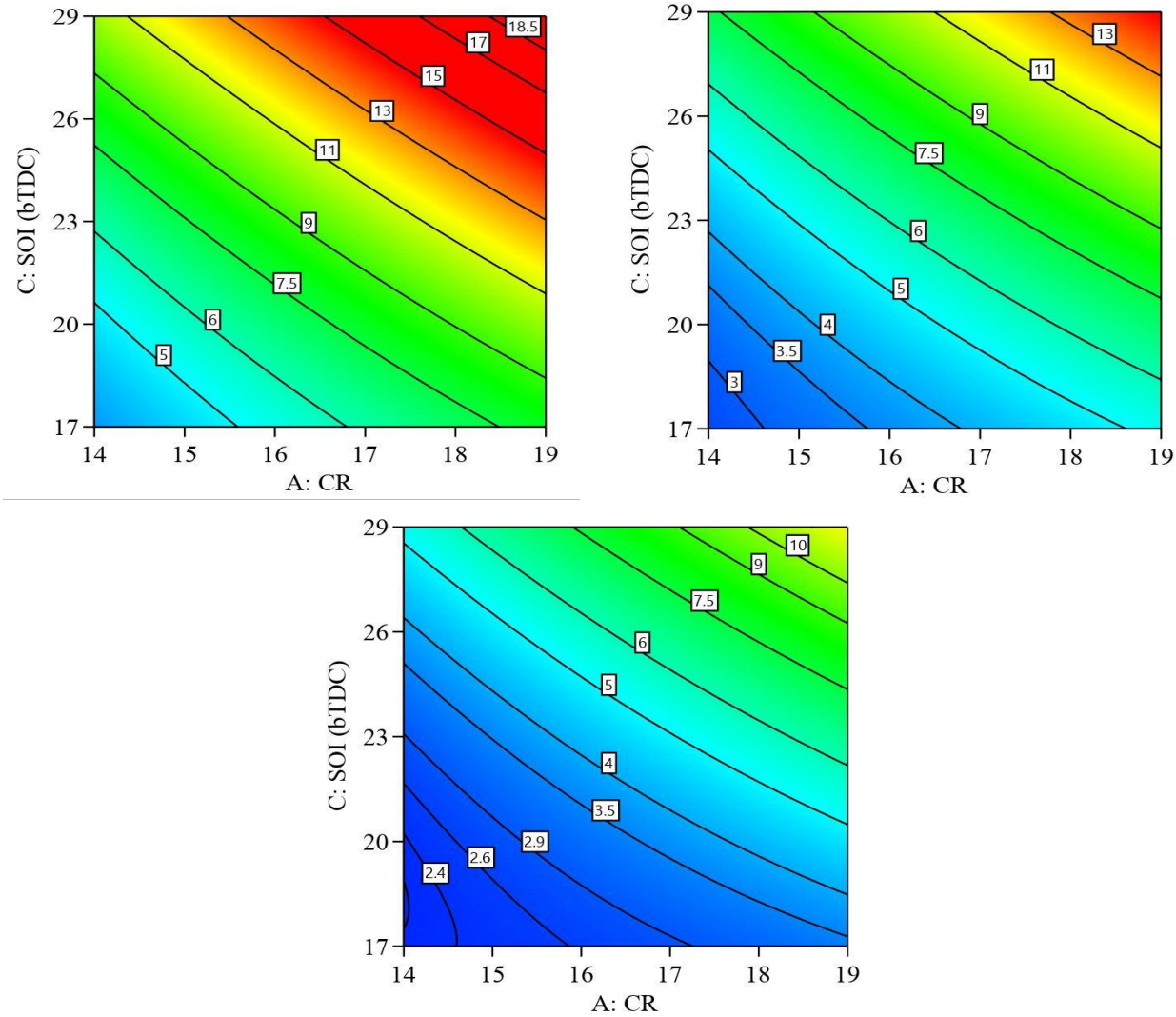

Fig. 6.4. Interaction effect of CR and SOI on the NOx at different EGR rates (i) 0 (ii) 15 and (iii) 30% for Bu00.

6.1.5. Optimization of the DI-CI engine fuelled with diesel fuel (Bu00) using desirability approach

The effect of the four significant parameters on the performance and emission were analyzed for the given set of operating ranges. Table 6.7 shows the criteria of optimization used for the desirability method for the engine operating on diesel fuel. Therefore, it is important to optimize the significant parameters in order to minimize the emissions and ISFC.

Table 6.7. Criteria of optimization used for desirability method for engine operating with diesel fuel.

Parameters /Response	Limits		Criterion	Desirability
	Lower	Upper		
Compression Ratio	14	19	In range	1
Fuel Injection Pressure (bar)	200	280	In range	1
Start of Injection (CA bTDC)	17	29	In range	1
Exhaust Gas Recirculation (%)	0	30	In range	1
ISFC (g/kWh)	183.1	354.3	Minimum	0.989
Soot (g/kWh)	0.52	4	Minimum	0.992
NOx (g/kWh)	1.8	14.8	Minimum	0.945
Combined				0.977

Based on the regression analysis, the following equations were developed for the ISFC, soot and NOx as shown in Equations 6.1 to 6.3. These equations provide the relation between the input parameters and the output response.

$$\begin{aligned} ISFC = {} & 2715.8 - 185.12*CR - 1.50*FIP - 46.56*SOI - 0.41*EGR + 0.1*CR*FIP \\ & + 1.9*CR*SOI - 0.07*CR*EGR + 0.022*FIP*SOI + 0.0079*FIP*EGR \\ & + 0.023*SOI*EGR + 2.93*CR^2 - 0.002*FIP^2 + 0.127*SOI^2 - 0.011EGR^2 \end{aligned} \quad (6.1)$$

$$\begin{aligned} Soot = {} & -18.14 + 1.5*CR + 0.084*FIP + 0.35*SOI - 0.03*EGR - 0.000725*CR*FIP \\ & + 0.0163*CR*SOI - 0.0022*CR*EGR - 0.000865*FIP*SOI - 0.000045*FIP*EGR \\ & + 0.00496*SOI*EGR - 0.066*CR^2 - 0.000123*FIP^2 - 0.01186*SOI^2 - 0.00011*EGR^2 \end{aligned} \quad (6.2)$$

$$NO_x = 27.60 - 1.57 * CR - 0.026 * FIP - 2.25 * SOI + 0.73 * EGR + 0.00095 * CR * FIP + 0.086 * CR * SOI - 0.031 * CR * EGR + 0.0017 * FIP * SOI - 0.00064 * FIP * EGR - 0.0151 * SOI * EGR + 0.021 CR^2 + 0.000054 * FIP^2 + 0.0252 * SOI^2 + 0.00232 * EGR^2 \quad (6.3)$$

Table 6.8. Comparison of optimized and baseline configuration values for Bu00.

Parameters	**Baseline configuration (Bu00)**	**Optimum configuration (Bu00)**
CR	17.5	18.9
FIP (bar)	220	279.9
EGR (%)	0	29.9
SOI (CA bTDC)	23°	25.2°

In the next step, optimization of operating parameters was carried out, as there exists an inherent trade-off relation between NOx, smoke and ISFC. The optimum combination of the input parameters were determined to be CR of 18.9, SOI of 25.2° bTDC, FIP of 279.9 bar, and EGR of 29.9% with a composite desirability of 0.97. From Table 6.8 it is observed that the values of the parameters for the optimum configuration are higher than the corresponding values at the base line configuration.

6.1.6. Comparison of optimized and baseline configuration for diesel fuel (Bu00)

As a final step of evaluation, the engine performance at the baseline engine configuration was compared with the optimal case, i.e., the simulation results corresponding to the engine baseline configuration and the set of optimum values of the input parameters were compared. Figures 6.5 to 6.8 show the comparison of in-cylinder pressure, IHRR, in-cylinder temperature and IHR for baseline configuration and optimum configuration. It can be seen from the in-cylinder pressure vs. crank angle diagram that the characteristics are almost similar, except that the peak values of in-cylinder pressure was slightly higher for the optimum case. It was observed that the pressure rise after TDC is more in case of optimized case as compared to the baseline case. The peak value of the in-cylinder temperature was lower for the optimized case compared to the baseline case. Similarly, the peak value of IHRR and IHR was also higher for the optimum case. NOx, soot, UBHC and CO emissions were also compared for both optimized and baseline cases as shown in figure 6.9 to 6.12 respectively. It is observed from the figures that all the four emissions, viz., NOx, soot,

UBHC and CO emission were lower for the optimized case compared to the baseline configuration. It can be seen from Table 6.9 that there was considerable decrease in the ISFC, NOx and soot emissions when the engine was running with the optimum values of the input parameters compared to the baseline configuration. Along with ISFC, ISEC (Indicated specific energy consumption) was also introduced to compare them with respect to energy consumption since the blends may have different calorific values. Soot and NOx emissions decreased considerably by 40.3% and 21.6%, respectively, along with a small reduction in ISFC/ISEC (2.9%).

Table 6.9. Comparison of the performance and emissions for the optimized and baseline configuration for diesel fuel operation.

	ISFC (g/kWh)	**ISEC (MJ/kWh)**	**Soot (g/kWh)**	**NOx (g/kWh)**
Baseline configuration	205	8.917	1.51	8.3
Optimized configuration	199	8.656	0.90	6.5
Change w.r.t. baseline (%)	2.9	2.9	40.3	21.6

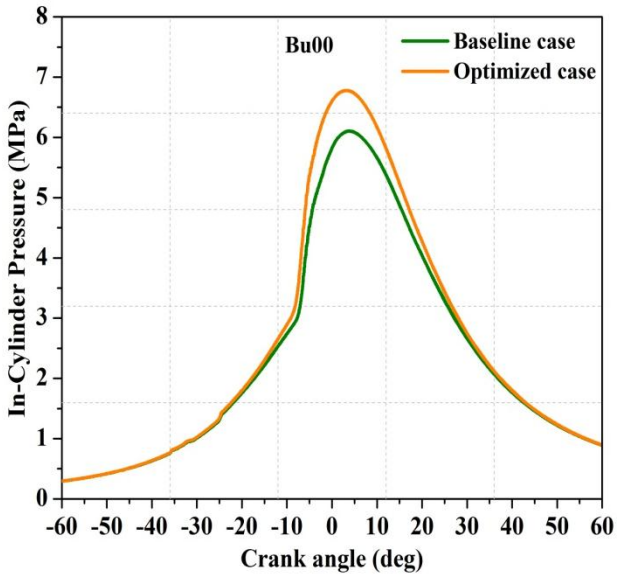

Fig. 6.5. Comparison of in-cylinder pressure for baseline and optimized case for Bu00.

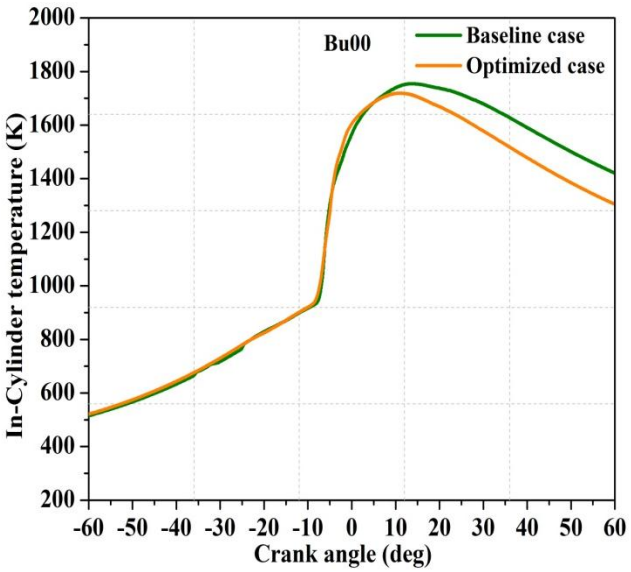

Fig. 6.6. Comparison of in-cylinder temperature for baseline and optimized case for Bu00.

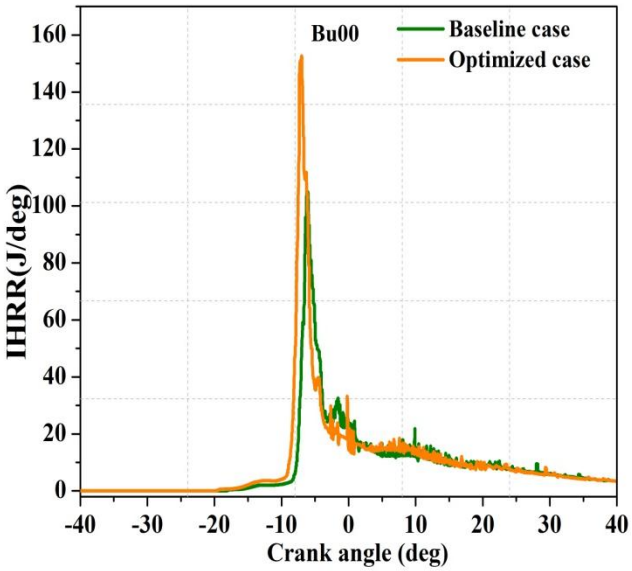

Fig. 6.7. Comparison of IHRR for baseline and optimized case for Bu00.

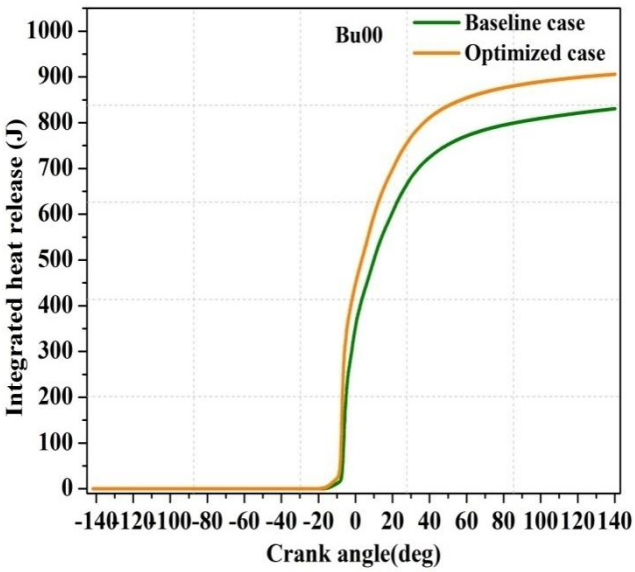

Fig. 6.8. Comparison of IHR for baseline and optimized case for Bu00.

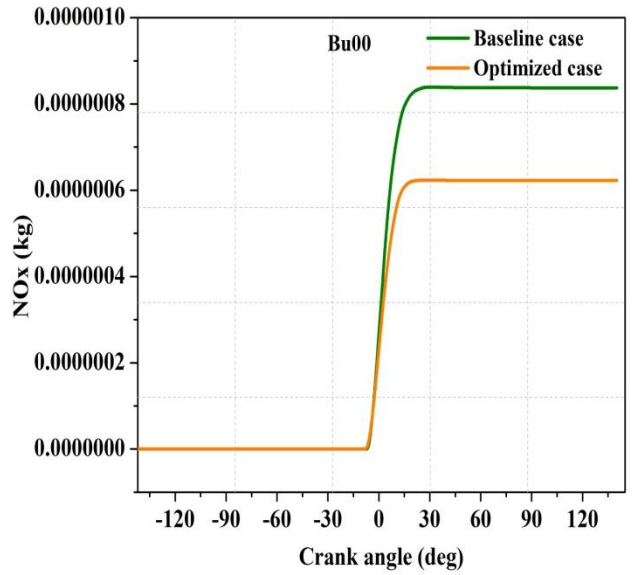

Fig. 6.9. Comparison of NOx for baseline and optimized case for Bu00.

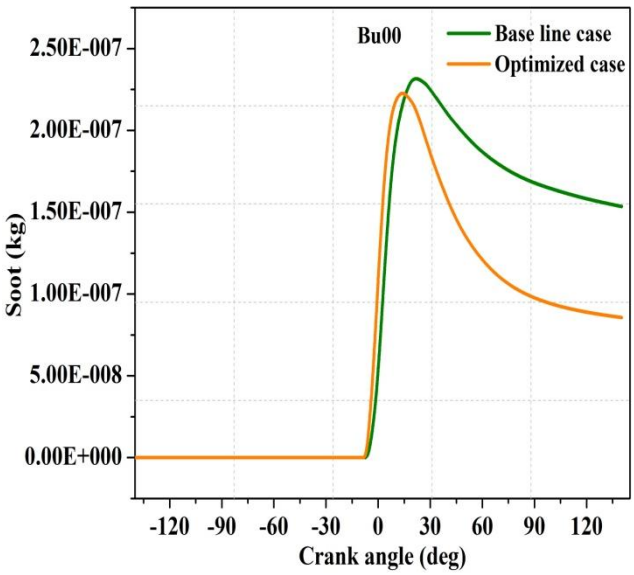

Fig. 6.10. Comparison of soot for baseline and optimized case for Bu00.

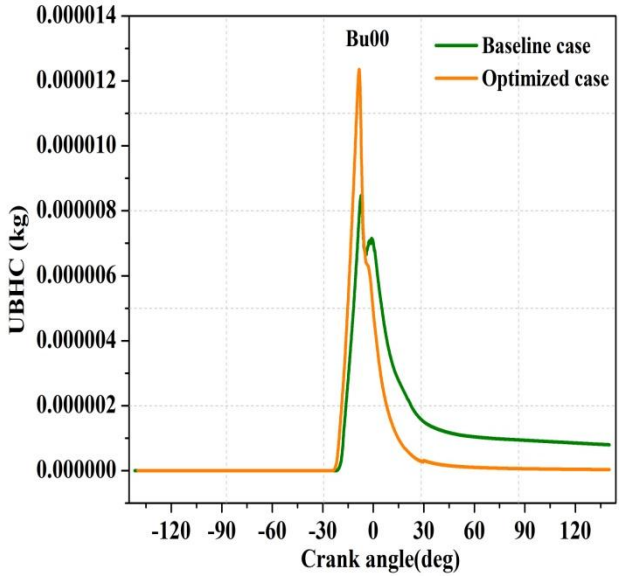

Fig. 6.11. Comparison of UBHC for baseline and optimized case for Bu00.

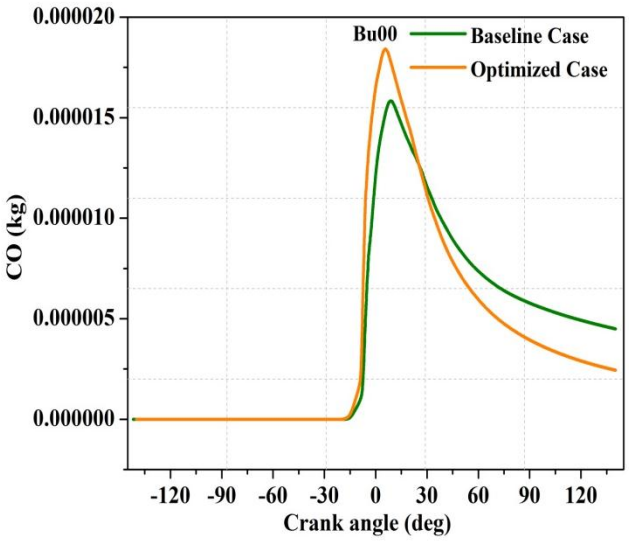

Fig. 6.12. Comparison of CO for baseline and optimized case for Bu00.

6.1.7. Comparison of homogeneity index for the optimized and baseline configurations for diesel fuel (Bu00) operation

Crank angle	Baseline case (Bu00)	Optimized case (Bu00)
0	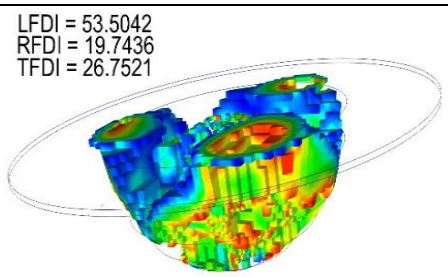	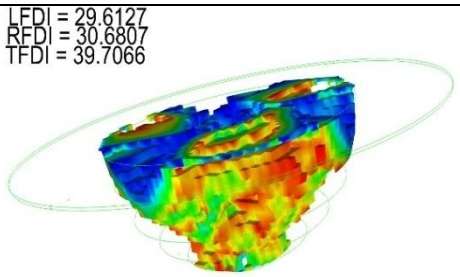
40	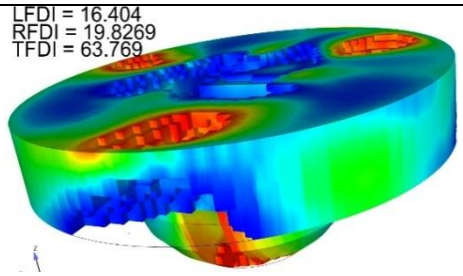	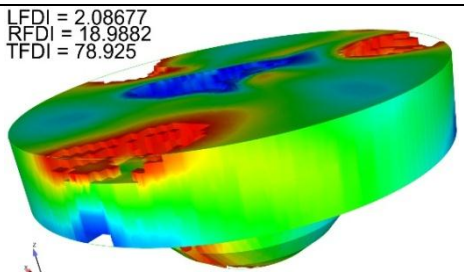

Fig. 6.13. Comparison of fuel distribution index for baseline and optimum cases for diesel fuel (Bu00).

The fuel distribution index at different crank angles (from crank angle 0 to 40°aTDC) is shown in figure 6.13 for the baseline and optimized cases. At 0° CA aTDC, the TFDI of baseline and optimized configurations were observed to be 28.2% and 39.7% respectively. Similarly, at all the instances, the homogeneity index (TFDI) was better for the optimized case. At 40° CA aTDC, the TFDI of baseline and optimized case are 63.7% and 78.9% respectively. The TFDI increased for the optimized case by 19.3% compared to the baseline configuration. This indicates that the TFDI is better for the optimized case as compared to the baseline configuration.

6.2. Determination of optimal engine parameters for the DI-CI engine fuelled with Bu40 butanol/diesel blend

The present section discusses the validation of Bu40 butanol/diesel blend by comparing the numerical results with the experimental results. The same procedure as was adopted in the case of Bu00 is used even here also. The influence of the input parameters (CR, FIP, SOI and EGR) and their interaction effects on the output responses (ISFC, soot and NOx) was studied. In the final step, the values of the optimum set was determined based on the minimization of the output responses i.e., ISFC, NOx and soot.

6.2.1. Validation of the simulation model for the Bu40 butanol/diesel blend

Initially, the numerical model was validated by comparing the simulation results with experimental results for the Bu40 test fuel. Experiments were carried out as discussed in Chapter 4, on the VCR engine with Bu40 as the test fuel. Validation of the numerical results was done using this experimental data by comparing the performance (in-cylinder pressure) and emission (NOx and soot) characteristics. In this study, three different conditions (**case 1:** CR: 17.5, FIP: 220 bar, SOI: -23º bTDC, EGR: 0%; **case 2:** CR: 17.5, FIP: 240 bar, SOI: -23º bTDC, EGR: 0%, and **case 3:** CR: 17.5, FIP: 220 bar, SOI: -23º bTDC, EGR: 20%,) were taken for validation and attempts were made to check the errors and trends between experimental and simulation results.

The simulation results of the model for the Bu40 case was validated by comparing with the experimental data. Figure 6.14 shows the comparison of the simulation results with the experimental results in terms of pressure vs. crank angle variation. From the figure, it is observed that the maximum difference between the experimental and simulation is around 7.48%. From the Table 6.10, it is clear that the maximum error between experimental and

simulation results is around 8%. Therefore, it is considered that the simulation results are in good agreement with experimental values and further studies were carried out using the simulation model.

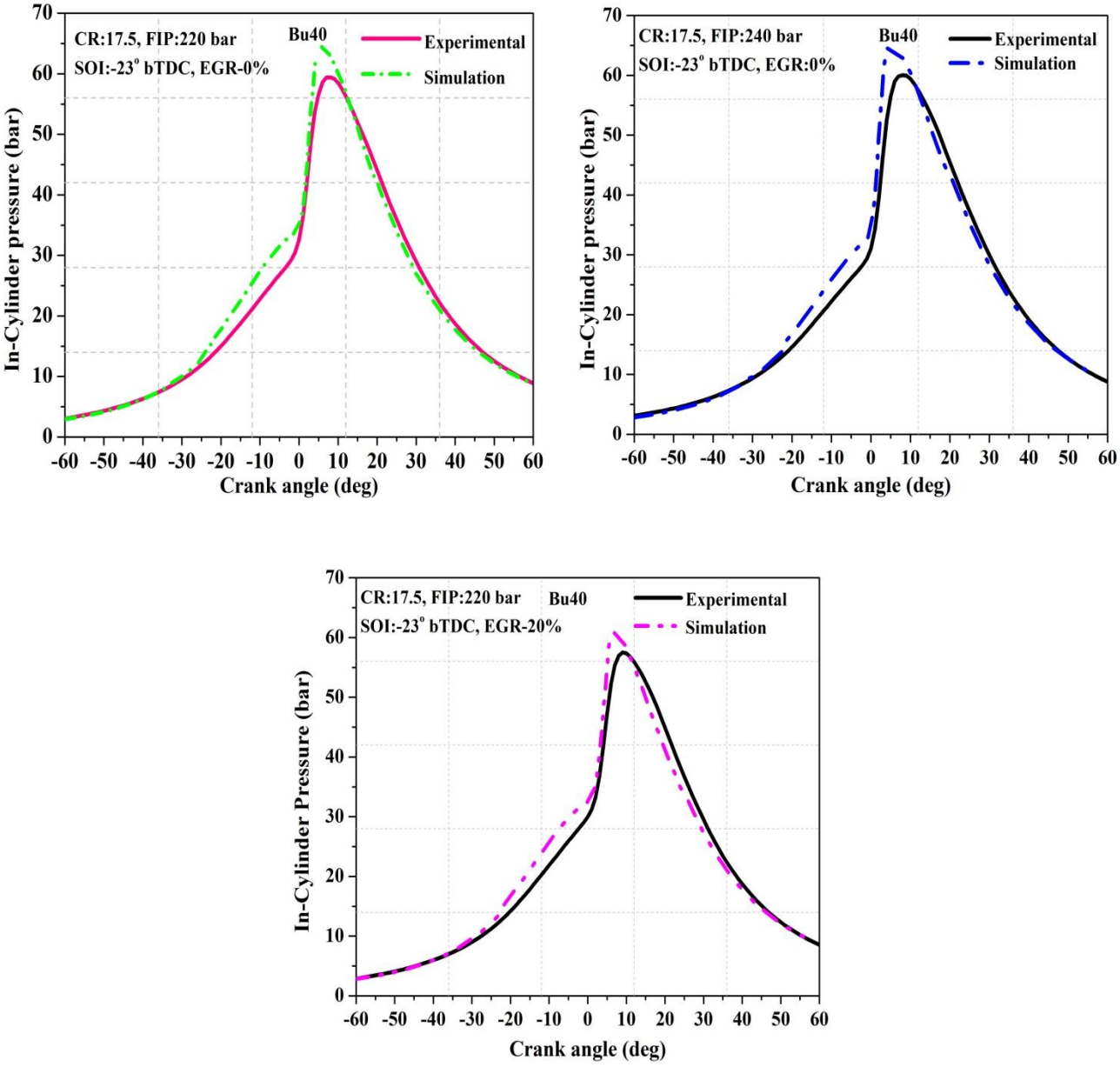

Fig. 6.14. Comparison of the simulation results with experimental data of the variation of in-cylinder pressure with crank angle for Bu40.

Table 6.10. Comparison of experimental and simulation results of performance and emissions for Bu40.

	In-Cylinder pressure (bar)			NOx (g/kWh)			Soot (g/kWh)		
	Case 1	**Case 2**	**Case 3**	**Case 1**	**Case 2**	**Case 3**	**Case 1**	**Case 2**	**Case 3**
Experimental	59.88	60.4	57.49	7	7.29	3.9	0.855	0.687	0.99
Simulation	63.1	64.9	60.7	749	7.65	4.1	0.89	0.708	1.01
Error (%)	3.4	7.48	5.2	6.3	4.7	4.87	3.9	3.1	1.98

6.2.2. Enabling HCCI mode of the DI-CI engine with Bu40 butanol/diesel blend

In the previous section, the validation of Bu40 blend was carried out. Based on the confidence attained by the validation, the present study was extended to analyze the effect of varying the operating parameters using the RSM technique. The same ranges of the parameters as were used for the Bu00 test fuel were considered here also for the Bu40 test fuel. 29 simulation experiments were carried out for the four input factors and with three levels for each factor. The outcomes are summarized in Table 6.11.

Table 6.11. Experimental design matrix with the three responses ISFC, soot and NOx for Bu40.

Run Order	CR	FIP (bar)	SOI (bTDC)	EGR (%)	ISFC (g/kWh)	Soot (g/kWh)	NOx (g/kWh)
1	14	240	23	0	390	2.56	2.43
2	16.5	240	17	0	281.88	1.8	3.2
3	16.5	240	23	15	242	1.3	3.1
4	16.5	240	23	15	242	1.3	3.1
5	19	240	23	30	195	0.18	4
6	16.5	200	23	30	334.3	1.6	1.36
7	19	280	23	15	178	0.46	7.5
8	16.5	280	23	30	295	2.22	1.36
9	19	240	23	0	218.3	0.2	9.16
10	16.5	240	23	15	242	1.3	3.1
11	19	240	17	15	224	0.05	2.58

12	19	240	29	15	185	0.179	11.7
13	16.5	240	23	15	242	1.3	3.1
14	16.5	280	23	0	232	1	7
15	16.5	280	29	15	225	0.36	8.39
16	19	200	23	15	235.44	0.54	4.69
17	16.5	280	17	15	300.8	2.01	1.54
18	16.5	240	29	30	211	0.79	4.66
19	16.5	240	29	0	197	0.35	7.48
20	16.5	200	29	15	197	1.27	3.72
21	16.5	200	23	0	248.81	2.5	2.1
22	14	200	23	15	500	3.66	1.5
23	14	240	17	15	600	4.2	2.75
24	16.5	240	23	15	245	1.3	3.1
25	14	240	29	15	381.06	1.75	1.15
26	14	240	23	30	589	3.4	0.59
27	16.5	240	17	30	402	1.55	0.4
28	14	280	23	15	530	3.37	1.8
29	16.5	200	17	15	385.23	1.99	1.28

6.2.3. ANOVA analysis for DI-CI engine fuelled with Bu40 butanol/diesel blend

Tables 6.12 to 6.14 show the ANOVA analysis results of ISFC, NOx and soot respectively. From the ANOVA analysis it is observed that the ISFC was influenced by all the linear and square terms while their *p*-values were less than 0.05. But the interaction effect of FIP x EGR was not significant because the *p*-value was greater than 0.05. The other two interaction effects are only significant as their *p*-values are less than 0.05. As far as the response of soot was concerned, all the linear and squared effects were significant. The interaction effects of CR x SOI (4.71%), FIP x EGR (3.18%), FIP x SOI (0.61%) and CR x EGR (05%) were significant. Three-square terms (CR (191%), SOI (0.8%) and FIP (2.61%)) had more effect on the soot emission. ANOVA analysis shows that the NOx was most influenced by CR (32.44%), followed by SOI (24.1%), EGR (13.53%) and FIP (6.27). SOI had a moderate effect on NOx and in the decreasing order of influence, EGR and FIP had the least influence on the NOx. The interaction of CR x SOI (12.93%) had strong influence on

the NOx followed by FIP x EGR (2.7%), FIP x SOI (2.18%), CR x EGR (1.24%) and CR x FIP (0.71%). Two-square terms (CR and SOI) had more effect on the soot emission.

Table 6.12. ANOVA analysis for ISFC for Bu40 blend.

Source	**Sum of Squares**	**Mean Square**	**F-value**	**p-value**		**Percentage Contribution**
Model	414000	29599.21	415.89	< 0.0001	significant	99.45
A-CR	257000	257000	3603.62	< 0.0001		61.8
B-FIP	1632.87	1632.87	22.94	0.0003		0.39
C-SOI	53047.05	53047.05	745.36	< 0.0001		12.78
D-EGR	17504	17504	245.95	< 0.0001		4.21
AB	1911.44	1911.44	26.86	0.0001		0.46
AC	8094.6	8094.6	113.74	< 0.0001		1.95
AD	12354.32	12354.32	173.59	< 0.0001		2.97
BC	3160.13	3160.13	44.4	< 0.0001		0.76
BD	126.45	126.45	1.78	0.2038		0.03
CD	2815.36	2815.36	39.56	< 0.0001		0.67
A^2	56867.32	56867.32	799.03	< 0.0001		13.7
B^2	3462.75	3462.75	48.65	< 0.0001		0.83
C^2	1299.43	1299.43	18.26	0.0008		0.31
D^2	1400.47	1400.47	19.68	0.0006		0.33
Residual	996.38	71.17				
Lack of Fit	889.58	88.96	3.33	0.1287	not significant	
Pure Error	106.8	26.7				
Total	415000					

Table 6.13. ANOVA analysis for soot for Bu40 blend.

Source	Sum of Squares	Mean Square	F-value	p-value		Percentage Contribution
Model	34.91	2.49	112.16	< 0.0001	significant	98.25
A-CR	25.03	25.03	1125.86	< 0.0001		60.1
B-FIP	0.3816	0.3816	17.17	0.001		1.08
C-SOI	3.97	3.97	178.51	< 0.0001		11.27
D-EGR	0.1474	0.1474	6.63	0.022		0.41
AB	0.011	0.011	0.4959	0.4929		0.031
AC	1.66	1.66	74.79	< 0.0001		4.71
AD	0.1849	0.1849	8.32	0.012		0.52
BC	0.2162	0.2162	9.73	0.0075		0.61
BD	1.12	1.12	50.54	< 0.0001		3.18
CD	0.119	0.119	5.35	0.0364		0.33
A^2	0.6757	0.6757	30.39	< 0.0001		1.91
B^2	0.9201	0.9201	41.39	< 0.0001		2.61
C^2	0.282	0.282	12.68	0.0031		0.8
D^2	0.0034	0.0034	0.1527	0.7019		0.009
Residual	0.3113	0.0222				
Lack of Fit	0.2793	0.0279	3.5	0.1193	not significant	
Pure Error	0.0319	0.008				
Total	35.22					

Table 6.14. ANOVA analysis for NOx for Bu40 blend.

Source	Sum of Squares	Mean Square	F-value	p-value		Percentage Contribution
Model	220.4	15.74	123.44	< 0.0001	significant	98.18
A-CR	72.08	72.08	565.15	< 0.0001		32.44
B-FIP	13.95	13.95	109.41	< 0.0001		6.27
C-SOI	53.55	53.55	419.89	< 0.0001		24.1

D-EGR	30.08	30.08	235.88	< 0.0001		13.53
AB	1.58	1.58	12.35	0.0034		0.71
AC	28.73	28.73	225.26	< 0.0001		12.93
AD	2.76	2.76	21.61	0.0004		1.24
BC	4.86	4.86	38.12	< 0.0001		2.18
BD	6	6	47.06	< 0.0001		2.7
CD	0.0001	0.0001	0.0008	0.9781		0.00045
A^2	3.8	3.8	29.82	< 0.0001		1.71
B^2	0.2232	0.2232	1.75	0.2071		0.1
C^2	2.66	2.66	20.88	0.0004		1.17
D^2	0	0	0.0002	0.9888		0
Residual	1.79	0.1275				
Lack of Fit	1.61	0.1612	3.71	0.1092	not significant	
Pure Error	0.1739	0.0435				
Total	222.18					

6.2.4. Error analysis of the regression model for the Bu40 butanol/diesel blend

Figure 6.15 shows that the residuals have been falling in a straight line. This indicates that the errors are normally distributed. Further, the model evaluation (Table 6.15) was carried out and the model values are within the range. Hence, the fitted models adequately represent the simulation results. This indicates that the regression equations are accurate enough.

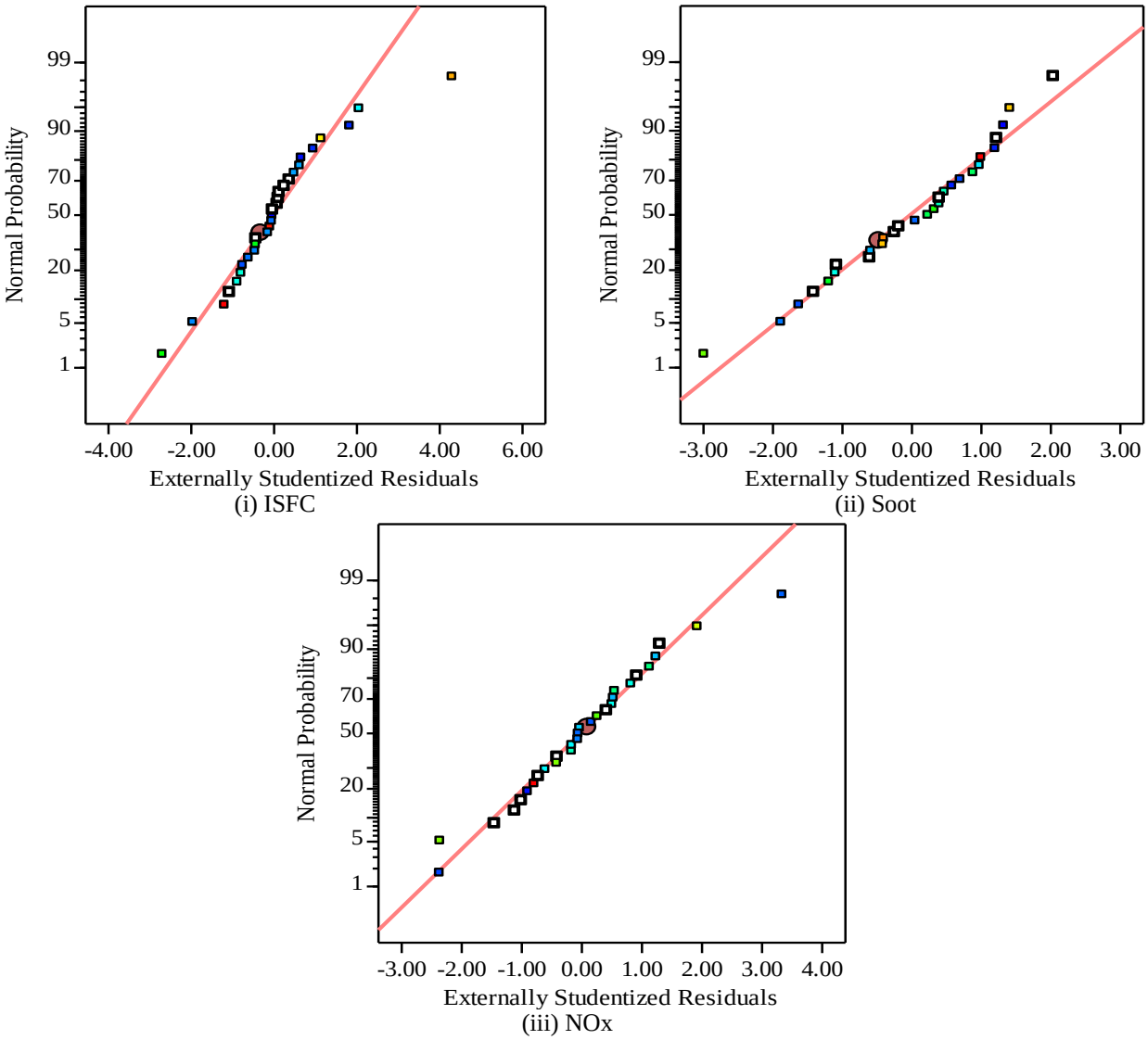

Fig. 6.15. Normal probability plot of the response ISFC, soot and NOx for Bu40 blend.

Table 6.15. Model evaluation for ISFC, soot and NOx for Bu40 blend.

Parameters	**ISFC**	**Soot**	**NOx**
R^2	0.9976	0.9912	0.992
Adjusted R^2	0.9952	0.9823	0.9839
Predicted R^2	0.9873	0.9529	0.957
(Adjusted R^2) - (Predicted R^2)	0.0079	0.0294	0.0269
Adeq. precision	70.61	38.96	45.54

6.2.5. Interaction effects of the DI-CI engine fuelled with Bu40 butanol/diesel blend

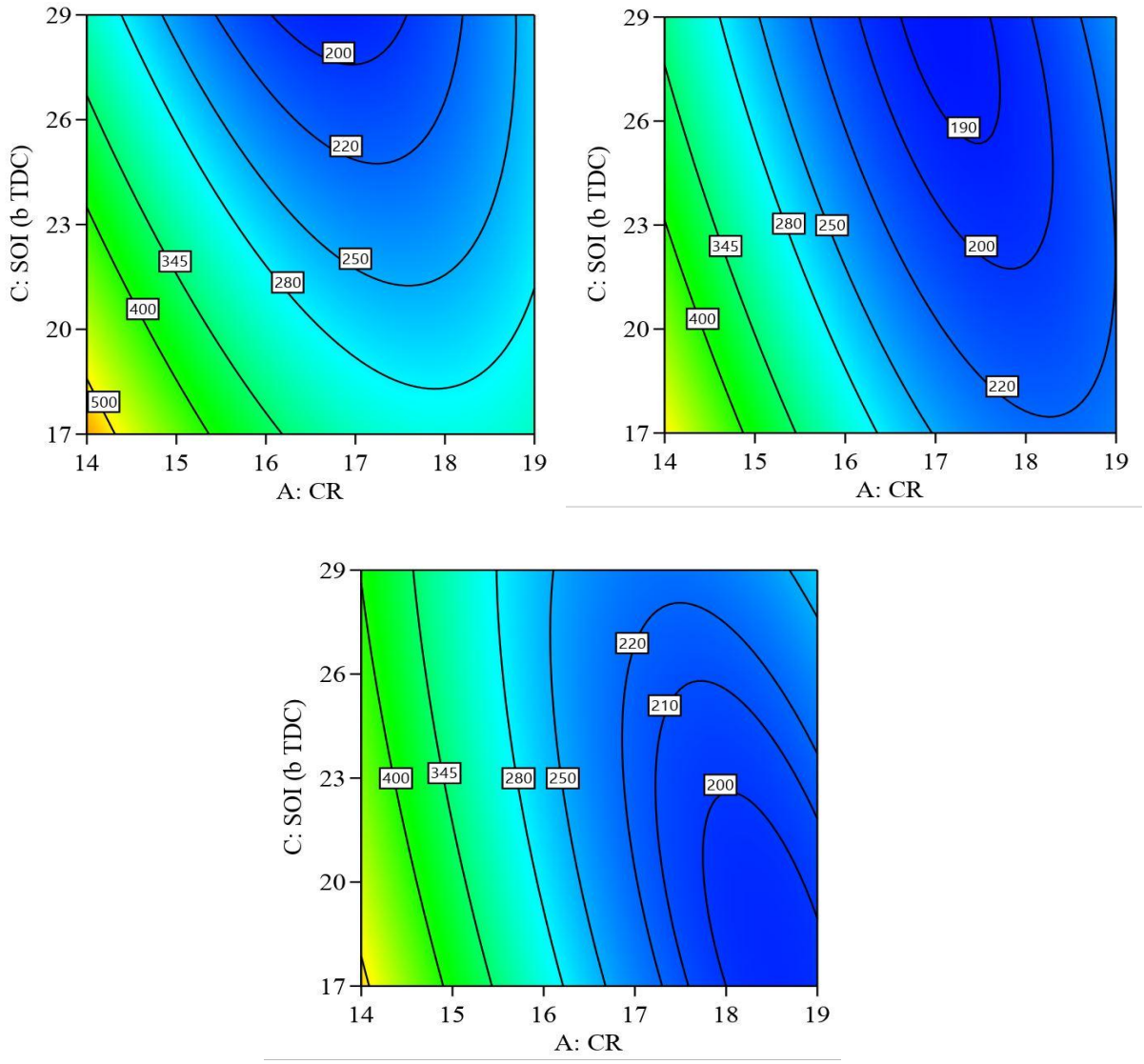

Fig. 6.16. Interaction effect of CR and SOI on the ISFC at different FIPs (i) 200 bar (ii) 240 bar and (iii) 280 bar for Bu40 blend.

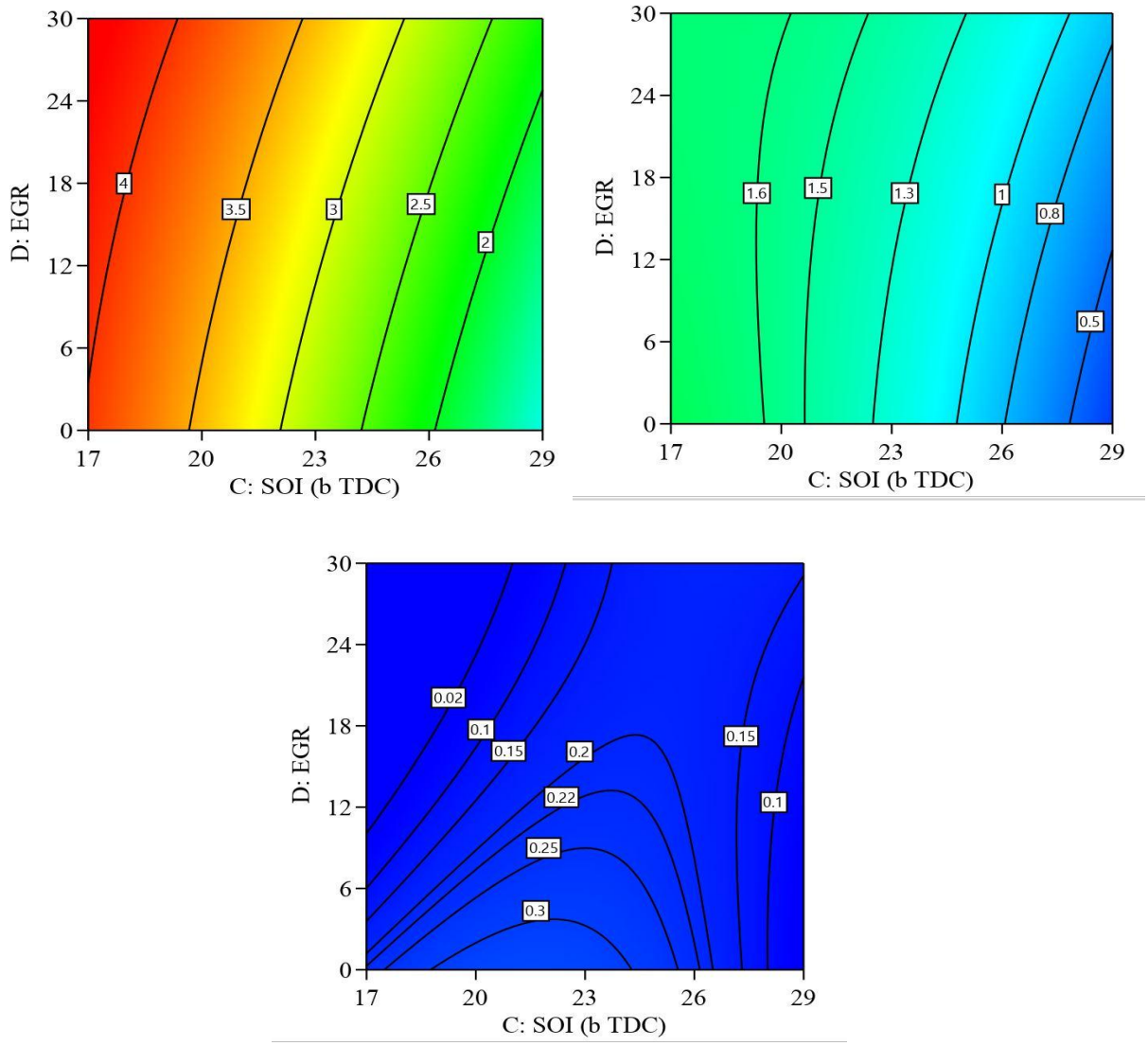

Fig. 6.17. Interaction effect of SOI and EGR on the soot at different CRs (i) 14 (ii) 16.5 and (iii) 19 for Bu40 blend.

Figures 6.16, 6.17 and 6.18 show the interaction effects between different operating parameters on the ISFC, soot and NOx emissions for the Bu40 fuel operation. It can be seen that similar effects to that of Bu00 operation were observed in this case also. There is not much effect of the addition of butanol except that the absolute value of ISFC was higher. This is plausible since the calorific value of butanol is lower than that of diesel. Similarly, absolute values of soot and NOx emission are lower compared to Bu00. This was because of the higher oxygen content in the molecular structure and higher latent heat of evaporation of butanol.

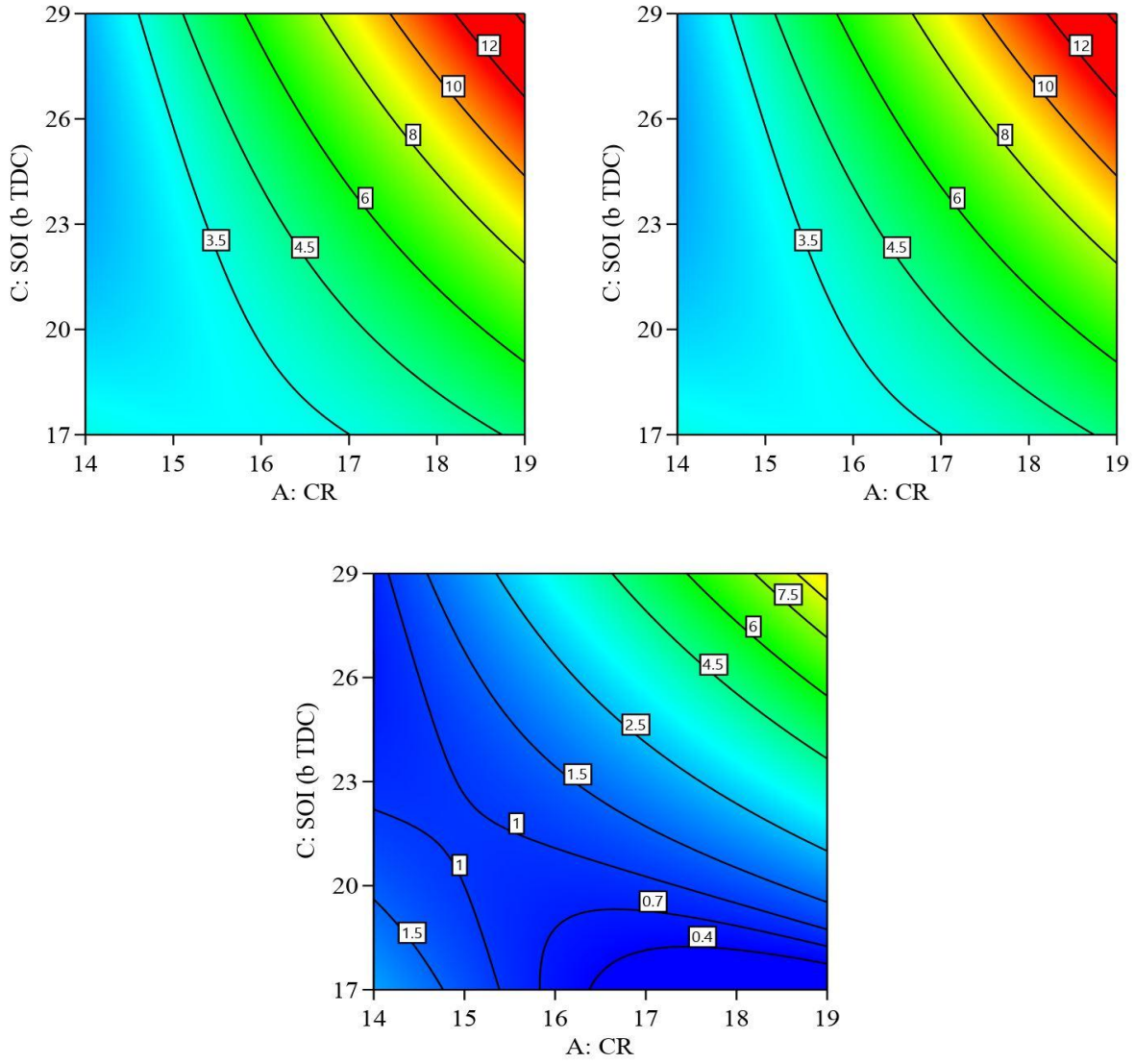

Fig. 6.18. Interaction effect of CR and SOI on the NOx at different EGR rates (i) 0 (ii) 15 and (iii) 30% for Bu40 blend.

6.2.6. Optimization using desirability approach for Bu40 butanol/diesel blend

Desirability technique was used to optimize the emission and performance characteristics. The desirability approach values are given in Table 6.16.

Based on the regression analysis, the regression equation was developed for the ISFC, soot and NOx as shown in Equations 6.4 to 6.6. The optimum combination of input parameters for Bu40 case were determined to be CR of 19, FIP of 248 bar, SOI of 19° bTDC, and EGR of 22% with a composite desirability of 0.98.

From the Table 6.17 it is observed that the optimum values for Bu40 operation are lower than the optimum values of Bu00. It indicated that as butanol content increases from 0 to 40%, the requirement of higher parameter level reduces.

Table 6.16. Optimization standards used for the desirability of the responses for Bu40 blend.

Parameters /Response	**Limits**		**Criterion**	**Desirability**
	Lower	**Upper**		
Compression Ratio	14	19	In range	1
Fuel Injection Pressure (bar)	200	280	In range	1
Start of Injection (bTDC)	17	29	In range	1
Exhaust Gas Recirculation (%)	0	30	In range	1
ISFC (g/kWh)	178	600	Minimum	0.95
Soot (g/kWh)	0.05	4.2	Minimum	0.995
NOx (g/kWh)	0.4	11.7	Minimum	0.97
Combined				0.98

Table 6.17. Comparison of the optimized and baseline configuration values for Bu40 blend.

Parameters	**Baseline configuration (Bu00)**	**Optimum configuration (Bu00)**	**Optimum configuration (Bu40)**
CR	17.5	18.9	19
FIP (bar)	220	279.9	248
EGR (%)	0	29.9	22
SOI (CA bTDC)	23°	25.2°	19

$$ISFC = 7042.53 - 547.13*CR - 6.169*FIP - 102.33*SOI + 34.06*EGR - 0.218*CR*FIP$$
$$+2.99*CR*SOI - 1.820*CR*EGR + 0.117*FIP*SIO - 0.0093*FIP*EGR$$
$$-0.294*SOI*EGR + 14.9*CR^2 + 0.0144*FIP^2 + 0.39*SOI^2 + 0.065*EGR^2 \quad (6.4)$$

$$Soot = 54.06 - 3.31*CR - 0.117*FIP - 0.335*SOI - 0.157*EGR + 0.000525*CR*FIP$$
$$+0.042*CR*SOI - 0.0057*CR*EGR - 0.000969*FIP*SOI + 0.000883*FIP*EGR$$
$$+0.0019*SOI*EGR + 0.0516*CR^2 + 0.000235*FIP^2 - 0.0058*SOI^2 + 0.000102*EGR^2 \quad (6.5)$$

$$NO_x = 115.35 - 8.35*CR - 0.096*FIP - 4.52*SOI + 0.75*EGR + 0.0063*CR*FIP$$
$$+0.1787*CR*SOI - 0.022*CR*EGR + 0.0046*FIP*SOI - 0.002*FIP*EGR$$
$$-0.000056*SOI*EGR + 0.1225*CR^2 - 0.000116*FIP^2 + 0.0178*SOI^2 + 0.000089*EGR^2 \quad (6.6)$$

6.2.7. Comparison of the optimized and baseline configuration for Bu40 blend

The comparison of the optimized and baseline cases of Bu40 is shown in Table 6.18. Figures 6.19 to 6.22 show the comparison of the in-cylinder pressure, temperature, IHRR and IHR for the baseline configuration and the optimum configuration. The optimum case results have lower ISFC and lower emissions compared to the baseline case. From the figures 6.23 to 6.26, it is observed that all the emissions decreased for the optimized case compared to the baseline configuration. The corresponding soot and NOx emissions decreased by 53.9 % and 77.5%, respectively, and a marginal reduction in ISFC/ISEC (1.7%) was accomplished. This shows better performed of the optimum case than the baseline case in terms of both ISEC and emissions aspects.

Table 6.18. Comparison of the optimized and baseline configuration for the Bu40 blend operation.

	ISFC (g/kWh)	ISEC (MJ/kWh)	Soot (g/kWh)	NOx (g/kWh)
Baseline configuration	223	7.530	0.89	7.49
Optimized configuration	219	7.401	0.2	3.4
Change w.r.t. baseline	1.7	1.7	77.5	53.9

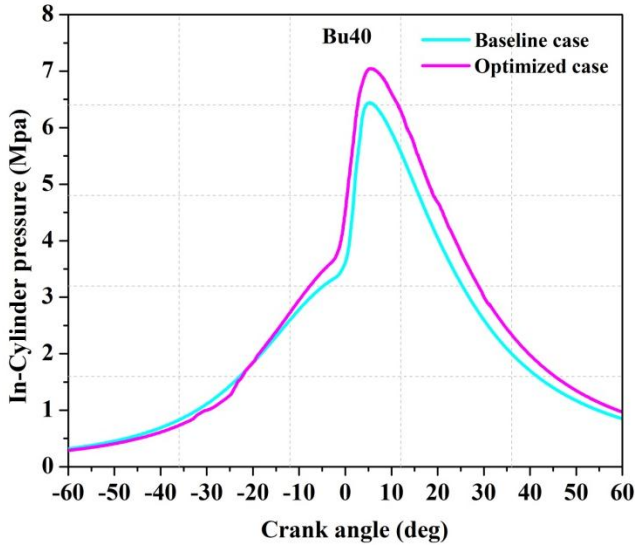

Fig. 6.19. Comparison of in-cylinder pressure

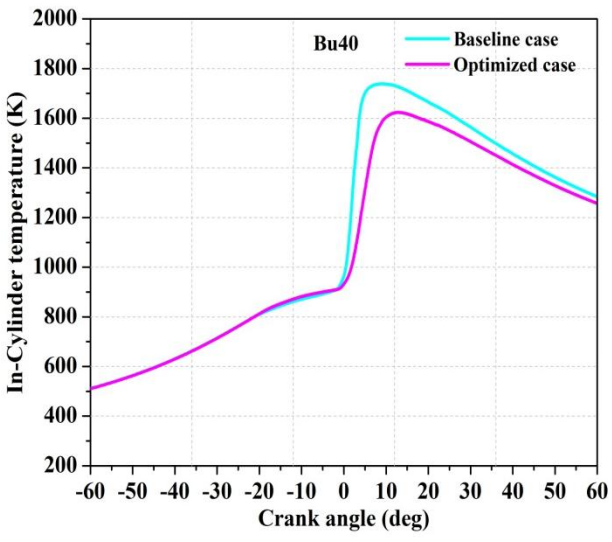

Fig. 6.20. Comparison of in-cylinder temperature

with crank angle between baseline and optimized case for Bu40 blend.

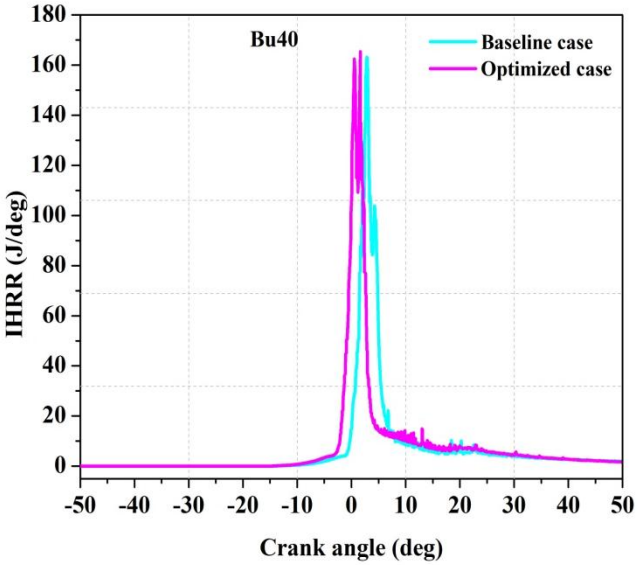

Fig. 6.21. Comparison of IHRR with crank angle between baseline and optimized case for Bu40 blend.

with crank angle between baseline and optimized case for Bu40 blend.

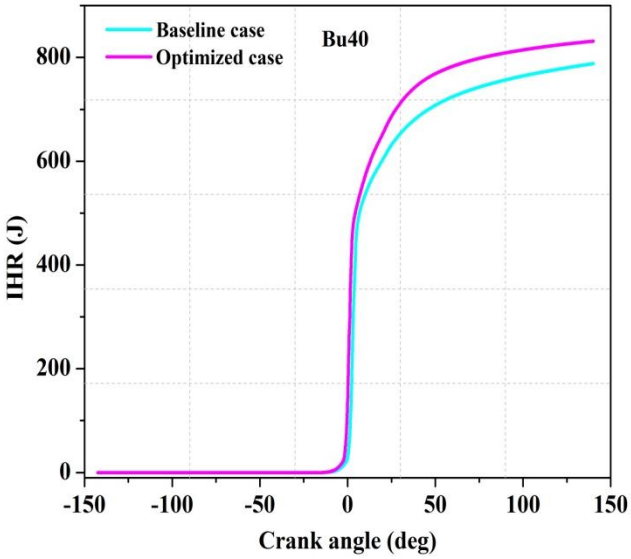

Fig. 6.22. Comparison of IHR with crank angle between baseline and optimized case for Bu40 blend.

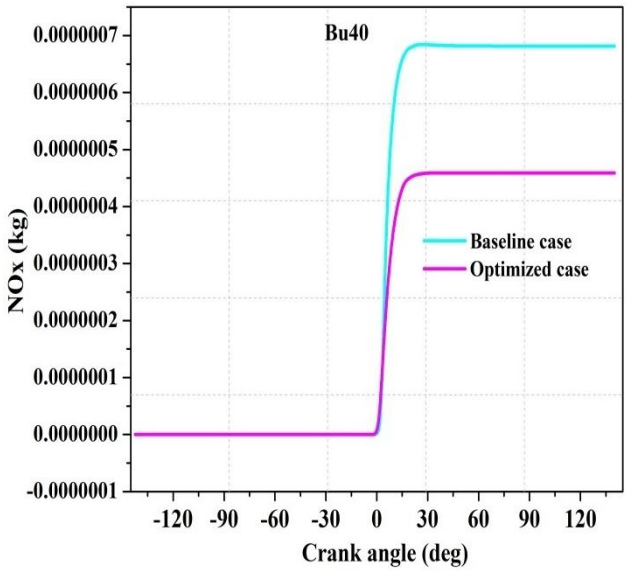

Fig. 6.23. Comparison of NOx with crank angle between baseline and optimized case for Bu40 blend.

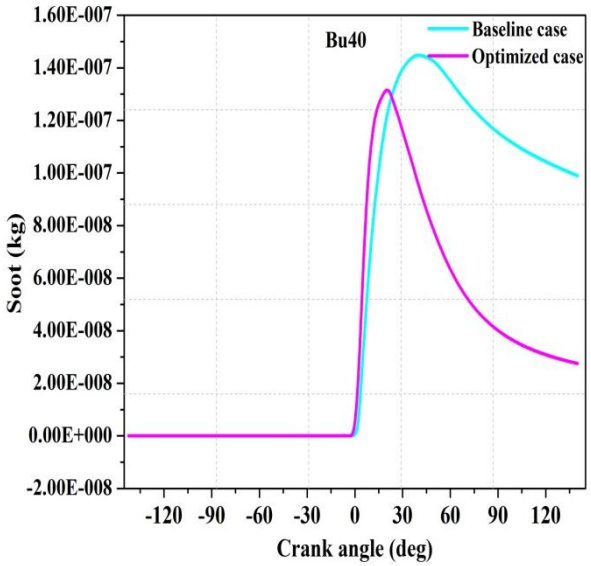

Fig. 6.24. Comparison of soot with crank angle between baseline and optimized case for Bu40 blend.

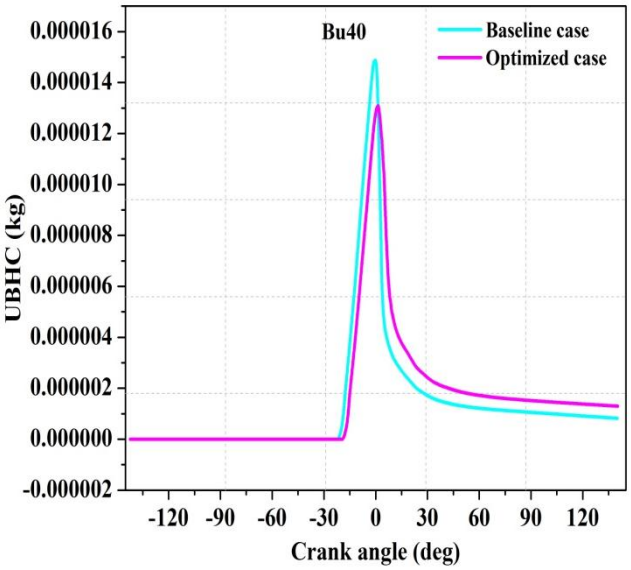

Fig. 6.25. Comparison of UBHC with crank angle between baseline and optimized case for Bu40 blend.

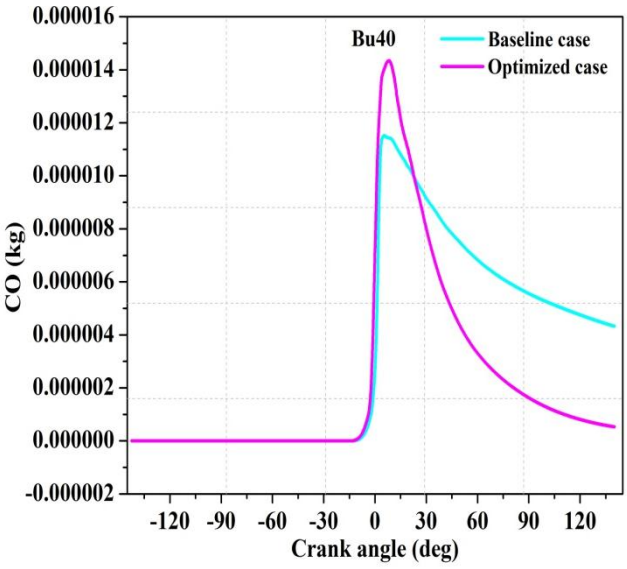

Fig. 6.26. Comparison of CO with crank angle between baseline and optimized case for Bu40 blend.

6.2.8. Comparisons of homogeneity of the baseline and optimized cases for Bu40 blend operation

Crank angle (deg)	Baseline Case (Bu40)	Optimized Case (Bu40)
0	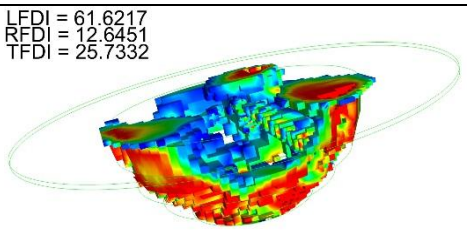	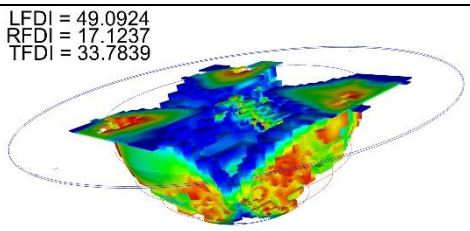
40	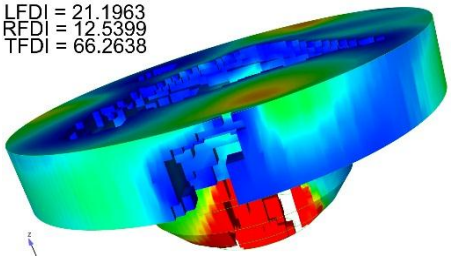	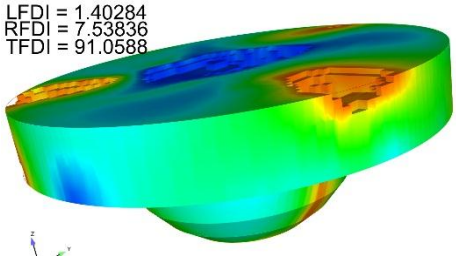

Fig. 6.27. Comparisons of homogeneity of the baseline and optimized cases for Bu40 blend.

The comparison of air-fuel mixture homogeneity for the baseline and the optimized case of Bu40 operation at different crank angles is shown in figure 6.27. The optimized case of Bu40 improved the TFDI by 27.02% compared to the baseline case. The LFDI and RFDI

reduced for the optimum case by 93.3% and 40% respectively compared to the baseline configuration.

6.3. Comparison of the Optimum performance configuration for the four test fuels

Table 6.19 shows a comparison of the values of the operating parameters for the baseline configuration and the optimum cases for the four different test fuels. From the table it can be observed that with increase in the butanol content in the blends from Bu00 to Bu40, the optimum FIP, optimum SOI and the optimum EGR are decreasing, while the optimum CR is more or less constant. Table 6.20 shows the properties of diesel and butanol. The difference in the values of the operating parameters for the butanol/diesel blends can be attributed to these differences in the properties of the test fuels.

Table 6.19. Comparison of optimum values with baseline values for all test fuels.

S. No.	Test fuel	CR	FIP (bar)	SOI (CA bTDC)	EGR (%)
1.	**Bu00 (baseline)**	17.5	220	23	0
2.	**Bu00 (Optimum)**	18.9	279	25.2	29.9
3.	**Bu20 Optimum)**	18.9	275	23.4	28.2
4.	**Bu30 (Optimum)**	18.9	260	21.2	24.5
5.	**Bu40 (Optimum)**	19	248	19	22

Table 6.20. Properties of the diesel and butanol.

Properties	Diesel fuel	Butanol
Boiling point (^{o}C)	180 to 360	117
Self-ignition point (^{o}C)	250 to 300	350
Cetane number	52	25
Latent heat of evaporation (kJ/kg)	270-375	580

Table 6.21. Comparison of ISFC, ISEC, soot, NOx and TFDI of the optimum cases with baseline values for all test fuels.

S. No.	Test fuel	ISFC (g/kWh)	(ISEC) (MJ/kWh)	Soot (g/kWh)	NOx (g/kWh)	TFDI (%)
1.	**Bu00 (baseline)**	205	8.917	1.51	8.3	63.7
2.	**Bu00 (Optimum)**	209	8.656	0.90	6.5	78.92
3.	**Bu20 Optimum)**	205.2	8.57	0.68	5.56	81.07
4.	**Bu30 (Optimum)**	214	8.006	0.42	4.9	85.9
5.	**Bu40 (Optimum)**	219	7.401	0.2	3.4	91.05
6.	**Change w.r.t. baseline (Bu00) and optimized case (Bu40)**	**2.69%** ↑	**17.00** ↓	**86.7** ↓	**59.0** ↓	**30.03** ↑

From Table 6.21 it is observed that the ISEC, soot and NOx reduced by 17%, 86.7% and 59.0% respectively, for the Bu40 optimum case compared to the baseline configuration of Bu00 case. Hence, Bu40 blend with the optimized set of operating parameters was found to give better performance with lower emissions. The TFDI also increased by 30% for the optimum case of Bu40 blend as compared to the baseline case of Bu00. This indicates that the TFDI is better for the optimized case, which is an index of the homogeneous charge preparation. This shows that all four optimized cases achieved the HCCI combustion characteristics. Therefore, the use of Bu40 is justified as a replacement for the conventional diesel in a CI engine with minor modification of the engine operating parameters viz., CR, FIP, SOI and EGR.

6.4. Comparison of parameter influence on the performance and emission characteristics for Bu00, Bu20, Bu30 and Bu40

The effect of CR, SOI, FIP, EGR and their interactions were studied on the performance and emission characteristics of a DI-CI engine fuelled with four different butanol/diesel blends, viz., (Bu00, Bu20, Bu30 and Bu40). It was observed that the individual parameters have more influence on the performance and emissions characteristics than the interaction effects. The optimum combination set of parameters for each one of these four test fuels was determined based on the minimization of ISFC and lower emissions.

Table 6.22. Influential strength of the parameters on ISFC for the four test fuels.

Percentage of contribution by individual parameters				
	Bu00	**Bu20**	**Bu30**	**Bu40**
A-CR	71.8	70.1	64.21	61.8
B-FIP	2.37	2.2	2.19	0.39
C-SOI	9.75	10.8	10.74	12.78
D-EGR	1.74	2.25	3.62	4.21
AB	0.83	2.1	0.94	0.46
AC	7.28	8.48	3.77	1.95
AD	0.06	1.47	1.71	2.97
BC	0.39	0.43	0.28	0.76
BD	0.117	0.01	0.02	0.03
CD	0.0003	0.08	0.37	0.67
A^2	4.06	7.79	11.48	13.7
B^2	0.05	0.08	0.37	0.83
C^2	0.14	0.005	0.48	0.31
D^2	0.11	0.0004	0.03	0.33

The impact of the individual parameters and their interaction effects on the ISFC, soot and NOx are shown in Tables 6.22, 6.23 and 6.24. From Table 6.22, it is observed that the ISFC was most influenced by CR for all the four cases. The SOI is the second most influential parameter on the ISFC. This indicates that CR and SOI are the two potential parameters in deciding the engine performance. The individual parameters have major

influence on the ISFC. However, the interaction terms and square terms also have moderate influence on the ISFC.

From Table 6.23 it is observed that the soot emission was most influenced by the CR and SOI for all the four cases. FIP and EGR have moderate effect on the soot emission. From Table 6.24 it is observed that the EGR has a strong influence on the NOx emission followed by SOI, CR and FIP. On the other hand, for higher butanol content blend, i.e., Bu40, the effect of EGR on the NOx was the minimum.

Table 6.23. Influential strength of the parameters on soot for the four test fuels.

Percentage of contribution by individual parameters				
	Bu00	**Bu20**	**Bu30**	**Bu40**
A-CR	73.24	70.4	63.16	60.1
B-FIP	2.92	0.66	0.99	1.08
C-SOI	5.24	9.0	10.3	11.27
D-EGR	4.66	0.8	0.52	0.41
AB	0.071	2.08	1.25	0.031
AC	0.81	0.12	0.02	4.71
AD	0.00034	0.2	0.21	0.52
BC	0.58	0.86	1.22	0.61
BD	0.0098	0.2	0.079	3.18
CD	4.46	2.94	3.53	0.33
A^2	4.084	32.3	11.15	1.91
B^2	1.082	0.98	0.35	2.61
C^2	3.36	17.18	6.5	0.8
D^2	0.013	1	1.34	0.009

Table 6.24. Influential strength of the parameters on NOx for the four test fuels.

Percentage of contribution by individual parameters				
	Bu00	**Bu20**	**Bu30**	**Bu40**
A-CR	17.45	23.28	32.15	32.44
B-FIP	2.98	3.1	3.95	6.27
C-SOI	34.85	33.2	29.15	24.1
D-EGR	36.85	35.3	22.36	13.53
AB	0.01	0.0001	0.321	0.71
AC	1.92	4.14	5.717	12.93
AD	1.32	0.75	1.77	1.24
BC	0.21	0.21	0.97	2.18
BD	0.16	0.04	0.65	2.7
CD	1.91	1.51	0.708	0.00045
A^2	0.03	0.15	0.0705	1.71
B^2	0.003	0.0001	0.166	0.1
C^2	1.478	4.16	0.66	1.17
D^2	0.57	0.0009	0.001	0

6.5. Major observations

In chapter 6, a numerical model was developed for analysing the effect of the engine operating parameters on the performance and emission characteristics of a DI-CI engine. In the next step, the optimum combination of operating parameters were determined by using RSM technique with an objective of minimization of ISFC, soot and NOx emissions. The homogeneity index was also compared for the optimum and the baseline cases.

The following major conclusions have been drawn from the numerical analysis:

For ISFC

- For all the four test fuels (Bu00, Bu20, Bu30 and Bu40), ISFC was most impacted by CR.
- SOI has a moderate effect on the ISFC for all the four test fuels.

- CR and SOI are two potential parameters in deciding the engine performance and emission characteristics. However, there is a limit in advancing the SOI due to the possibility of negative work.

For Soot

- For all the four test fuels (Bu00, Bu20, Bu30 and Bu40), soot was most affected by CR.
- SOI is the second most influential parameter on the soot emission for all the four test fuels.

For NOx

- In case of Bu00 fuel, EGR has a strong influence on the NOx emission followed by SOI, CR and FIP. On the other hand for higher butanol content blend, i.e., Bu40, the effect of EGR on NOx was minimum.

Comparison of the optimization case with baseline configuration

For Bu00 case

- The soot and NOx emissions decreased by 40.3% and 21.6%, respectively, and a marginal reduction in ISFC (2.9%) was observed with the optimum values of the operating parameters compared to the baseline configuration of the engine. Similarly, the TFDI increased by 19.3% for the optimized configuration compared to the baseline configuration

- The optimum combination of input parameters were determined to be CR of 18.9, SOI of 25.2° CA bTDC, FIP of 279.9 bar, and EGR of 29.9% with a composite desirability of 0.97.

For Bu40 case

- The optimum combination of input parameters for the Bu40 case was determined to be CR of 19, FIP of 248 bar, SOI of 19° CA bTDC, and EGR of 22% with a composite desirability of 0.98.
- With the set of the optimum values of the operating parameters, the soot and NOx emissions decreased by 77.5% and 53.9%, respectively, and a marginal reduction in ISFC (1.8%) was accomplished. Similarly, the TFDI improved by 27.2% compared to the baseline case. The ISEC reduced by 17% for the Bu40 optimum case compared to the baseline configuration of Bu00 case.

Therefore, the use of Bu40 as the fuel is justified as a replacement for the conventional diesel in a DI-CI engine with suitable modification of the engine operating parameters, viz., CR, FIP, SOI and EGR.

Chapter 7

Conclusions

7.1. Over all conclusions

Numerical and experimental studies were carried out to evaluate the performance and emission characteristics of a DI-CI engine operated with different butanol/diesel blends (Bu00 to Bu40). The numerical analysis was carried out to study the influence of four different operating parameters (CR, SOI, FIP and EGR). RSM methodology was used to find the set of optimum values for these four operating parameters with an objective of minimization of three output parameters, viz., ISFC, soot and NOx. Homogeneity index of the fuel-air mixture inside the cylinder was evaluated based on the fuel distribution index. Experimental investigations were carried out on a DI-CI engine operating with butanol/diesel blends (0% and 40% of butanol-by volume) to assess the effect of EGR (0-30%), CR (14-18) and FIP (200-280 bar) on the combustion, performance and emission characteristics. The numerical results were validated by comparing them with the experimental results.

The following important conclusions were drawn from the present study:

1. Numerical studies were carried out to identify the operating ranges for the four input parameters considered (CR, SOI, FIP and EGR) based on their effect on the three output parameters considered, viz., ISFC, soot and NOx. From the analysis the optimum operating ranges were identified as CR from 14 to 19, FIP from 200 to 280 bar, SOI from -17^{o} to -29^{o} CA bTDC, and EGR from 0 to 30%.
2. From the ANOVA analysis, it was observed that CR and SOI were the most influential factors on the ISFC and soot for all the four cases of butanol/diesel blends. It was also found from the ANOVA analysis that in case of diesel fuel (Bu00), EGR has a strong effect on the NOx emission followed by SOI, CR and FIP. On the other

hand, for higher butanol content blend, i.e., Bu40, the effect of EGR on the NOx was minimum.

3. From the ANOVA analysis, it was observed that individual parameters have a strong effect on the output parameters, i.e., ISFC, soot and NOx emission. This means that the linear relation with respect to individual parameters were dominant over the interaction effects and quadratic terms.
4. From a comparison of the optimum values for different blends, it was observed that with an increase in the butanol content in the blends from Bu00 to Bu40, the optimum values of FIP, SOI and EGR were decreasing, while the optimum CR was more or less constant for all the blends.
5. From a comparison of the Bu00 and Bu40 operation of the engine at the respective optimized configurations, for the Bu40 operation the soot and NOx emissions reduced by 77.7%, 47.69% respectively, while the ISEC reduced by 14.4%,compared to the optimized case of Bu00.
6. Homogeneity of the fuel - air mixture inside the cylinder was evaluated in terms of the TFDI. It was observed that the TFDI increased for the optimized case by 19.3%, 21.3%, 24.1% and 27.02% for Bu00, Bu20, Bu30 and Bu40 respectively compared to their respective baseline configurations. This indicates that the TFDI is better for the optimized cases, which is an index of homogeneous charge preparation. This shows that all the four optimized cases provided nearly HCCI combustion characteristics.
7. From the present study, it was concluded that butanol/diesel blends engine upto a maximum of 40% of butanol content (Bu40) can be substituted for pure diesel in the CI engine without major modifications to the.

Therefore, it can be concluded that a conventional CI engine can operate with butanol/diesel blends with slight modifications to the engine in terms of operating parameters for better performance and minimum emissions. Hence the use of Bu40 blend is justified and recommended as a replacement for the conventional diesel fuel in a CI engine.

7.2. Scope for future work

- Further studies are required to investigate the effect of higher than 40% (v/v) butanol blend on the combustion, performance and emissions characteristics of a CI engine.
- The effect of butanol/diesel blends on the formation of other emissions is to be thoroughly studied, before the butanol/diesel blends are used in the vehicles.
- Further studies can be carried out to achieve better homogeneous charge in the DI-CI engine for enabling HCCI mode by varying the piston bowl shape, swirl generation through inlet manifold, ultra high injection pressure and fuel additives.
- For better LTC mode with butanol, a combination of SOI, FIP, and O_2 concentration at intake can be examined using optimization techniques without depending much on the EGR rate.

References

[1] Feng H, Zheng Z, Yao M, Cheng G, Wang M, Wang X. Effects of exhaust gas recirculation on low temperature combustion using wide distillation range diesel. Energy 2013;51:291–6. doi:10.1016/j.energy.2012.12.023.

[2] Maurya RK, Agarwal AK. Experimental investigation of cyclic variations in HCCI combustion parameters for gasoline like fuels using statistical methods. Appl Energy 2013;111:310–23. doi:10.1016/j.apenergy.2013.05.004.

[3] Fathi M, Saray RK, Checkel MD. The influence of Exhaust Gas Recirculation (EGR) on combustion and emissions of n-heptane/natural gas fueled Homogeneous Charge Compression Ignition (HCCI) engines. Appl Energy 2011;88:4719–24. doi:10.1016/j.apenergy.2011.06.017.

[4] Agarwal D, Singh SK, Agarwal AK. Effect of Exhaust Gas Recirculation (EGR) on performance, emissions, deposits and durability of a constant speed compression ignition engine. Appl Energy 2011;88:2900–7. doi:10.1016/j.apenergy.2011.01.066.

[5] Siebers DL. SAE TECHNICAL Liquid-Phase Fuel Penetration in Diesel Sprays 2018.

[6] Kim K, Kim D, Jung Y, Bae C. Spray and combustion characteristics of gasoline and diesel in a direct injection compression ignition engine. Fuel 2013;109:616–26. doi:10.1016/j.fuel.2013.02.060.

[7] Wang WG, Clark NN, Lyons DW, Yang RM, Gautam M, Bata RM, et al. Emissions comparisons from alternative fuel buses and diesel buses with a chassis dynamometer testing facility. Environ Sci Technol 1998;31:3132–7. doi:10.1021/es9701063.

[8] Shahabuddin M, Kalam MA, Masjuki HH, Bhuiya MMK, Mofijur M. An experimental investigation into biodiesel stability by means of oxidation and property determination. Energy 2012;44:616–22. doi:10.1016/j.energy.2012.05.032.

[9] No SY. Application of biobutanol in advanced CI engines – A review. Fuel 2016;183:641–58. doi:10.1016/j.fuel.2016.06.121.

[10] Jin C, Yao M, Liu H, Lee CFF, Ji J. Progress in the production and application of n-butanol as a biofuel. Renew Sustain Energy Rev 2011;15:4080–106.

doi:10.1016/j.rser.2011.06.001.

[11] Dernotte J, Mounaim-Rousselle C, Halter F, Seers P. Évaluation De Mélange Butanol-Essence Dans Un Moteur À Allumage Commandé À Injection Indirecte. Oil Gas Sci Technol 2010;65:345–51. doi:10.2516/ogst/2009034.

[12] Chen C, Fawcett A. Butanol by Two Stage Fermentation. Thesis 2009:213.

[13] Al- Hasan MI, Al- Momany M. The effect of iso- butanol- diesel blends on engine performance. Transport 2008. doi:10.3846/1648-4142.2008.23.306-310.

[14] Chen Z, Liu J, Han Z, Du B, Liu Y, Lee C. Study on performance and emissions of a passenger-car diesel engine fueled with butanol-diesel blends. Energy 2013;55:638–46. doi:10.1016/j.energy.2013.03.054.

[15] Rakopoulos DC, Rakopoulos CD, Hountalas DT, Kakaras EC, Giakoumis EG, Papagiannakis RG. Investigation of the performance and emissions of bus engine operating on butanol/diesel fuel blends. Fuel 2010;89:2781–90. doi:10.1016/j.fuel.2010.03.047.

[16] Karabektas M, Hosoz M. Performance and emission characteristics of a diesel engine using isobutanol-diesel fuel blends. Renew Energy 2009;34:1554–9. doi:10.1016/j.renene.2008.11.003.

[17] Doğan O. The influence of n-butanol/diesel fuel blends utilization on a small diesel engine performance and emissions. Fuel 2011;90:2467–72. doi:10.1016/j.fuel.2011.02.033.

[18] Ozsezen AN, Turkcan A, Sayin C, Canakci M. Comparison of performance and combustion parameters in a heavy-duty diesel engine fueled with iso-butanol/diesel fuel blends. Energy, Explor Exploit 2011;29:525–41. doi:10.1260/0144-5987.29.5.525.

[19] Satsangi DP, Tiwari N. Experimental investigation on combustion, noise, vibrations, performance and emissions characteristics of diesel/n-butanol blends driven genset engine. Fuel 2018;221:44–60. doi:10.1016/j.fuel.2018.02.060.

[20] Al- Hasan MI, Al- Momany M. The effect of iso- butanol- diesel blends on engine performance. Transport 2008;23:306–10. doi:10.3846/1648-4142.2008.23.306-310.

[21] Lamani VT, Yadav AK, Gottekere KN. Performance, emission, and combustion characteristics of twin-cylinder common rail diesel engine fuelled with butanol-diesel blends. Environ Sci Pollut Res 2017;24:23351–62. doi:10.1007/s11356-017-9956-7.

[22] Merola SS, Tornatore C, Iannuzzi SE, Marchitto L, Valentino G. Combustion process investigation in a high speed diesel engine fuelled with n-butanol diesel blend by conventional methods and optical diagnostics. Renew Energy 2014;64:225–37. doi:10.1016/j.renene.2013.11.017.

[23] Liu B, Cheng X, Liu J, Pu H. Investigation into particle emission characteristics of partially premixed combustion fueled with high n-butanol-diesel ratio blends. Fuel 2018;223:1–11. doi:10.1016/j.fuel.2018.02.196.

[24] Chen Z, Wu Z, Liu J, Lee C. Combustion and emissions characteristics of high n-butanol/diesel ratio blend in a heavy-duty diesel engine and EGR impact. Energy Convers Manag 2014;78:787–95. doi:10.1016/j.enconman.2013.11.037.

[25] Huang H, Liu Q, Yang R, Zhu T, Zhao R, Wang Y. Investigation on the effects of pilot injection on low temperature combustion in high-speed diesel engine fueled with n - butanol – diesel blends 2015;106:748–58. doi:10.1016/j.enconman.2015.10.031.

[26] Nayyar A, Sharma D, Soni SL, Mathur A. Experimental investigation of performance and emissions of a VCR diesel engine fuelled with n-butanol diesel blends under varying engine parameters. Environ Sci Pollut Res 2017;24:20315–29. doi:10.1007/s11356-017-9599-8.

[27] Maurya RK, Saxena MR, Rai P, Bhardwaj A. Effect of compression ratio, nozzle opening pressure, engine load, and butanol addition on nanoparticle emissions from a non-road diesel engine. Environ Sci Pollut Res 2018:1–16. doi:10.1007/s11356-018-1644-8.

[28] He T, Chen Z, Zhu L, Zhang Q. The in fl uence of alcohol additives and EGR on the combustion and emission characteristics of diesel engine under high-load condition. Appl Therm Eng 2018;140:363–72. doi:10.1016/j.applthermaleng.2018.05.064.

[29] Fayad MA. Effect of renewable fuel and injection strategies on combustion characteristics and gaseous emissions in diesel engines. Energy Sources, Part A Recover Util Environ Eff 2020;42:460–70. doi:10.1080/15567036.2019.1587091.

[30] Emiroğlu AO. Effect of fuel injection pressure on the characteristics of single cylinder diesel engine powered by butanol-diesel blend. Fuel 2019;256:115928. doi:10.1016/j.fuel.2019.115928.

[31] Saravanan S, Rajesh Kumar B, Varadharajan A, Rana D, Sethuramasamyraja B, Lakshmi Narayana rao G. Optimization of DI diesel engine parameters fueled with iso-butanol/diesel blends – Response surface methodology approach. Fuel 2017;203:658–70. doi:10.1016/j.fuel.2017.04.083.

[32] Nayyar A, Sharma D, Soni SL, Mathur A. Characterization of n-butanol diesel blends on a small size variable compression ratio diesel engine: Modeling and experimental investigation. Energy Convers Manag 2017;150:242–58. doi:10.1016/j.enconman.2017.08.031.

[33] Ballesteros R, Hernández JJ, Guillén-Flores J. Carbonyls speciation in a typical European automotive diesel engine using bioethanol/butanol-diesel blends. Fuel 2012;95:136–45. doi:10.1016/j.fuel.2011.09.012.

[34] Zhang ZH, Chua SM, Balasubramanian R. Comparative evaluation of the effect of butanol-diesel and pentanol-diesel blends on carbonaceous particulate composition and particle number emissions from a diesel engine. Fuel 2016;176:40–7. doi:10.1016/j.fuel.2016.02.061.

[35] Zhang ZH, Balasubramanian R. Influence of butanol-diesel blends on particulate emissions of a non-road diesel engine. Fuel 2014;118:130–6. doi:10.1016/j.fuel.2013.10.059.

[36] Choi B, Jiang X. Individual hydrocarbons and particulate matter emission from a turbocharged CRDI diesel engine fueled with n-butanol/diesel blends. Fuel 2015;154:188–95. doi:10.1016/j.fuel.2015.03.084.

[37] Fang Q, Fang J, Zhuang J, Huang Z. Effects of ethanol-diesel-biodiesel blends on combustion and emissions in premixed low temperature combustion. Appl Therm Eng 2013;54:541–8. doi:10.1016/j.applthermaleng.2013.01.042.

[38] Zhang Q, Yao M, Zheng Z, Liu H, Xu J. Experimental study of n-butanol addition on performance and emissions with diesel low temperature combustion. Energy 2012;47:515–21. doi:10.1016/j.energy.2012.09.020.

[39] Kook S, Bae C, Miles PC, Choi D, Pickett LM. The Influence of Charge Dilution and Injection Timing on Low-Temperature Diesel Combustion and Emissions 2005. doi:10.4271/2005-01-3837.

[40] Rajesh Kumar B, Saravanan S, Rana D, Nagendran A. Combined effect of injection timing and exhaust gas recirculation (EGR) on performance and emissions of a DI diesel engine fuelled with next-generation advanced biofuel – diesel blends using response surface methodology. Energy Convers Manag 2016;123:470–86. doi:10.1016/j.enconman.2016.06.064.

[41] Valentino G, Corcione FE, Iannuzzi SE, Serra S. Experimental study on performance and emissions of a high speed diesel engine fuelled with n-butanol diesel blends under premixed low temperature combustion. Fuel 2012;92:295–307. doi:10.1016/j.fuel.2011.07.035.

[42] Han X, Zheng M, Wang J. Fuel suitability for low temperature combustion in compression ignition engines. Fuel 2013;109:336–49. doi:10.1016/j.fuel.2013.01.049.

[43] Gu X, Li G, Jiang X, Huang Z, Lee CF. Experimental study on the performance of and emissions from a low-speed light-duty diesel engine fueled with n-butanol-diesel and isobutanol-diesel blends. Proc Inst Mech Eng Part D J Automob Eng 2013;227:261–71. doi:10.1177/0954407012453231.

[44] Yang B, Yao M, Cheng WK, Zheng Z, Yue L. Regulated and unregulated emissions from a compression ignition engine under low temperature combustion fuelled with gasoline and n-butanol/gasoline blends. Fuel 2014;120:163–70. doi:10.1016/j.fuel.2013.11.058.

[45] Zhou X, Song M, Huang H, Yang R, Wang M. Numerical Study of the Formation of Soot Precursors during Low- Temperature Combustion of a n ‑ Butanol − Diesel Blend. Energy & Fuels 2014;28:7149–58. doi:10.1021/ef501370u.

[46] Zheng M, Han X, Asad U, Wang J. Investigation of butanol-fuelled HCCI combustion on a high efficiency diesel engine. Energy Convers Manag 2015;98:215–24. doi:10.1016/j.enconman.2015.03.098.

[47] Rajesh Kumar B, Saravanan S. Effect of iso-butanol addition to diesel fuel on performance and emissions of a di diesel engine with exhaust gas recirculation. Proc

Inst Mech Eng Part A J Power Energy 2016;230:112–25. doi:10.1177/0957650915617107.

[48] Rajesh Kumar B, Saravanan S. Effects of iso-butanol/diesel and n-pentanol/diesel blends on performance and emissions of a di diesel engine under premixed LTC (low temperature combustion) mode. Fuel 2016;170:49–59. doi:10.1016/j.fuel.2015.12.029.

[49] Zhu J, Huang H, Zhu Z, Lv D, Pan Y, Wei H, et al. Effect of intake oxygen concentration on diesel–n-butanol blending combustion: An experimental and numerical study at low engine load. Energy Convers Manag 2018;165:53–65. doi:10.1016/j.enconman.2018.03.045.

[50] Şahin Z, Aksu ON. Experimental investigation of the effects of using low ratio n-butanol/diesel fuel blends on engine performance and exhaust emissions in a turbocharged DI diesel engine. Renew Energy 2015;77:279–90. doi:10.1016/j.renene.2014.11.093.

[51] Siwale L, Kristóf L, Adam T, Bereczky A, Mbarawa M, Penninger A, et al. Combustion and emission characteristics of n-butanol / diesel fuel blend in a turbo-charged compression ignition engine. Fuel 2013;107:409–18. doi:10.1016/j.fuel.2012.11.083.

[52] Rakopoulos DC, Rakopoulos CD, Giakoumis EG, Dimaratos AM, Kyritsis DC. Effects of butanol-diesel fuel blends on the performance and emissions of a high-speed di diesel engine. Energy Convers Manag 2010;51:1989–97. doi:10.1016/j.enconman.2010.02.032.

[53] Campos-Fernández J, Arnal JM, Gómez J, Dorado MP. A comparison of performance of higher alcohols/diesel fuel blends in a diesel engine. Appl Energy 2012;95:267–75. doi:10.1016/j.apenergy.2012.02.051.

[54] Miers S a., Carlson RW, Mcconnell SS, Ng HK, Wallner T, Esper JL. Drive Cycle Analysis of Butanol/Diesel Blends in a Light-Duty Vehicle. SAE Pap 2008;2008-01–23. doi:10.4271/2008-01-2381.

[55] Yao M, Wang H, Zheng Z, Yue Y. Experimental study of n-butanol additive and multi-injection on HD diesel engine performance and emissions. Fuel 2010;89:2191–201. doi:10.1016/j.fuel.2010.04.008.

[56] Zheng Z, Yue L, Liu H, Zhu Y, Zhong X, Yao M. Effect of two-stage injection on combustion and emissions under high EGR rate on a diesel engine by fueling blends of diesel/gasoline, diesel/n-butanol, diesel/gasoline/n-butanol and pure diesel. Energy Convers Manag 2015;90:1–11. doi:10.1016/j.enconman.2014.11.011.

[57] Huang H, Zhou C, Liu Q, Wang Q, Wang X. An experimental study on the combustion and emission characteristics of a diesel engine under low temperature combustion of diesel/gasoline/n-butanol blends. Appl Energy 2016;170:219–31. doi:10.1016/j.apenergy.2016.02.126.

[58] Rajesh Kumar B, Saravanan S, Rana D, Nagendran A. A comparative analysis on combustion and emissions of some next generation higher-alcohol/diesel blends in a direct-injection diesel engine. Energy Convers Manag 2016;119:246–56. doi:10.1016/j.enconman.2016.04.053.

[59] Zhang T, Jacobson L, Björkholtz C, Munch K, Denbratt I. Effect of using butanol and octanol isomers on engine performance of steady state and cold start ability in different types of Diesel engines. Fuel 2016;184:708–17. doi:10.1016/j.fuel.2016.07.046.

[60] Kumar N, Pali HS. Effects of n-Butanol Blending with Jatropha Methyl Esters on Compression Ignition Engine. Arab J Sci Eng 2016;41:4327–36. doi:10.1007/s13369-016-2127-1.

[61] Zheng Z, Wang XF, Zhong X, Hu B, Liu H, Yao M. Experimental study on the combustion and emissions fueling biodiesel/n-butanol, biodiesel/ethanol and biodiesel/2,5-dimethylfuran on a diesel engine. Energy 2016;115:539–49. doi:10.1016/j.energy.2016.09.054.

[62] Wei M, Li S, Xiao H, Guo G. Combustion performance and pollutant emissions analysis using diesel/gasoline/iso-butanol blends in a diesel engine. Energy Convers Manag 2017;149:381–91. doi:10.1016/j.enconman.2017.07.038.

[63] Lapuerta M, Hernández JJ, Rodríguez-Fernández J, Barba J, Ramos A, Fernández-Rodríguez D. Emission benefits from the use of n-butanol blends in a Euro 6 diesel engine. Int J Engine Res 2017:146808741774257. doi:10.1177/1468087417742578.

[64] Emiroğlu AO, Şen M. Combustion, performance and emission characteristics of various alcohol blends in a single cylinder diesel engine. Fuel 2018;212:34–40.

doi:10.1016/j.fuel.2017.10.016.

[65] Ahmed SA, Zhou S, Zhu Y, Feng Y. Numerical investigation of n-butanol addition on the performance and emission characteristics of CI diesel engine. Int Energy J 2018;18:25–38.

[66] Choi B, Jiang X, Kim YK, Jung G, Lee C, Choi I, et al. Effect of diesel fuel blend with n-butanol on the emission of a turbocharged common rail direct injection diesel engine. Appl Energy 2015;146:20–8. doi:10.1016/j.apenergy.2015.02.061.

[67] López AF, Cadrazco M, Agudelo AF, Corredor LA, Vélez JA, Agudelo JR. Impact of n-butanol and hydrous ethanol fumigation on the performance and pollutant emissions of an automotive diesel engine. Fuel 2015;153:483–91. doi:10.1016/j.fuel.2015.03.022.

[68] Valentino G, Corcione FE, Iannuzzi SE. Effects of gasoline-diesel and n-butanol-diesel blends on performance and emissions of an automotive direct-injection diesel engine. Int J Engine Res 2012. doi:10.1177/1468087412441879.

[69] Iannuzzi SE, Valentino G. Comparative behavior of gasoline-diesel/butanol-diesel blends and injection strategy management on performance and emissions of a light duty diesel engine. Energy 2014;71:321–31. doi:10.1016/j.energy.2014.04.065.

[70] Reitz RD, Beale JC. Modeling Spray Atomization With the Kelvin-Helmholtz/Rayleigh-Taylor Hybrid Model. At Sprays 1999;9:623–50. doi:10.1615/AtomizSpr.v9.i6.40.

[71] Ra Y, Reitz RD. A vaporization model for discrete multi-component fuel sprays. Int J Multiph Flow 2009;35:101–17. doi:10.1016/j.ijmultiphaseflow.2008.10.006.

[72] Kennedy IM. Models of soot formation and oxidation. Prog Energy Combust Sci 1997;23:95–132. doi:10.1016/S0360-1285(97)00007-5.

[73] Ramesh N, Mallikarjuna JM. Evaluation of in-cylinder mixture homogeneity in a diesel HCCI engine – A CFD analysis. Eng Sci Technol an Int J 2016;19:917–25. doi:10.1016/j.jestch.2015.11.013.

[74] Akihama K, Takatori Y, Inagaki K, Sasaki S, Dean AM. Mechanism of the Smokeless Rich Diesel Combustion by Reducing Temperature 2001;2001. doi:10.4271/2001-01-

0655.

[75] Pradeep V, Sharma RP. Use of HOT EGR for NOx control in a compression ignition engine fuelled with bio-diesel from Jatropha oil. Renew Energy 2007;32:1136–54. doi:10.1016/j.renene.2006.04.017.

[76] Uyumaz A. An experimental investigation into combustion and performance characteristics of an HCCI gasoline engine fueled with n -heptane , isopropanol and n -butanol fuel blends at different inlet air temperatures 2015;98:199–207.

[77] Rajesh Kumar B, Saravanan S, Rana D, Nagendran A. A comparative analysis on combustion and emissions of some next generation higher-alcohol/diesel blends in a direct-injection diesel engine. Energy Convers Manag 2016;119:246–56. doi:10.1016/j.enconman.2016.04.053.

[78] Sayin C. Engine performance and exhaust gas emissions of methanol and ethanol-diesel blends. Fuel 2010;89:3410–5. doi:10.1016/j.fuel.2010.02.017.

[79] Sarathy SM, Thomson MJ, Togbé C, Dagaut P, Halter F, Mounaim-Rousselle C. An experimental and kinetic modeling study of n-butanol combustion. Combust Flame 2009;156:852–64. doi:10.1016/j.combustflame.2008.11.019.

[80] Rakopoulos DC, Rakopoulos CD, Hountalas DT, Kakaras EC, Giakoumis EG, Papagiannakis RG. Investigation of the performance and emissions of bus engine operating on butanol/diesel fuel blends. Fuel 2010;89:2781–90. doi:10.1016/j.fuel.2010.03.047.

[81] Prasad KS, Rao SS, Raju VRK. Performance and emission characteristics of a DI-CI engine operated with n-butanol/diesel blends. Energy Sources, Part A Recover Util Environ Eff 2019;7036. doi:10.1080/15567036.2019.1685611.

[82] De Serio D, de Oliveira A, Sodré JR. Effects of EGR rate on performance and emissions of a diesel power generator fueled by B7. J Brazilian Soc Mech Sci Eng 2017;39:1919–27. doi:10.1007/s40430-017-0777-x.

[83] Hountalas DT, Mavropoulos GC, Binder KB. Effect of exhaust gas recirculation (EGR) temperature for various EGR rates on heavy duty DI diesel engine performance and emissions. Energy 2008;33:272–83. doi:10.1016/j.energy.2007.07.002.

[84] Singh AP, Agarwal AK. An experimental investigation of combustion, emissions and performance of a diesel fuelled HCCI engine. SAE Tech Pap 2012. doi:10.4271/2012-28-0005.

[85] Purushothaman K, Nagarajan G. Effect of injection pressure on heat release rate and emissions in CI engine using orange skin powder diesel solution 2009;50:962–9. doi:10.1016/j.enconman.2008.12.030.

[86] Kannan GR, Anand R. Effect of injection pressure and injection timing on DI diesel engine fuelled with biodiesel from waste cooking oil. Biomass and Bioenergy 2012;46:343–52. doi:10.1016/j.biombioe.2012.08.006.

[87] Wang H, Deneys Reitz R, Yao M, Yang B, Jiao Q, Qiu L. Development of an n-heptane-n-butanol-PAH mechanism and its application for combustion and soot prediction. Combust Flame 2013;160:504–19. doi:10.1016/j.combustflame.2012.11.017.

[88] Moffat RJ. Using uncertainty analysis in the planning of an experiment. J Fluids Eng Trans ASME 1985;107:173–8. doi:10.1115/1.3242452.

List of Publications

Journal paper:

S. No.	Authors (*)	Title of the Paper	Journal Details (Journal, Year, Vol., pp)	Indexing: SCI/SCOPUS	Impact factor
1	K Siva Prasad, S Srinivasa Rao, VRK Raju, and G Prabhakara Rao	Effect of n-butanol/diesel blends and piston bowl geometry on combustion and emission characteristics of CI engine	Environmental Science and Pollution Research, 2019, no. 2 : 1661-1674	SCI	3.056
2	K Siva Prasad, S Srinivasa Rao and VRK Raju	Performance and emission characteristics of a DI-CI engine operated with n-butanol/diesel blends	Energy Sources, Part A: Recovery, Utilization, and Environmental Effects (2019): 1-12	SCI	1.18
3	K Siva Prasad, S Srinivasa Rao and VRK Raju	Parametric optimization of a direct injection-compression ignition engine fuelled with butanol/diesel blend using response surface methodology	Environmental Progress & Sustainable Energy (2020):no. 3, e13355	SCI	1.989
4	K Siva Prasad, S Srinivasa Rao and VRK Raju	Comparative study on single-injection and pilot-injection strategies for DI CI engine fuelled with the butanol/diesel blend	." *International Journal of Ambient Energy* 2020, no. 11 : 1227-1234	ESCI	NA
5	K Siva Prasad, S Srinivasa Rao and VRK Raju	Effect of compression ratio and fuel injection pressure on the characteristics of a CI engine operating with butanol/diesel blends	Alexandria Engineering Journal, 2021: no. 1, 1183-1197.	SCI	2.46
6	K Siva Prasad, S Srinivasa Rao and VRK Raju	Effect of EGR on the performance and emission characteristics of DI-CI engine fuelled with butanol/diesel blends	Environmental progress & Sustainable Energy,(2021) ep.13658	SCI	1.989

Conference paper:

S. No.	Authors (*)	Title of the Paper	Presentation: Oral / Poster	Event Details (Event, Place, Dates)
1	K. Siva Prasad, S. S Rao, and V.R.K Raju	Performance and Emission Analysis of CI Engine with Butanol-Diesel Blends	Presentation	25th National Conference on Internal Combustion Engines and Combustions at NIT Karnataka, December 15-17, 2017
2	K. Siva Prasad, S. S Rao, and V.R.K Raju	Effect of n-butanol/diesel blends on the performance and emission characteristics of DI CI engine	Presentation	2nd International Conference on New Frontiers in Chemical, Energy and Environmental Engineering (INCEEE-2019) at NIT Warangal, 15 to 16 February 2019

Appendix A

A.1 Test fuel preparation

N-butanol (normal butanol) is a 4-carbon structure straight-chain alcohol (the chemical formula is C_4H_9OH) purchased from a local retailer at Warangal. N-butanol was used in the present study. Butanol (20%, and 40% by volume) was blended with diesel fuel individually (no external agent added) and was denoted as Bu20 and Bu40. The mixing of diesel and butanol was carried out in a high-pressure Homogenizer (figure 1). Homogenizer is manufactured by Ormerod Engineers and has a capacity of 10 GPH (gallons per hour) and can generate a maximum pressure of 1000 lb/in^2 (pounds per inch square). It has a rated power input of 0.25 HP (horsepower). A 250 mm diameter stainless steel coned hopper feed is used to store and supply the blended mixture to the main unit were homogenization takes place. The mixture passes through a very small and narrow gap at a very high pressure. This mechanical action on fluid particles creates very high shear stress, which aids in forming very fine emulsified droplets. The very high pressures in the homogenizer are generated by a high-pressure positive displacement pump. Then, the high-pressure liquid droplets enter the nozzle at the end. As the liquid droplets pass through the nozzle, the pressure reduces and finally the homogenized liquid droplets fall in a beaker or container. To further improve the miscibility of the blended mixture, a mechanical stirrer arrangement was attached and positioned at the centre of the coned feed to stir the mixture thoroughly before passing through the restricted passage. The mechanical stirrer was powered by a motor of Remi Udyog make with a power input of 20 Watts and a rated speed of 4000 rpm. The speed of the motor was adjusted using a variable speed regulator. With the help of the homogenizer, blends of 20%, 30% and 40% by volume of n-butanol in diesel were prepared. The same blends were used in the experimentation. The density of diesel, butanol and their blends were measured using Hydrometer. The calorific value of test fuels was measured using a Bomb calorimeter, and the viscosity was measured using Red-Wood viscometer. Stoichiometric air/fuel ratio and oxygen content (by % wt) were estimated based on the balanced combustion equation of test fuel.

Fig.1. Photographic view of Homogenizer.

A.2. Measurement of test fuel Properties

A.2.1. Measurement of density for diesel, butanol and their blends using Hydrometer

After the preparation of blends, the next step in the experimentation stage was to measure the densities of diesel, butanol and their blends. A hydrometer was used for measuring the density of test fuels (figure 2). The hydrometer is made of clear glass and contains a bulb with mercury or lead at the bottom. It operates on the principle of buoyancy: whenever a lighter object is immersed in a fluid, a buoyant force is exerted on the object, which is equal to the weight of the displaced fluid. A sample of 250 ml. of diesel was heated up to 40 ^{0}C and poured in a graduated cylinder. The hydrometer was immersed in the fuel slowly and it was left to float after it was submerged inside for more than half the length of a hydrometer. After it stopped oscillating inside the graduating cylinder, the density value was recorded by reading the scale below the meniscus. The same procedure was followed for all test fuels.

Fig. 2. Density measurement using Hydrometer.

A.2.2. Measurement of viscosity for diesel, butanol and their blends using Redwood Viscometer

Viscosity is the property of a fluid. It can be expressed as "The internal resistance offered by the fluid to the moment of one layer of fluid over a contiguous layer ". It is due to the collision between the molecules of the fluid. The fluids, which obey Newton's law of viscosity are called Newtonian fluid. Redwood Viscometer was used for measuring the viscosity of test fuels. Redwood Viscometer comprises a cylindrical oil cup furnace with a metallic orifice jet at the bottom (figure 3). A ball can close the orifice. The oil cup is surrounded by a water bath with a circular electrical immersion heater. Two thermometers were used for measuring water and oil temperature. A 50 ml flask was used for collecting the fuel under orifice against time. The given test fuel was heated by warming the water by electric heater in the water bath. The stir was provided for mixing water and oil separately, to keep constant temperature in the water bath and oil cylinder. After reaching oil temperature 40 ^{0}C, the spherical ball was lifted and simultaneously the time was noted for collecting 50 ml of oil in the flask. The same method was repeated for all test fuel.

Fig. 3. Redwood viscometer set-up.

A.2.3. Measurement of calorific value for diesel, butanol and their blends using a Bomb calorimeter

A bomb calorimeter is a type of constant-volume calorimeter used for measuring energy change in the chemical process. Bomb calorimeter comprises a sample cup, sealed bomb, insulated container, ignition wires, motorized stirrer and thermometers. The fuel is weighed (1 gram) in the weighing machine and placed inside the sample cup. The sample cup is placed inside the bomb. The bomb is sealed and filled with oxygen. The sealed bomb is placed inside the insulated container that contains cooled water. Ignition wires are used to ignite the fuel. The motorized stirrer is placed above the insulated container for mixing water. After reaching stable water temperature, fire bottom is turn on. The fuel is burned by electrical energy. The burning fuel deliveries the heat energy to the surrounding air and transfer, it to the water. The changes in the temperature of water were used for calculating the calorific value of the fuel. Figure 4 shows the experimental set-up of bomb calorimeter.

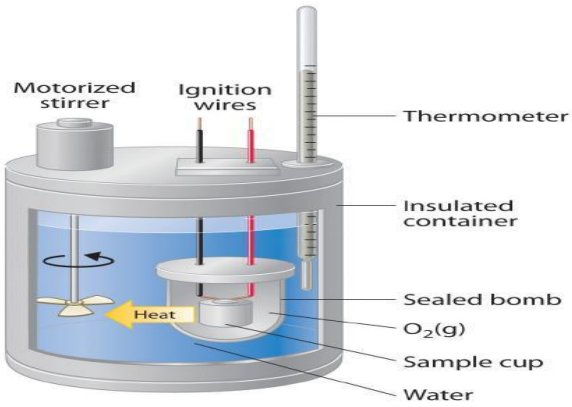

Fig. 4. Bomb calorimeter set-up.

A.3. Experimental set-u of the VCR engine Test Rig.

The details of the experimental set-up are discussed in this section. Figure 5 (a) shows the schematic diagram of the engine set-up. Experiments were conducted on a normal four-stroke, water-cooled, single-cylinder VCR engine. Minor modifications have been carried out on this set-up by attaching an EGR line. Figure 5 (b) shows the layout of the experimental set-up.

The engine set-up has all the essential components for measuring of combustion pressure and crank-angle. A piezoelectric diaphragm pressure sensor was used for the measurement of pressure inside the cylinder. In addition to that, a crank angle encoder of Kubler-Germany make was incorporated to measure the crank angle in a cycle. Also, a K-type thermocouple was used for the measurement of exhaust gas temperature. The inlet water temperature and exit water temperature, from the engine were measured using RTD temperature sensors. All the values measured were digitally stored in data acquisition system (DAS) and displayed on the computer screen. The test rig also consisted of fuel flow, air-flow, temperatures and load measurements. Rotameters were also provided for cooling water and calorimeter water flow measurement. A battery, starter and battery charger were provided for engine electric start arrangement. The engine and the dynamometer were interfaced with a control panel, which was connected to a computer. The computerized set-up was used to record all the observation parameters such as load, speed, fuel flow rate, water flow rate, air-flow rate and temperature. The computerized set-up gave a summary of the engine performance and combustion values such as BSFC, in-cylinder pressure rise, net heat release, temperature and BTE. Exhaust emissions (NOx, CO and HC) were measured with AVL gas analyzer. The soot emission was measured by AVL smoke meter.

Initially, the engine was run at no load condition and constant speed (1500±10). The experiments were performed at different loads and at a constant engine speed (1500 rpm), operated with diesel fuel and different butanol/diesel blends. Experimental studies were carried out by varying three engine parameters, viz., compression ratio (CR) (14, 16, 17.5 and 18), fuel injection pressure (FIP) (200bar, 220bar, 240bar, 260bar and 280bar) and exhaust gas recirculation (EGR) (0, 10%, 20% and 30%) at diesel and different butanol/diesel blends. All the experiments were conducted at a rated load and at a constant engine speed (1500).

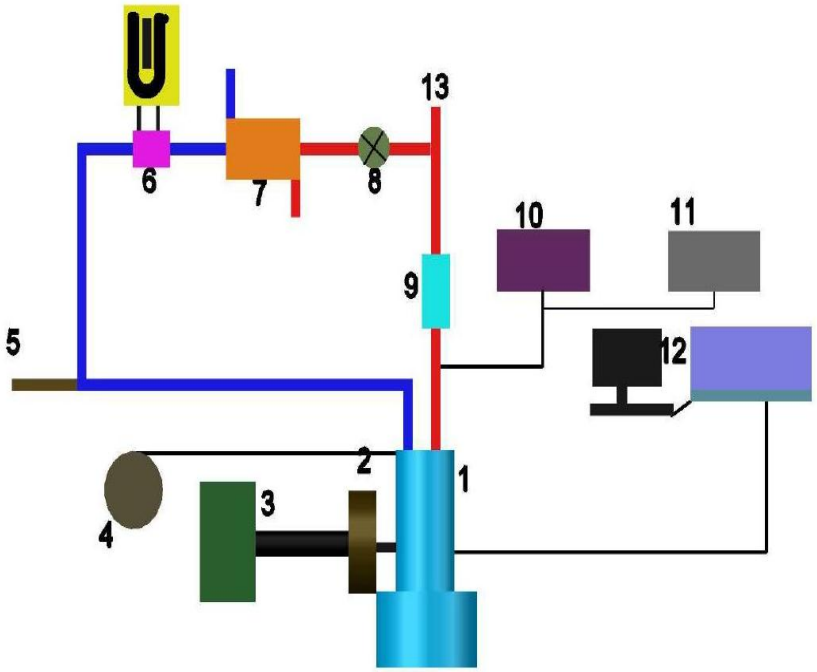

1-Engine block 2- Flywheel 3-Dynamometer 4-Fuel tank 5-Air inlet 6-Orifice meter set-up 7-Heat exchanger 8-Control Valve 9- Calorimeter 10-Gas analyzer 11- Smoke meter 12- Data acquisition system and computer 13-Exhaust outlet

Fig. 5 (a) Schematic diagram of the Engine set-up.

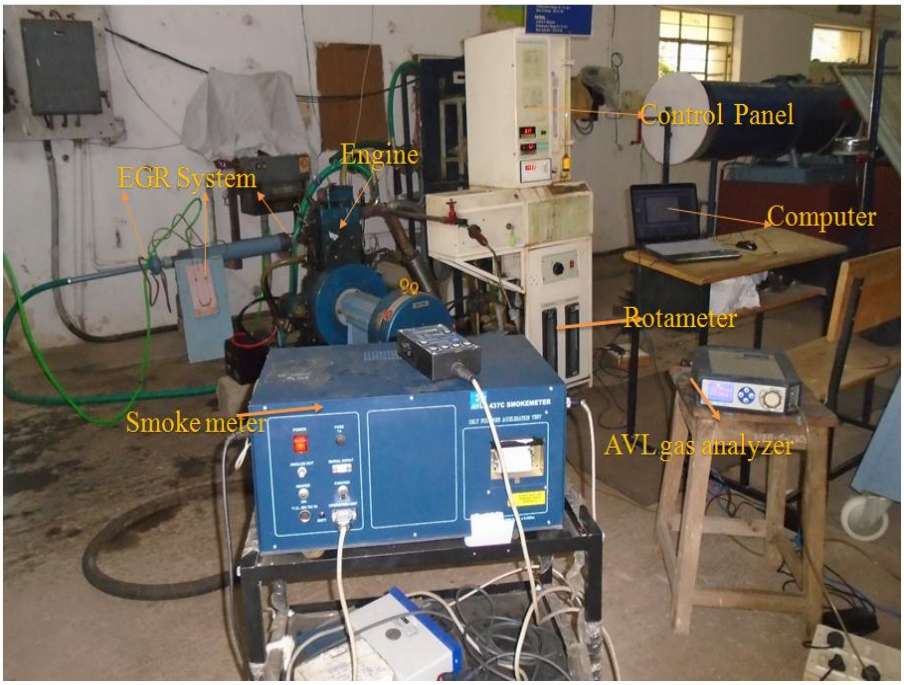

Fig. 5 (b) Layout of the engine experimental set-up

A.3.1. Modified EGR set-up

EGR is one of the techniques for reducing NOx formation by reduction of in-cylinder charge temperature and in-cylinder temperature. Externally cooled EGR system was coupled to the engine set-up. The EGR external cooled system consists of orifice meter, u-tube manometer, counter flow heat exchanger and control valve. The exhaust gas flow rate was measured by orifice meters set-up. A control valve was used for controlling EGR flow rate. EGR cooling system was used as a counter-flow heat exchanger, in which the water flow absorbs heat from hot exhaust gases to reduce exhaust gas temperature. In this experimental study, EGR was cooled up to 35^0C. It was observed that the temperature of the cooled exhaust gas was lower than exhaust gas temperature and higher than intake air temperature. Figure 6 shows the Schematic diagram engine EGR set-up. The EGR rate was calculated using the following equations (1) – (4).

$$EGRrate(\%) = \frac{Q_{withoutEGR} - Q_{EGR}}{Q_{withoutEGR}} x100 \quad (1)$$

$$Q_{withEGR} = \frac{C_d a_0 a_1 \sqrt{2gh}}{\sqrt{a_1^2 - a_0^2}} \quad (2)$$

$$Mass\ flowrate = \rho \times Q_{withEGR} \tag{3}$$

$$Dry\ air\ density, \rho = \frac{P}{RT} \tag{4}$$

Where $Q_{withoutEGR}$ represents the total amount of air supplied (26 kg/h) to the engine during the suction stroke. Q_{EGR} represents the amount of exhaust gas supplied to intake manifold during suction stroke. The C_d is coefficient of discharge for orifice meter, a_0, a_1 are the area of orifice and pipe, h is manometer difference, P is atmospheric pressure, R is gas constant and T is cooled exhaust gas temperature. The exhaust gas supplied to fresh charge is 2.6 kg/h, 5.2 kg/h and 7.8 kg/h for 10%, 20% and 30% of EGR respectively.

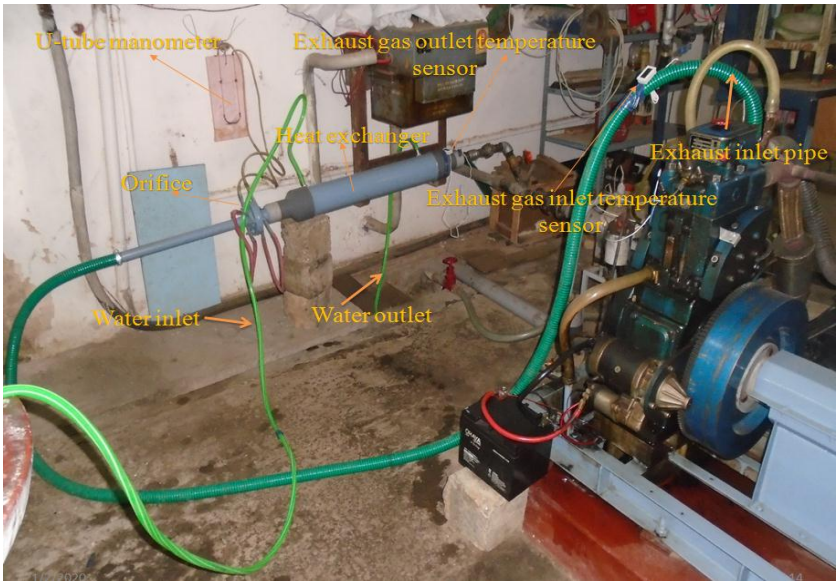

Fig. 6. Photographic view of EGR set-up for engine.

A.3.2. Compression ratio adjustment

The compression ratio can be varied by utilizing allen bolt, CR adjuster, lock nut and CR indicator. Figure 7 shows the location of the components on the engine. The fixed compression ratio of an engine is generally varied by increasing/decreasing clearance volume between the cylinder head and piston. To achieve this, firstly allen bolts should slightly loosen and later loosen the lock nut on the CR adjuster. The CR adjuster is rotated clockwise or anticlockwise for moving the CR adjuster up and down for the required CR (by following

the scale on CR indicator). After fixing the CR the lock nut is locked and the allen bolts are tightened.

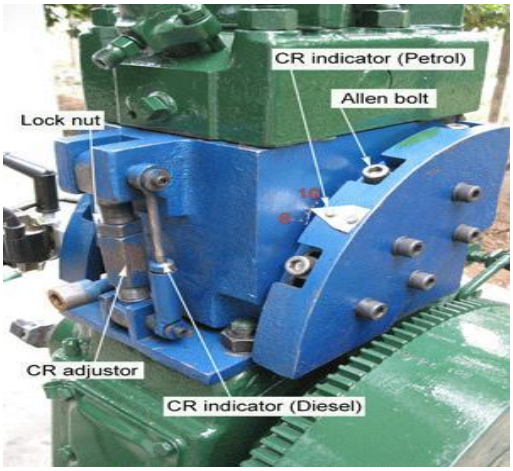

Fig. 7. Diesel engine depicting the components to varying compression ratio.

A.3.3. Error analysis

The errors allied with different instruments and calculations of parameters are computed in this section. Moffat [88] was given a correlation for estimating the maximum possible error in calculation. Errors were calculated from the minimum values of the output and accuracy of the instrument. If an estimated quantity S, the depends on independent variable like (a_1, a_2, a_3.....,a_n), the error value S calculated by using Eq. (5).

$$\frac{\partial S}{S}=\left\{\left(\frac{\partial a_1}{a_1}\right)^2+\left(\frac{\partial a_2}{a_2}\right)^2+\left(\frac{\partial a_3}{a_3}\right)^2+.....+\left(\frac{\partial a_n}{a_n}\right)^2\right\}^{\frac{1}{2}} \quad (5)$$

Where $\frac{\partial a_1}{a_1}, \frac{\partial a_2}{a_2}$, etc. are the errors in independent variables. The a_1 represents the minimum value measured during experimentation and ∂a_1 represents minimum accuracy of the measuring instrument. The brake thermal efficiency (BTE) is function of speed (N), torque (T), time (t) and mass of fuel consumption (t). The maximum possible error in the calculation of BTE was found by 5.3% using Eq. (7). Type of Instruments used in experiments and their ranges is shown in Table A1.

$$\frac{\partial BTE}{BTE} = \left\{ \left(\frac{\partial N}{N} \right)^2 + \left(\frac{\partial T}{T} \right)^2 + \left(\frac{\partial t}{t} \right)^2 + \left(\frac{\partial m}{m} \right)^2 \right\}^{\frac{1}{2}} \quad (3.6)$$

Table A1. Type of Instruments used in experiments and their ranges.

Quantity	Range	Accuracy
AVL smoke meter	0-100%	±0.2%
AVL gas analyzer	NOx:0-5000 ppm	±10 ppm
	UBHC:0-20000 ppm	±1 ppm
	CO: 0 – 10% vol.	±0.01%
In-cylinder pressure	(0-110 bar)	±0.05 bar
Crank angle encoder		±1°
Fuel flow sensor	0-5 psi	±0.1 psi
Speed measuring	0-5000 rpm	±5rpm
Burette		±1ml
Load		±0.2 Nm
Stop watch		±0.1 sec

$$\frac{\partial BTE}{BTE} = \left\{ \left(\frac{5}{1500} \right)^2 + \left(\frac{0.2}{12} \right)^2 + \left(\frac{0.1}{60} \right)^2 + \left(\frac{1}{20} \right)^2 \right\}^{\frac{1}{2}} \quad (7)$$

A.3.4. NOx emission error analysis

NOx emission error analysis was carried out using standard deviation. The sample calculations were shown in Table A2.

Standard deviation (s) = $(((\text{sum}(X-x)^2)/(n-1)))^{1/2}$ (8)

X = The values in the data distribution

x= The sample mean

n = number of trials =9

Table A2. Standard deviation calculation for NOx emission.

Test	NOx (g/kWh)	(X- x)	Square(X- x)=A
Trail 1	7.8	-0.242222	0.05867
Trail 2	7.99	-0.052222	0.00273
Trail 3	7.96	-0.082222	0.00676
Trail 4	8.05	0.007778	6E-05
Trail 5	8.06	0.017778	0.00032

Trail 6	8.11	0.067778	0.00459
Trail 7	8.12	0.077778	0.00605
Trail 8	8.15	0.107778	0.01162
Trail 9	8.14	0.097778	0.00956
Total	72.38		
Avg. (*x*)	8.042222222	**Sum of A**	0.10036
	A/(n-1)	0.012544	
Std	**Root of (A/n-1)=**		**0.112001984**

The maximum deviation in NOx emission was found by 0.112% using Eq. (8). Similar method was used to finding the error analysis for soot emission also.

A.4. Model calculations

(1) Stoichiometric Equation

For Bu00 case,

Molecular weight of C7H16=100 g/mol

Molecular weight of C4H9OH=74 g/mol

C7H16+ 11(O2+3.76N2) = >7CO2+8H2O+11*3.76*N2

Stoichiometric ratio for Bu00 = Air/fuel = 11 (32+3.76*28)/ (100) = 15.1

For Bu20 case (80% C7H16+20%C4H9OH)

0.8 C7H16+0.2C4H9OH + 10 (O2+3.76N2) => 6.4 CO2+7.4H2O+10*3.76*N2

Stoichiometric ratio for Bu20 = 10(32+3.76*28)/ ((0.8*100)+0.2*74))= 14.4

(2) Brake thermal efficiency (BTE)

For Bu00 case, at full load condition i.e., 3.5 kW

BTE= (BP)/ (mf*CV)

CV- Calorific value= 43.5 MJ/kg

BP- Brake power= 3.5 kW

mf - Mass of fuel= 1.02 kg/h

BTE= (3.5)* (3600)/ (1.02*43.5*1000) = 28.4%

(3) Brake specific energy consumption (BSEC)

For Bu00 case, at full load condition i.e., 3.5 kW

*BSEC= SFC*CV*

Specific fuel consumption (SFC) = mf/BP= (1.02/3.5)= 0.29 kg/kWh

BSEC= 0.29*43500= 12615 kJ/kWh

A.5. Emission conversion ppm to g/kWh

The following equations are used for converting the ppm to g/kWh.

(a) NOx emission conversion ppm to g/kWh

$$NOx(g/h) = \frac{M_{NO_2}.NOx(ppm).Q_{exhaustdry}}{10^3.V_m}$$

Where M_{NO2}= 46.005 g/mol and V_m= 22.4411/mol

$Q_{exhaust}$ = non conducted exhaust flow

$$Q_{exhaust} = FMF\left[\frac{1+AFR_{st}}{\rho_{burnedgas}} + \frac{(\lambda-1).AFR_{st}}{\rho_{air}}\right]$$

Stoichiometric air/fuel ratio (AFR_{st}) = 14.4 and , FMF= fuel mass = 1 kg/h, flow burned gas density ($\rho_{burned\ gas}$)= 1.33 kg/m^3 and air density(ρ_{air})= 1.293 kg/m^3

$Q_{exhaustdry=}$ dry exhaust gas flow

$$Q_{exhaustdry} = FMF\left[\frac{(1+AFR_{st}).\alpha}{\rho_{burnedgas}} + \frac{(\lambda-1).AFR_{st}}{\rho_{air}}\right]$$

α= mass of dry exhaust gases in one kilogram non-condensed exhaust gas= 0.924 kg for diesel fuel.

$$\lambda = \frac{AMF}{AFR_{st}.FMF}$$

(a) Soot emission conversion percentage to g/kWh

$$Smoke(mg/m^3) = \frac{1}{0.405}.5.32.FSN.\exp(0.3062.FSN)$$

$$Smoke(g/h) = 10^{-3}.smoke(mg/m^3).Q_{exhaust}$$

FSN= filter smoke number

(c) **Model calculation for NOx and soot emission:**

(i) NOx emission (ppm to g/kWh)

For diesel fuel NOx emission= 700 ppm

$Q_{exhaust\ dry}$= 19.9

$Q_{exhaust}$ = 20.82

NOx (g/kWh) = (46.05*700*19.9)/(1000*3.5*22.411)

= 8.04 g/kWh

(ii) **Soot emission (percentage to g/kWh)**

For diesel fuel soot emission= 32.5%

From the emission conversion chart, 32.5% of soot emission equivalent value in mg/m^3= 242 mg/m^3

Soot emission (g/kWh) = (0.001*242*20.82)/3.5= 1.44 g/kWh

Appendix B

B.1. Description of CONVERGE software

CONVERGE is an innovative computer software product based on the principles of CFD (Computational Fluid Dynamics) developed by the experts in the field of engine simulations. Unlike the traditional CFD software packages, where grid generation is manually developed by the user, CONVERGE eliminates the unnecessary and time-consuming effort of the user in generation of grids and gives more time in varying the important parameters and performing a detailed analysis of simulations in an engine study. CONVERGE can not only model the engine environment, but can also be used to simulate a non-engine environment with the same computational efficiency. Therefore, CONVERGE can be regarded as a very powerful CFD simulation software with a wide variety of capabilities which can find solutions for difficult real-life problems. Other CFD solvers were used whose approach for engine modelling is to have an add-on to an existing solver. CONVERGE was designed from its inception to be a leading CFD solver for modelling IC engines. The ease of grid generation for moving boundaries, adaptive mesh refinement, improved numerical accuracy, and latest sub-models are evidence of this pioneering code. The fluid dynamics of the problems involve governed equations, which are included in solver i.e., conservations of mass, momentum and energy. In addition, conservation equations, transport of passive scalars, species and turbulence are also incorporated to simulate the IC engine combustion phenomena.

B.1.1. Governing Equations

The dynamics of fluid flow inside the in-cylinder is simulated by solving the governing equations that describe the conservation of mass, momentum, and energy. The transport and turbulence of passive species and other species are also required to solve the in-cylinder flow. It is necessary to solve both the mass and momentum equations together for suitable computations of the pressure gradient in the momentum equation. Momentum and mass transport can be solved for both compressible and incompressible flows.

B.1.1.1. Mass and Momentum transport

The compressible equations for mass transport and momentum transport are given by:

$$\frac{\partial \rho}{\partial t} + \frac{\partial \rho u_i}{\partial x_i} = S, \tag{i}$$

$$\frac{\partial \rho u_i}{\partial t} + \frac{\partial \rho u_i u_j}{\partial x_i} = -\frac{\partial p}{\partial x_i} + \frac{\partial \sigma_{i\ j}}{\partial x_i} + S, \tag{ii}$$

Where the stress tensor is given by

$$\sigma_{ij} = \mu\left(\frac{\partial u_i}{\partial x_j} + \frac{\partial u_j}{\partial x_i}\right) + \left(\mu' - \frac{2}{3}\mu\right)\left(\frac{\partial \mu_k}{\partial x_k}\delta_{ij}\right) \tag{iii}$$

Where u is the velocity, ρ is density, S is the source term, P is a pressure term, μ is viscosity, μ' is dilatational viscosity (set to zero), and δ_{ij} is Kronecker delta. For turbulence model, the viscosity is replaced by turbulence viscosity (μ_t) given by

$$\mu_t = \mu + C_\mu \rho \frac{k^2}{\varepsilon'} \tag{iv}$$

Where C_μ a turbulence model is constant, k is the turbulence kinetic energy and ε' is the turbulence dissipation.

B.1.1.2. Energy transport

The compressible form of the energy equation if given by

$$\frac{\partial \rho e}{\partial t} + \frac{\partial u_j \rho e}{\partial x_i} = -P\frac{\partial u_i}{\partial x_i} + \sigma_{ij}\frac{\partial u_i}{\partial x_j} + \frac{\partial}{\partial x_i}\left(K\frac{\partial T}{\partial x_i}\right) + \frac{\partial}{\partial x_i}\left(\rho D \sum_m h_m \frac{\partial Y_m}{\partial x_i}\right) + S, \tag{v}$$

Where ρ is density, Y_m is the mass fraction of species m, D is mass diffusion coefficient, S is source term, P is pressure, *e* is specific internal energy, *K* is conductivity, h_m is species enthalpy, σ_{ij} is stress tensor and *T* is temperature. For turbulence model the conductivity is replaced by turbulence conductivity (K_t) given by

$$K_t = K + c_p \frac{\mu_t}{\mathrm{Pr}_t} \tag{vi}$$

Where Pr_t is the turbulence Prandtl number and μ_t is the turbulent viscosity.

B.1.1.3. Species Transport

The species transport equation is solved for the mass fraction of all species in the domain. The species mass fraction is defined as:

$$Y_m = \frac{M_m}{M_{tot}} = \frac{\rho_m}{\rho_{tot}} \tag{vii}$$

Where M_m the mass of species m in the cell, M_{tot} is the total mass in the cell, ρ_m is the density of species, ρ_{tot} is the density in the cell. The species equation can be solved along or together with any of the transport equations.

The compressible form of the species conservation equation is given by

$$\frac{\partial \rho_m}{\partial t} + \frac{\partial \rho_m u_j}{\partial x_j} = \frac{\partial}{\partial x_j}\left(\rho D \frac{\partial Y_m}{\partial x_j} \right) + S_m \tag{viii}$$

Where $\rho_m = Y_m \rho$ (ix)

Where u is velocity, ρ_m is the species density, Y_m is mass fraction of species m, D is the mass diffusion coefficient, and S_m is the source term.

The molecular diffusion coefficient is calculated by :

$$D = \frac{\nu}{Sc_t} \tag{x}$$

Where Sc_t is the turbulence Schmidt number.

B.1.1.4. Passive Transport

A passive is a transported scalar that does not affect the solution of other transport equations (e.g., mass, momentum and energy etc.). Some of the sub-models require that passive element be added in order to activate the models (e.g., soot models). The passive transport equation can be solved only when passive elements are defined in the program. The compressible form of the passive scalar transport equation is given by:

$$\frac{\partial \rho \phi}{\partial t} + \frac{\partial \rho u_i \phi}{\partial x_i} = \frac{\partial}{\partial x_i}\left(\rho D \frac{\partial \phi}{\partial x_i}\right) + S \qquad \text{(xi)}$$

Where u is velocity, ρ is density, D is the diffusion coefficient, S is the source term and ϕ is a passive scalar.

B.1.1.5. Turbulence Modelling

Turbulence significantly increases the rate of mixing of momentum, energy and species. For many applications, such as internal combustion engine, turbulence is critical to an accurate simulation. Turbulence model interacts with many of the other models in CONVERGE (e.g., Spray combustion, wall heat transfer and auto ignition). The Reynolds Averaged Navier-Stroke (RANS) model was widely used in IC engines. In these models, two equation models are widely used because of their simplicity and effectiveness. When a turbulence model is activated, boundary conditions must be specified for turbulence kinematic energy equation (TKE) and the turbulence dissipation equation. The boundary conditions for these equations are shown below.

For the turbulence intensity condition, the boundary TKE is given as:

$$k = \frac{3}{2} u_i^2 I \qquad \text{(xii)}$$

Where k is turbulence kinematic energy equation and I is the turbulence intensity.

The turbulence dissipation equation is given as below

$$\varepsilon = \frac{c_\mu^{\frac{3}{4}} k^{\frac{3}{2}}}{le} \qquad \text{(xiii)}$$

Where C_μ a model constant, k is turbulence kinetic energy and *le* is the turbulent scale length.

B.2. Reaction Mechanism

The reaction mechanism of fluids, gas or liquid, is the most important input to CONVERGE software for the execution of the simulations. The oxidation process of the fuel is modelled using a chemical kinetics reaction mechanism that contains species and their reactions with specified thermodynamic data ('therm.dat') and reaction mechanism data ('mech.dat') for any given fuel. The chemical kinetics essentially contains reactions that form products such as hydrocarbons, CO and CO_2. In addition, Hiroyasu-NSC model and Zeldovich mechanism were employed in the simulation analysis to compute soot and NOx formation, respectively**.** A chemical reaction mechanism containing about 349 reactions and 76 species, developed by Wang et al. (2013), was chosen to simulate the butanol-diesel blend. The same reaction mechanism was used for diesel fuel and different butanol/diesel blends validation purpose.

Appendix C

C.1. Determination of optimal engine parameters using RSM for VCR engine fuelled with 20% of butanol/diesel blend (Bu20)

The main aim of the present work is to minimize the ISFC and emissions using RSM technique for Bu20 blend.

C.1.1. Validation of VCR engine model for 20% of butanol/diesel blend (Bu20)

The butanol/diesel blend of numerical simulation model was validated against experimental data using Bu20 (20% butanol+ 80% diesel) as fuel for its operation at different conditions. Figure 1 shows variation of in-cylinder pressure with crank angle for the experimental and simulation results. The trends of the simulation results were similar to that of the experimental results. However, a slight difference of around 7% in the peak pressure was observed. From the Table C1 it is observed that the simulation results were nearly in good agreement with the experimental results as the maximum error between them is around 7%. Based on the comparison of these characteristics, it was concluded that the simulation results are nearly in good agreement with the experimental results, and further studies were carried out using the simulation model.

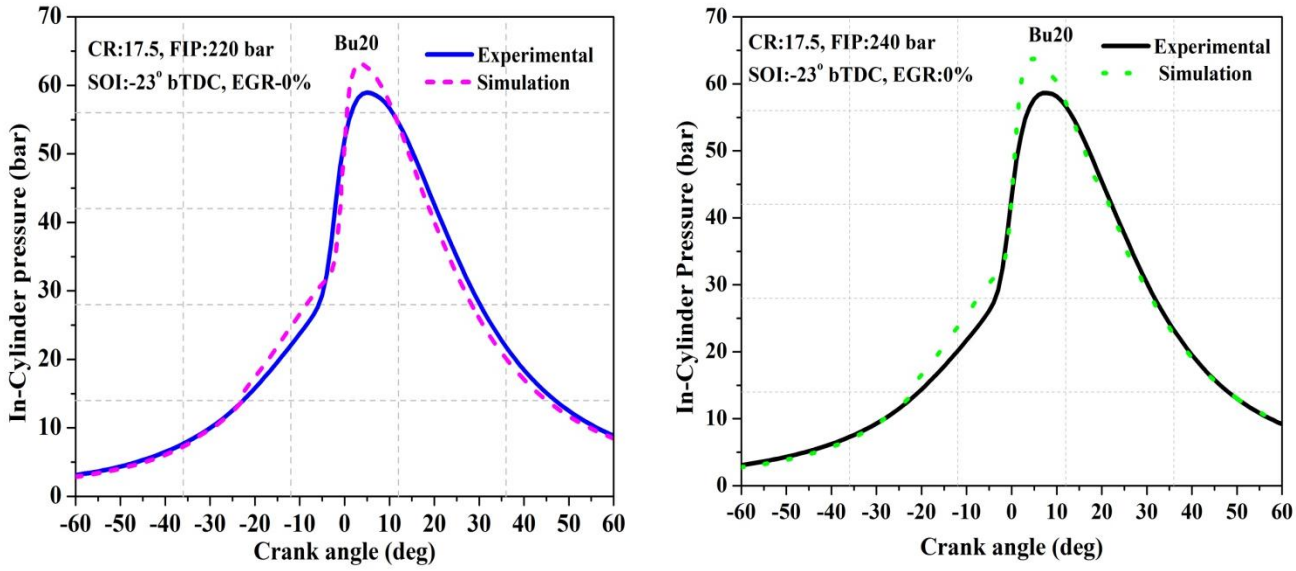

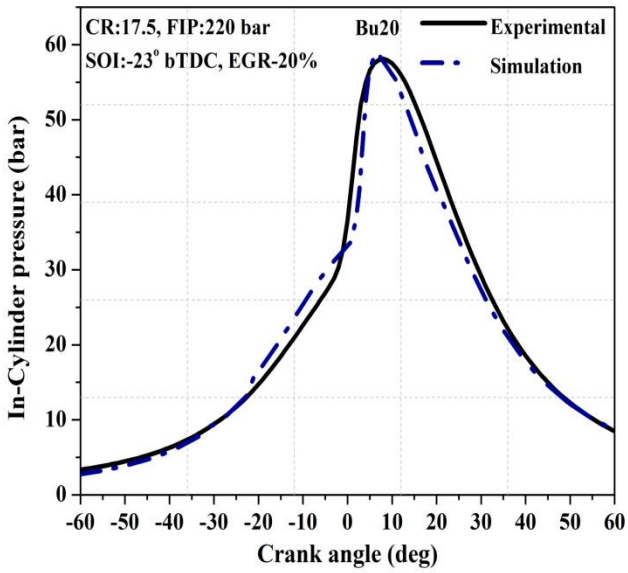

Fig. 1. Comparison of the in-cylinder pressure with crank of the simulation with experimental result for B20 at rated load.

Table C1. Comparison of the experimental and simulation results of performance and emission characteristics for 20% butanol/diesel blend (Bu20).

	In-Cylinder pressure (bar)			**NOx (g/kWh)**			**Soot (g/kWh)**		
	Case 1	**Case 2**	**Case 3**	**Case 1**	**Case 2**	**Case 3**	**Case 1**	**Case 2**	**Case 3**
Experimental	58.97	59.22	58.11	7.4	7.51	5.4	1.18	0.985	1.41
Simulation	62.4	63.7	58.96	7.73	7.82	5.72	1.22	0.925	1.48
Error (%)	5.49	7.03	1.44	4.5	3.96	5.5	3.2	6.48	4.7

C.1.2. Enabling HCCI mode of the CI engine with 20% of butanol/diesel blend (Bu20) using RSM technique

In the previous section, we analyzed the VCR DI-CI engine fuelled with diesel fuel. In the present section, the performance and emission characteristics of the VCR DI- CI engine operating with butanol/diesel blend (Bu20) as the fuel were also analysed.

In the present study also, four different engine parameters were considered (CR, FIP, SOI and EGR) and their ranges are shown in Table C2. The engine performance was evaluated in terms of three output parameters, viz., ISFC, NOx and soot. Box–Behnken design was used for developing the design matrix for numerical analysis. All these set of experiments were simulated in CONVERGECFD code and the results are summarized Table C2 as responses (ISFC, soot and NOx).

Table C 2. Experimental design matrix and their responses for Bu20 blend.

Run Order	CR	FIP	SOI	EGR	ISFC (g/kWh)	Soot (g/kWh)	NOx (g/kWh)
1	14	240	23	0	318	1.69	3.34
2	16.5	240	17	0	267	1.9	4.03
3	16.5	240	23	15	238	1.96	4.69
4	16.5	240	23	15	238	1.96	4.69
5	19	240	23	30	199	0.71	3.56
6	16.5	200	23	30	278	1.88	1.7385
7	19	280	23	15	200	0.3	7.8
8	16.5	280	23	30	236	1.9	2.89
9	19	240	23	0	204	0.46	10.1
10	16.5	240	23	15	238	1.96	4.69
11	19	240	17	15	190	0.533	3.3
12	19	240	29	15	204	0.11	14.2
13	16.5	240	23	15	238	1.96	4.69
14	16.5	280	23	0	202	1.53	8.19
15	16.5	280	29	15	187	0.72	11.08
16	19	200	23	15	197	0.88	6.33
17	16.5	280	17	15	255	1.73	2.73
18	16.5	240	29	30	202	1.32	6.02
19	16.5	240	29	0	183	0.64	13.7
20	16.5	200	29	15	207	1.2	8.6
21	16.5	200	23	0	252	1.79	6.2
22	14	200	23	15	432	1.56	0.89
23	14	240	17	15	477	1.63	1.65
24	16.5	240	23	15	238	1.96	4.69
25	14	240	29	15	258	0.99	4.72
26	14	240	23	30	410	1.66	0.133
27	16.5	240	17	30	309	1.51	1.09
28	14	280	23	15	319	1.88	2.4
29	16.5	200	17	15	328	1.63	2.02

C.1.3. ANOVA analysis for VCR engine fuelled with 20% of butanol/diesel blend (Bu20)

Table C3-C5 show the ANOVA analysis of the three responses. The regression models were analyzed based on ANOVA, which gives the ‘p’ value for different response parameters such as ISFC, soot and NOx emissions. This analysis shows that the ISFC is most influenced by CR (70.1%), followed by SOI (10.2%), EGR (2.25%) and FIP (2.2%), as shown in Table. This indicates that even a small increase in the CR has significant effect on ISFC. SOI has a moderate effect on ISFC. The interaction CR x SOI (8.48%) has a strong influence on ISFC followed by CR x FIP (2.1%), CR x EGR (1.47%), FIP x SOI

(0.43%) and SOI x EGR (0.08%). The square terms of the CR (7.79%) and FIP (0.08%) also have some impact on ISFC. For Soot emission, CR (70.4%) is the most influential, followed by SOI (9%), EGR (0.8%) and FIP (0.66%). The interaction SOI x EGR (2.94%) has a strong influence on soot followed by CR x FIP (2.08%), FIP x SOI (0.86%), FIP x EGR (0.2%), CR x EGR (0.2%) and CR x SOI (0.12%). The square terms of the CR (32.3%), SOI (17.18%), EGR (1%) and FIP (0.98%) also have some impact on soot emission. EGR (35.3%) also has a strong influence on NOx emission, followed by SOI (33.2%), CR (23.28%) and FIP (3.1%). The interaction CR x SOI (4.14%) has a strong influence on NOx emission, followed by SOI x EGR (1.51%), CR x EGR (0.75%) and FIP x SOI (0.21%). The square term of SOI (4.16%) also has some influence on the NOx emissions.

Table C3. ANOVA analysis for ISFC for Bu20 blend.

Source	**Sum of Squares**	**Mean Square**	**F-value**	**p-value**		**percentage Contribution**
Model	159400	11382.95	461.88	< 0.0001	significant	99.25
A-CR	86700	86700	3517.97	< 0.0001		70.1
B-FIP	7252.08	7252.08	294.26	< 0.0001		2.2
C-SOI	28518.75	28518.75	1157.19	< 0.0001		10.82
D-EGR	3605.33	3605.33	146.29	< 0.0001		2.25
AB	3364	3364	136.5	< 0.0001		2.1
AC	13572.25	13572.25	550.71	< 0.0001		8.48
AD	2352.25	2352.25	95.45	< 0.0001		1.47
BC	702.25	702.25	28.49	0.0001		0.43
BD	16	16	0.6492	0.4339		0.01
CD	132.25	132.25	5.37	0.0362		0.08
A^2	12464.78	12464.78	505.78	< 0.0001		7.79
B^2	129.12	129.12	5.24	0.0381		0.08
C^2	9.52	9.52	0.3864	0.5442		0.005
D^2	0.7352	0.7352	0.0298	0.8653		0.0004
Residual	345.03	24.64				
Lack of Fit	322.92	32.29	5.84	0.0518	not significant	
Pure Error	22.11	5.53				
Total	160000					

Table C4. ANOVA analysis for soot for Bu20 blend.

Source	**Sum of Squares**	**Mean Square**	**F-value**	**p-value**		**Percentage Contribution**
Model	9.65	0.6893	130.46	< 0.0001	significant	99.21
A-CR	3.43	3.43	649.5	< 0.0001		70.4

B-FIP	0.0645	0.0645	12.21	0.0036		0.66
C-SOI	1.3	1.3	246.47	< 0.0001		9.0
D-EGR	0.0784	0.0784	14.84	0.0018		0.8
AB	0.2025	0.2025	38.33	< 0.0001		2.08
AC	0.0118	0.0118	2.23	0.1577		0.12
AD	0.0196	0.0196	3.71	0.0746		0.2
BC	0.0841	0.0841	15.92	0.0013		0.86
BD	0.0196	0.0196	3.71	0.0746		0.2
CD	0.2862	0.2862	54.18	< 0.0001		2.94
A^2	3.14	3.14	594.73	< 0.0001		32.3
B^2	0.0956	0.0956	18.09	0.0008		0.98
C^2	1.67	1.67	315.9	< 0.0001		17.18
D^2	0.0975	0.0975	18.46	0.0007		1
Residual	0.074	0.0053				
Lack of Fit	0.066	0.0066	3.3	0.1307	not significant	
Pure Error	0.008	0.002				
Total	9.72					

Table C5. ANOVA analyses for NOx for Bu20 blend.

Source	**Sum of Squares**	**Mean Square**	**F-value**	**p-value**		**Percentage Contribution**
Model	369.57	26.4	702.38	< 0.0001	significant	98.25
A-CR	75.64	75.64	2012.67	< 0.0001		23.28
B-FIP	7.23	7.23	192.25	< 0.0001		3.1
C-SOI	157.69	157.69	4195.61	< 0.0001		33.2
D-EGR	86.17	86.17	2292.81	< 0.0001		35.3
AB	0.0004	0.0004	0.0106	0.9193		0.0001
AC	15.33	15.33	407.81	< 0.0001		4.14
AD	2.78	2.78	73.89	< 0.0001		0.75
BC	0.7832	0.7832	20.84	0.0004		0.21
BD	0.1758	0.1758	4.68	0.0484		0.04
CD	5.62	5.62	149.45	< 0.0001		1.51
A^2	0.5751	0.5751	15.3	0.0016		0.15
B^2	0.0004	0.0004	0.0108	0.9186		0.0001
C^2	15.42	15.42	410.29	< 0.0001		4.16
D^2	0.0035	0.0035	0.0936	0.7641		0.0009
Residual	0.5262	0.0376				
Lack of Fit	0.4765	0.0476	3.84	0.1035	not significant	

Pure Error	0.0497	0.0124				
Total	370.1					

C.1.4. Error analysis of the regression model for VCR engine fuelled with 20% of butanol/diesel blend

The regression statistics of fit (R^2), adjusted R^2 and predicated R^2 for three output responses are shown in Table C6. It can be seen from the table that the difference between the values of adjusted R^2 and predicated R^2 is less than 0.2 for all the responses, which indicates that the models were able to fit the data with reasonably good accuracy. From the normal probability plots (Fig.2) observed that the residuals have been falling almost in a straight line. This is an indication that errors for ISFC, soot and NOx are normally distributed. Hence, the fitted models adequately represent the simulation results. This implies that the regression equations are accurate enough.

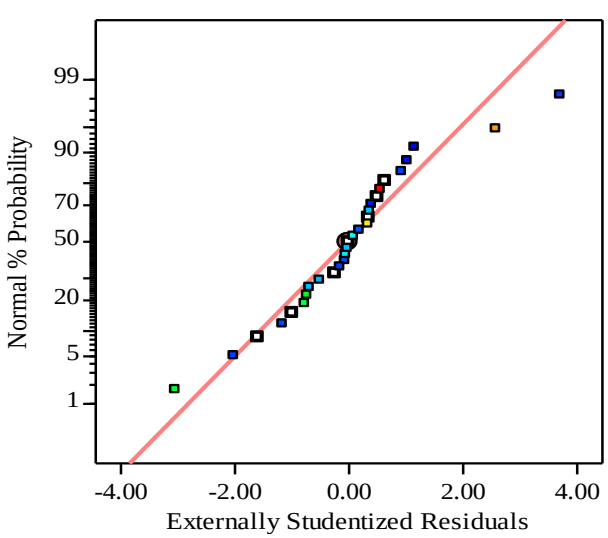

(i) ISFC

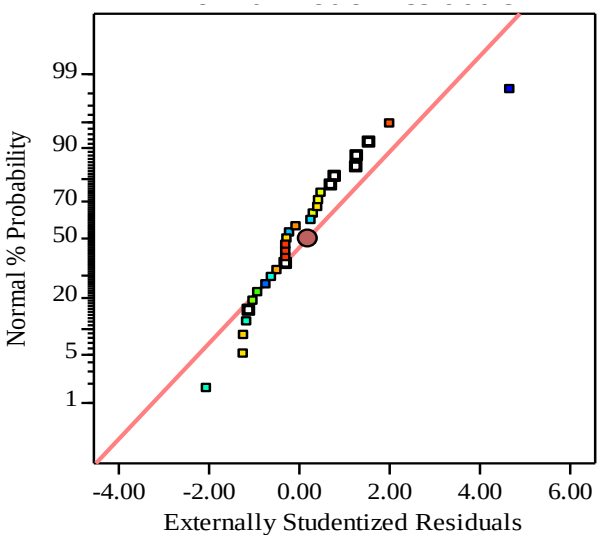

(ii) Soot

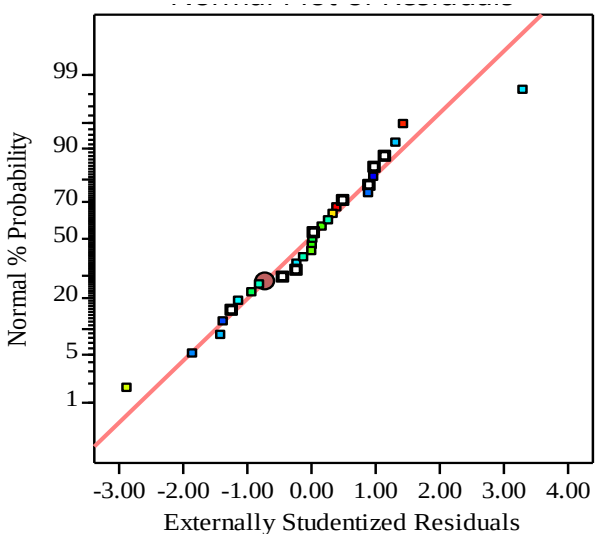

(iii) NOx

Fig. 2. Normal probability plot of the response ISFC, soot and NOx for VCR engine for Bu20 blend.

Table C6. the regression statistics of fit for three output responses.

Parameters	ISFC	Soot	NOx
R^2	0.9978	0.9924	0.9986
Adjusted R2	0.9957	0.9848	0.9972
Predicted R2	0.9881	0.9596	0.9924
(Adjusted R2) - (Predicted R2)	0.0076	0.0252	0.0048
Adeq. precision	82.85	38.51	101.4

C.1.5. Interaction effects of VCR engine fuelled with 20% of butanol/diesel blend (Bu20)

Figure 3 illustrations the interaction effect of CR and SOI on ISFC at different FIPs. The reddish and bluish colour zones in contour plots represent higher and lower values of ISFC. From the figure it is observed that ISFC is lower at higher CR and advanced SOI at all FIPs. As CR increases from 14 to 19, ISFC decreases. This is because of higher initial pressure and temperature of the charge at higher CR, which helps in better mixing of the fuel and air, and hence better combustion. As a result there is lowering of ISFC at higher CR. Similarly, as SOI is advanced, ISFC is reduced. This is because of the lower initial temperature and pressure at the time of advanced SOI which prolonged the ignition delay. This helps in more homogeneous charge preparation. Because of the homogeneous charge preparation, ignition occurs simultaneously at a number of locations, resulting in greater

combustion (lowering the ISFC). Simultaneously, higher FIP provides better atomized fuel droplets in a short interval of time, which helps in easy evaporation of the fuel droplets in the combustion chamber in smaller intervals of time. Because of this, the combustion process enhances, which leads to reduced ISFC. Thus, the cumulative effect of these three input parameters is that at higher CR, higher SOI (advanced SOI) and higher FIP, ISFC is the lowest.

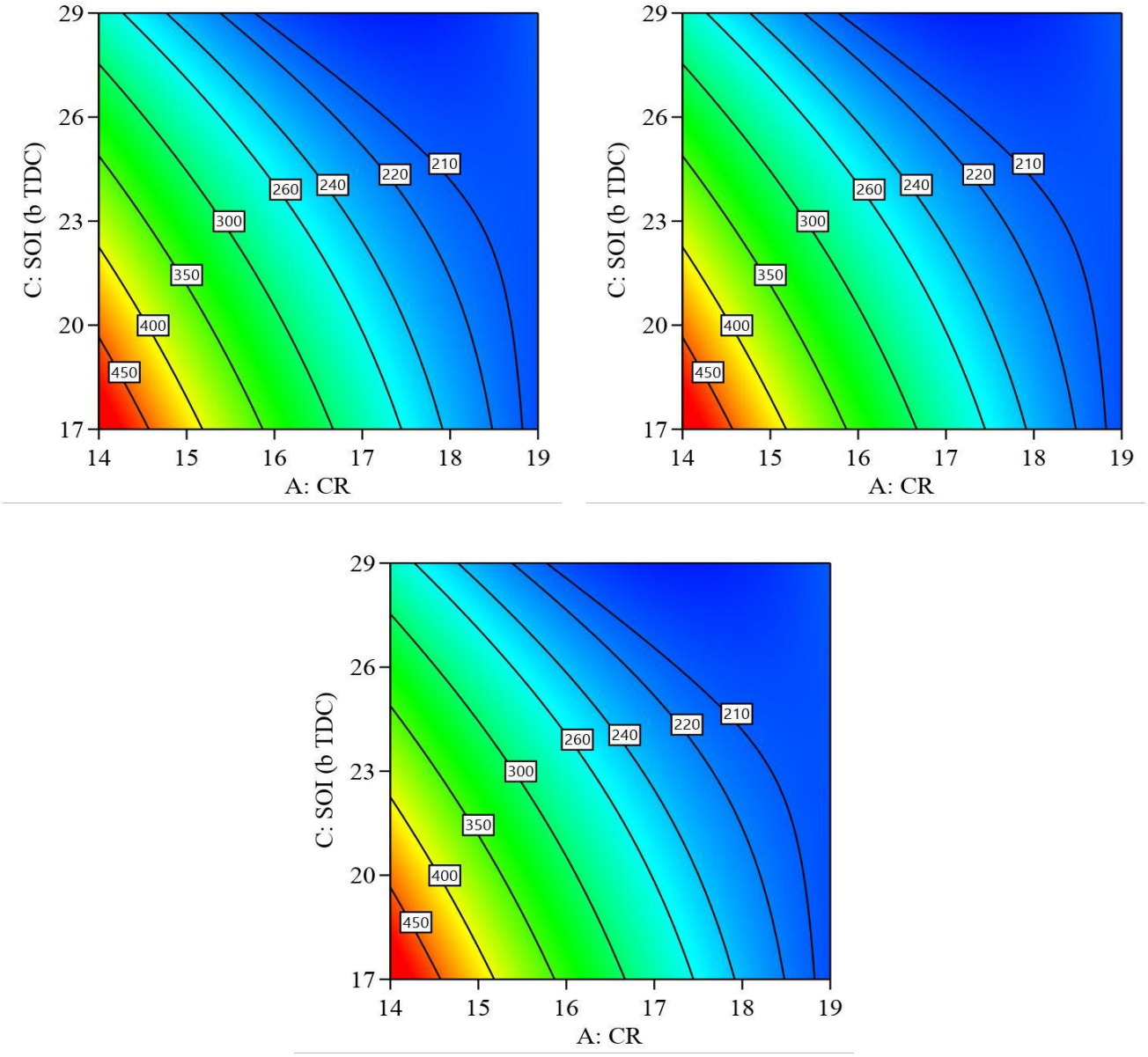

Fig. 3. Interaction effect of CR and SOI on the ISFC at different FIPs (i) 200 bar (ii) 240 bar and (iii) 280 bar for Bu20.

Figure 4 depicts the interaction effect of SOI and EGR at different CRs for Bu20 blend. From the figure it is observed that soot emission is lower at advanced SOI and lower EGR rate at all CRs. As CR increases from 14 to 19, the soot emission decreases. This may

be because of the increased soot oxidation process caused by the higher swirl ratio and turbulence, which is attained at higher CR. Similarly, advanced SOI provides sufficient time for homogeneous charge preparation, which causes better combustion. The cumulative effect of a higher swirl ratio and homogeneous charge causes reduction in soot emission.

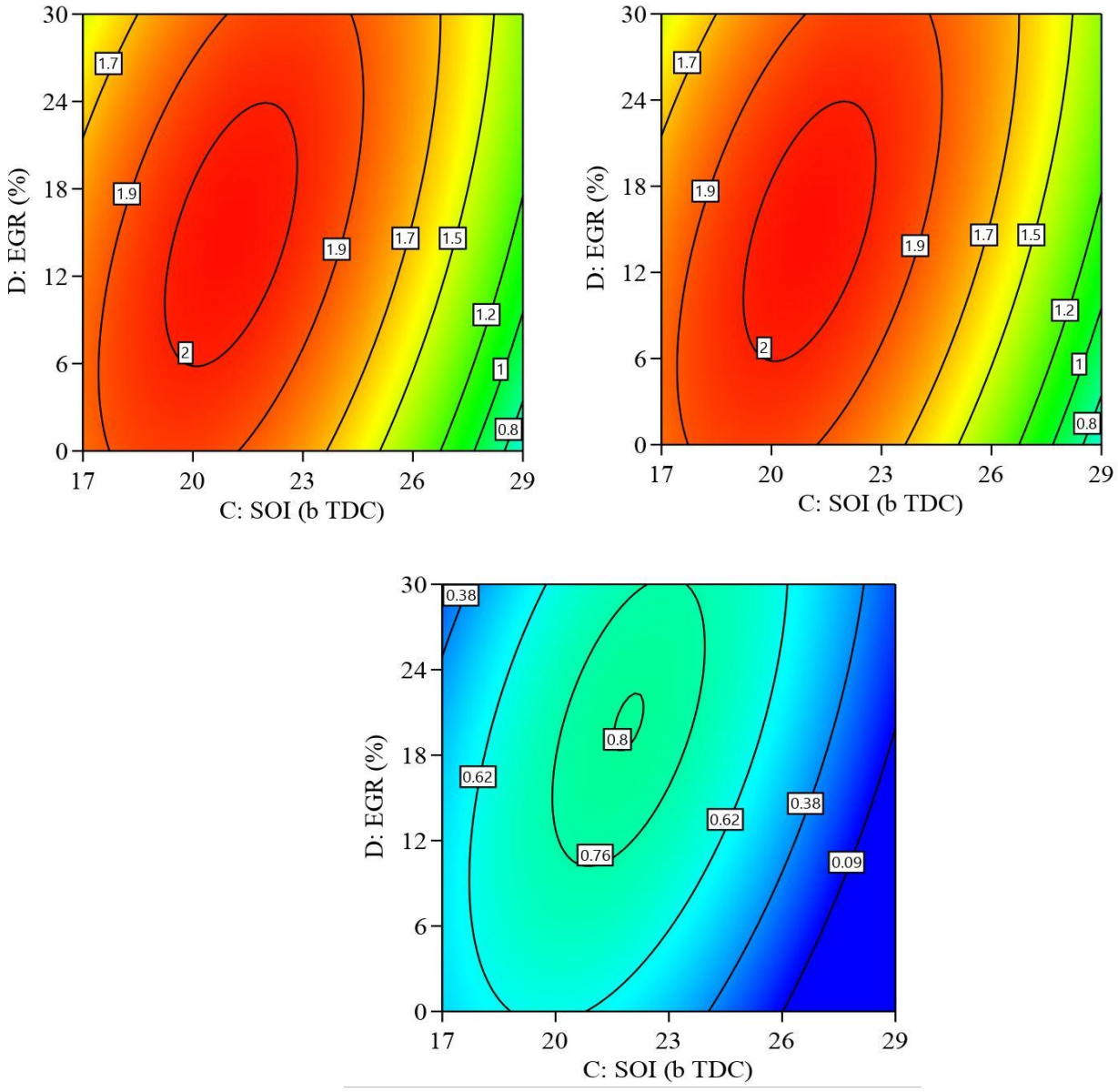

Fig. 6.4. Interaction effect of SOI and EGR on the soot at different CRs (i) 14 (ii) 16.5 and (iii) 19 for Bu20.

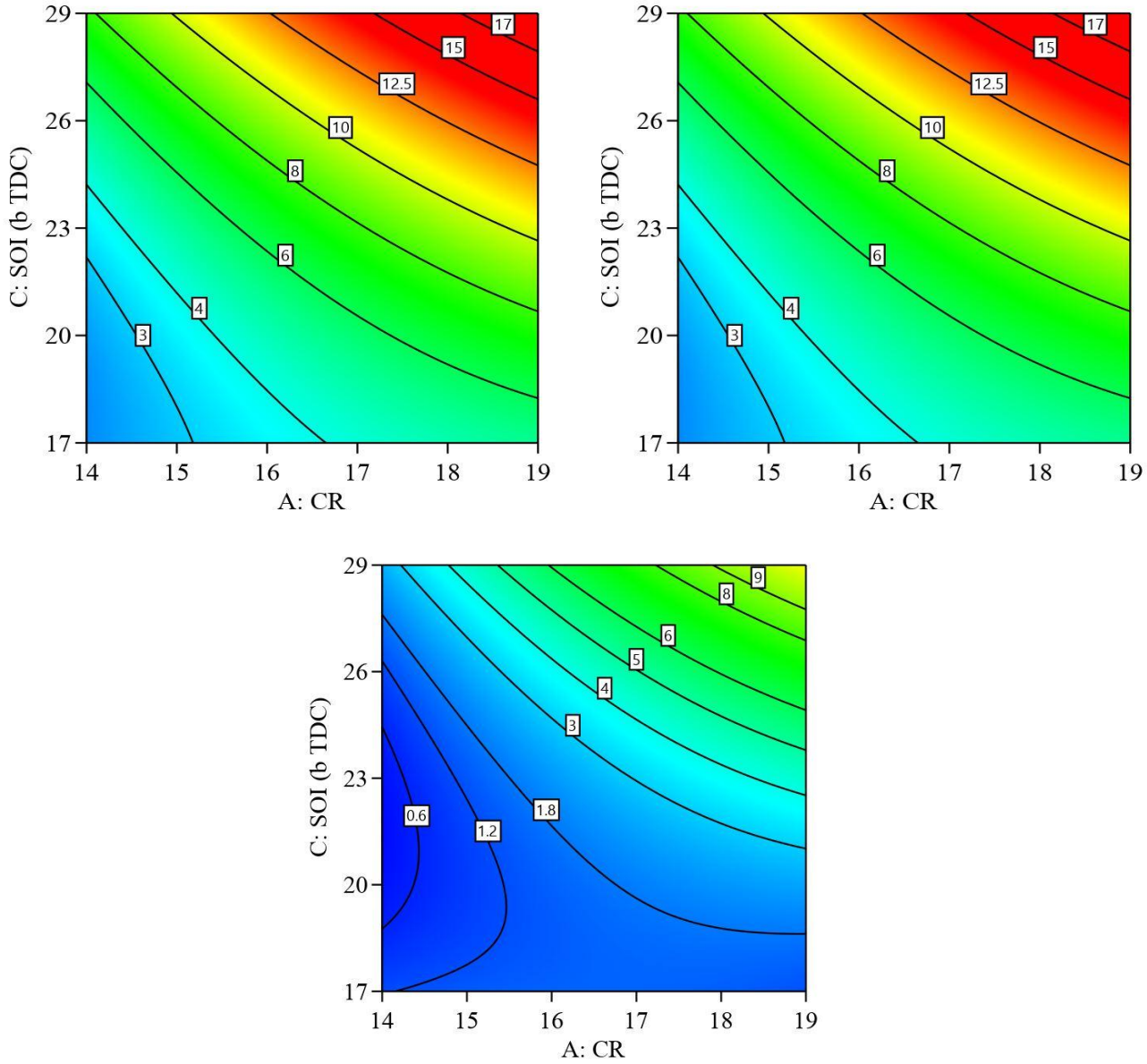

Fig. 5. Interaction effect of CR and SOI on the NOx at different EGR rates (i) 0(ii) 15 and (iii) 30% for Bu20.

The interaction effect of CR and SOI at different EGR rates for Bu20 blend is shown in figure 5. From the figure it is observed that NOx emissions are lower at lower CR and late SOI at all EGR rates. And it is also observed that as EGR rate increases from 0 to 30%, NOx emission decreases. This is because EGR percentage increases the specific heat of intake mixture (which contains CO_2 and H_2O), and hence decreases the combustion flame temperature. In addition, it reduces the amount of oxygen content in intake mixture. The combination of decreased combustion flame temperature and decreased oxygen content lowers NOx emission formation. The interaction effect of CR and SOI is favourable at lower CR and late SOI at higher EGR rate.

C.1.6. Optimization using desirability approach for 20% of butanol/diesel blend (Bu20)

The composite desirability approach was used for finding the best optimum combination of the parameters. Equal weights were assigned for all the output responses in order to simultaneously minimize ISFC, soot and NOx. Table C7 shows the criteria of optimization used for desirability method for Bu20 blend.

Table C7 Criteria of optimization used for desirability method for Bu20 blend.

Parameters /Response	Limits		Criterion	Desirability
	Lower	Upper		
Compression Ratio	14	19	In range	1
Fuel Injection Pressure (bar)	200	280	In range	1
Start of Injection (bTDC)	17	29	In range	1
Exhaust Gas Recirculation (%)	0	30	In range	1
ISFC (g/kWh)	183	477	Minimum	0.98
Soot (g/kWh)	0.11	2.06	Minimum	0.985
NOx (g/kWh)	0.133	14.2	Minimum	0.955
Combined				0.98

Based on the regression analysis, the regression equation was developed for the ISFC, soot and NOx as shown in Equations 1, 2 and 3. The optimum combination of input parameters were determined to be CR of 18.9, FIP of 276 bar, SOI of 24.3° bTDC, and EGR of 28.2% with a composite desirability of 0.98.

$$\begin{aligned} ISFC = {} & 5961.27 - 414.67*CR - 8.05*FIP - 86.03*SOI + 12.45*EGR + 0.29*CR*FIP \\ & + 3.88*CR*SOI - 0.646*CR*EGR + 0.055*FIP*SOI + 0.0033*FIP*EGR \\ & - 0.06388*SOI*EGR + 7.01*CR^2 + 0.0027*FIP^2 + 0.033*SOI^2 + 0.00149*EGR^2 \end{aligned} \quad (1)$$

$$\begin{aligned} Soot = {} & -44.29 + 3.91*CR + 0.083*FIP + 0.6340*SOI - 0.09641*EGR - 0.00225*CR*FIP \\ & + 0.0036*CR*SOI + 0.0014*CR*EGR - 0.00060*FIP*SOI + 0.00011*FIP*EGR \\ & + 0.00294*SOI8EGR - 0.11CR^2 - 0.000075*FIP^2 - 0.014079*SOI^2 - 0.000560*EGR^2 \end{aligned} \quad (2)$$

$$\begin{aligned} NOx = {} & 28.87 + 0.0056*CR - 0.0186*FIP - 3.764*SOI + 0.58*EGR - 0.00010*CR*FIP \\ & + 0.13*CR*SOI - 0.022*CR*EGR + 0.0018*FIP*SOI - 0.00034*FIP*EGR \\ & - 0.013*SOI*EGR - 0.0477*CR^2 + 0.000052*FIP^2 + 0.042*SOI^2 + 0.0001*EGR^2 \end{aligned} \quad (3)$$

C.1.7. Comparison of baseline and optimized configuration for Bu20 blend

The baseline and optimized cases were compared for VCR Bu20 in the current section. The optimum combination parameters were simulated and compared with the baseline configuration. The comparison of optimized and baseline cases of VCR Bu20 is shown in Table C8. Figures 6 to 9 show the comparison of in-cylinder pressure, temperature,

IHRR and IHR for baseline configuration and optimum configuration. The optimum case results have lower ISFC compared to baseline case. NOx, soot, UBHC and CO emissions were also compared for both optimized and baseline cases as shown in Fig 10 to 13 respectively. All the emissions decreased for the optimized case compared to baseline configuration. The corresponding soot and NOx emissions decreased by 44.2% and 28% respectively, and a marginal reduction in ISFC/ISEC was accomplished (2.28%).This shows the superior quality of the optimum case than the baseline case in terms of both performance and emission aspects.

Table C8. Comparison of optimized and baseline configuration for Bu20 blend.

	ISFC (g/kWh)	**ISEC (MJ/kWh)**	**Soot (g/kWh)**	**NOx (g/kWh)**
Baseline configuration	210	8.77	1.22	7.73
Optimized configuration	205.2	8.57	0.68	5.56
Change w.r.t baseline	2.28	2.28	44.2	28

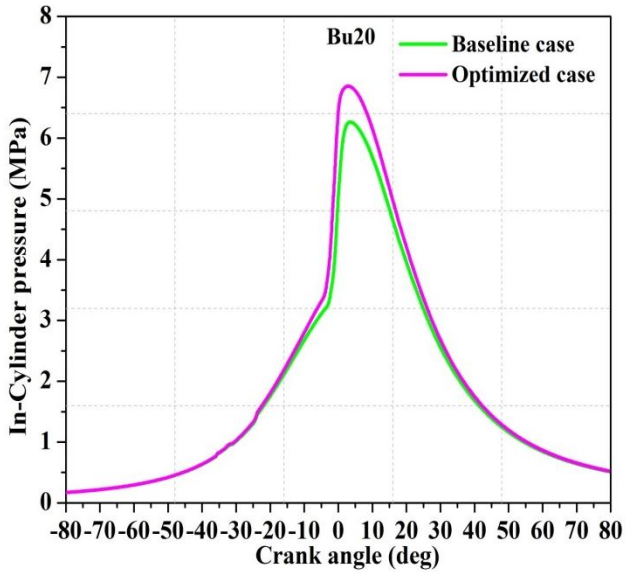

Fig. 6. Comparison of in-cylinder pressure with crank angle between baseline and optimized case for Bu20 at rated load.

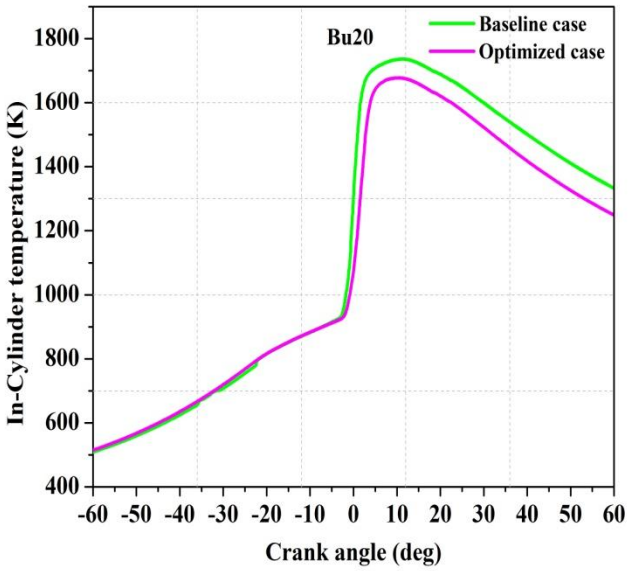

Fig. 7. Comparison of in-cylinder temperature with crank angle between baseline and optimized case for Bu20 at rated load.

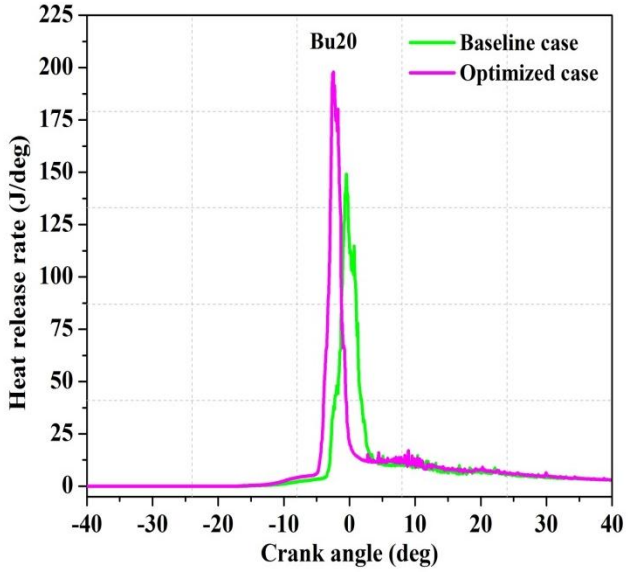

Fig. 8. Comparison of IHRR with Crank Angle for optimized and baseline cases for Bu20 at rated load.

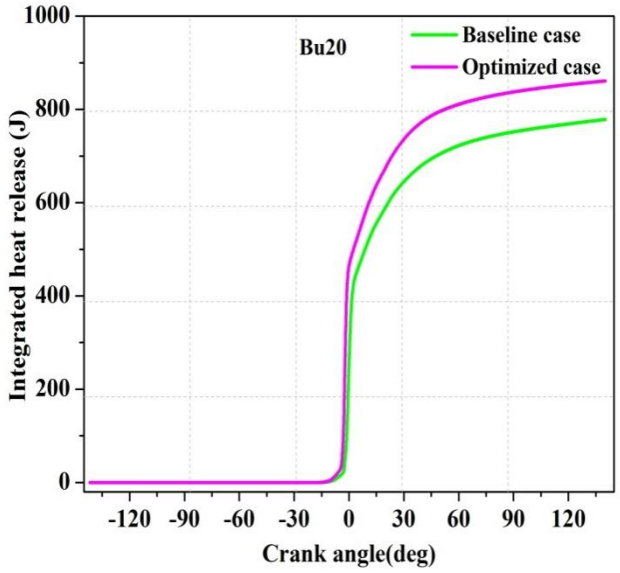

Fig. 9. Comparison of IHR with Crank Angle for optimized and baseline cases for Bu20 at rated load.

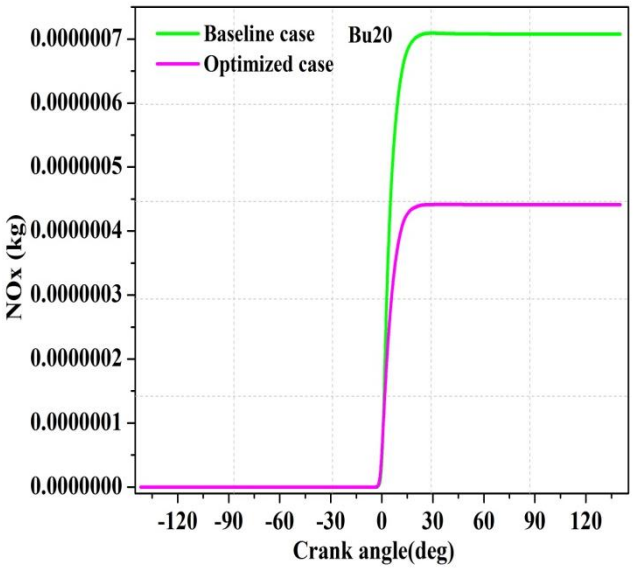

Fig. 10. Comparison of NOx with Crank Angle for optimized and baseline cases for Bu20 at rated load.

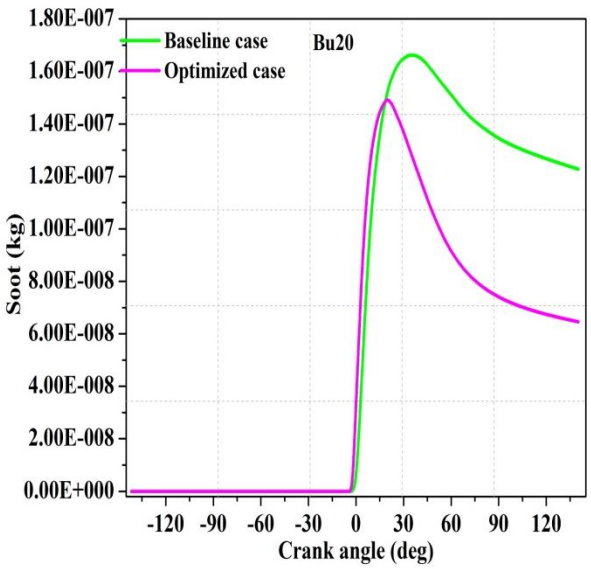

Fig. 11. Comparison of soot with Crank Angle for optimized and baseline cases for Bu20 at rated load.

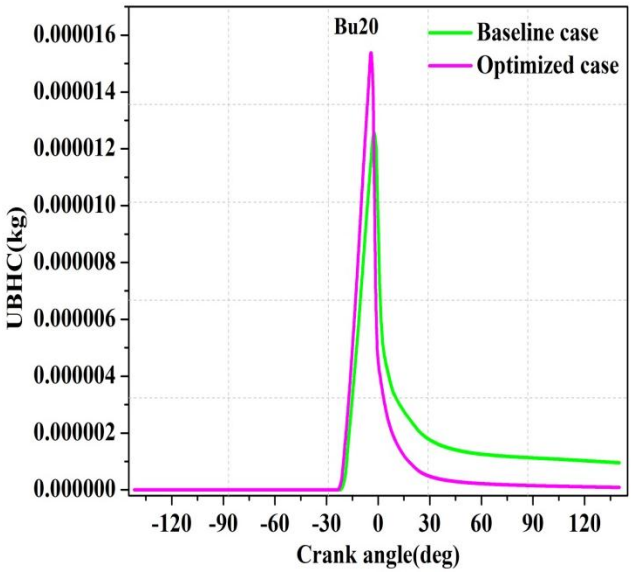

Fig. 12. Comparison of UBHC with Crank Angle for optimized and baseline cases for Bu20 at rated load.

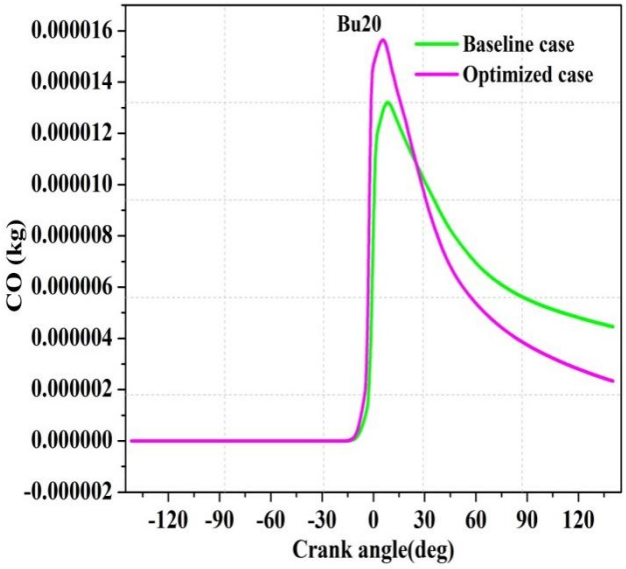

Fig. 13. Comparison of CO with Crank Angle for optimized and baseline cases for Bu20 at rated load.

C.1.8. Comparison of homogeneity index for optimized and baseline configuration for Bu20 case

Crank angle	Baseline case (Bu00)	Optimized case (Bu20)
0	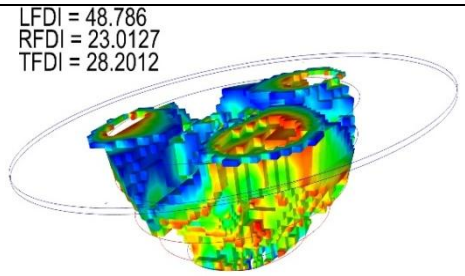	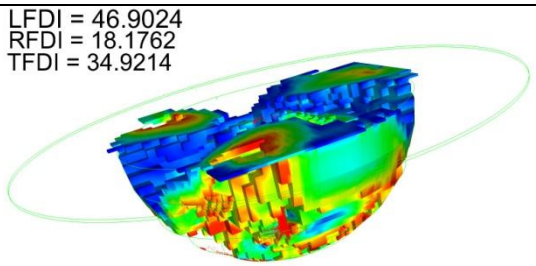
40	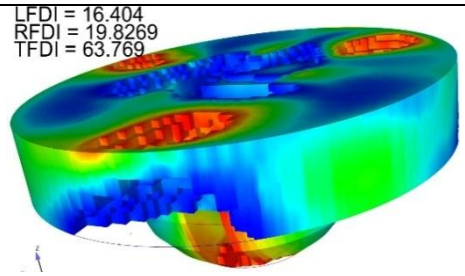	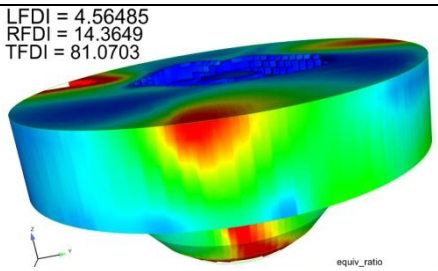

Fig. 14. Comparison of fuel distribution index for baseline and optimized case for Bu20 blend.

Figure 14 shows the comparison of fuel distribution index for baseline and optimized cases. TFDI increased for optimized Bu20case by 21.3% compared to baseline configuration. Similarly, RFDI and LFDI decreased by 27.54% and 72% respectively for optimized configuration compared to baseline configuration. This shows that TFDI is better for the optimized cases compared to baseline configuration, which is an index of the homogeneous charge preparation.

C.2. Determination of optimal engine parameters using RSM for VCR engine fuelled with 30% of butanol/diesel blend (Bu30)

In the present section, validation of 30% butanol/diesel blend model was carried out by comparing the simulation results with experimental results. This study also emphasizes the effect of CR, FIP, EGR and SOI on optimal engine parameters using CONVERGE CFD software with DOE adoption. In this numerical analysis also, four operating parameters and 3 out responses (ISFC, NOx and soot) were considered. The main aim of the present work is to reduce the ISFC and emissions for Bu30 blend using optimization technique.

C.2.1. Validation of VCR engine model for 30% of butanol/diesel blend (Bu30)

The butanol/diesel blend (bu30) numerical model was validated by comparing the numerical results with experimental results. The comparison of experimental and numerical results for Bu30 are shown in figure 15. The experimental and numerical results trends appeared to be similar. From the Table C9, it is observed that the maximum error obtained between experimental and numerical results was around 7.66%. Therefore, based on the comparison of these characteristics, it was concluded that the simulation results were nearly in good agreement with the experimental results, and further studies were carried out using the same numerical model.

Table C9. Comparison of the experimental and simulation results of peak in-cylinder pressure and emissions for 30% butanol/diesel blend (Bu30).

Characteristics	Experimental	Simulation	Error (%)
Peak in-Cylinder pressure (bar)	59.11	62.8	5.87
NOx (g/kWh)	7.21	7.6	5.13
Soot (g/kWh)	1.016	1.1	7.66

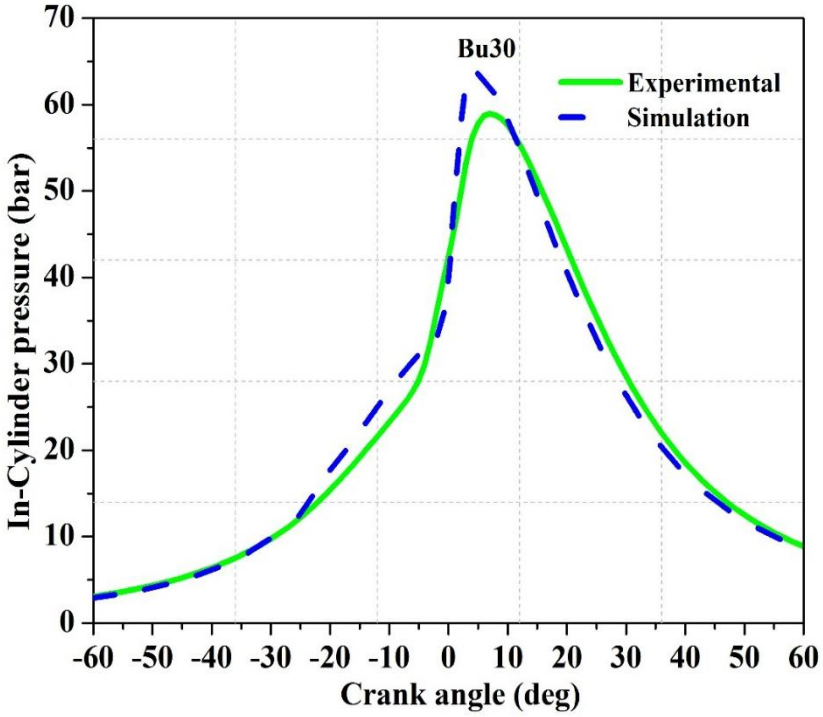

Fig. 15. Comparison of the in-cylinder pressure with crank of the simulation with experimental result for B30 blend.

C.2. 2. Enabling HCCI mode of the CI engine with 30% of butanol/diesel blend (Bu30) using RSM technique

Based on the confidence levels attained by the validation of Bu30 blend, the present study was extended to analyse the effect of different parameters on the output responses. Based on the DOE analysis, a set of 29 experiments were obtained. All the 29 simulation were simulated using CONVERGE CFD software and three responses were considered. The experimental design matrix and their responses are listed in Table C10.

Table C10. Experimental design matrix and their responses for Bu30 blend.

Run order	CR	FIP (bar)	SOI (bTDC)	EGR (%)	ISFC (g/kWh)	Soot (g/kWh)	NOx (g/kWh)
1	14	240	23	0	356	1.78	2.75
2	16.5	240	17	0	265	1.75	3.595
3	16.5	240	23	15	242	1.84	4.2
4	16.5	240	23	15	242	1.84	4.2
5	19	240	23	30	192	0.41	3.85
6	16.5	200	23	30	300	1.86	1.505
7	19	280	23	15	196	0.73	7.71
8	16.5	280	23	30	270	1.58	2.03
9	19	240	23	0	192.2	0.3	10.2

10	16.5	240	23	15	242	1.84	4.2
11	19	240	17	15	205	0.53	2.94
12	19	240	29	15	210	0.1	10.4
13	16.5	240	23	15	242	1.84	4.2
14	16.5	280	23	0	215	1.6	7
15	16.5	280	29	15	211	0.922	8.6
16	19	200	23	15	203	0.38	5.2
17	16.5	280	17	15	276	1.98	1.87
18	16.5	240	29	30	216	1.16	4.32
19	16.5	240	29	0	193	0.7	9.74
20	16.5	200	29	15	220.62	1.41	5.36
21	16.5	200	23	0	260	1.69	4.05
22	14	200	23	15	490	2.7	1.14
23	14	240	17	15	543	1.91	2.175
24	16.5	240	23	15	242	1.84	4.2
25	14	240	29	15	350	1.366	2.47
26	14	240	23	30	489	2.2	0.39
27	16.5	240	17	30	350	1.46	0.7
28	14	280	23	15	384	1.78	1.95
29	16.5	200	17	15	340	1.72	1.59

C.2.3. ANOVA analysis for VCR engine fuelled with 30% of butanol/diesel blend (Bu30)

Table C11 to C13 shows the ANOVA analysis of the three responses. From the ANOVA table it is apparent that CR (64.21%) had the most impact on ISFC, followed SOI (10.74%), EGR (4.21%) and FIP (0.39%). The interaction effect of CR x SOI (3.77) strongly affected ISFC followed by CR x EGR (1.71%), CR x FIP (0.94%), SOI x EGR (0.37%) and FIP x SOI (0.28%). The square terms of CR (11.48%), SOI (0.48%) and FIP (0.37%) also have some impact on ISFC. In case of soot emission, CR (63.61%) was the most significant parameter, followed by SOI (10.3%), FIP (0.99%) and EGR (0.5%). The interaction effect of SOI x EGR (3.53%) exercised a strong influence on soot followed by CR x FIP (1.25%), FIP x SOI (1.22%) and CR x EGR (0.21%). The square terms of CR (11.15%), SOI (6.5), EGR (1.34%) and FIP (0.35%) also had some impact on soot emission. CR (32.15%) was a strong impact on NOx emission, followed by SOI (29.15%), EGR (22.36%) and FIP (395%). The interaction effect of CR x SOI (4.14%) had a strong effect on NOx emission, followed by CR x EGR (1.77%), FIP x SOI (0.97%) and SOI x EGR (0.708).

Table C11 ANOVA analysis of ISFC for 30% butanol/diesel blend (Bu30 blend)

Source	Sum of Squares	df	Mean Square	F-value	p-value		Percentage contribution
Model	258369	14	18454.93	257.436	< 0.0001	significant	99.61
A-CR	166569.2	1	166569.2	2323.548	< 0.0001		64.21
B-FIP	5703.752	1	5703.752	79.56417	< 0.0001		2.19
C-SOI	27876.95	1	27876.95	388.868	< 0.0001		10.74
D-EGR	9396.803	1	9396.803	131.0802	< 0.0001		3.62
AB	2450.25	1	2450.25	34.17963	< 0.0001		0.94
AC	9801	1	9801	136.7185	< 0.0001		3.77
AD	4435.56	1	4435.56	61.8736	< 0.0001		1.71
BC	739.2961	1	739.2961	10.31277	0.006277		0.28
BD	56.25	1	56.25	0.784656	0.390683		0.02
CD	961	1	961	13.40542	0.002567		0.37
A^2	29779.97	1	29779.97	415.4141	< 0.0001		11.48
B^2	963.0761	1	963.0761	13.43438	0.002546		0.37
C^2	1259.573	1	1259.573	17.57035	0.000905		0.48
D^2	91.58145	1	91.58145	1.27751	0.277355		0.03
Residual	1003.624	14	71.68744				
Lack of Fit	932.8242	10	93.28242	5.270193	0.061678	not significant	
Pure Error	70.8	4	17.7				
Total	259372.7	28					

Table C12 ANOVA analysis of soot emission for 30% butanol/diesel blend (Bu30 blend).

Source	Sum of Squares	df	Mean Square	F-value	p-value		Percentage contribution
Model	11.23	14	0.8021	71.75	< 0.0001	significant	98.5
A-CR	7.19	1	7.19	642.79	< 0.0001		63.16
B-FIP	0.1137	1	0.1137	10.17	0.0066		0.99
C-SOI	1.14	1	1.14	101.61	< 0.0001		10.3
D-EGR	0.0602	1	0.0602	5.39	0.0359		0.52
AB	0.4032	1	0.4032	36.07	< 0.0001		1.23
AC	0.0032	1	0.0032	0.2906	0.5983		0.02
AD	0.024	1	0.024	2.15	0.1648		0.21
BC	0.1399	1	0.1399	12.51	0.0033		1.22
BD	0.009	1	0.009	0.8073	0.3841		0.079
CD	0.1406	1	0.1406	12.58	0.0032		3.53
A^2	1.27	1	1.27	113.27	< 0.0001		11.15
B^2	0.0404	1	0.0404	3.61	0.0781		0.35
C^2	0.7458	1	0.7458	66.71	< 0.0001		6.5
D^2	0.1535	1	0.1535	13.73	0.0024		1.34
Residual	0.1565	14	0.0112				

Lack of Fit	0.1398	10	0.014	3.35	0.1274	not significant	
Pure Error	0.0167	4	0.0042				
Cor Total	11.39	28					

Table C13 ANOVA analysis of NOx emission for 30% butanol/diesel blend (Bu30 blend).

Source	**Sum of Squares**	**df**	**Mean Square**	**F-value**	**p-value**		Percentage contribution
Model	221.75	14	15.84	96.81	< 0.0001	significant	98.81
A-CR	72.15	1	72.15	440.98	< 0.0001		32.15
B-FIP	8.87	1	8.87	54.19	< 0.0001		3.95
C-SOI	65.43	1	65.43	399.87	< 0.0001		29.15
D-EGR	50.18	1	50.18	306.72	< 0.0001		22.36
AB	0.7225	1	0.7225	4.42	0.0542		0.321
AC	12.83	1	12.83	78.44	< 0.0001		5.717
AD	3.98	1	3.98	24.33	0.0002		1.77
BC	2.19	1	2.19	13.39	0.0026		0.97
BD	1.47	1	1.47	8.99	0.0096		0.65
CD	1.59	1	1.59	9.74	0.0075		0.708
A^2	0.1584	1	0.1584	0.9679	0.3419		0.0705
B^2	0.3736	1	0.3736	2.28	0.153		0.166
C^2	1.49	1	1.49	9.11	0.0092		0.66
D^2	0.0043	1	0.0043	0.026	0.8741		0.001
Residual	2.29	14	0.1636				
Lack of Fit	2.12	10	0.2123	5.05	0.0662	not significant	
Pure Error	0.168	4	0.042				
Cor Total	224.04	28					

C.2.4. Error analysis of the regression model for VCR engine fuelled with 30% of butanol/diesel blend

Figure 16 shows the normal probability plots of three responses. It can be seen from the figures that the residuals have been falling almost in a straight line. Hence, the fitted models adequately represent the simulation results. This indicates that the regression equations are accurate enough. From the Table C14, it is observed that the difference between the values of adjusted R^2 and predicated R^2 is less than 0.2 for all the responses, which indicates that the models were able to fit the data with reasonably good accuracy.

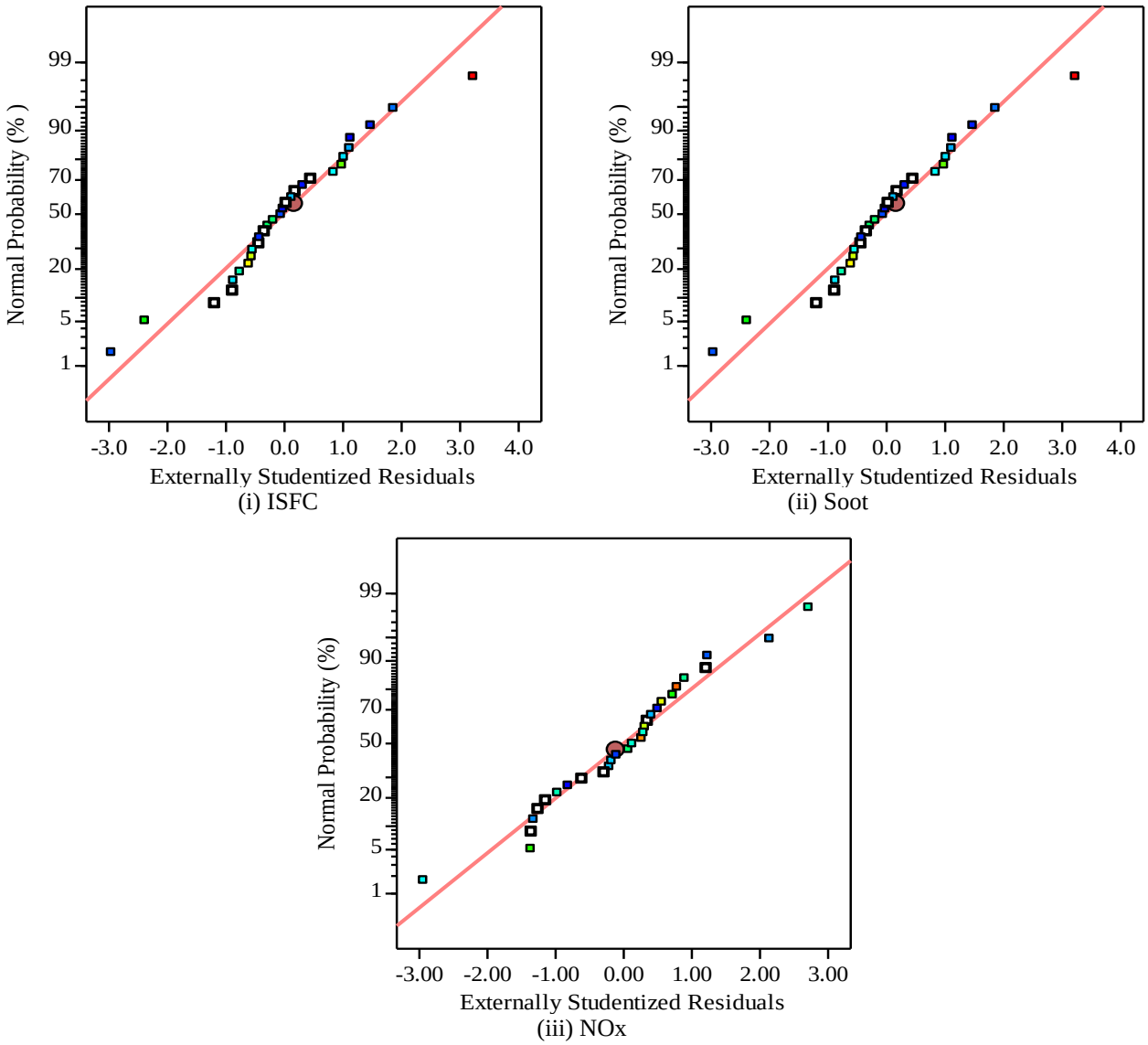

Fig. 16. Normal probability plot of the response ISFC, soot and NOx for VCR engine for Bu30 blend.

Table C14. Model evaluation for ISFC, Soot and NOx for Bu30 blend.

Parameters	**ISFC**	**Soot**	**NOx**
R^2	0.996	0.986	0.99
Adjusted R^2	0.992	0.973	0.98
Predicted R^2	0.979	0.948	0.949
(Adjusted R^2) - (Predicted R^2)	0.013	0.025	0.031
Adeq. precision	57.28	44.43	36.2

C.2.5. Interaction effects of VCR engine fuelled with 20% of butanol/diesel blend (Bu20)

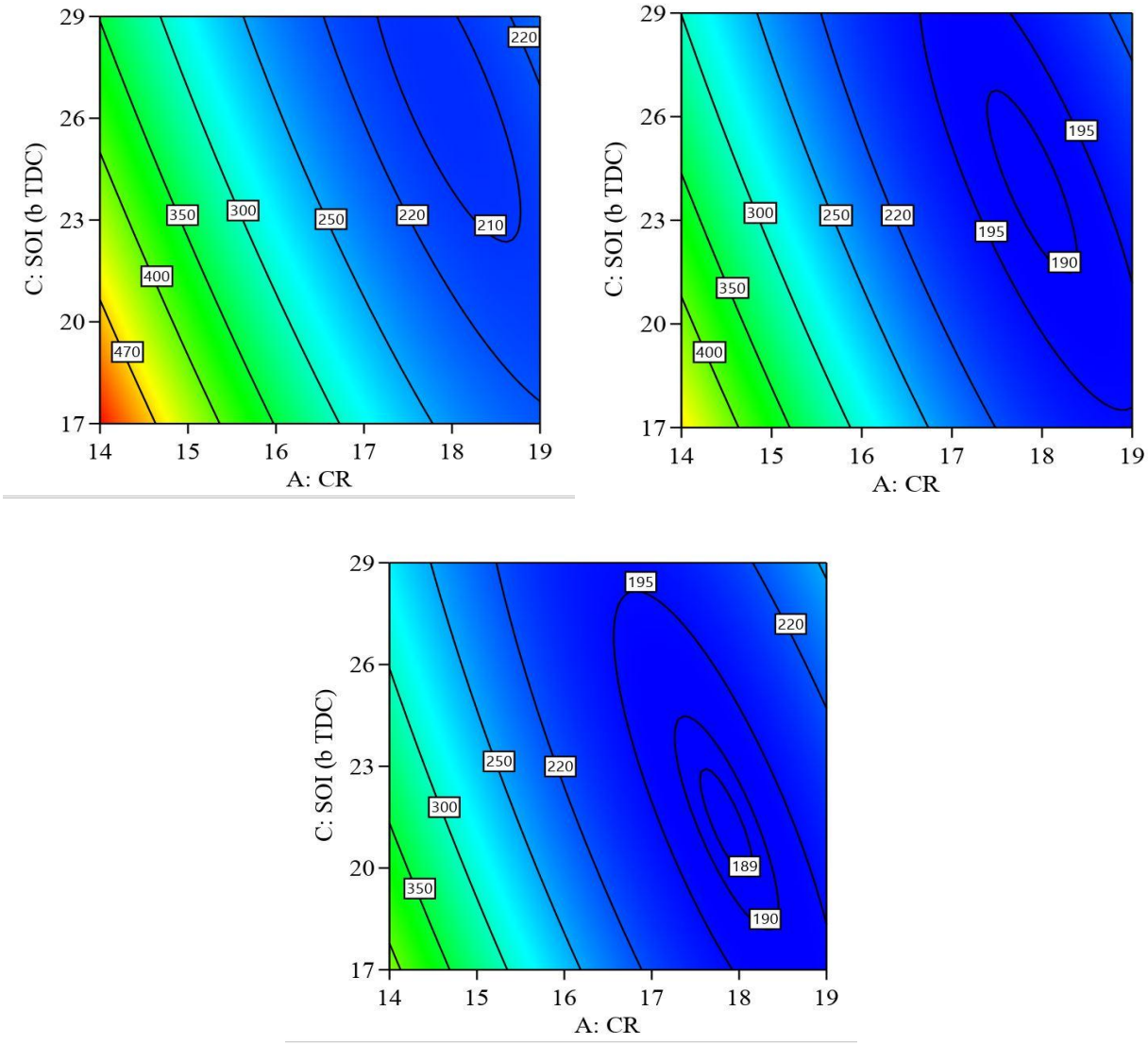

Fig. 17. Interaction effect of CR and SOI on the ISFC at different FIPs (i) 200 bar (ii) 240 bar and (iii) 280 bar for Bu30.

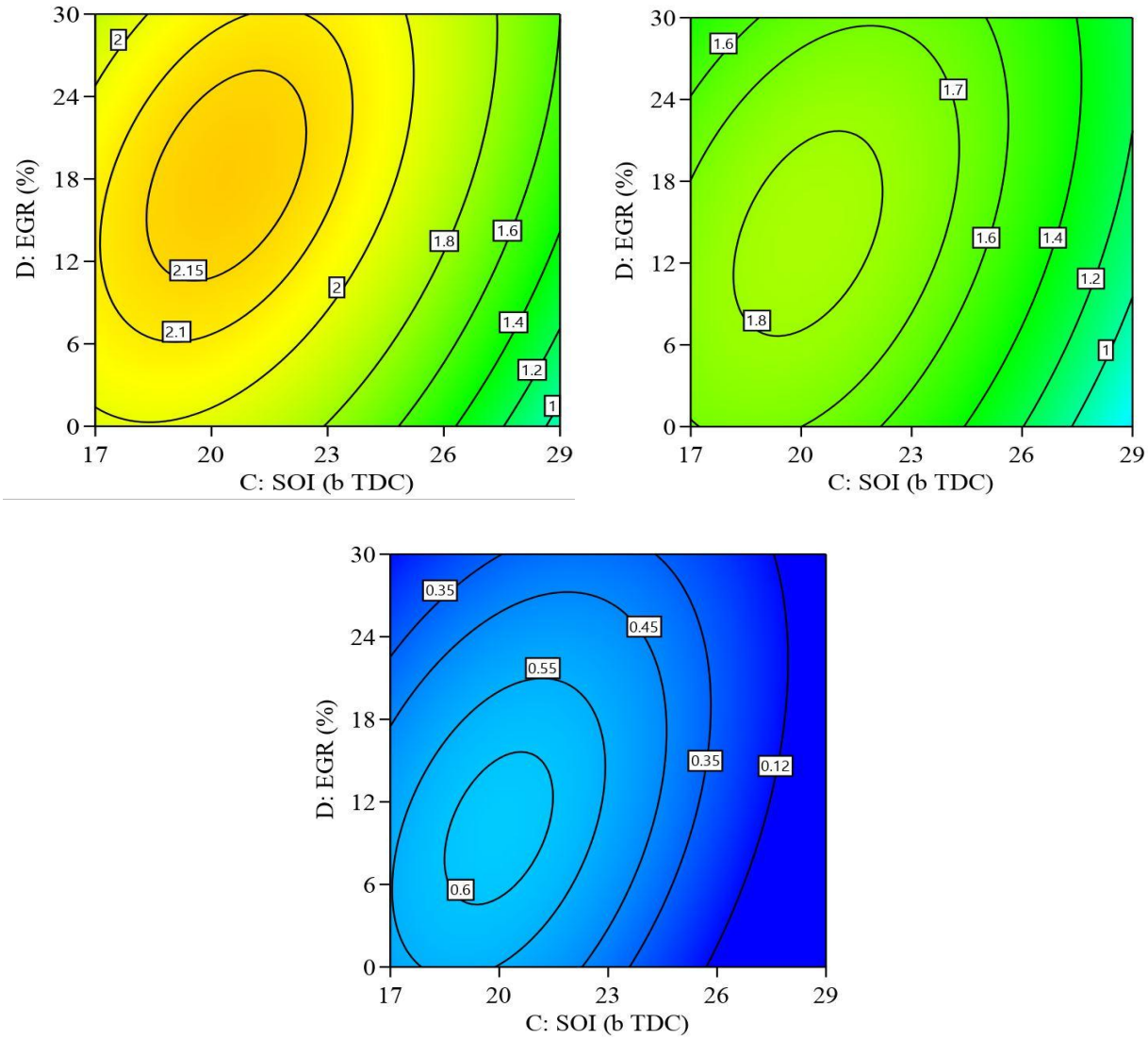

Fig.18. Interaction effect of SOI and EGR on the soot at different CRs (i) 14 (ii) 16.5 and (iii) 19 for Bu30.

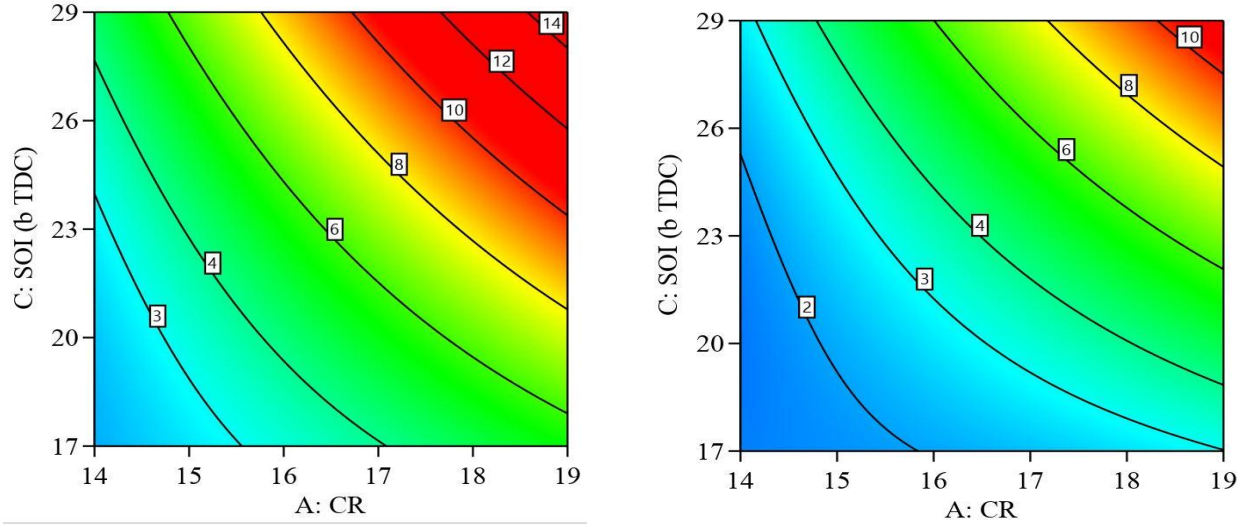

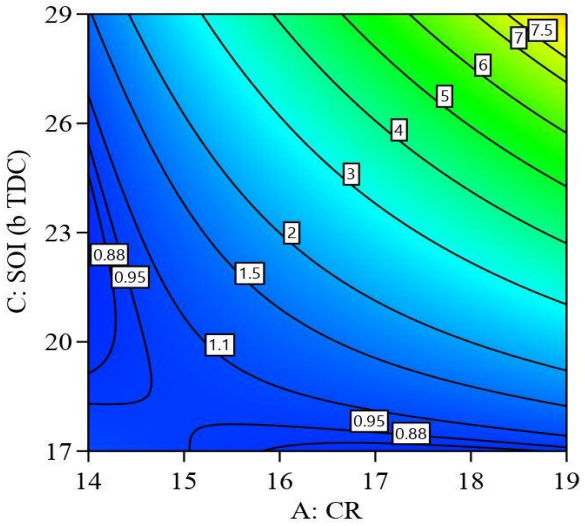

Fig. 19. Interaction effect of CR and SOI on the NOx at different EGR rates (i) 0(ii) 15 and (iii) 30% for Bu30.

Figures 16, 17 and 18 show the interaction effects between different operating parameters on the ISFC, soot and NOx for Bu30 fuel operations. It can be seen that similar effects were observed in these cases and also in the case of Bu00 and Bu20. There is not much effect of the addition of butanol except that the absolute value of ISFC was higher. This is plausible since the calorific value of butanol is lower than that of diesel. Similarly, absolute values of soot and NOx emission are lower compared to Bu00. This was because of higher oxygen content in the molecular structure and higher latent heat of evaporation.

C.2.6. Optimization using desirability approach for 30% of butanol/diesel blend (Bu30)

Composite desirability technique was used to optimize the output responses. Equal weights were assigned for all the responses in order to simultaneously minimize ISFC, soot and NOx. Table C15 shows the criteria of optimization used for desirability method for Bu30 blend.

Table C15.Criteria of optimization used for desirability method for Bu30 blend.

Parameters /Response	Limits		Criterion	Desirability
	Lower	Upper		
Compression Ratio	14	19	In range	1
Fuel Injection Pressure (bar)	200	280	In range	1
Start of Injection (bTDC)	17	29	In range	1
Exhaust Gas Recirculation (%)	0	30	In range	1
ISFC (g/kWh)	192	543	Minimum	0.958
Soot (g/kWh)	0.1	2.7	Minimum	0.975
NOx (g/kWh)	0.39	10.4	Minimum	0.951
Combined				0.961

Based on the regression analysis, the regression equation was developed for ISFC, soot and NOx emission as shown in Equations 4, 5 and 6. In the next step optimum values were found based on the minimization of ISFC and emissions. The optimum combination of input parameters were determined to be CR of 18.9, FIP of 261.2 bar, SOI of 21° bTDC, and EGR of 24.1% with a composite desirability of 0.961.

$$\begin{aligned} ISFC = {} & 7192.11 - 526.86*CR - 9.68*FIP - 91.30*SOI + 18.47*EGR + 0.247*CR*FIP \\ & + 3.3*CR*SOI - 0.88*CR*EGR + 0.056*FIP*SOI + 0.0062*FIP*EGR \\ & - 0.1722*SOI*EGR + 10.841*CR^2 + 0.007616*FIP^2 + 0.387*SOI^2 + 0.0167*EGR^2 \end{aligned} \quad (4)$$

$$\begin{aligned} Soot = {} & -4.06 + 1.248*CR - 0.059*FIP + 0.5063*SOI + 0.030417*EGR + 0.003175*CR*FIP \\ & + 0.0019*CR*SOI - 0.002067*CR*EGR - 0.000779*FIP*SOI - 0.000079*FIP*EGR \\ & + 0.002083*SOI*EGR - 0.07069*CR^2 + 0.000049*FIP^2 - 0.009419*SOI^2 - 0.000684*EGR^2 \end{aligned} \quad (5)$$

$$\begin{aligned} NOx = {} & 47.53 - 3.211*CR - 0.0323*FIP - 2.82*SOI + 0.7029*EGR + 0.004250*CR*FIP \\ & + 0.1194*CR*SOI - 0.0266*CR*EGR + 0.003083*FIP*SOI - 0.00101*FIP*EGR \\ & - 0.007014*SOI*EGR + 0.025*CR^2 - 0.00015*FIP^2 + 0.01338SOI^2 + 0.000114*EGR^2 \end{aligned} \quad (6)$$

C.2.7. Comparison of baseline and optimized configuration for Bu30 blend

In this section, for Bu30 blend, the optimized case was compared with and baseline case. The comparison of optimized and baseline cases of VCR Bu30 is shown in Table C16. From the table it is observed that ISFC/ISEC, NOx and soot emissions are reduced for optimum case by 1.15%, 35.52% and 57.57% respectively, compared to baseline case. Figures 20 to 23 show the comparison of the in-cylinder pressure, temperature, IHRR and IHR for the baseline configuration and optimum configuration. It can be seen from the figures that Peak in-cylinder pressure, IHRR and IHR increase for optimized cases compared to baseline case. The in-cylinder temperature reduces for optimized case compared to baseline case. From the figure 24 to 27, it is observed that all the emissions decreased for the optimized case compared to the baseline configuration. This indicates that the optimum case has superior quality than the baseline case.

Table C16. Comparison of optimized and baseline configuration for Bu30 blend.

	ISFC (g/kWh)	ISEC (MJ/kWh)	Soot (g/kWh)	NOx (g/kWh)
Baseline configuration	216.5	81	0.99	7.6
Optimized configuration	214	8.006	0.42	4.9
Change w.r.t baseline	1.15	1.15	57.57	35.52

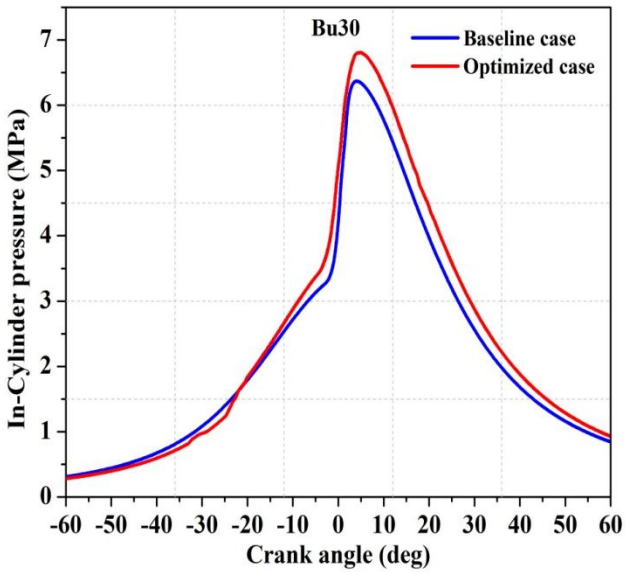

Fig. 20. Comparison of in-cylinder pressure with crank angle between baseline and optimized case for Bu30 blend at rated load.

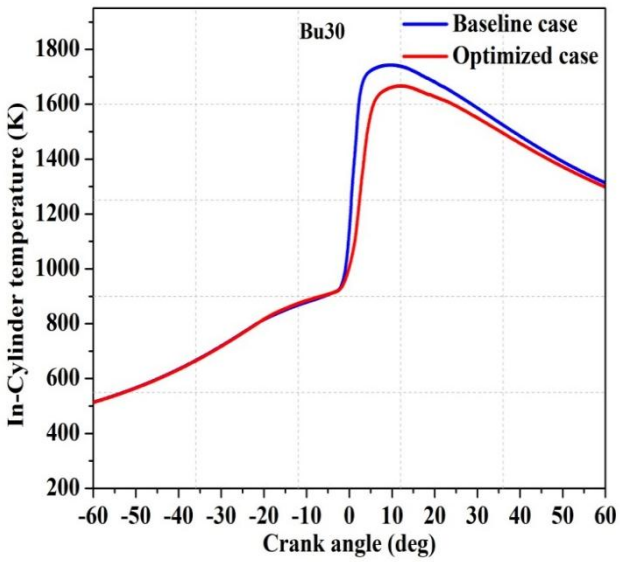

Fig. 21. Comparison of in-cylinder temperature with crank angle between baseline and optimized case for Bu30 blend at rated load.

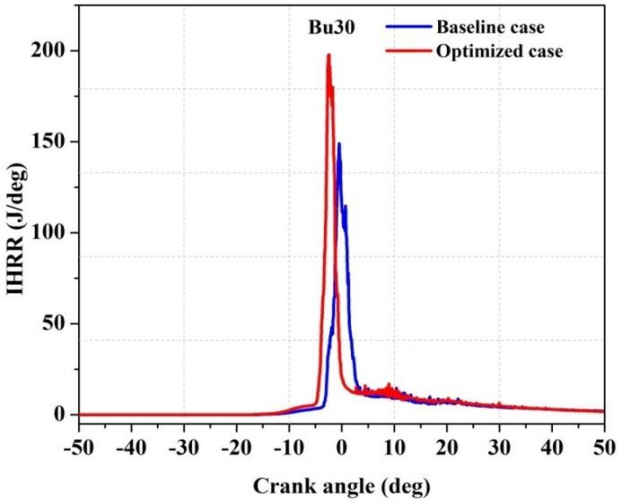

Fig. 22. Comparison of IHRR with crank angle between baseline and optimized case for Bu30 blend at rated load.

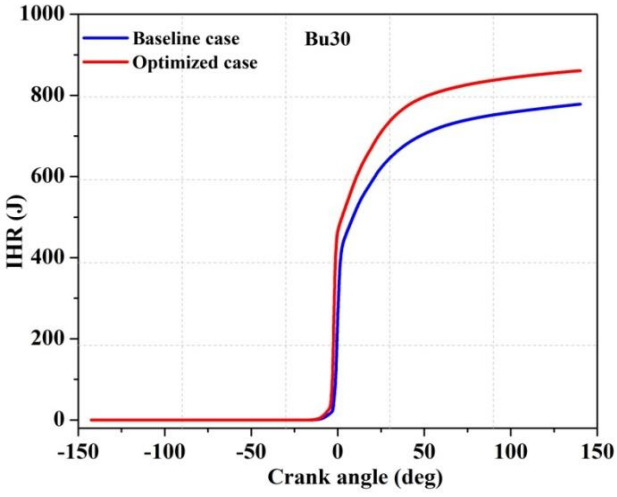

Fig. 23. Comparison of IHR with crank angle between baseline and optimized case for Bu30 blend at rated load.

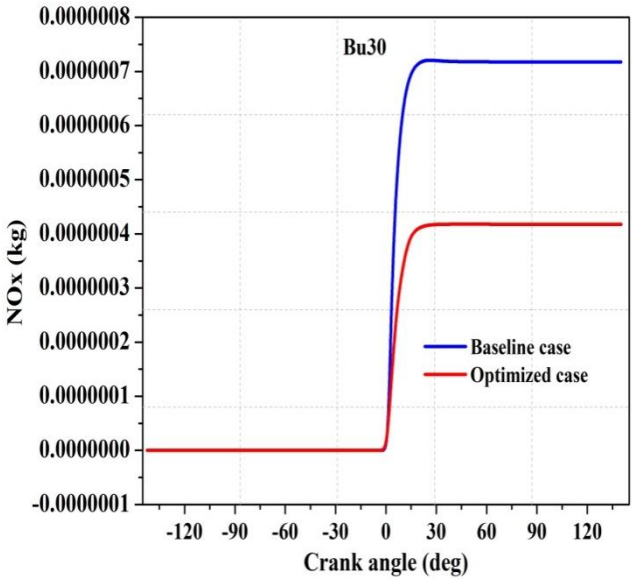

Fig. 24. Comparison of NOx with crank angle between baseline and optimized case for Bu30 blend at rated load.

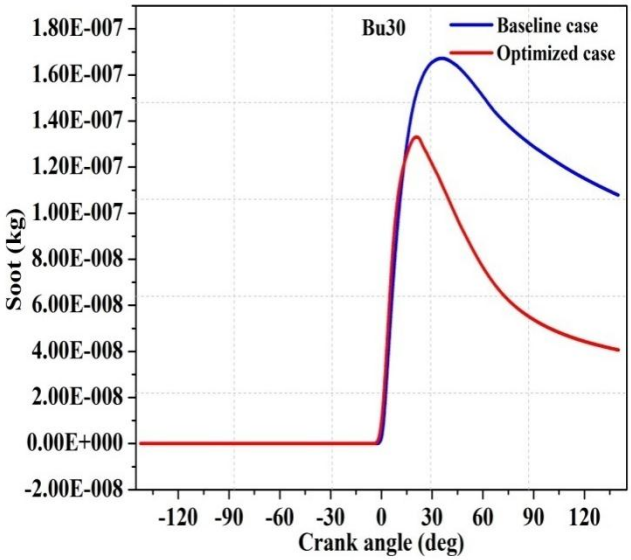

Fig. 25. Comparison of soot with crank angle between baseline and optimized case for Bu30 blend at rated load.

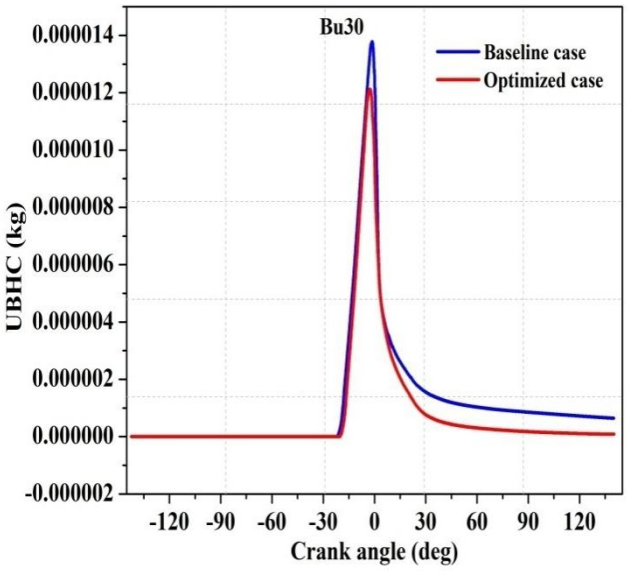

Fig. 26. Comparison of UBHC with crank angle between baseline and optimized case for Bu30 blend at rated load.

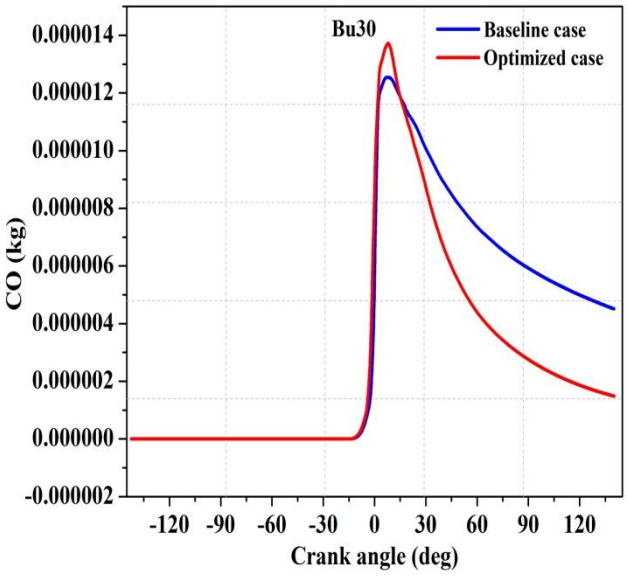

Fig. 27. Comparison of CO with crank angle between baseline and optimized case for Bu30 blend at rated load.

C.2.8. Comparison of homogeneity index for optimized and baseline configuration for Bu30 blend

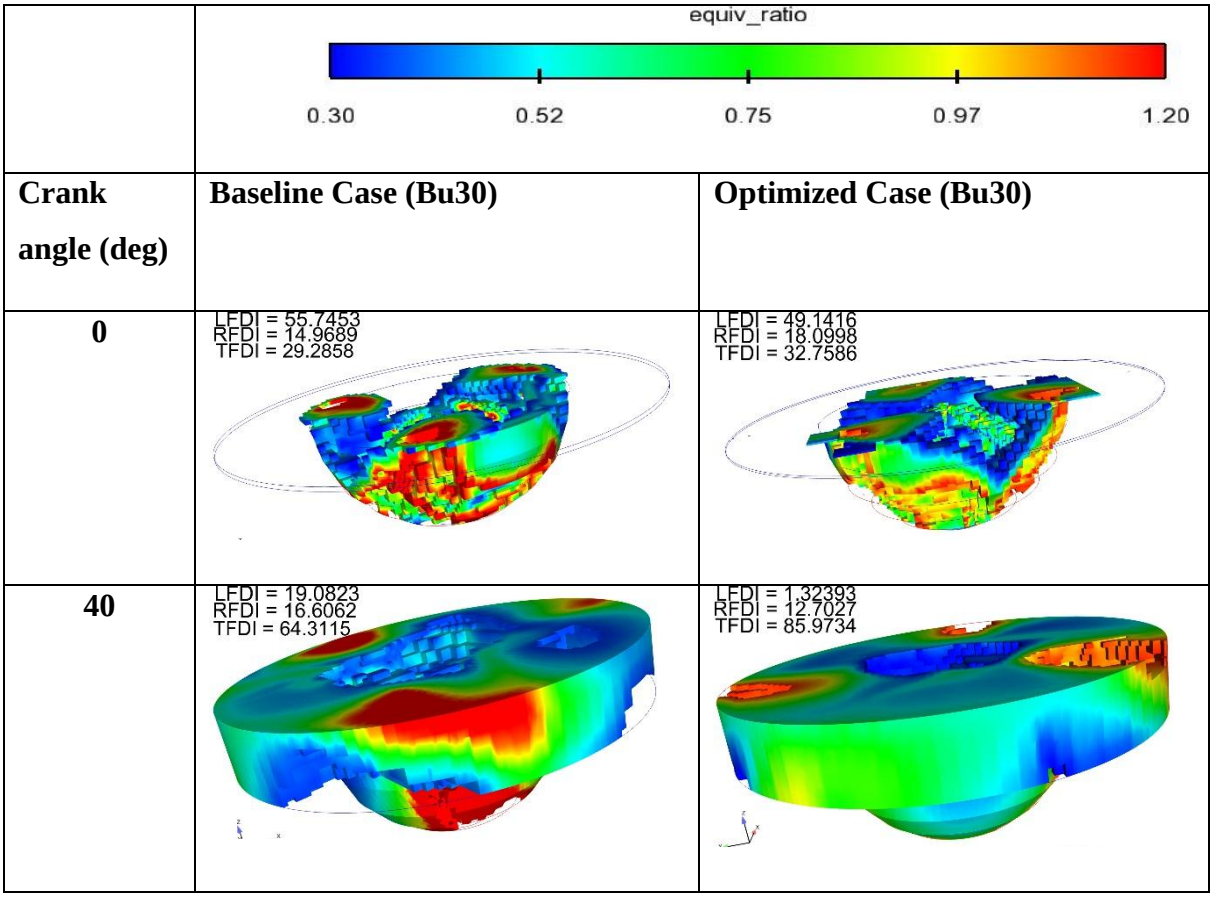

Fig. 28. Comparison of fuel distribution index for baseline and optimized case for Bu30 blend.

Figure 28 shows the comparison of fuel distribution index for baseline and optimized cases. TFDI increased for optimized Bu30case by 25.1% compared to baseline configuration. Similarly, LFDI and RFDI decreased for optimized configuration by 30.6% and 23.49% respectively, compared to baseline configuration.